Effects of Nutritional Perturbations on the Metabolomic Homeostasis of HepG2 Cells

A

Dissertation Submitted

By

Nehal

Roll No. 302101015

Under Supervision of

Dr. Priyankar Dey

Assistant Professor

Department of Biotechnology

In Partial Fulfillment of the Requirements for the Award of the Degree of

Master of Science

In

Biotechnology

Thapar Institute of Engineering and Technology, Patiala, Punjab

July, 2023

CANDIDATE'S DECLARATION

I, **Ms. Nehal**, do hereby declare that the work presented in this dissertation entitled **"Effects of Nutritional Perturbations on the Metabolomic Homeostasis of HepG2 Cells"** is an authentic record of my work during the period of six months from January 2023 to June 2023. This dissertation is submitted in partial fulfillment of the requirement for the award of the degree of **"Master in Science in Biotechnology"** from Thapar Institute of Engineering and Technology, Patiala, Punjab. The information derived from the literature has been duly acknowledged in the text and a list of references is provided. No part of this dissertation is submitted for the reward of any other degree or certificate in this or any other university or institute.

Date: 17-7-23

Place: Patiala

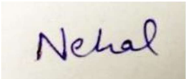

Nehal

CERTIFICATE

This is to certify that the dissertation entitled **"Effects of Nutritional Perturbations on the Metabolomic Homeostasis of HepG2 Cells"** submitted by **Ms. Nehal** (Roll No. 302101015) in partial fulfillment of the requirement for the award of the degree of **"Master of Science in Biotechnology"** from Thapar Institute of Engineering and Technology, Patiala, Punjab, is an authentic record of the student's work during the period of six months, i.e. from January 2023 to June 2023. This work has not been submitted for the reward of any other degree or certificate in this or any other university or institute.

Dr. Priyankar Dey
Supervisor
Assistant Professor
Department of Biotechnology
Thapar Institute of Engineering and Technology
Patiala

ACKNOWLEDGEMENT

The contentment and joy of completing any scientific project are incomplete without acknowledging the people who made this possible, whose persistent support and assistance can't be neglected and paved my way to success. I take this privilege to express my heartfelt thanks and gratitude to all those who helped me with the successful completion of this project.

I owe my deepest gratitude to my family who always supported me and stick by my side regardless of any situation and whose sacrifices will always inspire me to do well in life. My sincere thanks go to my esteemed supervisor **Dr. Priyankar Dey**, Assistant Professor, Department of Biotechnology, Thapar Institute of Engineering and Technology (TIET), Patiala for his precious guidance, constructive criticism, convergent thinking, and positive attitude towards my abilities. You always inspired me to think "out of the box" and handle every situation with patience.

I would like to acknowledge **Dr. Siddharth Sharma**, PG coordinator and Associate Professor, and **Dr. Anil Kumar**, Coordinator TIFAC-CORE and Professor for providing me with the facilities for easy and smooth working of the project.

Also, I would like to thank 3M research group members, **Ms. Jyoti Sharma**, **Ms. Nisha Tewari**, **Ms. Sayantani Bhattacharya**, and **Ms. Dwinder Sidhu** for their constant support and motivation. You always helped me and created a cooperative lab environment throughout my work.

Place: Patiala

Nehal

LIST OF TABLES

LIST OF FIGURES

LIST OF ABBREVIATIONS

AMP	Adenosine monophosphate
NADPH	Nicotinamide adenine dinucleotide phosphate hydrogen
ATP	Adenosine triphosphate
MetS	Metabolic syndrome
MTT	3-(4,5-Dimethylthiazol-2-yl)-2,5-diphenyltetrazolium bromide
NaCl	Sodium chloride
BSA	Bovine serum albumin
GC-MS	Gas chromatography-mass spectrometry
KEGG	Kyoto encyclopedia of genes and genomes
HMDB	Human metabolome database
SMPDB	Small molecule pathway database
NAFLD	Non-alcoholic fatty liver disease
ALT	Alanine aminotransferase
AST	Aspartate aminotransferase
NASH	Nonalcoholic steatohepatitis
HCC	Hepatocellular carcinoma
HILIC-TOF	Hydrophilic time-of-flight
GC-TOF-MS	Gas chromatography time-of-flight mass spectrometry
LC-MS	Liquid chromatography-mass spectrometry
LC-QTOF-MS	Liquid chromatography quadrupole time-of-flight mass spectrometry
UHPLC-QTOF/MS	Ultra-high performance liquid chromatography-quadrupole time-of-flight mass spectrometry
TCA	Tricarboxylic acid cycle
IL-6	Interleukin-6
TNF-α	Tumor necrosis factor-alpha
MAPKs	Mitogen-activated protein kinase
NF-κb	Nuclear factor kappa B

ROS	Reactive oxygen species
DNA	Deoxyribonucleic acid
LPL	Lipoprotein lipase
VLDL	Very low-density lipo-proteins
HFD	High-fat diet
NAD	Nicotinamide adenine dinucleotide
PUFAs	Polyunsaturated fatty acids
RAS	Renin-angiotensin system
PEPCK	Phosphoenolpyruvate carboxykinase
BCAAs	Branched-chain amino acids
AAAs	Aromatic amino acids
DF	Dietary fiber
SCFAs	Short-chain fatty acids
LPS	Lipopolysaccharide
HAMRS-2	High-amylose-maize resistant starch type 2
ETWB	Enzyme-treated wheat bran
SREBP	Sterol regulatory element-binding protein 1
LDL	Low-density lipoprotein
HDL	High-density lipoprotein
SAMe	S-adenosylmethionine
DPA	Docosapentaenoic acid
EPA	Eicosapentaenoic acid
DHA	Docosahexaenoic acid
NCCS	National center for cell science
MEM	Minimum essential medium
CO_2	Carbon dioxide
ELISA	Enzyme-linked immuno sorbent assay
PBS	Phosphate saline buffer

N_2	Nitrogen
BSTFA	N,O-Bis(trimethylsilyl)trifluoroacetamide
AMDIS	Automated mass spectral deconvolution and identification system
NIST	National institute of standards and technology
ANOVA	Analysis of variance
MW	Molecular weight
RT	Retention time

CONTENTS

ABSTRACT

Background: Normal body function is based on the metabolic processes going inside the body which require energy (ATP) as fuel for the formation of metabolic intermediates to enrich other metabolic pathways and perform cellular functions. This energy is provided by diet which includes carbohydrates, fats, proteins, fiber, and minerals. The diet consumed is digested in the small intestine and enters the liver via the portal vein. The liver plays a significant role in the metabolism of gut-derived dietary components. Metabolism of these components will lead to the production of metabolites conferring physiological roles. Consumption of these dietary elements in adequate amounts maintains metabolic homeostasis. But excess intake for prolonged periods may cause toxicity and affect the metabolic processes and metabolites composition in the human body. This can lead to the development of metabolic syndrome (MetS) which may cause several metabolic diseases. These metabolomic shifts may negatively affect the liver and its function as the liver is the first line of detoxification for gut-derived metabolites. Scientists have shown the effects of different dietary elements on liver function with gene expression studies but the metabolome call remains critically underexplored. Metabolomic studies would help in understanding the interaction between diet and biomolecules in the body and identifying disease-associated markers specific to certain dietary stress.

Aim: The effects of high concentrations of each diet were evaluated using human hepatoma (liver tumor) cells, (in this study, HepG2 cells), in which various chemicals were used to mimic the dietary stress and untargeted metabolome analysis was done to understand the changes in metabolites caused by various dietary stress.

Method: HepG2 cells were cultured in standard conditions and used to mimic liver responses to dietary stress. A sub-lethal dose for each treatment was selected using a standard MTT assay. Cells were treated with five dietary stresses (high glucose, high palmitic acid, high salt (NaCl), high bovine serum albumin (BSA), and high butyrate) and later metabolomics study was conducted. GC-MS technique was used for untargeted metabolomic analysis and relevant metabolites were obtained for each nutritional stress. Later, metabolites were mapped using PubChem, KEGG, HMDB, and SMPDB databases. Metabolic pathway enrichment, disease signatures, and sub-classes for the metabolite set of each treatment were evaluated using Metaboanalyst (5.0) tool, and corresponding results were recorded.

Result: Different metabolites were identified after GC-MS analysis. 54 metabolites were identified in control, 137 after glucose treatment, 211 after palmitic acid treatment, 92 after NaCl treatment, 231 after BSA treatment, and 122 after butyrate treatment. Out of all metabolites, cholesterol, 2-propyl-1-pentanol, palmitic acid, benzoic acid, acetamide, and leucine were common among all treatments. Three disease signatures were common in all which are phenylketonuria, phosphoenolpyruvate carboxykinase (PEPCK) deficiency, and type VI hers disease, and seven classes of metabolites were also found to be common, which include straight chain fatty acids, benzoic acids, carboximidic acids, amino acids, hydrocarbons, saturated fatty acids, and alkanes.

Conclusion: Palmitic acid showed more deleterious effects on HepG2 cells in comparison to all other treatments and butyrate revealed a negative association with liver dysfunction.

Keywords: liver, diet, metabolites, metabolomics, MTT, glucose, palmitic acid, NaCl, BSA, butyrate, HepG2 cells, GC-MS

INTRODUCTION

It is well known that there is a huge network of metabolism going inside the body and maintenance of this metabolism is important for survival. Disturbances in this metabolism and related metabolites can cause metabolic syndrome (MetS). Metabolic syndrome can be caused by various reasons in which dietary stress act as an important factor. Dietary stress includes our daily diet but in higher concentrations for a prolonged time. Throughout our lives, we consume vast quantities of food, various beverages, numerous medications, antibiotics, syrups, and other substances, some of which are extremely hazardous, and all of these go through the liver (Hajdarevic *et al.*, 2020). The liver is the first line of detoxification and filtration system for gut-derived dietary metabolites. According to food type and its availability, the liver can switch between different metabolic pathways (De Chiara *et al.*, 2019).

The liver is regarded as the "Central Laboratory" of the human as it plays a vital role in the detoxification of toxic compounds, nutrient storage, and multiple metabolic processes of the body. Major metabolic roles are executed by parenchymal cells and hepatocytes which include anabolism and catabolism of carbohydrates, proteins, and fats that possess a huge impact on body functions. Liver disorders can be classified as focal or diffuse based on their ability to affect specific liver regions or the whole liver. Consequently, the duration of an illness can be acute if it occurs abruptly and lasts for a limited amount of time (up to six months) or chronic if it is characterized by a slow progression and lasts for longer than six months, typically years. All liver diseases can be subdivided conditionally into inflammatory (acute and chronic hepatitis) and non-inflammatory (toxic lesions, liver tumors, cirrhosis, hepatic steatosis, and vascular disorders). The most prevalent viral liver diseases are hepatitis A, B, C, and D (Hajdarevic *et al.*, 2020).

Dietary stress (specifically, calorie overload) can result in MetS and this can further lead to chronic liver diseases like Non-alcoholic Fatty Liver Disease (NAFLD) spectrum. So, a healthy and balanced diet is important to maintain nutrient balance and liver function in the body. Liver dysfunction impacts the health of the digestive organs, which are crucial for the cleansing of the body. The body progressively encounters a condition of chronic toxicity if its liver function slows down. Diet management has been an integral element of liver disease treatment. The curative approach is more commonly referred to as the "liver diet." In addition to replenishing nutrients and calories, the liver diet significantly impacts the progression of the disease. Understanding metabolic conditions in the liver leads the way for appropriate diet therapy, which consists of an adequate amount of calorie intake and an appropriate proportion of essential nutrients, with a focus on proteins (Hajdarevic *et al.*, 2020).

NAFLD is a spectrum of liver diseases, which is linked to weight gain and MetS (Stachowska *et al.*, 2022). NAFLD spectrum includes fat accumulation (steatosis), fibrosis, and cirrhosis (Maciejewska-Markiewicz *et al.*, 2022). NAFLD is associated with increased triglyceride levels, shifts in alanine transaminase (ALT), and histopathological modifications in the liver. The occurrence of steatosis acts as a biomarker for NAFLD (Boyce *et al.*, 2020). Development of NAFLD can also occur by gut microbiome dysbiosis which negatively affects intestinal barrier function and leads to leaky gut. This will allow the movement of bacterial endotoxins to the liver via the portal vein and cause inflammation in the liver. Thus, diet can play an important role in maintaining gut commensals and intestinal barrier and NAFLD can be prevented (Stachowska *et al.*, 2022).

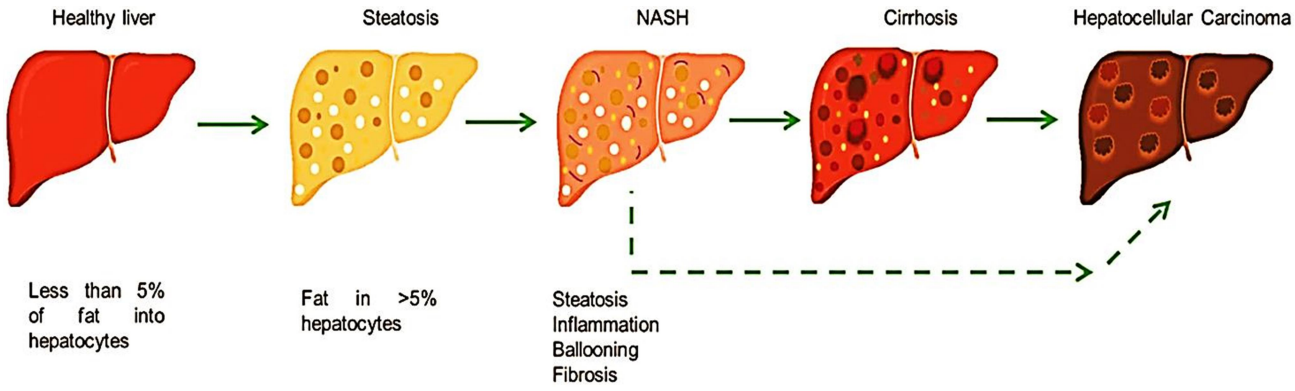

Figure 1: Non-alcoholic Fatty Liver Disease (NAFLD) Progression; This represents a gradual progression of hepatocellular carcinoma and steatosis, inflammation and fibrosis of the liver plays a major in it. NASH: non-alcoholic steatohepatitis, (Rojas *et al.*, 2022)

According to De Chiara *et al,* NAFLD is frequently described as the hepatic manifestation of MetS. When >5% of the liver's hepatocytes indicate fat accumulation (steatosis), as determined by histology or imaging, non-alcoholic fatty liver disease is suspected. Non-alcoholic steatohepatitis (NASH), a more severe version of NAFLD, is marked by inflammation and hepatocyte ballooning (given in Figure 1). The most striking indicator of fatality and liver-specific damage is the development of advanced fibrosis in patients with NAFLD and NASH (De Chiara *et al.*, 2019). The progression of liver fibrosis is significantly influenced by the lack of metabolic homeostasis (Wang *et al.*, 2016). Unregulated extracellular matrix accumulation, mostly brought on by hepatic stellate cells, is what drives the development of fibrosis and cirrhosis. In a hepatic damage situation, these cells get activated (De Chiara *et al.*, 2019), (Rojas *et al.*, 2022). The risk of developing hepatocellular carcinoma (HCC), colorectal cancer, and breast cancer is increased in NAFLD/NASH individuals who have elevated fibrosis stage scores than in people with lower scores (De Chiara *et al.*, 2019).

Various *in vitro, in vivo*, *ex vivo*, and *in silico* studies are conducted to understand the complex functioning of the liver. *In silico* studies include drug-response studies, gene expression studies,

and metabolomics studies; *in vivo* studies include animal studies; *ex vivo* studies include studying liver biopsy samples; and *in vitro* studies include liver cell line studies. Due to their resemblance to main tissue, low cost, and simplicity of use and culture, cell lines have transformed scientific research. Cell lines are widely used for cytotoxicity testing, vaccine production, studying tissue and organ function, and the production of certain proteins having therapeutic value. Also, it helps in evading ethical issues regarding the usage of animals for human studies (Arzumanian *et al.*, 2021).

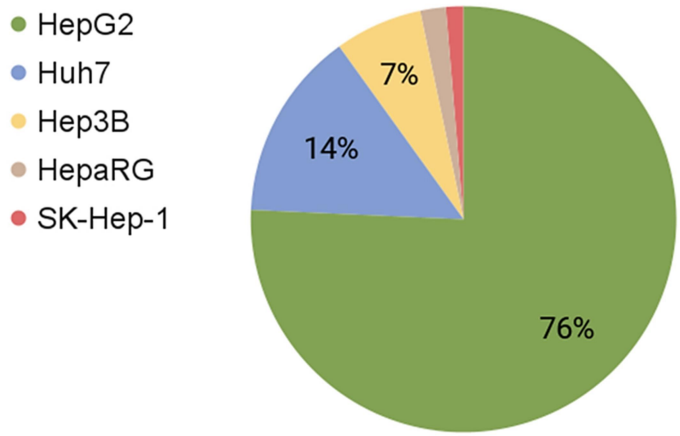

Figure 2: Pie-chart representing the percentage of studies utilizing human liver cell lines; It is based on the associated PubMed search keyword, (Arzumanian *et al.*, 2021).

For understanding liver functions, various hepatic cell lines can be used. There are approximately 40 different types of liver tumor cell lines, but HepG2, Huh7, HepaRG, Hep3B, and SK-Hep-1 are the most frequently used. Due to its numerous applications in scientific research, the HepG2 cell line continues to rise in popularity (as given in Figure 2). They maintain characteristics of regular hepatocytes and contain mixed features of normal hepatocytes and tumor cells (Arzumanian *et al.*, 2021).

Metabolomics is an appropriate technology for differentiating phenotypes and identifying potential biomarkers correlated to particular traits. Human and animal research identified several metabolites that are potential biomarkers of adiposity and associated illnesses (Kim *et al.*, 2011). So, a metabolomics study will help identify the relationship between dietary stress and associated shifts in metabolites that may cause NAFLD in humans. Several researchers have used metabolomics methods to understand the liver, its functioning, and liver-associated diseases, given Table 1.

Table 1: Metabolomics methods used in various studies

Methods	**References**
HILIC-TOF and GC-TOF mass spectroscopy method was used to validate the effects of glucose, fructose, and its combination on HepG2 cells.	(Meissen *et al.*, 2015)
GC-TOF-MS method was used to effects of a high-fat diet enriched with resistant starch in a murine model.	(Kieffer, Piccolo*, et al.*, 2016)
LC-MS method was used to know the effects of a high-fat diet on rat liver.	(Boyce *et al.*, 2020)
Partial least squares-discriminant analysis, GC-MS, and ultraperformance LC-QTOF-MS were used to analyze the effects of high-fat on mice.	(Kim *et al.*, 2011)
GC-MS was used to know the effects of high fiber on NAFLD subjects	(Stachowska *et al.*, 2022)
UHPLC-Q-TOF/MS method was used to understand the effects of high fat in mice.	(Cai *et al.*, 2021)

REVIEW OF LITERATURE

After a literature survey, it has been found that diet and liver function are closely related in terms of, physiology, morphology, metabolic alterations, and disease pathogenesis. Our daily diet includes carbohydrates, proteins, fats, fibers, and salt. Diet influences the genetic expression of the host and metabolites in the body that directly or indirectly alter liver function (Figure 3). Various shreds of evidence have shown the effects of dietary stress on liver function but only a few studies have been conducted that are based on diet-induced alteration in the liver and related metabolites. Five dietary stresses, i.e., high-carbohydrate, high-fat, high-protein, high-fiber, and high-salt diet, will be used to know the effects on the liver and its related metabolites. So, the related literature has been reviewed and key observations from each study have been collected.

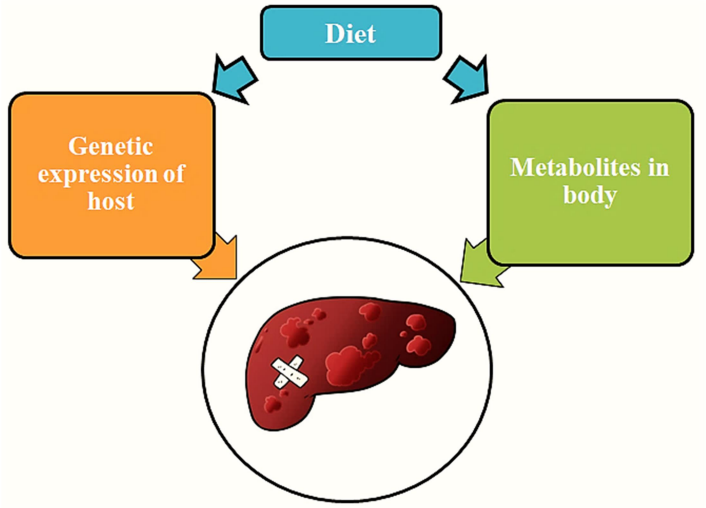

Figure 3: Diet-induced alterations in liver function; Diet alters gene expression patterns and metabolites in the body directly or indirectly, which in turn affects various metabolic processes and functions of organs including the liver.

A. High-carbohydrate diet-induced alterations in liver

Consumption of simple sugars like glucose, galactose, fructose, etc. can cause obesity, weight gain, and diabetes (Pitsavos *et al.*, 2006). It is also responsible for hyperglycemia (Chandrasekaran

et al., 2010), insulin resistance, inflammation (Panahi *et al.*, 2018), and diabetic liver disease (Chen *et al.*, 2013). Chronic liver disease can be induced by diabetes (NAFLD) or developed by diabetes (diabetic hepatosclerosis and glycogenic hepatopathy) or occur at the same time with diabetes (autoimmune biliary disease and chronic active autoimmune hepatitis) (described in Figure 4). About 50 to 90 percent of diabetics have NAFLD. Diabetes may accelerate the development of cirrhosis, severe fibrosis, hepatocellular cancer, and NAFLD into NASH (Hamed *et al.*, 2018).

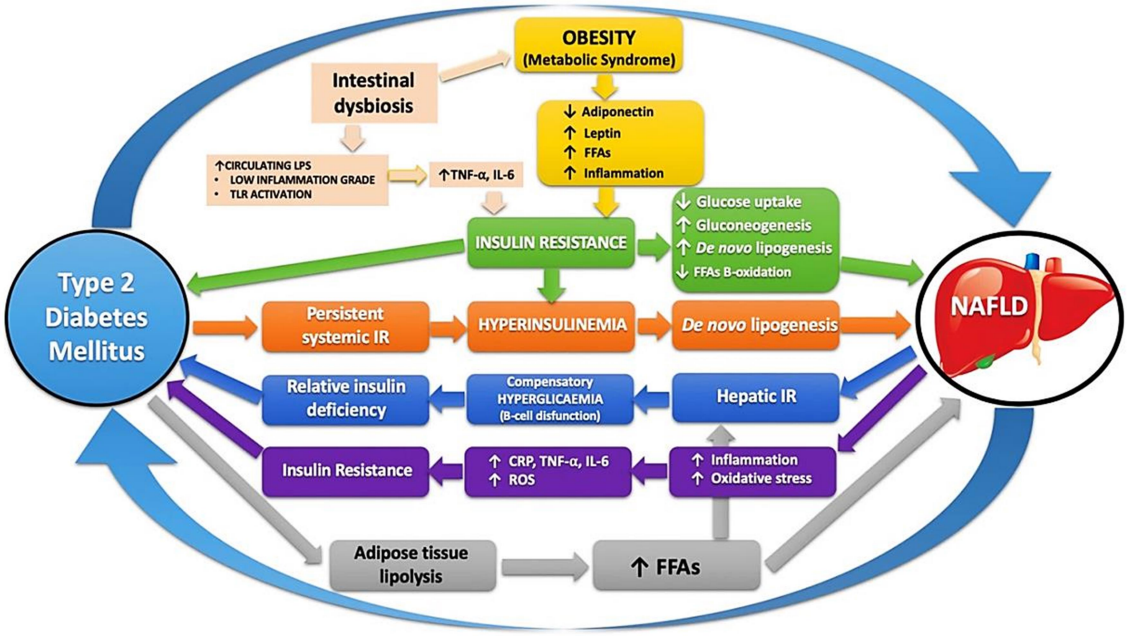

Figure 4: Diagrammatic representation of the relation between diabetes and NAFLD; Diabetes and NAFLD show bi-directional inter-relation. Both can occur due to each other or simultaneously. TNF-α: tumor necrosis factor-α, IL-6: interleukin-6, FFAs: free fatty acids, ROS: reactive oxygen species, CRP: C-reactive protein, LPS: lipopolysaccharides, TLR: toll-like receptor, IR: insulin resistance, (Acierno *et al.*, 2020)

Glucose is taken up by the liver from the gut via the portal vein and enters into glycolysis. This can help in the production of glycogen or can be directed towards the pentose phosphate pathway to

yield NADPH. Furthermore, in a fasted state, glucose is produced by glycolysis intermediate in the endoplasmic reticulum. Pyruvate (end product of glycolysis) is used to produce ATP via the TCA cycle and oxidative phosphorylation. Also, pyruvate can act as a precursor for lipogenesis (Rui, 2014). It has been seen that, even at reduced BMIs, type 2 diabetes is prevalent among South Asians. This could be due to increased visceral adiposity which further increases the risk of insulin resistance (Narayan & Kanaya, 2020). It was also observed that diabetes cases in Australia were substantially lower and extremely uncommon in the Philippines (Johnson *et al.*, 2009).

In comparison to a normal diet, excess glucose intake can develop a diabetic liver condition. Chen *et al.* used Chang liver cells to validate the effects of high glucose on the liver and found alterations in protein expression. At 25 mM glucose treatment, down-regulation of calcium signaling regulatory protein and up-regulation of glycolysis, protein degradation, cytoskeleton regulation, protein folding, mitosis, heat-shock proteins, redox regulation, and vesicle transport was seen (Chen *et al.*, 2013). Chandrasekaran *et al.* used HepG2 cells to study the effects of high glucose and found low survival rates after incubation of cells with 50 or 72 mM glucose concentrations. After long exposure, changes in cell morphology were also seen (Chandrasekaran *et al.*, 2010). Furthermore, excess monosaccharides can alter proteins at amino groups. These modified proteins are called glycated proteins and the process is called glycoxidation. This causes – the activation of protein kinases, oxidative stress, and the development of proinflammatory conditions in cells (Chen *et al.*, 2013). It was validated that high glucose in HepG2 cells tends to increase translation of IL-6, and TNF-α, and encourage the production of ROS. This leads to inflammation and triggers MAPKs and NF-κB associated signaling (Panahi *et al.*, 2018). High glucose or glucose/fructose mixture (10.5 mM) alters acylcarnitines formation leading to lower β-oxidation of fat in mitochondria. Fructose bypasses the regulatory step in glycolysis and leads to –

elevated glycolysis metabolites, increased lipid production, induced esterification of fatty acids, low concentrations of carnitine palmitoyltransferase 1, and less lipid oxidation in the liver (Meissen *et al.*, 2015).

Human apolipoprotein A-II gene activity was upregulated in HepG2 cells cultivated at high glucose concentrations. This can cause elevation of triglycerides and glucose resistance. A key enzyme in the regulation of cellular energy homeostasis, 5′AMP-activated protein kinase, is also inhibited by high glucose levels in HepG2 cells (Chen *et al.*, 2013) (Chandrasekaran *et al.*, 2010). Elevated hepatic lipase production was seen in HepG2 cells treated with high glucose due to enhancement in upstream stimulatory elements 1 and 2 and this causes dyslipidemia. High glucose is associated with insulin receptor substrate-1 phosphorylation resulting in the inhibition of insulin signaling. Also, the absorption of cholesterol was decreased in high glucose-treated HepG2 cells (Chandrasekaran *et al.*, 2010). Hyperglycemia is linked to decreased Akt activity producing insulin-tolerance state and production of ROS which alter lipids, proteins, and DNA. Earlier it was observed that high glucose increases the translation of peroxiredoxin-1 and peptidyl-prolyl cis-trans isomerase A (a potential marker for inflammation) (Chen *et al.*, 2013). This also leads to alterations in triglyceride, glucose, and bile acid metabolism and may cause NAFLD due to fat accumulation in the liver (Chandrasekaran *et al.*, 2010).

According to Wehmeyer *et al.*, subjects with NAFLD consumed considerably more glucose per 1000 calories than healthy controls. In other studies, it was demonstrated that high carbohydrate intake was related to the development of NASH. In contrast, the occurrence of NAFLD was inversely correlated with total carbohydrate intake in the Rotterdam trial. Likewise, Rietman *et al*. discovered that consumption of monosaccharides and disaccharides was negatively related to

NAFLD, but that consumption of soft drinks was related to NAFLD (Perdomo *et al.*, 2019). It has been recorded that fructose intake can promote lipid production and abdominal fat and reduces insulin sensitivity in humans who are overweight or obese. After 10 weeks of glucose consumption, triglyceride concentrations elevated in individuals, and post-prandial post-heparin lipoprotein lipase function appeared to surge (Stanhope *et al.*, 2009).

B. High-fat diet-induced alterations in liver

Following a meal, the majority of dietary fat is broken down in the small intestine and transported into enterocytes, where triacylglyceride is formed (from fatty acids) and released as chylomicrons into the gut lymphatic system. Chylomicrons enter the liver through the bloodstream and produce non-esterified fatty acids through a process called lipolysis that is mostly mediated by the enzyme lipoprotein lipase (LPL). Fatty acids may combine with cholesterol to yield cholesterol esters that are reserved in hepatocytes as lipid droplets or may circulate in the blood as VLDL molecules (Rui, 2014). Basic fat metabolism in the liver is described in Figure 5.

Increased alterations in levels of lipids in blood can cause hyperglycemia (Kim *et al.*, 2011), hypercholesterolemia and hyperlipidemia, and NAFLD (Cai *et al.*, 2021)**.** Saturated lipids cause dyslipidemias, hypertension, atherogenesis, and metabolic syndrome in the body (Pitsavos *et al.*, 2006). Asian Americans have a lower prevalence of NAFLD and fibrosis (18%) than non-Hispanic Whites (28%). Also, the data indicate that the Western way of life may have a predominate effect on the occurrence of NAFLD in Asian Americans born in the US. The average incidence of NAFLD in Asian has been estimated at approximately 27%; however, these rates can differ by place of birth (Golabi *et al.*, 2019).

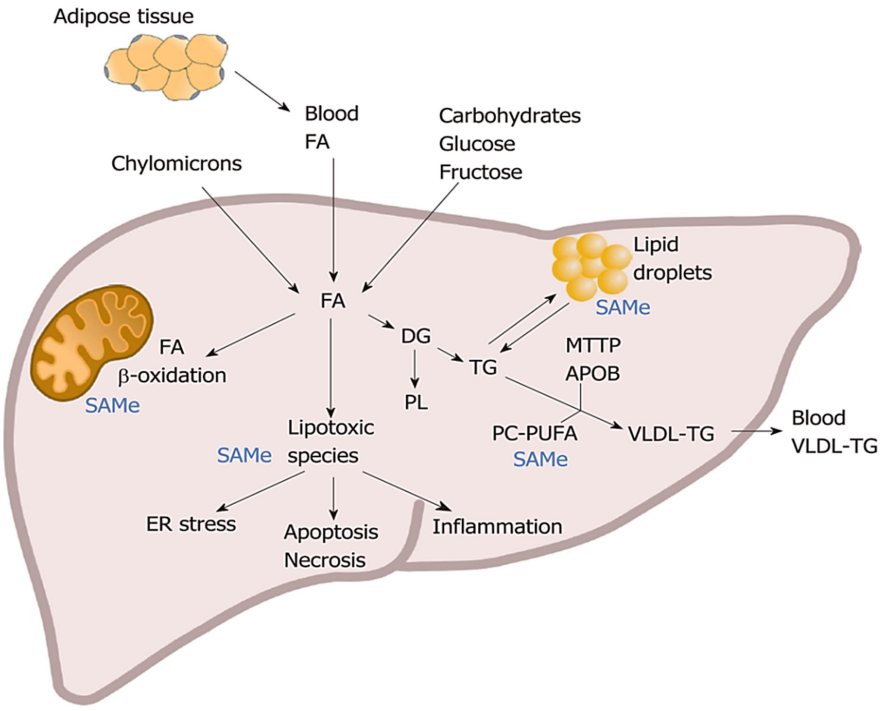

Figure 5: General fatty acid metabolism in the liver; Excess fatty acids in the liver can cause apoptosis, inflammation, and ER stress, or can be diverted towards different metabolic pathways. FA: fatty acids, DG: diglycerides, ER: endoplasmic reticulum, PL: phospholipids, TG: triglycerides, SAMe: S-adenosylmethionine, APOB: apolipoprotein B, MTTP: microsomal triglycerides transfer protein, PC-PUFA: phosphatidylcholines containing polyunsaturated fatty acids, VLDL: very low density lipo-proteins, (Mato *et al.*, 2019).

A diet rich in fat influences the host's metabolic processes and induces hepatic damage in animals by modifying the gut microbiota. Also, it induced a rise in total cholesterol, triglycerides, alanine transaminase (ALT), and aspartate aminotransferases (AST) levels in the blood and cause steatosis in the liver. Fatty acid and glycerophospholipid metabolic alterations can cause the progression of hyperlipidemia. Excessive glycerophospholipids are responsible for steatosis. Excessive choline in the liver is related to inflammation, steatosis, and NASH. Reduced phosphatidylcholines production affects the liver's ability to secrete VLDL, which promotes the development of hepatic steatosis. Elevated levels of taurochenodeoxycholic acid, as given in Table 2, may indicate

dysfunction of the liver. alpha-linolenic acid is associated with inflammation and insulin resistance reduction (Cai *et al.*, 2021).

Table 2: Effects of HFD on metabolites in liver, (Cai *et al.*, 2021).

Effects	Metabolites	Classification of metabolites
Elevation	❖ Glycerophosphocholine ❖ CDP-choline ❖ Phosphorylcholine ❖ sn-glycerol 3-phosphoethanolaminesn ❖ O-phosphoethanolamine ❖ Choline	Glycerophospholipids in liver
	❖ Oleic acid ❖ Adrenic acid ❖ Stearic acid ❖ Icosenoic acid	Unsaturated fatty acid biosynthesis in liver
	❖ Taurochenodeoxycholic acid ❖ Chenodeoxycholic acid ❖ Tauroursodeoxycholic acid	Primary bile acids biosynthesis in liver
	❖ Taurodeoxycholic acid ❖ Taurolithocholic acid	Secondary bile acids biosynthesis in liver
Depletion	❖ Phosphatidylcholines (16:0/16:0) ❖ 1-stearoyl-2-oleoyl-sn-glycerol 3-phosphocholine	Phosphatidylcholines in liver
	❖ Eicosapentaenoic acid ❖ alpha-linolenic acid ❖ Docosahexaenoic acid	Unsaturated fatty acids biosynthesis in liver
	❖ Taurine ❖ Cholic acid ❖ Taurocholic acid	Potential biomarkers for obesity

Boyce *et al*. used three different rat strains, i.e. Brown Norway, Fisher 344, and Sprague Dawley to know the effects of a high-fat diet (HFD) in NAFLD progression, and strain-specific effects of HFD are given in Table 3. It was seen that HFD given to all three strains elevates triglycerides in the blood and depletes the metabolites like serotonin, (20:4) Lyso-phosphatidylcholine, 18:1 (Omega-9) Lyso-phosphatidylcholine, and 2-hydroxydodecanimidic acid. These metabolic intermediates are implicated in insulin signaling and fat metabolism. It has been demonstrated that

serotonin controls lipid homeostasis (Boyce *et al.*, 2020). Serotonin plays a vital role in controlling weight gain, and the development of inflammatory responses (Kim *et al.*, 2011).

HFD induces the formation of metabolites involved in amino acids and carnitine metabolism. Elevated metabolites from the carnitine pathway comprise L-Palmitoylcarnitine, L-Carnitine, g-Butyrobetaine, O-oleoylcarnitine, and L-Lysine. Also, alterations in citric acid cycle metabolites and enzyme kinetics were common in all three strains. These changes can lead to gluconeogenesis in the liver, which is a potential biomarker of insulin resistance caused by diet. Up-regulation of lactate and fumarate is associated with HFD and these metabolites are linked to NAFLD and hepatic fibrosis (Boyce *et al.*, 2020).

Table 3: Strain-specific alterations in metabolites in response to HFD, (Boyce *et al.*, 2020).

Rat strains	Observations
Brown Norway	❖ Elevated levels of succinate after 4 and 12 weeks of HFD ❖ Elevated levels of lactate after HFD ❖ Elevated levels of fumarate after HFD
Fisher 344	❖ Elevated levels of fumarate after 4-weeks of HFD ❖ Elevated levels of pyruvate after 4 weeks of HFD ❖ Elevated levels of succinate after 4 and 12 weeks of HFD ❖ Elevated levels of lactate after HFD
Sprague Dawley	❖ Elevated levels of lactate after HFD after 24 weeks ❖ Elevated levels of citrate after HFD

A previous metabolic study demonstrated that HepG2 cells when treated with oleic acid can develop deficiencies in the levels of carnitine, betaine, and methionine. 7-ketodeoxycholic acid is required for balancing cholesterol levels and absorption of fats. Elevation of PCs in the liver leads to release in the blood causing its accumulation and this is related to fat accumulation. Alterations in lipid metabolites and low NAD/NADH ratio due to HFD can lead to disrupted energy

homeostasis. The decrease in betaine levels causes the buildup of transported fatty acids in fat cells. Also, the enzyme activity of carnitine palmitoyltransferase-1, involved in the β-oxidation of fatty acids dwindled. These are related to the dysfunction of peroxisome (Kim *et al.*, 2011). List of affected metabolites after HFD is given below in Table 4.

Table 4: List of metabolites affected by HFD in mice, (Kim *et al.*, 2011).

Serum		**Liver**	
Elevation	**Depletion**	**Elevation**	**Depletion**
❖ L-carnitine ❖ Stearoylcarnitine ❖ Phenylpyruvic acid ❖ Phenylacetamide ❖ Pantothenic acid ❖ Phosphatidyl-cholines ❖ 3 lysophosphatidyl-cholines ❖ Arginine ❖ Serotonin ❖ Tyrosine ❖ Valine ❖ Uric acid ❖ Pipecolic acid ❖ Benzoic acid ❖ Triglycerides ❖ Cholesterol	❖ 11 lysophosphatidyl-cholines ❖ 4 acyl-carnitines ❖ Betaine	❖ Pantothenic acid ❖ 7-ketodeoxycholic acid ❖ Phosphatidylcholines ❖ Triglycerides ❖ Cholesterol	❖ 3-metylgutaryl-carnitine ❖ Glycerol ❖ Tyrosine ❖ *trans*-palmitoleic acid ❖ Glucose ❖ L-carnitine ❖ Lysophosphatidyl-cholines ❖ Betaine ❖ Valine

After lipid profiling of the NAFLD subject, low phosphatidylcholines titers and elevated triglyceride levels were seen in the liver. Also, low levels of cholic acid were seen in the liver of NASH subjects (Cai *et al.*, 2021). Subjects with NASH consumed significantly more saturated fat and omega-6 polyunsaturated fatty acids (PUFAs) and substantially fewer PUFAs. It was observed

that significant elevation in the omega-6/omega-3 ratio is a feature of the liver in NAFLD patients (Perdomo *et al.*, 2019).

C. High-salt diet-induced alterations in liver

One of the most popular food additions both at home and in the food industry is salt. A diet rich in salt can cause oxidative stress and inflammation in the liver of rats leading to NAFLD and NASH. A high salt diet and NAFLD have a positive association, showed by recent metabolic studies (Shojaei-Zarghani *et al.*, 2022). High consumption of salt can lead to metabolic syndrome (Li *et al.*, 2021), (da Silva Ferreira *et al.*, 2023). It was also seen that sodium supplementation can lead to insulin resistance, weight gain, etc. in mice. Also, elevated levels of AST and ALT were seen after a high-salt diet (da Silva Ferreira *et al.*, 2023).

The regions with the highest sodium intake include Eastern Europe, East and Central Asia, and the Middle East. As of the 2010 survey, average salt intake was 3.95 g/day, which is double the World Health Organization's recommendation. It was also seen that men tend to consume high salt than women (8.9% less in South Asia and 10.7% less in Western Europe). Also, sodium intake was affected by age as mean intake increased by ~ 6% from age 25 to 40. East Asia showed the highest consumption of salt in all Asian regions (Powles *et al.*, 2013).

A high-salt diet can increase blood osmolality, induce polyol pathways, cause mitochondrial dysfunction, and elevation of total cholesterol (da Silva Ferreira *et al.*, 2023). It also produces fructose, due to the induction of the aldose reductase pathway (da Silva Ferreira *et al.*, 2023), (Li *et al.*, 2021) and (Shojaei-Zarghani *et al.*, 2022). When fructose is broken down, oxidative stress is triggered, resulting in fat buildup, reduced insulin responses in the liver, and resistance to leptin in

the hypothalamus. By increasing appetite and possibly lowering energy expenditure, leptin intolerance leads to hepatic steatosis (da Silva Ferreira *et al.*, 2023). Diet rich in salt increases leptin titers in blood, fat mass, and glucose degradation in adipocytes of rats. Elevation of leptin titers can inhibit insulin release (Shojaei-Zarghani *et al.*, 2022). A relation between salt induced hypertension and HCC is given in Figure 6.

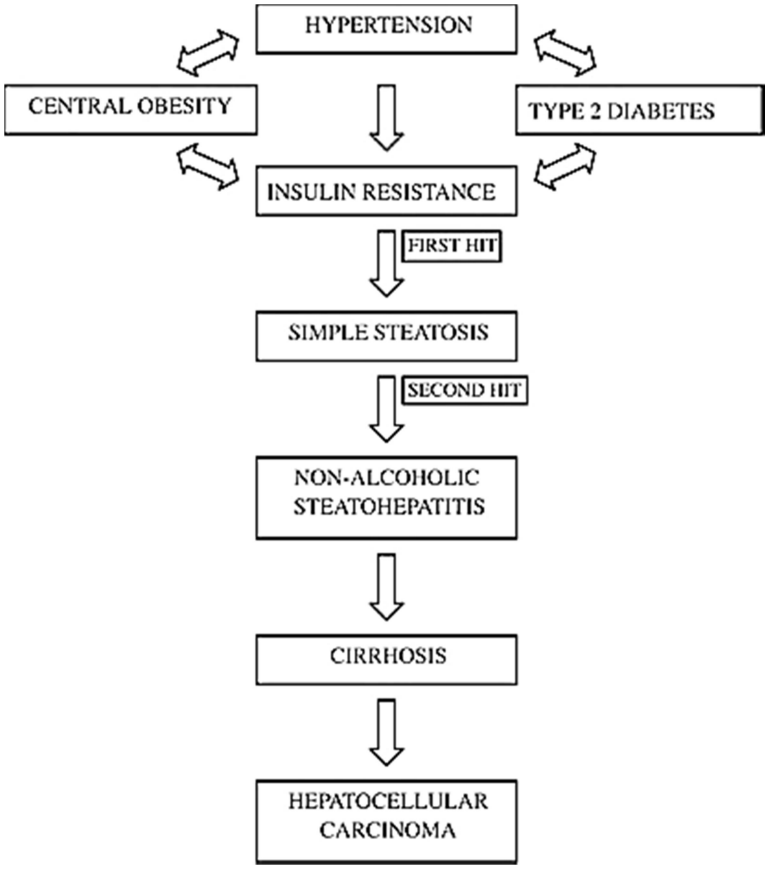

Figure 6: Flow-chart showing the relation between hypertension and NAFLD; Hypertension can cause hepatocellular carcinoma (end stage of NAFLD spectrum) directly or via diabetes or obesity, (Brookes & Cooper, 2007)

At a genetic level, high salt can cause epigenetic modifications, like elevated H3K27 acetylation. This lowers sirtuin 3 and induces inflammatory cytokine translation. Sirtuin 3 is an important deacetylase that prevents the development of ROS in mitochondria and its low expression can cause the progression of NAFLD in mice (da Silva Ferreira *et al.*, 2023). High-salt consumption in

chick causes the production of ROS and induces liver injury (Wang *et al.*, 2016). The formation of lipogenic enzymes like fatty acid synthase, acetyl CoA carboxylase, and TNF was inhibited due to high salt intake. In the research conducted by Cabrera *et al.*, the investigators hypothesized that high salt consumption reduces the production of aldosterone and mineralocorticoid receptors, thereby permitting an elevated level of salt-inducible kinase1 which inhibits the production of lipogenic enzymes, thus decreasing steatosis (da Silva Ferreira *et al.*, 2023).

Table 5: Genes affected by high-salt diet in mice, (Li *et al.*, 2021).

Up-regulation	*rad51b* gene	Involved in DNA repair
	cyp4a10 gene	Associated with the development of NAFLD
	cyp4a14 gene	Associated with the development of NAFLD
	cyp2e1 gene	Induce lipid peroxidation and oxidative stress, leading to hepatocyte injury
Suppression	*cyp17a1* gene	Inducing steroid hormone production
	cyp2a4 gene	Induces numerous substances and chemicals metabolism and degradation
	nr4a1 gene	Involved in apoptosis and cell proliferation

It was previously investigated that the biochemical indices for regular and high-salt-consuming mice did not differ significantly. Also, H&E staining revealed no physiological shifts in the liver, but the primary vein of the liver lobule was swollen (Li *et al.*, 2021). The hepatic cords in the high salt-treated livers were organized haphazardly and loosely. In addition, several hepatocytes had a balloon-like morphology and contained more collagen fibers (Wang *et al.*, 2016). This indicates that no physical injury in the liver. *cyp4a10* and *cyp4a14* genes develop NAFLD, as these are associated with oxidative stress, peroxisome proliferator-activated receptors signaling, and lipid peroxidation. Also, the cellular production of ROS-activating protein and NADPH oxidase 4 was enhanced. High-salt diet suppresses the *cyp1a2* gene in rats and mice (as

given in Table 5) which indicates the onset of NAFLD. It has been demonstrated that high-salt elevates osmotic pressure in the liver and induces the production of the TonEBP transcription factor. Cyp4a protein from the *cyp4a* gene converts arachidonic acid to 20-hydroxyeicosapentaenoic acid which causes hypertension (Li *et al.*, 2021).

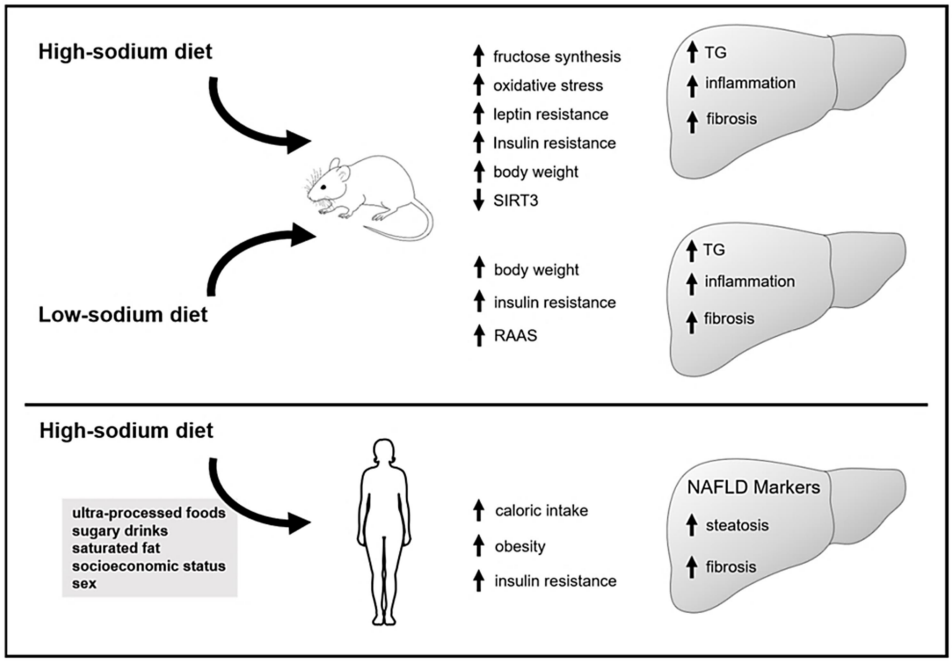

Figure 7: Effects of altered salt diet on mice and humans; High salt diet can increase fibrosis in both humans and mice. TG: triglycerides, RAAS: renin- angiotensin-aldosterone system, SIRT3: sirtuin 3, (da Silva Ferreira *et al.*, 2023).

It was also seen that high-salt expression led to high expression of desmin (causing liver fibrosis) and lead to the hepatic cords that are organized erratically, and hepatocytes that appear foamy and have less cell density. The high-salt diet also affects cell proliferation, and growth, and led to lipid buildup by disturbing the transport of lipoprotein. It was seen that high salt in hepatocytes of mice negatively affects kelch-like ECH-associated protein 1 and positively affects nuclear factor erythroid 2-related factor 2 expression. When chick embryo was exposed to high salt, disrupted glycogen production and increased apoptosis were seen (Wang *et al.*, 2016). A high-salt diet is

directly co-related to C-reactive protein and TNF-α in blood. It also elevates the levels of trimethylamine N-oxide (a metabolite of betaine, choline, and carnitine) in the blood and causes intestinal dysbiosis in rats after 2 weeks of high-salt treatment. Trimethylamine N-oxide disturbs the signaling of the farnesoid X receptor in the liver which causes the development of steatosis. The high salt disturbs the renin-angiotensin system (RAS) and renin biosynthesis, as given in Figure 7, and induces the activity of mineralocorticoid receptors. The pathophysiology of NAFLD is influenced by the stimulation of RAS and mineralocorticoid receptors, which are connected to oxidative damage and inflammation. RAS suppression may also stop the onset and progression of NAFLD (Shojaei-Zarghani *et al.*, 2022).

But RAS inhibition by salt was seen to be least in NAFLD subjects. So, RAS activity is not affected by high salt in these subjects (Shojaei-Zarghani *et al.*, 2022). According to Shojaei-Zarghani *et al.*, high-sodium consumption will increase the chances of NAFLD by 60% in human subjects (da Silva Ferreira *et al.*, 2023), (Shojaei-Zarghani *et al.*, 2022). It has been found that 50% of hypertensive non-obese subjects have hyperinsulinaemia. In a study by Ramsay, it has been observed that tests for liver function were impaired in 15% of male hypertension patients. Fatty liver was more common in hypertensive patients (Brookes & Cooper, 2007).

D. High-protein diet-induced alterations in liver

The liver, kidney, and small intestine help in amino acid degradation. Due to their numerous metabolic entry locations, amino acids are essential to numerous biological processes. These can produce glucose, urea, fatty acids, ketone bodies, ammonia, and polyamines (De Chiara *et al.*, 2019). Nutritional studies indicate that we require a small quantity of protein for optimal health. For obese individuals as well as people with kidney disease, a higher protein consumption may be

harmful (Pitsavos *et al.*, 2006). High-protein can affect kidneys and bones negatively. It tends to produce acids in the body, which can lead to hypercalciuria, loss of bone mass, and kidney stones. Also, animal protein consumption in high amounts can cause hyperuricosuria, as it is a nutritional carrier of purines (uric acid precursor). High-meat diet (rich in proteins) can induce the development of prostrate, breast, and bowel cancers. In addition, it can cause hyperalbuminemia, liver dysfunction, elevated transaminases, and coronary artery disease (Delimaris, 2013).

About the EAT-Lancet standard diet, the average calorie consumption from plant-based and animal-based products, high in protein, is low in various regions of India. Low-calorie consumption from protein-rich foods is prevalent across every sector, area, and income category in India. In rural areas, only 6 percent of total calorie consumption comes from protein-rich foods, compared to 29 percent according to the EAT-Lancet diet. Even for the wealthiest 5% of India's population, protein-derived calories account for less than 50% of the 726 kcal in the standard diet. In Indian diets, legumes are the primary provider of non-cereal plant-based protein. In India, dairy goods are the most prevalent sources of animal protein (Sharma *et al.*, 2020).

High protein diets can act as a possible weight loss treatment. It was observed that tryptophan can form serotonin (an anorexigenic neurotransmitter) and develop a satiated state in the body. Satiety due to a high-protein diet could be developed due to – the formation of anorexigenic factors, huge energy usage, and unregulated gluconeogenesis. Titers of amino acids in the body tend to increase and gluconeogenesis in the liver is induced due to high-protein consumption, as given in Figure 8. Rats on a high-protein diet exhibit upregulation of the glucose-6-phosphatase and PEPCK, two essential gluconeogenesis enzymes. Also, researchers found that high-protein intake can induce the formation of ketone bodies (specifically β-hydroxybutyrate). High-protein diets can – negatively affect the formation of adipose tissue and positively affect triglycerides, lipids, and total

cholesterol. Consumption of aromatic amino acids (AAAs) and branched-chain amino acids (BCAAs) can cause metabolic syndrome (Pesta & Samuel, 2014). But a vegetable protein diet with low carbohydrates has the greatest impact on halting the onset and development of metabolic diseases. (De Chiara *et al.*, 2019).

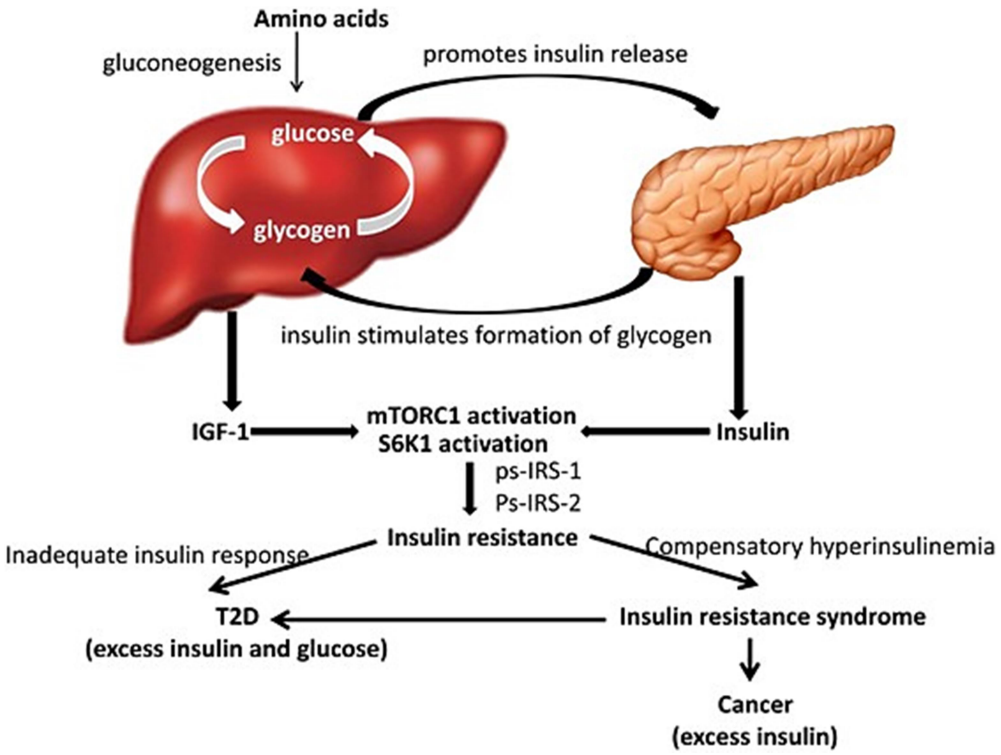

Figure 8: Relation between amino acids, liver, and pancreas; Amino acid induces gluconeogenesis which promotes insulin release and glycogen formation. Increased insulin release can cause insulin resistance which can later induce diabetes and cancer. T2D: type 2 diabetes, IRS: insulin receptor substrate, IGF-1: insulin-like growth factor 1, mTORC1: mammalian target of rapamycin complex 1, S6K1: ribosomal protein S6 kinase β1 (Bi & Henry, 2017)

BCAAs degenerate into metabolites - succinyl-CoA and propionyl-CoA, which get accumulated in the body. This affects fatty acid oxidation by reducing citrate synthase activity leading to the accumulation of acylcarnitines. This causes mitochondrial dysfunction, altered glucose metabolism, and disrupted insulin signaling (Pesta & Samuel, 2014). BCAAs help in the movement of glucose from the liver and induce insulin release. Additionally, BCAAs intake could

minimize the chances of HCC progress and increases endurance. Also, it acts as a potential anti-tumor in subjects with HCC (De Chiara *et al.*, 2019). High protein consumption leads to liver dysfunction and elevated titers of ammonia (by ~59%). In SH-SY5Y differentiated cells, reduced viability was seen after 90 μM ammonium chloride treatment. This suggested that high ammonia (due to a high protein diet) is harmful for cells. Hepatic encephalopathy can develop due to high protein consumption. Also, retinoic acid-associated differentiation method can be employed to promote generation of ROS in SH-SY5Y differentiated cells and this can lead to the cells more sensitive to the toxicity of ammonia. High protein diets are linked to shorter lifespan, according to murine studies (Griffin & Bradshaw, 2019).

The development of NAFLD due to high protein intake will depend on the type of proteins in a diet. Vegetable proteins tend to decrease NAFLD progression but animal protein showed direct relation with NAFLD. According to previous animal studies, taurine (bile acid conjugate and amino acid) can help lower inflammation, insulin levels, steatosis, and triglycerides, and improve liver health. So, it can act as a potential therapy for NAFLD (Perdomo *et al.*, 2019). In another study, it was observed that diets focusing on high protein had the best success rate for reversing NAFLD. This diet includes vegetable protein with reduced sugars and carbohydrates. It was found that a vegetable protein diet enhances glucose levels in the blood of cirrhosis patient with diabetes and overall help in curing hepatic encephalopathy and boosting nitrogen metabolism. In other experiments, it was found that a soy diet decreases the levels of alanine aminotransferase in NAFLD patients. A diet with high BCAAs and reduced AAAs and methionine; ameliorate the health of those with cirrhosis (De Chiara *et al.*, 2019).

In an experiment, subjects were given a diet rich in animal protein or a diet rich in vegetable protein without a limitation on calories. The macronutrient ratio in both diets was the same (30% protein, 40% carbs, and 30% fat). After six weeks, indicators of hepatic necrosis, insulin resistance, and intrahepatic lipid content, all decreased (Perdomo *et al.*, 2019). In addition, individuals on a 6-week low-carbohydrate, high-protein diet had low calcium balance, elevated urinary calcium levels, and reduced serum osteocalcin concentrations. A higher intake of vegetable protein and a lower intake of animal protein may reduce bone loss and decrease the likelihood of hip fracture. It was also found that people eating lamb, pork, or beef, at least five times a week had a greater risk of developing colon cancer (Delimaris, 2013).

E. High-fiber diet-induced alterations in liver

Various types of indigestible carbohydrates are referred to as "dietary fiber". Fiber can be of 2 types: first is dietary fiber (DF) which is non-digestible lignin and carbohydrates present in plants and second are functional fibers comprising non-digestible carbohydrates which possess favorable physiological impacts on humans (Kieffer, Martin*, et al.*, 2016). Intestinal bacteria ferment DF, resulting in the formation of short-chain fatty acids (SCFAs). In addition to lowering endogenous cholesterol synthesis and fat storage, SCFA can modulate several systems involved in lipid and glucose metabolism (Maciejewska-Markiewicz *et al.*, 2022). High-fiber diets cure multiple diseases like diabetes, heart disease, hypertension, obesity, and colon cancer (Pitsavos *et al.*, 2006).

The fermentation of DF by intestinal microbiota causes the synthesis of SCFAs. SCFA can regulate multiple reactions associated with carbohydrate and fatty acid metabolism and decrease endogenous cholesterol synthesis and fat storage (Maciejewska-Markiewicz *et al.*, 2022). DF can

also change the microbes in the gut and frequently enhances the metabolic profile of the host, like increasing insulin sensitivity (Kieffer, Piccolo*, et al.*, 2016). Intake of insufficient fiber is typically associated with NAFLD and NASH. Fiber intake may help in decreasing hepatic steatosis and body fat in rodents (Perdomo *et al.*, 2019). DF derivatives like acetic acid, propionic acid, and butyric acid are the primary byproducts of saccharolytic fermentation. SCFAs nourish intestinal cells, activate goblet cells to generate an adequate amount of mucus, regulate tight junctions, and preserve the functioning of the intestinal wall (Stachowska *et al.*, 2022) by enhancing the differentiation and proliferation of gut cells. DFs also induce the production of goblet cells. Mucus helps in maintaining the gut barrier and restricts the transportation of LPS from the gut (Kieffer, Martin*, et al.*, 2016). The decreased barrier function is associated with the transport of LPS into the body causing "leaky gut syndrome" which causes inflammation. So, propionate or butyrate (SCFAs) from a fiber diet can reduce inflammation, maintain tight junction, and gut barrier, and reduce the chances of NAFLD (Stachowska *et al.*, 2022). DFs reduce the transport of LPS and other pro-inflammatory compounds from the gut leading to the least chances of NAFLD and NASH (Kieffer, Martin*, et al.*, 2016).

Using cell line models, it was demonstrated that butyrate feeding can cause low oxygen leading to Hif-1α transcription factor stability. This factor is present in the gut barrier and controls apoptosis and inflammation. Also, it enhances the activity of detoxification and antioxidant enzymes that could prevent the development of NASH from fatty liver. In an experiment using rats on a fiber diet, low titers of triglycerides were seen in the liver and decreased expression of unique genes associated with inflammation, fibrosis, and lipid metabolic processes was seen at a genetic level. Inulin treatment decreased the expression of decorin and connective tissue growth regulator that is

linked to fibrosis (Kieffer, Martin, *et al.*, 2016). Effects of high diet in humans are given in Figure 9.

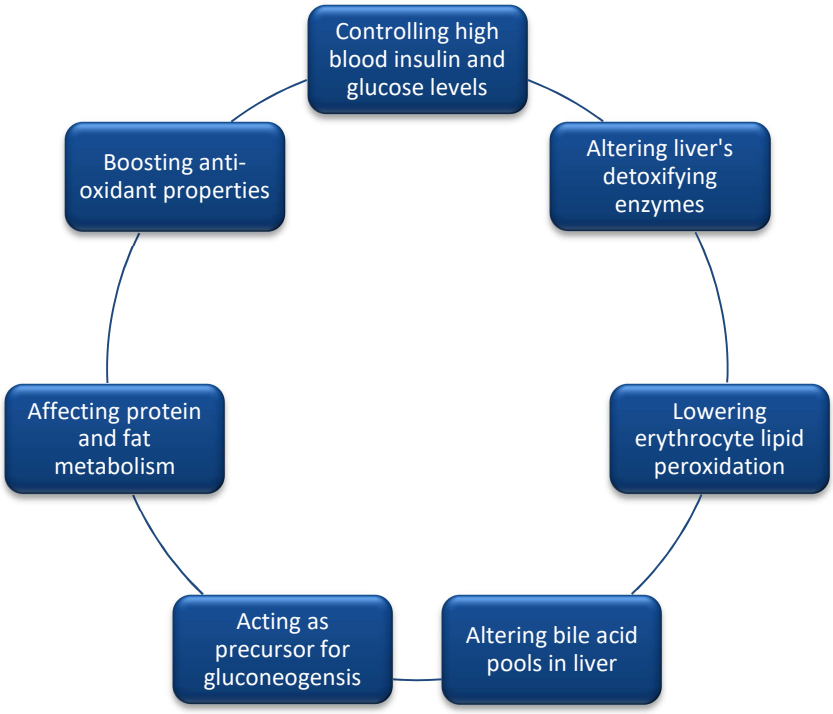

Figure 9: Effects of high fiber diets in humans; Fiber tends to show beneficial effects on the body. Majority of the effects are given in the picture, (Kieffer, Martin, *et al.*, 2016).

A further investigation that supplemented nonfermentable viscous DF hydroxypropyl-methylcellulose to high fat-fed mice discovered a reduction in hepatic lipid levels as well as modified expression of liver genes associated with glucocorticoid metabolism, estrogen hormone production, steroid metabolism, androgen hormone production and, oxidative stress, and methylation reduction. Decreased levels of amino acids in the liver were seen after high-amylose-maize-resistant starch type 2 (HAMRS-2) supplementation in mice. Also, alterations in nitrogen metabolism were seen after DF supplementation, as given in Table 6 (Kieffer, Martin, *et al.*, 2016). In mice given HAMRS2, numerous cytochrome P450 enzymes associated with drug/xenobiotic

and fat metabolism were elevated. Transforming growth factor-β, Jak-STAT, and Wnt signaling pathways were all impacted by HAMRS2 supplementation (Kieffer, Piccolo*, et al.*, 2016).

Table 6: Effects of HAMRS2 diet on metabolites in mice, (Kieffer, Piccolo*, et al.*, 2016).

Elevation	❖ Cholesterol output ❖ Glycolysis ❖ Lipid oxidation	General metabolism in mice
	❖ Sorbitol ❖ 2-deoxyerythritiol	Sugar alcohols
	❖ Glutamine	Amino acid
	❖ Capric acid ❖ Pelargonic acid	Fatty acids
	❖ β-hydroxybutyrate	Ketone body
Depletion	❖ Lipogenesis ❖ Amino acid metabolism	General metabolism in mice
	❖ 1,5-anhydroglucitol ❖ Myo-inositol ❖ Ribitol ❖ Xylitol	Sugar alcohols
	❖ Aspartic acid	Amino acid
	❖ Urea ❖ Creatinine ❖ Ornithine ❖ Purine-related metabolites	Nitrogenous metabolites
	❖ Fumaric acid ❖ Pyruvic acid ❖ Malic acid	Ketoacids
	❖ Maltose ❖ Glucose ❖ Maltotriose	Sugars
	❖ Palmitic acid ❖ Palmitoleic acid ❖ Oleic acid ❖ Arachidonic acid ❖ Linoleic acid	Lipid metabolites (fatty acids)

Metabolic studies evidenced the improvement of liver-associated biomarkers after a high-fiber diet (10-12 weeks). These biomarkers include AST, ALT, and insulin resistance index. The introduction of fiber in the daily diet decreased the amounts of choline and proline in the blood. Reduced choline is harmful to the liver as it forms phosphatidylcholine, used for VLDL

production. This causes the development of the fatty liver. Proline act as an indicator of fatty liver development and its deficiency after a fiber diet indicates the curing of liver disease (Stachowska *et al.*, 2022). Other surprising results proved that mice fed enzyme-treated wheat bran (ETWB) had dramatically different metabolic and gene activity patterns in their livers, which somewhat resembled fasting conditions. For instance, ETWB-fed animals showed up-regulation of phosphoenolpyruvate carboxykinase 1, the speed-limiting enzyme for gluconeogenesis, which is also elevated during fasting. Mice administered with ETWB also had higher blood and liver amounts for the ketone body β-hydroxybutyrate (Kieffer, Martin*, et al.*, 2016).

Animal studies revealed that DF standardized the formation of sterol regulatory element-binding protein 1 (SREBP1) and this regulates triglyceride and fatty acids production which induces the production of oleic acid, stearic acid, palmitoleic acid, and palmitic acid. These alterations are induced by cholesterol and insulin which stimulate steatosis in the liver. Recent investigations have demonstrated that the consumption of SCFAs tends to inhibit the production of SREBP-1C and fatty acid synthase (an enzyme involved in de novo lipogenesis) in the hepatic system (Maciejewska-Markiewicz *et al.*, 2022).

Oligo-fructose (dietary fiber in vegetables) showed positive changes in lipid and glucose metabolism and a decrease in body weight in humans after 12 weeks of supplementation. Also, better insulin and aminotransferase titers were observed in the blood (Perdomo *et al.*, 2019). Consuming fiber lowers hunger and eating frequency by indirectly controlling the orexigenic hormone ghrelin. Loss of weight and NAFLD regression are associated with adequate fiber consumption and a low-energy diet. The amount of hepatic steatosis among individuals who consumed high fiber was dramatically reduced. Also, the amount of polyunsaturated and monounsaturated fatty acids (oleic acid and palmitoleic acid) increased while saturated fatty acids

(stearic acid and palmitic acid) significantly decreased. High fiber diet tends to decrease total cholesterol, LDL, AST, ALT, and insulin and increase δ-linolenic acid, HDL, and docosahexaenoic acid (DHA). This may suggest a decrease in cyclooxygenase-2 activity in NAFLD subjects (Maciejewska-Markiewicz *et al.*, 2022).

The effects of various diets on liver and NAFLD progression are given in Figure 10 and biomarkers associated with liver diseases are provided in Table 7.

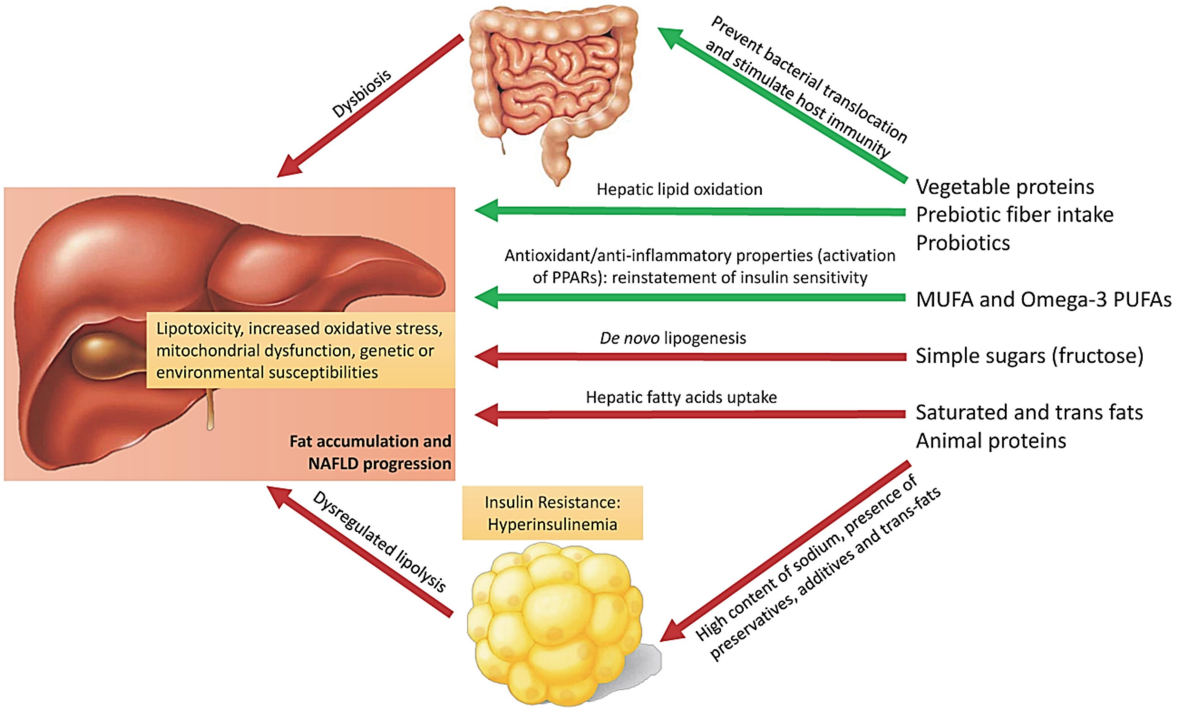

Figure 10: Effects of various diets on NAFLD progression; Various types of diets include simple sugars, vegetable proteins, fiber, trans fat, etc. They tend to have negative or positive effects on the liver as described above. PPARs: peroxisome proliferator-activated receptor, MUFA: monounsaturated fatty acids, PUFA: polyunsaturated fatty acids, (Perdomo *et al.*, 2019).

Table 7: Biomarkers related to liver diseases

Biomarkers description	References
❖ Although invasive, liver sampling is the most effective diagnostic method for NAFLD. Alanine aminotransferase and aspartate aminotransferase are blood-based biomarkers that are typically used to screen for and diagnose this condition.	(Shojaei-Zarghani *et al.*, 2022)
❖ Liver biopsy acts as the gold standard for diagnosis of NAFLD and NASH. But elevated de novo lipogenesis in NAFLD patients generates metabolic signals and indicates the pathogenesis of the disease. ❖ Also, in a subpopulation of NAFLD patients, *S*-Adenosyl methionine (SAMe) scarcity may be a key initiator of NASH.	(Mato *et al.*, 2019)
❖ An increase in omega-6/omega-3 ratio defines the NAFLD subjects' liver	(Perdomo *et al.*, 2019)
❖ Increased levels of vimentin, triosephosphate isomerase, retinoic acid receptor, glutathione S-transferase P, aldose reductase, syntenin-1, phosphoglycerate kinase 1, and galectin-3 act as a potential biomarker for diabetic liver disease	(Chen *et al.*, 2013)
❖ BCAAs and lysophophatidylcholines act as potential markers for obesity. ❖ Also, elevated primary bile acid amounts were present in NAFLD patients.	(Cai *et al.*, 2021)
❖ The branched-chain amino acids/aromatic amino acids ratio acts as a potential diagnostic marker for evaluating the extent of liver disease and liver disorder.	(De Chiara *et al.*, 2019)
❖ Alterations in glycine and glutamate levels can indicate the extent of liver fibrosis.	(Stachowska *et al.*, 2022)
❖ Elevated levels of docosapentaenoic acid (DPA), eicosapentaenoic acid (EPA), and DHA, and a reduction in palmitoleic acid levels are associated with a decrease in liver steatosis. ❖ DPA, DHA, EPA, vaccenic acid, and oleic acid act as potential biomarkers for liver fat accumulation ❖ High levels of inflammatory cytokines, 13-hydroxyloctadecadienoic acids, and 9-hydroxyloctadecadienoic acids are the most effective indicators of the advancement of steatosis.	(Maciejewska-Markiewicz *et al.*, 2022)
❖ L-carnitine, 7-ketodeoxycholic acid, Lysophosphatidylcholines, and betaine act as biomarker metabolites that distinguish HFD mice from control. ❖ Fatty acids, lysophosphatidylcholines, and BCAAs proved to be potential indicators of obesity and related disorders.	(Kim *et al.*, 2011)

RESEARCH GAP

Various pieces of evidence are based on the overall physiological effects of dietary stress on the liver. Also, it is well-known how dietary stress alters gene expression and signaling pathways for a specific liver function. But the effects of these dietary stresses on liver metabolites and overall metabolome remain critically unexplored. The relationship between dietary stress and liver metabolome and metabolites is yet to be developed. Diet-induced shifts in metabolites will not only provide information regarding the effects of daily diet on the liver but it may also lead to the identification of metabolite-based disease markers associated with diet and chronic metabolic disease. These disease markers can act as potential biomarkers for diagnosis of chronic liver diseases and later these biomarkers can be used to develop early predictive models that can be used to foretell the type of chronic liver disease and the dietary stress which resulted in it.

RESEARCH SIGNIFICANCE

a) Information regarding potential disease biomarkers associated with diet.

The results will indicate the disease-specific and diet-specific metabolites and the relationship between these metabolites can be inferred using pathway enrichment by various databases.

b) Early predictive models can be developed for diet-induced liver diseases.

Once a relationship between disease-specific and diet-specific metabolites is inferred, it will be easy to develop a predictive model for early diagnosis of liver diseases.

OBJECTIVES

The effects of high concentrations of each diet will be evaluated using human hepatoma (liver tumor) cells, (in this study, HepG2 cells), in which various chemicals will be used to mimic the dietary stress, and untargeted metabolome analysis will be done to understand the changes in metabolites caused by various dietary stress. The key objectives of the study include –

1. To identify the nutritional stress tolerance capacity of HepG2 cells by identifying lethal doses of selected nutrients.
2. To identify the metabolomic signatures of HepG2 cells under sub-lethal doses of selected nutrients.
3. To map the identified metabolites for pathway enrichments using HMDB and KEGG pathways.

MATERIALS AND METHODS

A. HepG2 cell culture (Biosafety Approval no. TIET/IBSC/23-24/03)

The human hepatocellular carcinoma, HepG2 cells (Figure 11.2) were obtained from National Center for Cell Science (NCCS), Pune, at passage no. 23. Cells were maintained using Minimum Essential Medium Eagle (MEM) (HiMedia, India) incorporated with 10% (v/v) Fetal Bovine Serum (HiMedia, India), 1% (v/v) Penstrep (HiMedia, India) and 0.5% (v/v) Amphotericin B (HiMedia). Cells were incubated at 37˚C, 5% CO_2, and 5% humidity. The growth of cells was regularly supervised using an inverted microscope (Nikon). After 70-80% confluency, the cells were subcultured into new T-flasks, and further growth was monitored.

Figure 11.1: HepG2 cell vial from NCCS, Pune

Figure 11.2: Cells under inverted microscope at 40X

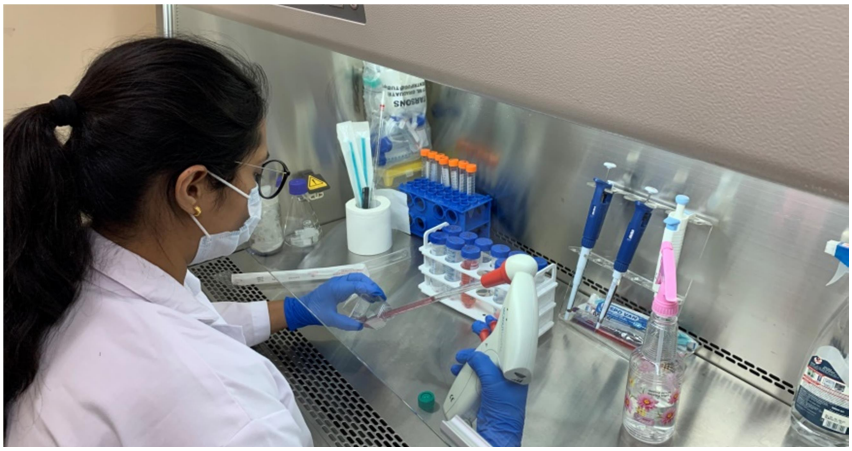

Figure 12: Performing cell culture

B. Cytotoxicity assay (MTT assay)

Different concentrations of stock and working solutions were made to test the cytotoxic effects of different dietary compounds (glucose, palmitic acid, NaCl, BSA, and butyrate) on HepG2 cells, as shown in Table 8 below.

Table 8: Range of concentrations of different treatments for MTT assay

Treatment	Concentration
Carbohydrate (glucose)	0-320 mM
Fat (palmitic acid)	0-1600 µM
Salt (NaCl)	0-800 mM
Protein (BSA)	0-40 mM
Fiber (sodium butyrate)	0-80 mM

HepG2 cell suspension of concentration $1X10^6$ cells/ml was made in MEM and 250 µl of cell suspension was seeded in a flat-bottom micro-well plate (as in Figure 13) and later incubated at 37˚C, 5% CO_2, and 5% humidity for 24-48 hours for cell attachment and attaining ~80% confluency. After this, the media was removed from wells and different concentrations of dietary compound solutions (100 µl) were added in each seeded wells in triplicates and incubated for 24 hours at 37˚C, 5% CO_2, and 5% humidity in an incubator.

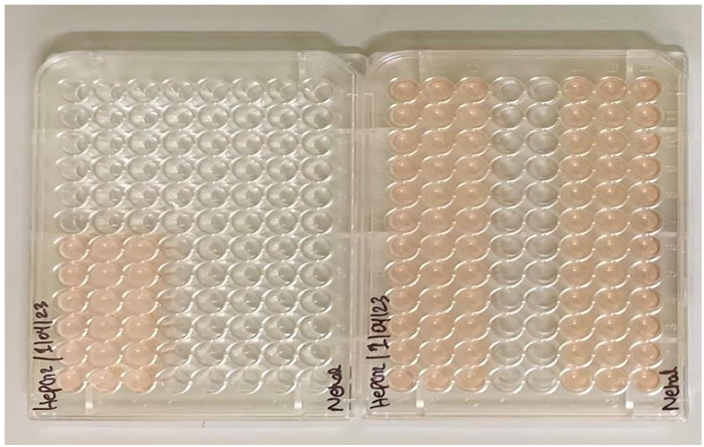

Figure 13: Cell seeded in flat-bottom micro-well plate

Next, the MTT cell viability test was performed by adding 10 µl MTT (5 mg/ml) to each well. The plate was covered with aluminium foil and incubated for 4 hours in the dark. Then, 100 µl of Dimethyl sulfoxide was added as a solubilizing agent to each well and mixed thoroughly. At last, the absorbance of the micro-well plate was taken at 570 nm using ELISA Plate Reader (ThermoScientific).

C. Preparation of treatment media

According to previous experiments in the lab, literature survey, and the MTT assay, the sub-lethal doses were selected for each dietary stress, given in Table 9.

Table 9: Sub-lethal dosage for each dietary component after the MTT assay

Treatment	Sub-lethal dosage
Carbohydrate (glucose)	80 mM
Fat (palmitic acid)	800 µM
Salt (NaCl)	200 mM
Protein (BSA)	5 mM
Fiber (sodium butyrate)	20 mM

i. Carbohydrate (glucose) treatment media preparation –

Final concentration = 80 mM or 0.08 M

Mol. weight of glucose = 180.156 g/mol

Total final volume = 6 ml or 0.006 l

$$Molarity\ (M) = \frac{\frac{Given\ mass\ (g)}{Molecular\ mass\ (g/mol)}}{Volume\ of\ solution\ (l)}$$

$$0.08 = \frac{\frac{m}{180.156}}{0.006}$$

m = 0.08 X 0.006 X 180.156

m = 0.0865 g

0.0865 g (86.5 mg) of glucose was added to 6 ml media

ii. Fat (palmitic acid) treatment media preparation –

Working concentration = 800 µM or 0.8 mM

Stock concentration = 10 mM

Total final volume = 6 ml

According to the equation,

$C_1V_1 = C_2V_2$

10 X V_1 = 0.8 X 6

$V_1 = \frac{0.8 \text{ X } 6}{10}$

V_1 = 0.48 ml

0.48 ml (480 µl) of palmitic acid stock was added to 5520 µl media.

iii. Salt (NaCl) treatment media preparation –

Final concentration = 200 mM or 0.2 M

Mol. weight of NaCl = 58.44 g/mol

Total final volume = 6 ml or 0.006 l

$$Molarity\ (M) = \frac{\frac{Given\ mass\ (g)}{Molecular\ mass\ (g/mol)}}{Volume\ of\ solution\ (l)}$$

$0.2 = \frac{\frac{m}{58.44}}{0.006}$

m = 0.2 X 0.006 X 58.44

m = 0.07 g

0.07 g (70 mg) of NaCl was added to 6 ml media

iv. Protein (bovine serum albumin) treatment media preparation –

Final concentration = 5 mM or 0.005 M

Mol. weight of BSA = 6.6 X 10^4 g/mol

Total final volume = 6 ml or 0.006 l

$$Molarity\ (M) = \frac{\frac{Given\ mass\ (g)}{Molecular\ mass\ (g/mol)}}{Volume\ of\ solution\ (l)}$$

$$0.005 = \frac{\frac{m}{6.6 \text{ X } 10000}}{0.006}$$

m = 0.005 X 0.006 X 6.6 X 10^4

m = 1.98 g

1.98 g of BSA was added to 6 ml media

v. Fiber (sodium butyrate) treatment media preparation –

Final concentration = 20 mM or 0.02 M

Mol. weight of sodium butyrate = 114.058 g/mol

Total final volume = 6 ml or 0.006 l

$$Molarity\ (M) = \frac{\frac{Given\ mass\ (g)}{Molecular\ mass\ (g/mol)}}{Volume\ of\ solution\ (l)}$$

$$0.02 = \frac{\frac{m}{114.058}}{0.006}$$

m = 0.02 X 0.006 X 114.058

m = 0.0137 g

0.0137 g (13.7 mg) of sodium butyrate was added in 6 ml media.

The five treatment media were prepared and filtered using 0.4 microns filters. After filtration, the treatment media were stored at 4˚C.

D. Treatment of HepG2 cells

The prepared treatment media were recovered from the 4˚C and thawed properly for the treatment. Six vials containing ~80% confluent cells were selected for the treatment and treatment was given according to Table 10.

Table 10: Treatment vials and their corresponding compositions

Treatment Vials	Treatment
Control	Cells + Serum-free media
Glucose	Cells + 80 mM glucose media
Palmitic acid	Cells + 800 µM palmitic acid media
NaCl	Cells + 200 mM NaCl media
BSA	Cells + 5 mM BSA media
Sodium butyrate	Cells + 20 mM sodium butyrate media

After the addition of treatment media, the vials were incubated for 24 hours at 37˚C, 5% CO_2, and 5% humidity.

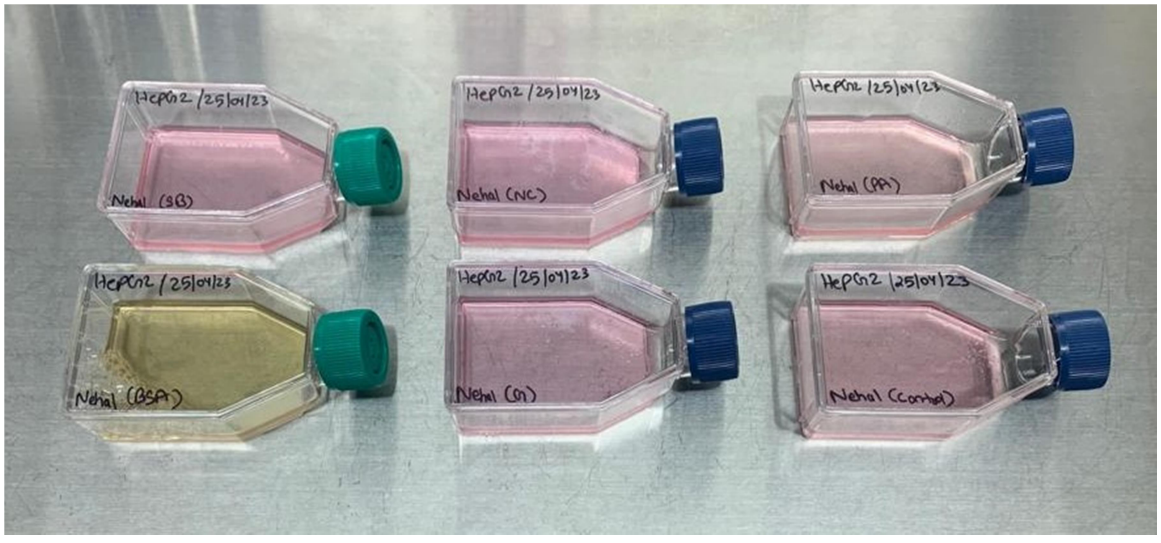

Figure 14: Cells treated with nutritional stress in T-flask

E. Sample preparation for GC-MS

After incubation, media was removed from the 6 vials and 1.5 ml of phosphate buffered saline (PBS) was added in each vial and scrapping was done. The cells scrapped into PBS were then added to eppendorf and centrifuged at 3000 rpm for 4 min. After this, the treated cell pellet was obtained and prepared for GC-MS. The sample preparation for GC-MS is given in Figure 15:

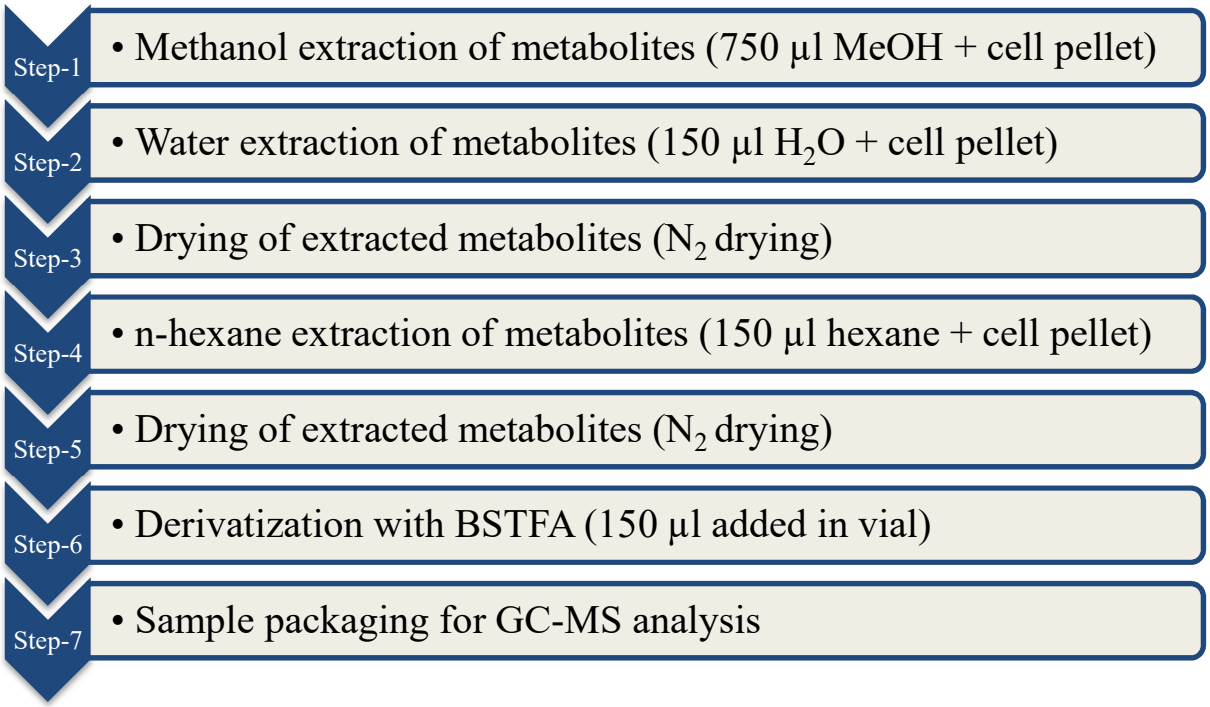

Figure 15: GC-MS sample preparation procedure

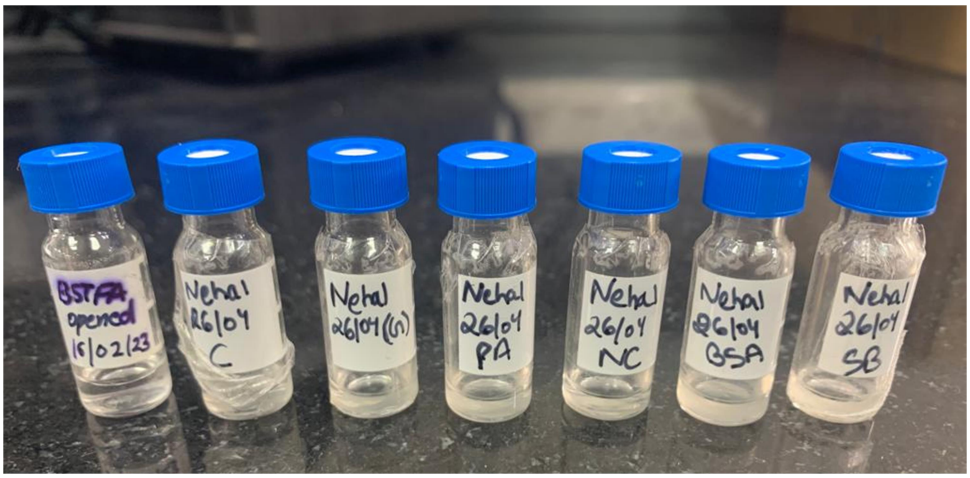

Figure 16: GC-MS vials containing derivatized samples

F. GC-MS analysis

GC-MS was carried out using GC-2014C AFsc-Shimadzu model with 5Sil-MS column.

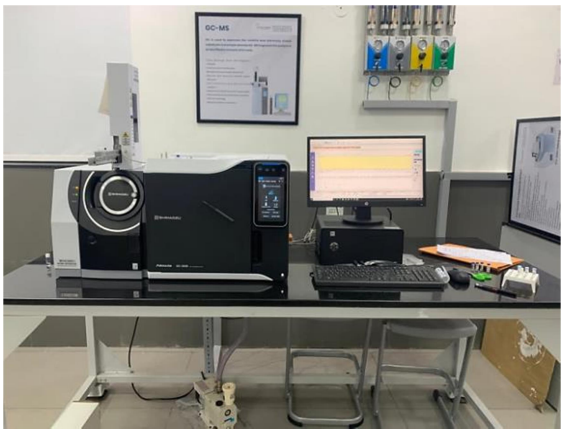

Figure 17: GC-2014C AFsc-Shimadzu GC-MS

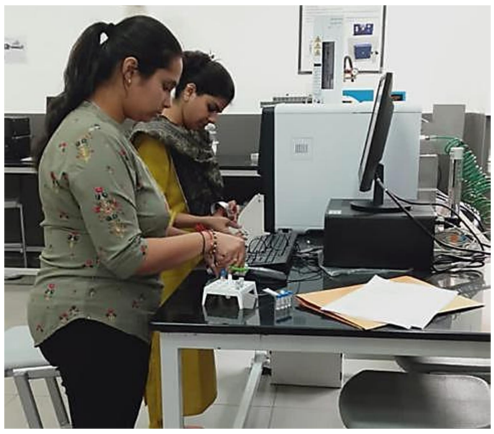

Figure 18: Performing GC-MS

The injection volume for conditioning the column was 1 µl and for a sample was 2 µl. Conditioning of the column was done with BSTFA.

Folder: D:\Data\Thapar_Nehal_28.04.2023

	Vial#	Sample Name	Sample ID	Sample Type	Analysis Type	Method File	Data File	Level#	Inj. Volume	Tuning File
1	0	Conditiong	bstfa	0:Unknown	IT QT	g method.qgm	oning1.qgd	1	1	uning File.qgt
2	1	C	1	0:Unknown	IT QT	r Analysis.qgm	C.qgd	1	2	uning File.qgt
3 >>	2	PA	2	0:Unknown	IT QT	r Analysis.qgm	PA.qgd	1	2	uning File.qgt
4	3	BSA	3	0:Unknown	IT QT	r Analysis.qgm	BSA.qgd	1	2	uning File.qgt
5	4	NC	4	0:Unknown	IT QT	r Analysis.qgm	NC.qgd	1	2	uning File.qgt
6	5	G	5	0:Unknown	IT QT	r Analysis.qgm	G.qgd	1	2	uning File.qgt
7	6	SB	6	0:Unknown	IT QT	r Analysis.qgm	SB.qgd	1	2	uning File.qgt

Figure 19: Batch setting for GC-MS analysis

Table 11: Run parameters for the GC-MS analysis

Parameters for a sample run	
Initial Run Temperature	60˚C
Initial Hold	4 min
Ramp	5˚C per min
End Temperature	300˚C
End Hold	2 min
Transfer Line Temperature	300˚C
MS Analyzer Range	50-650 amu
Total Run Time	55 min
Injection Volume	2 µL
Injection Type	Splitless mode

G. Peak identification and Characterization

The chromatogram of each sample was obtained in .qgd file format. This was later converted to .cdf file format using the OpenChrome tool as this format was compatible with AMDIS. Peaks were identified using AMDIS and characterized using the NIST library. The GC-MS files were loaded into the AMDIS tool and resolution, sensitivity, shape requirements, and peak subtraction was adjusted according to the requirements. Peaks were identified as "Components" and a list of retention time was provided in the tool. For a specific peak at a given retention time, the compounds were identified using the NIST library. Identified compounds were listed with respective retention time, area of peak, and probability. Later, the compounds identified were processed and mapping was done concerning PubChem, KEGG, and HMDB databases.

H. Enrichment analysis

Metaboanalyst (5.0) tool (https://www.metaboanalyst.ca/) was used for the enrichment analysis of compounds. A list of compounds was uploaded and relevant hits were obtained. After this, "Pathway", "Disease Signature" and "Chemical Structure" related bar graphs and metabolite sets were obtained and later used for analysis.

I. Pathway analysis

Metaboanalyst (5.0) tool (https://www.metaboanalyst.ca/) was used for pathway analysis of compounds. A list of compounds was uploaded and relevant hits were obtained. The scatter plot for each compound list was obtained and later used for the analysis.

Table 12: Parameters selected for pathway analysis

Visualization method	Scatter plot
Enrichment method	Fischer's Exact test
Topology analysis	Out-degree centrality
Reference metabolome	All compounds in the selected pathway library

RESULTS

HepG2 cells were treated with five nutritional stresses, i.e. high glucose treatment, high palmitic acid treatment, high sodium chloride treatment, high bovine serum albumin treatment, and high sodium butyrate treatment. A control was also taken in this study to compare the effect of each nutritional stress on HepG2 to normal conditions. Morphological changes in HepG2 cells were also recorded. Also, the metabolites, identified and characterized using GC-MS-based metabolomics, were used for identifying disease signatures, enriched metabolisms and pathways, and classes of molecules specific to each treatment.

MTT assay was conducted to know the dose-dependent effects of each dietary stress on HepG2 cells. Sub-lethal dose concentration for each dietary stress was selected for understanding the effects on HepG2 cells.

One-way ANOVA (Dunnett's multiple comparisons test) was used as a statistical tool to investigate independent single variables (each treatment) for significant variations ($P<0.05$). A P-value less than 0.05 indicate a significant difference between the two values.

As in Figure 20, Graph A represents HepG2 cell viability concerning different glucose concentrations with respect to control. Similarly, graphs B, C, D, and E for palmitic acid, sodium chloride, bovine serum albumin, and sodium butyrate, respectively. Cell viability is calculated as percentage of control. '*' represents significant difference ($P<0.05$), '**' represents high significant difference ($P<0.01$) and '***' represents very high significant difference ($P<0.001$).

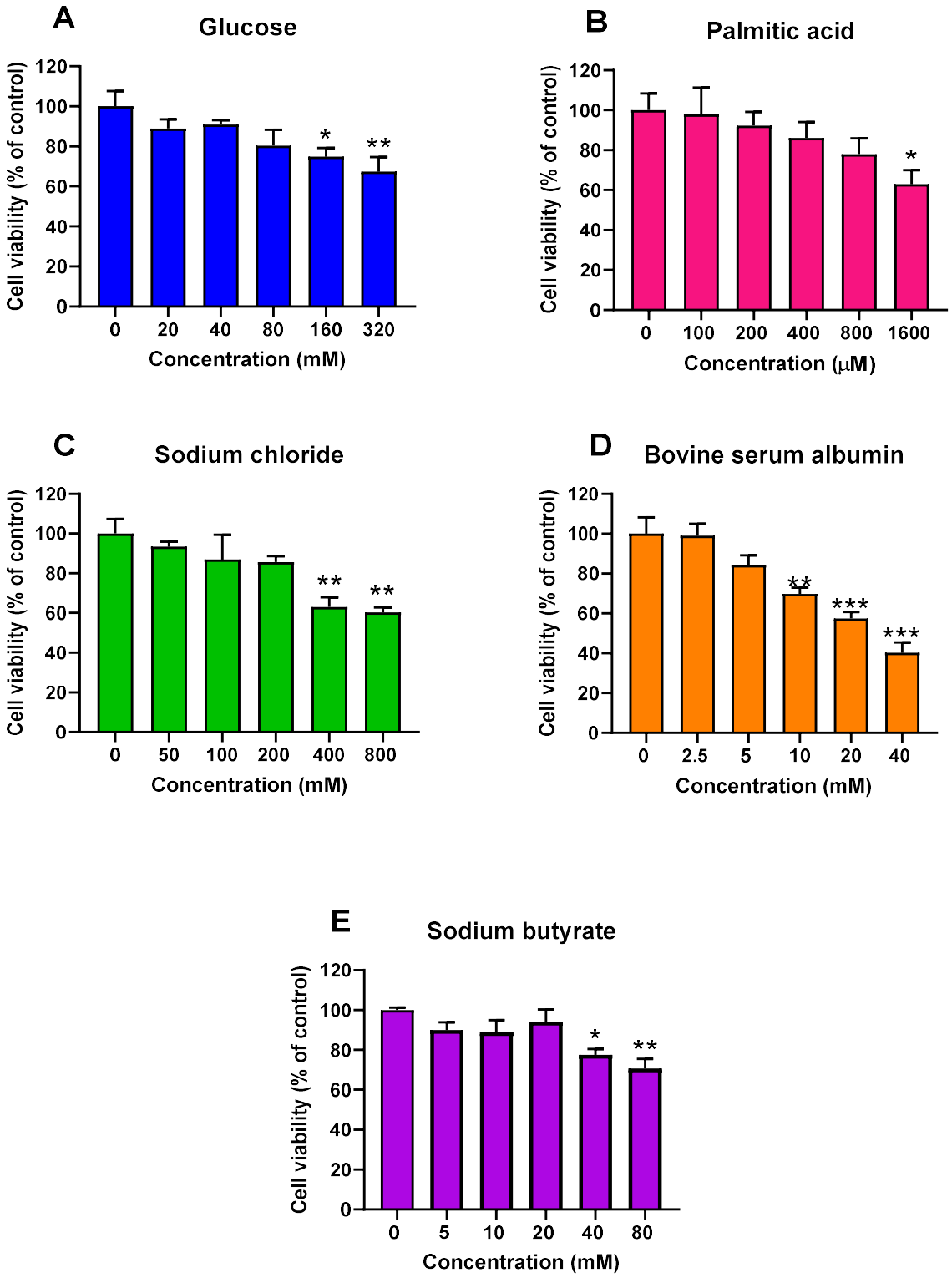

Figure 20: Graphs representing lethal doses for each dietary stress; a significant difference between the doses is represented with '*'.

I. Control

Cells were treated with serum-free media for 24 hours.

➢ GC-MS graph

GC chromatogram (given in Figure 21.1) of control depicts retention time (min) on X-axis and relative abundance (intensity) on Y-axis. A total of 54 metabolites (components) were identified in the control (given in Table 13.1). The most abundant metabolites are – Acetamide (62.732%), 2-Ethylhexanoic acid (25.649%), and 2-Ethylhexyl 2-ethylhexanoate (2.801%). The abundance is measured based on the % area of the peak of a specific component.

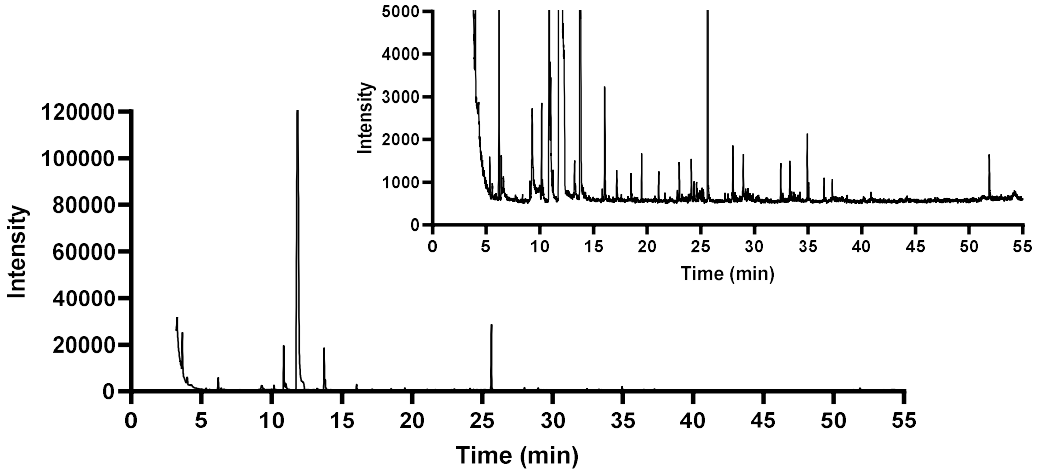

Figure 21.1: GC-MS graph obtained for the control treatment

Table 13.1: Metabolites identified in the control treatment

S.No.	Metabolites	Mol. Formula	MW (g/mol)	% Probability	RT (min)	Area	% Area
1	1,2,3,4-Tetrahydroisoquinoline	$C_9H_{11}N$	133.19	6.95	3.247	154489	0.434
2	Pyrrole-2-carboxaldehyde	C_5H_5NO	95.10	1.75	3.26	1357	0.004
3	Acetamide	C_2H_5NO	59.07	70.3	3.2785	22353662	62.732
4	4-Methylbenzoic acid	$C_8H_8O_2$	136.15	9.82	3.346	7477	0.021
5	Propionamide	C_3H_7NO	73.09	68.2	3.397	6047	0.017
6	3,4-Hexanedione	$C_6H_{10}O_2$	114.14	56.4	3.417	6189	0.017
7	Oxanilic acid	$C_8H_7NO_3$	165.15	28.6	3.4975	22030	0.062
8	2,6-Dimethylpyridine	C_7H_9N	107.15	22.6	3.5275	39113	0.110

9	2-(Acetamidomethylene)succinate	$C_7H_9NO_5$	187.15	61.4	3.585	27417	0.077
10	5-Amino-4-imidazole carboxylate	$C_4H_5N_3O_2$	127.1	42.2	3.642	38364	0.108
11	Cyclobutane	C_4H_8	56.11	47.8	3.672	6242	0.018
12	Valine	$C_5H_{11}NO_2$	117.15	8.91	3.757	11111	0.031
13	2,3,5,6-Pyridinetetracarbonitrile	C_9HN_5	179.14	51.6	3.807	4841	0.014
14	5-Methylhydantoin	$C_4H_6N_2O_2$	114.10	22.6	3.9675	1843	0.005
15	Thiodiacetonitrile	$C_4H_4N_2S$	112.16	21.7	3.9895	996	0.003
16	1-Propanesulfonic acid	$C_3H_8O_3S$	124.16	19.6	4.3425	9226	0.026
17	Benzoxazole	C_7H_5NO	119.12	69.4	4.362	1259	0.004
18	N,N-Dimethylformamide	C_3H_7NO	73.09	48	4.3775	14908	0.042
19	3-Butoxypropylamine	$C_7H_{17}NO$	131.22	36.1	4.437	7020	0.020
20	2-Ethylhexanal	$C_8H_{16}O$	128.21	66.4	6.1975	112098	0.315
21	2-Buten-1-ol	C_4H_8O	72.11	16.9	6.2035	4371	0.012
22	2,4,6-Trimethylpyridine	$C_8H_{11}N$	121.18	18.4	8.0295	11493	0.032
23	Ethyl diethylcarbamate	$C_7H_{15}NO_2$	145.20	74.6	10.022	29008	0.081
24	2-Propyl-1-pentanol	$C_8H_{18}O$	130.23	33.1	10.167	569584	1.598
25	Lactic acid	$C_3H_6O_3$	90.08	59.3	10.194	46391	0.130
26	2,4,4-Trimethylpentan-1-ol	$C_8H_{18}O$	130.23	30.3	10.2465	22919	0.064
27	2-Ethylhexyl formate	$C_9H_{18}O_2$	158.24	55.5	10.8635	505055	1.417
28	2-Ethylhexan-1-ol	$C_8H_{18}O$	130.23	15.3	11.0065	28994	0.081
29	2-Ethylhexyl acetate	$C_{10}H_{20}O_2$	172.26	43.4	13.234	27269	0.077
30	2-Ethylhexanoic acid	$C_8H_{16}O_2$	144.21	97.4	13.7405	9139797	25.649
31	Dihydropyrimidine	$C_4H_6N_2$	82.10	61.6	14.2005	142838	0.401
32	Benzoic acid	$C_7H_6O_2$	122.12	77	16.293	157305	0.441
33	Octanoic acid	$C_8H_{16}O_2$	144.21	15.9	16.426	78786	0.221
34	1,3-Oxazolidine-2-thione	C_3H_5NOS	103.15	19.1	17.586	33285	0.093
35	2-Ethylhexyl butyrate	$C_{12}H_{24}O_2$	200.32	33.7	18.5015	43778	0.123
36	Pregna-3,5-dien-9-ol-20-one	$C_{21}H_{30}O_2$	314.5	23.7	18.949	1197	0.003
37	Butyric acid	$C_4H_8O_2$	88.11	8.46	19.484	48474	0.136
38	Pentitol	$C_5H_{12}O_5$	152.15	17	19.942	62446	0.175
39	Valeric acid	$C_5H_{10}O_2$	102.13	44.8	20.156	14123	0.040
40	6-Hydroxyheptanoic acid	$C_7H_{14}O_3$	146.18	19.2	20.7165	19508	0.055
41	3-Ethyl-3-methylheptane	$C_{10}H_{22}$	142.28	16.6	22.995	15837	0.044
42	5-Ethyl-5-methyldecane	$C_{13}H_{28}$	184.36	16.2	24.122	21273	0.060
43	2-Ethylhexyl 2-ethylhexanoate	$C_{16}H_{32}O_2$	256.42	91.7	25.6385	998233	2.801
44	3,8-Dimethylundecane	$C_{13}H_{28}$	184.36	7.07	27.994	29584	0.083
45	Hexadecane	$C_{16}H_{34}$	226.44	8.61	28.9595	27780	0.078
46	Terephthalic acid	$C_8H_6O_4$	166.13	96.5	29.8565	72912	0.205
47	2-Methyltridecane	$C_{14}H_{30}$	198.39	8.16	32.4505	27129	0.076
48	D-Mannose	$C_6H_{12}O_6$	180.16	10.5	33.833	16282	0.046
49	Sulfurous acid	H_2SO_3	82.08	8.37	34.935	4023	0.011
50	7-Tridecanone	$C_{13}H_{26}O$	198.34	8.7	34.9385	45699	0.128

51	Palmitic acid	$C_{16}H_{32}O_2$	256.42	95.9	35.047	14737	0.041
52	Oleic acid	$C_{18}H_{34}O_2$	282.5	48.6	38.1485	16760	0.047
53	Stearic acid	$C_{18}H_{36}O_2$	284.5	88.7	38.6325	16179	0.045
54	Cholesterol	$C_{27}H_{46}O$	386.7	75.9	51.876	514724	1.444

- **Enrichment analysis**

Disease signatures (Figure 21.2 and Table 13.2), pathway enrichment from the KEGG database (Figure 21.3 and Table 13.3) and from the SMPDB database (Figure 21.4 and Table 13.4), and different classes of metabolites (Figure 21.5 and Table 13.5) are given below. The enrichment ratio is no. of hits observed divided by no. of hits expected.

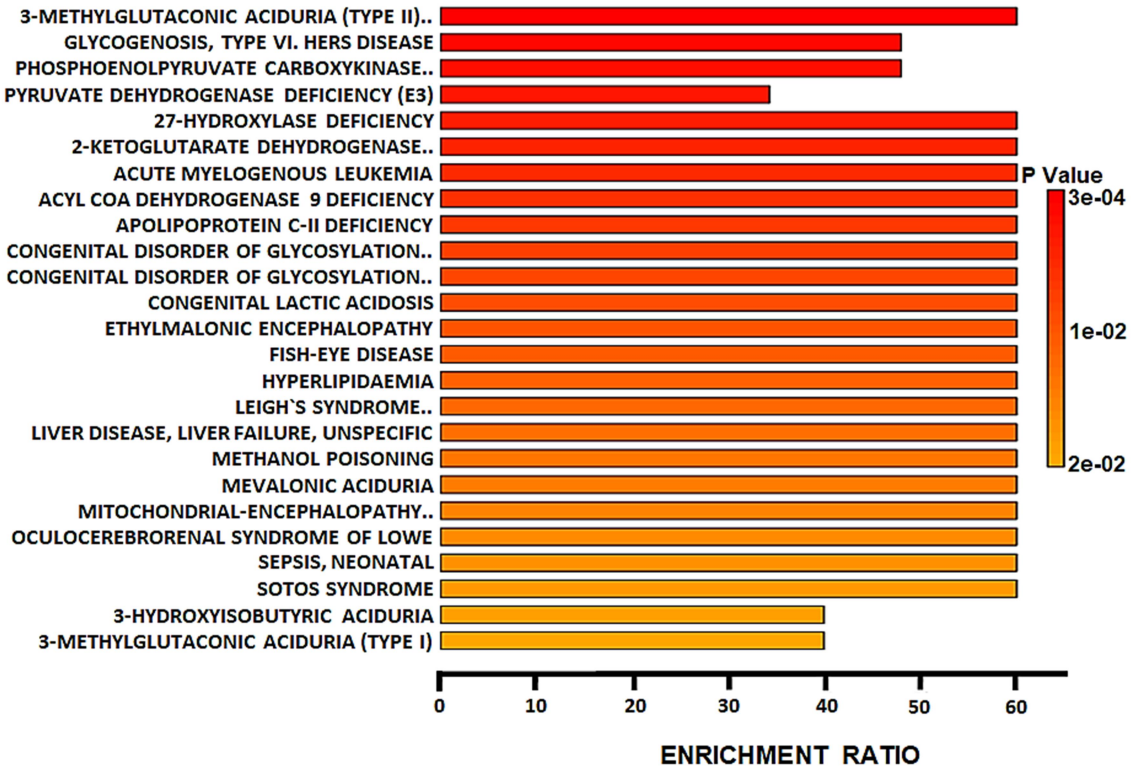

Figure 21.2: Disease signatures in control

The top 25 disease signatures were identified. Significantly enriched signatures (↓) include 3-methylglutaconic aciduria (type II), type VI. hers disease, phosphoenolpyruvate carboxykinase deficiency 2, pyruvate dehydrogenase deficiency (E3), and 27-hydroxylase deficiency. Highly

enriched signatures (←) include 3-methylglutaconic aciduria (type II), 27-hydroxylase deficiency, 2-ketoglutarate dehydrogenase complex deficiency, acute myelogenous leukemia, acyl CoA dehydrogenase 9 deficiency, apolipoprotein C-II deficiency, a congenital disorder of glycosylation CDG-IA and CDG-IB, congenital lactic acidosis, ethylmalonic encephalopathy, fish-eye disease, hyperlipidaemia, leigh's syndrome, liver disease, methanol poisoning, mevalonic aciduria, mitochondrial-encephalopathy-lactic-acidosis-stroke, oculocerebrorenal syndrome of lowe, sepsis, and sotos syndrome.

Table 13.2: Disease signatures in control

	Metabolite Set	Total	Hits	Expect	P Value	HolmP	FDR
	3-METHYLGLUTACONIC ACIDURIA (TYPE II), X-LINKED	4	2	0.0334	3.13E-4	0.0854	0.0473
	GLYCOGENOSIS (TYPE IA, IB, IC) | GLYCOGENOSIS, TYPE VI. HERS DISEASE	5	2	0.0418	5.2E-4	0.141	0.0473
	PHOSPHOENOLPYRUVATE CARBOXYKINASE DEFICIENCY 2 (PEPCK2)	5	2	0.0418	5.2E-4	0.141	0.0473
	PYRUVATE DEHYDROGENASE DEFICIENCY (E3)	7	2	0.0585	0.00109	0.293	0.0741
	27-HYDROXYLASE DEFICIENCY	2	1	0.0167	0.0166	1.0	0.194
	2-KETOGLUTARATE DEHYDROGENASE COMPLEX DEFICIENCY	2	1	0.0167	0.0166	1.0	0.194
	ACUTE MYELOGENOUS LEUKEMIA	2	1	0.0167	0.0166	1.0	0.194
	ACYL COA DEHYDROGENASE 9 DEFICIENCY | PYRUVATE DEHYDROGENASE DEFICIENCY (E2)	2	1	0.0167	0.0166	1.0	0.194
	APOLIPOPROTEIN C-II DEFICIENCY | CHOLESTERYL ESTER STORAGE DISEASE | GLYCOGENOSIS, TYPE IXB	2	1	0.0167	0.0166	1.0	0.194
	CONGENITAL DISORDER OF GLYCOSYLATION CDG-IA	2	1	0.0167	0.0166	1.0	0.194
	CONGENITAL DISORDER OF GLYCOSYLATION CDG-IB	2	1	0.0167	0.0166	1.0	0.194
	CONGENITAL LACTIC ACIDOSIS	2	1	0.0167	0.0166	1.0	0.194
	ETHYLMALONIC ENCEPHALOPATHY (EPEMA)	2	1	0.0167	0.0166	1.0	0.194

	FISH-EYE DISEASE	2	1	0.0167	0.0166	1.0	0.194
	HYPERLIPIDAEMIA	2	1	0.0167	0.0166	1.0	0.194
	LEIGH`S SYNDROME, SUBACUTE NECROTIZING ENCEPHALOPATHY, SNE	2	1	0.0167	0.0166	1.0	0.194
	LIVER DISEASE, LIVER FAILURE, UNSPECIFIC	2	1	0.0167	0.0166	1.0	0.194
	METHANOL POISONING	2	1	0.0167	0.0166	1.0	0.194
	MEVALONIC ACIDURIA	2	1	0.0167	0.0166	1.0	0.194
	MITOCHONDRIAL-ENCEPHALOPATHY-LACTIC ACIDOSIS-STROKE (MELAS) | MYOCLONIC EPILEPSY AND RAGGED RED FIBER DISEASE (MERRF) | PYRUVATE DEHYDROGENASE DEFICIENCY (E1)	2	1	0.0167	0.0166	1.0	0.194
	OCULOCEREBRORENAL SYNDROME OF LOWE	2	1	0.0167	0.0166	1.0	0.194
	SEPSIS, NEONATAL [DD]	2	1	0.0167	0.0166	1.0	0.194
	SOTOS SYNDROME	2	1	0.0167	0.0166	1.0	0.194
	3-HYDROXYISOBUTYRIC ACIDURIA	3	1	0.0251	0.0249	1.0	0.194
	3-METHYLGLUTACONIC ACIDURIA (TYPE I)	3	1	0.0251	0.0249	1.0	0.194

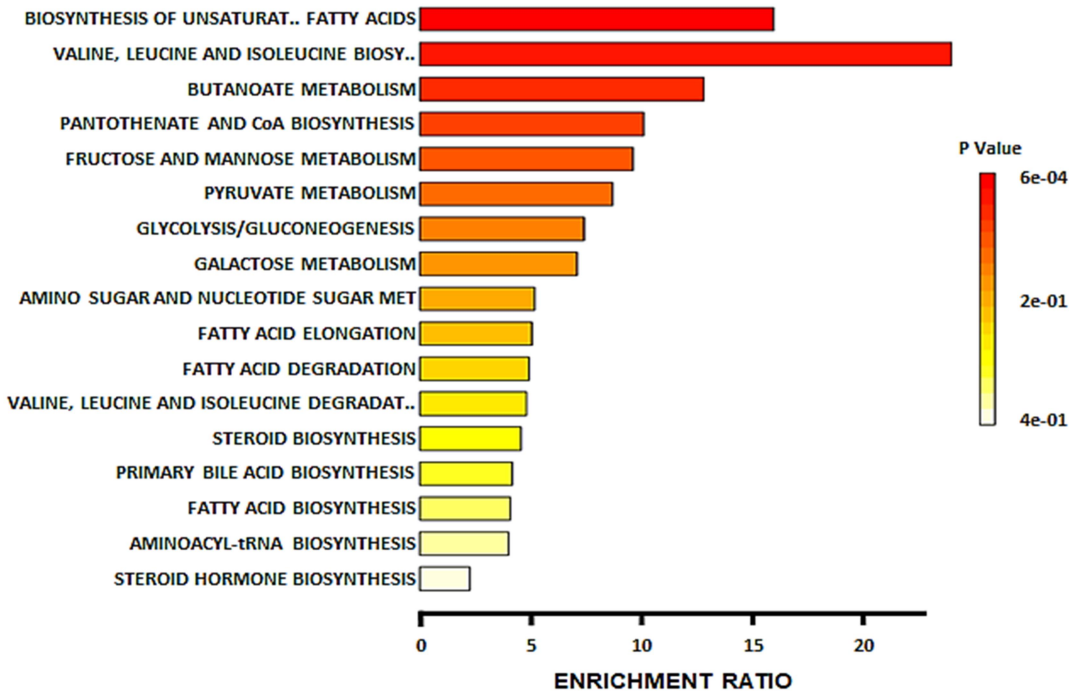

Figure 21.3: Control enrichment from the KEGG database

The top 17 metabolic pathways were identified. Significantly enriched pathways (↓) include biosynthesis of unsaturated fatty acids, valine, leucine, and isoleucine biosynthesis, butanoate metabolism, pantothenate and CoA biosynthesis, and fructose and mannose metabolism. Highly enriched pathways (←) include valine, leucine, and isoleucine biosynthesis, biosynthesis of unsaturated fatty acids, butanoate metabolism, pantothenate and CoA biosynthesis, and fructose and mannose metabolism.

Table 13.3: Control enrichment from the KEGG database

	Metabolite Set	Total	Hits	Expect	P Value	HolmP	FDR
	Biosynthesis of unsaturated fatty acids	36	3	0.188	6.12E-4	0.0514	0.0514
	Valine, leucine, and isoleucine biosynthesis	8	1	0.0417	0.041	1.0	1.0
	Butanoate metabolism	15	1	0.0781	0.0757	1.0	1.0
	Pantothenate and CoA biosynthesis	19	1	0.099	0.095	1.0	1.0
	Fructose and mannose metabolism	20	1	0.104	0.0998	1.0	1.0
	Pyruvate metabolism	22	1	0.115	0.109	1.0	1.0
	Glycolysis / Gluconeogenesis	26	1	0.135	0.128	1.0	1.0
	Galactose metabolism	27	1	0.141	0.133	1.0	1.0
	Amino sugar and nucleotide sugar metabolism	37	1	0.193	0.178	1.0	1.0
	Fatty acid elongation	38	1	0.198	0.182	1.0	1.0
	Fatty acid degradation	39	1	0.203	0.186	1.0	1.0
	Valine, leucine and isoleucine degradation	40	1	0.208	0.191	1.0	1.0
	Steroid biosynthesis	42	1	0.219	0.199	1.0	1.0
	Primary bile acid biosynthesis	46	1	0.24	0.216	1.0	1.0
	Fatty acid biosynthesis	47	1	0.245	0.221	1.0	1.0
	Aminoacyl-tRNA biosynthesis	48	1	0.25	0.225	1.0	1.0
	Steroid hormone biosynthesis	85	1	0.443	0.367	1.0	1.0

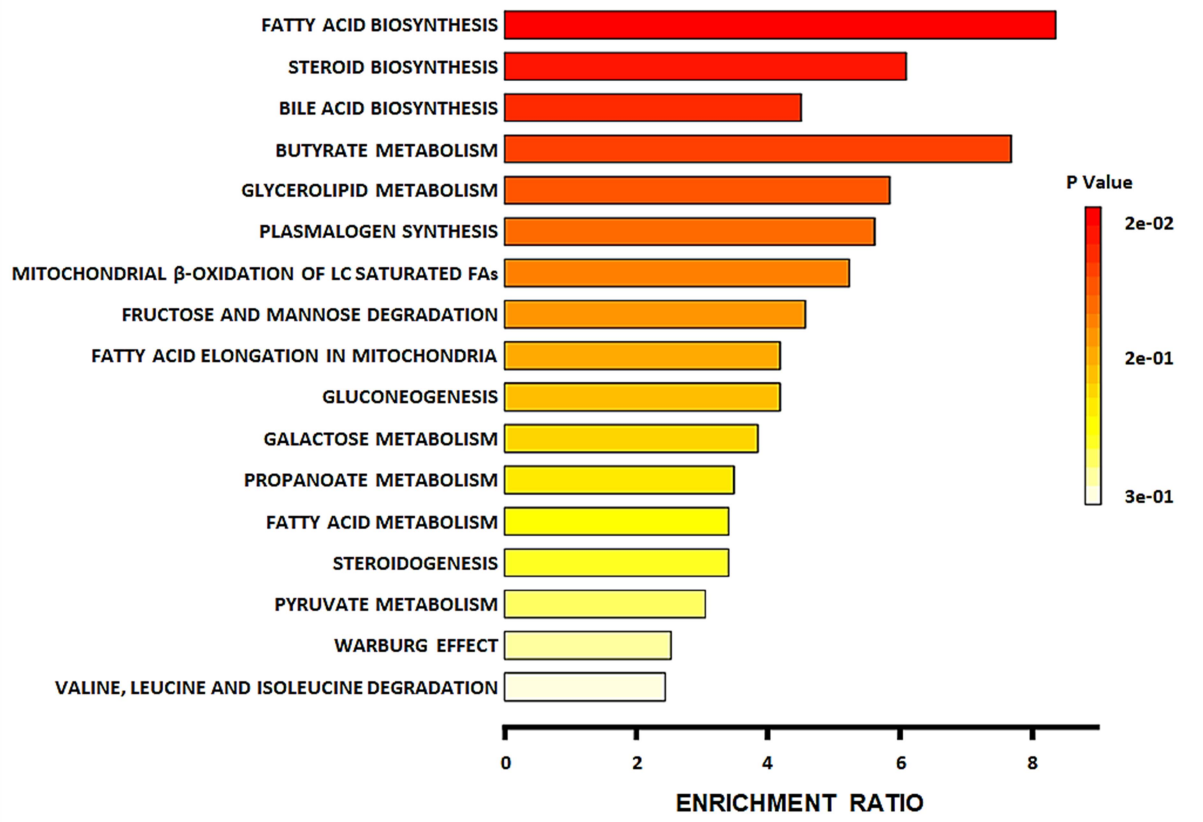

Figure 21.4: Control enrichment from the SMPDB database

The top 17 metabolic pathways were identified. Significantly enriched pathways (↓) include fatty acid biosynthesis, steroid biosynthesis, bile acid biosynthesis, butyrate metabolism, and glycerolipid metabolism. Highly enriched pathways (←) include fatty acid biosynthesis, butyrate metabolism, steroid biosynthesis, glycerolipid metabolism, and plasmalogen synthesis.

Table 13.4: Control enrichment from the SMPDB database

	Metabolite Set	Total	Hits	Expect	P Value	HolmP	FDR
	Fatty acid biosynthesis	35	3	0.273	0.00182	0.179	0.179
	Steroid biosynthesis	48	2	0.375	0.0503	1.0	1.0
	Bile acid biosynthesis	65	2	0.508	0.0867	1.0	1.0
	Butyrate metabolism	19	1	0.148	0.14	1.0	1.0
	Glycerolipid metabolism	25	1	0.195	0.18	1.0	1.0
	Plasmalogen synthesis	26	1	0.203	0.187	1.0	1.0
	Mitochondrial beta-oxidation of long chain saturated fatty acids	28	1	0.219	0.2	1.0	1.0

	Fructose and mannose degradation	32	1	0.25	0.225	1.0	1.0
	Fatty acid elongation in mitochondria	35	1	0.273	0.244	1.0	1.0
	Gluconeogenesis	35	1	0.273	0.244	1.0	1.0
	Galactose metabolism	38	1	0.297	0.262	1.0	1.0
	Propanoate metabolism	42	1	0.328	0.286	1.0	1.0
	Fatty acid metabolism	43	1	0.336	0.291	1.0	1.0
	Steroidogenesis	43	1	0.336	0.291	1.0	1.0
	Pyruvate metabolism	48	1	0.375	0.32	1.0	1.0
	Warburg effect	58	1	0.453	0.374	1.0	1.0
	Valine, leucine, and isoleucine degradation	60	1	0.469	0.384	1.0	1.0

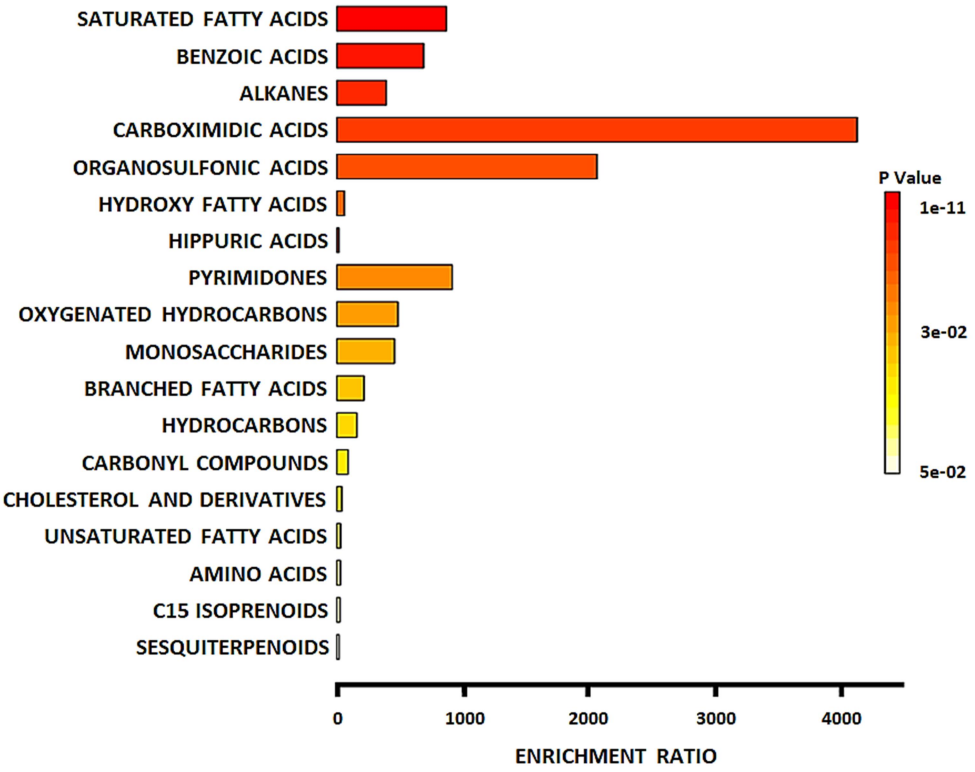

Figure 21.5: Different classes of identified metabolites in the control

The top 18 different classes of metabolites were identified. Significantly enriched classes (↓) include saturated fatty acids, benzoic acids, alkanes, carboximidic acids, and organosulfonic acids. Highly enriched classes (←) include carboximidic acids, organosulfonic acids, pyrimidones, saturated fatty acids, and benzoic acids.

Table 13.5: Different classes of identified metabolites in the control

	Metabolite Set	Total	Hits	Expect	P Value	HolmP	FDR
	Saturated fatty acids	38	4	0.0046	1.21E-11	8.88E-9	8.88E-9
	Benzoic acids	24	2	0.0029	3.87E-6	0.00282	0.00141
	Alkanes	42	2	0.00508	1.21E-5	0.00879	0.00294
	Carboximidic acids	2	1	2.42E-4	2.42E-4	0.176	0.0442
	Organosulfonic acids	4	1	4.84E-4	4.84E-4	0.352	0.0708
	Hippuric acids	1470	3	0.178	7.3E-4	0.53	0.0889
	Pyrimidones	9	1	0.00109	0.00109	0.789	0.114
	Oxygenated hydrocarbons	17	1	0.00206	0.00206	1.0	0.177
	Monosaccharides	18	1	0.00218	0.00218	1.0	0.177
	Branched fatty acids	38	1	0.0046	0.00459	1.0	0.335
	Hydrocarbons	52	1	0.00629	0.00628	1.0	0.417
	Carbonyl compounds	91	1	0.011	0.011	1.0	0.667
	Cholesterol and derivatives	203	1	0.0246	0.0243	1.0	1.0
	Unsaturated fatty acids	267	1	0.0323	0.0318	1.0	1.0
	Hydroxy fatty acids	274	1	0.0332	0.0326	1.0	1.0
	Amino acids	277	1	0.0335	0.033	1.0	1.0
	Hydroxy fatty acids	293	1	0.0355	0.0349	1.0	1.0
	C15 isoprenoids	333	1	0.0403	0.0395	1.0	1.0
	Sesquiterpenoids	452	1	0.0547	0.0533	1.0	1.0

- **Pathway analysis**

Impacted pathways from the KEGG database (Figure 21.6 and Table 13.6), and the SMPDB database (Figure 21.7 and Table 13.7) are given below. Pathway impact is calculated by using centrality and pathway enrichment results.

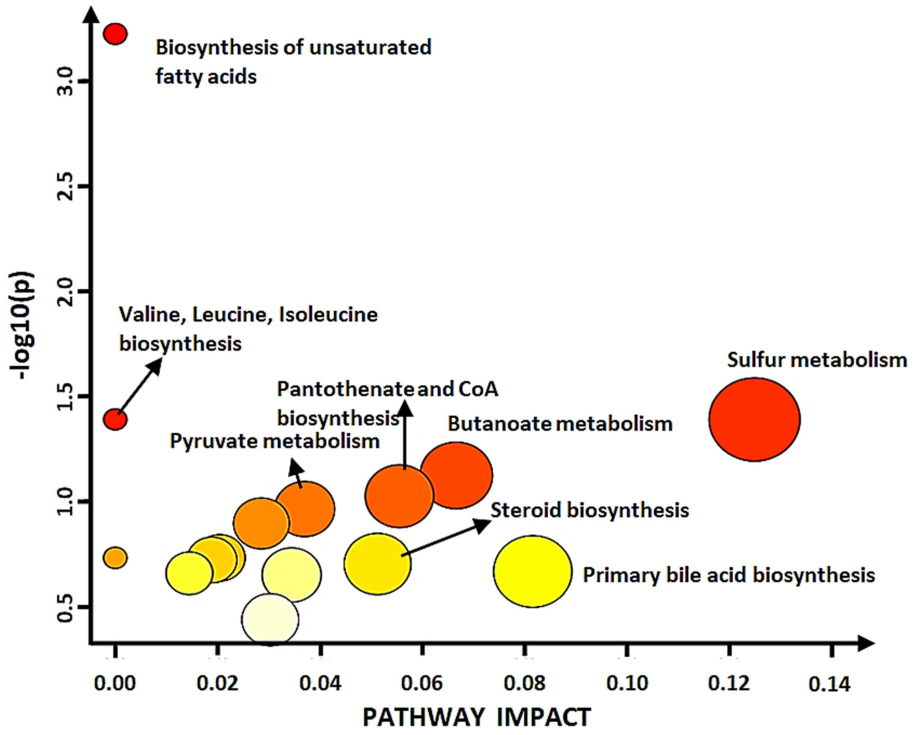

Figure 21.6: Control pathway analysis from the KEGG database

The top 15 impacted pathways were identified. Highly impacted pathways (←) include sulfur metabolism, primary bile acid biosynthesis, butanoate metabolism, pantothenate and CoA biosynthesis, and steroid biosynthesis. Significantly impacted pathways (↓) include biosynthesis of unsaturated fatty acids, sulfur metabolism, valine, leucine, and isoleucine biosynthesis, butanoate metabolism, and pantothenate and CoA biosynthesis.

Table 13.6: Control pathway analysis from the KEGG database

Pathway Name	Match Status	p	-log(p)	Holm p	FDR	Impact
Biosynthesis of unsaturated fatty acids	3/36	5.9553E-4	3.2251	0.050024	0.050024	0.0
Valine, leucine, and isoleucine biosynthesis	1/8	0.040642	1.391	1.0	1.0	0.0
Sulfur metabolism	1/8	0.040642	1.391	1.0	1.0	0.125
Butanoate metabolism	1/15	0.075011	1.1249	1.0	1.0	0.06667
Pantothenate and CoA biosynthesis	1/19	0.094163	1.0261	1.0	1.0	0.05556
Pyruvate metabolism	1/22	0.1083	0.96538	1.0	1.0	0.03704
Glycolysis / Gluconeogenesis	1/26	0.12684	0.89673	1.0	1.0	0.02857
Fatty acid elongation	1/39	0.18481	0.73328	1.0	1.0	0.0

Fatty acid degradation	1/39	0.18481	0.73328	1.0	1.0	0.02041
Valine, leucine and isoleucine degradation	1/40	0.18913	0.72325	1.0	1.0	0.01887
Steroid biosynthesis	1/42	0.1977	0.704	1.0	1.0	0.05128
Primary bile acid biosynthesis	1/46	0.2146	0.66836	1.0	1.0	0.08163
Fatty acid biosynthesis	1/47	0.21878	0.65999	1.0	1.0	0.01449
Aminoacyl-tRNA biosynthesis	1/48	0.22294	0.65181	1.0	1.0	0.03448
Steroid hormone biosynthesis	1/85	0.3638	0.43913	1.0	1.0	0.0303

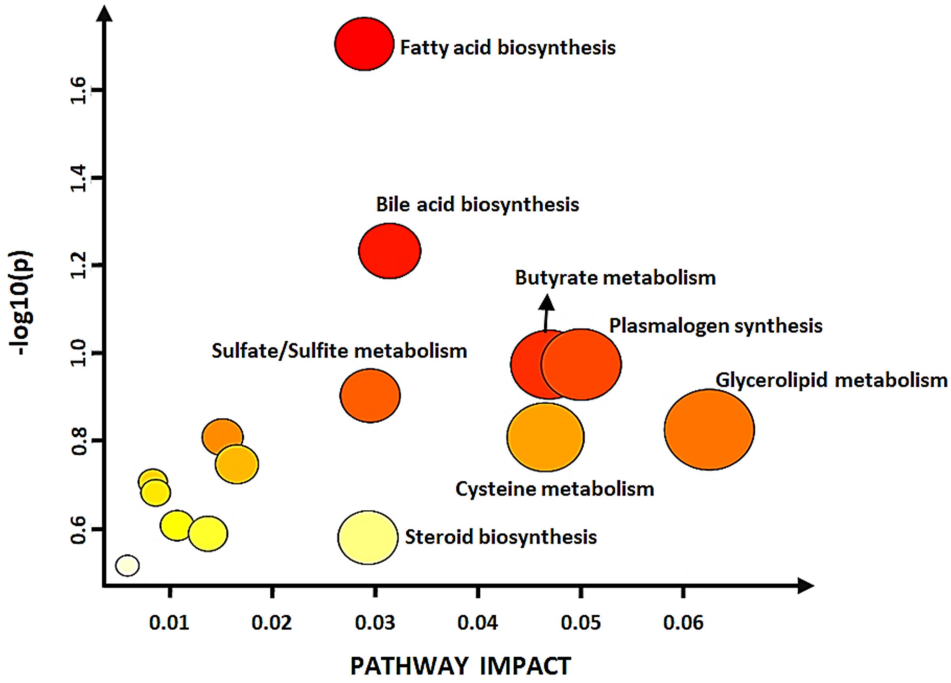

Figure 21.7: Control pathway analysis from the SMPDB database

The top 15 impacted pathways were identified. Highly impacted pathways (←) include glycerolipid metabolism, plasmalogen synthesis, cysteine metabolism, butyrate metabolism, and bile acid biosynthesis. Significantly impacted pathways (↓) include fatty acid biosynthesis, bile acid biosynthesis, plasmalogen synthesis, butyrate metabolism, and sulfate/sulfite metabolism.

Table 13.7: Control pathway analysis from the SMPDB database

Pathway Name	Match Status	p	-log(p)	Holm p	FDR	Impact
Fatty acid biosynthesis	2/33	0.019664	1.7063	1.0	1.0	0.028846
Bile acid biosynthesis	2/59	0.05839	1.2337	1.0	1.0	0.031311
Butyrate metabolism	1/16	0.10616	0.97404	1.0	1.0	0.046875
Plasmalogen synthesis	1/16	0.10616	0.97404	1.0	1.0	0.05

Sulfate/Sulfite metabolism	1/19	0.12495	0.90327	1.0	1.0	0.029412
Glycerolipid metabolism	1/23	0.14947	0.82544	1.0	1.0	0.0625
Mitochondrial beta-oxidation of long chain saturated fatty acids	1/24	0.15551	0.80824	1.0	1.0	0.015
Cysteine metabolism	1/24	0.15551	0.80824	1.0	1.0	0.046512
Fructose and mannose degradation	1/28	0.1793	0.74643	1.0	1.0	0.016393
Galactose metabolism	1/31	0.19676	0.70607	1.0	1.0	0.008196
Fatty acid elongation in mitochondria	1/33	0.20822	0.68147	1.0	1.0	0.008474
Fatty acid metabolism	1/40	0.24725	0.60687	1.0	1.0	0.010563
Steroidogenesis	1/42	0.25809	0.58823	1.0	1.0	0.013575
Steroid biosynthesis	1/43	0.26346	0.57929	1.0	1.0	0.029197
Valine, leucine, and isoleucine degradation	1/51	0.30524	0.51536	1.0	1.0	0.005714

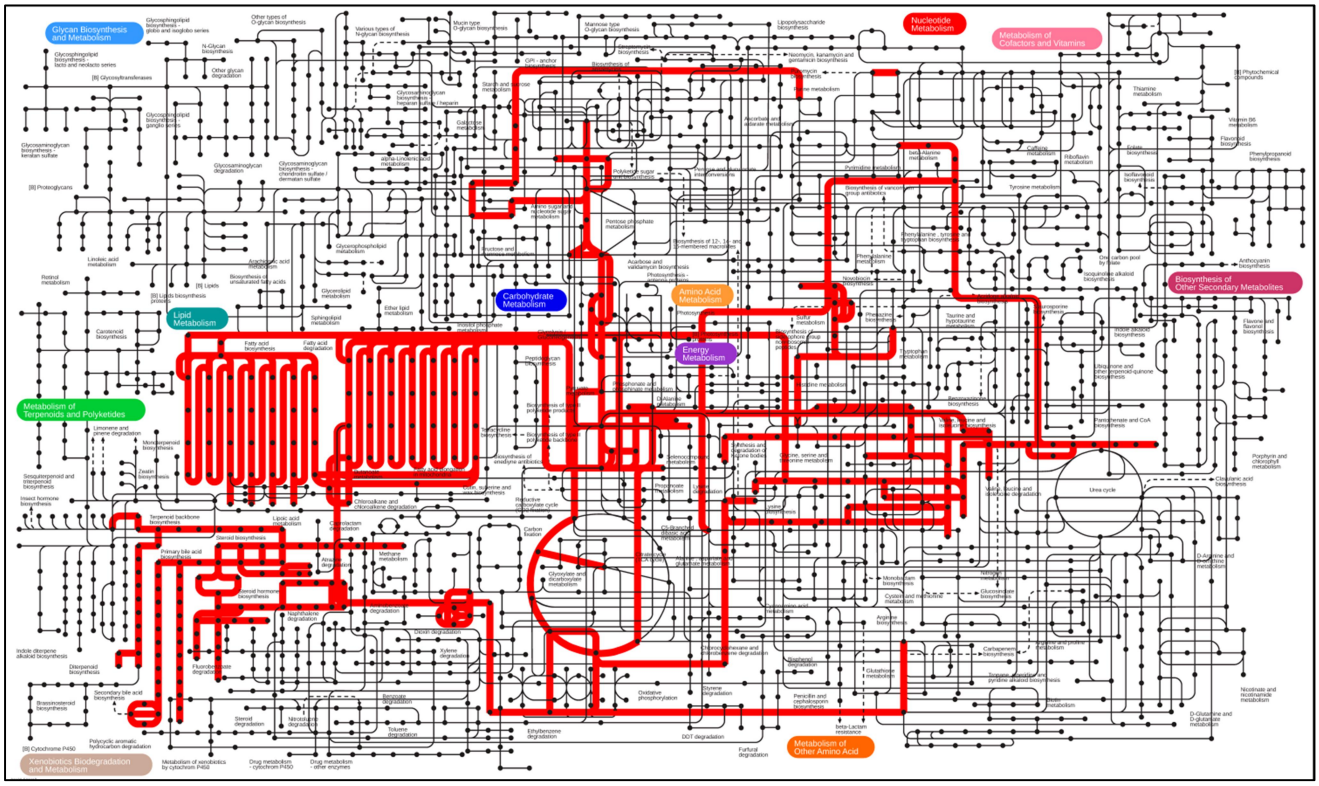

Figure 21.8: Metabolic pathways enriched in control after mapping with the KEGG database. The highlighted metabolisms show enrichment specific to control. Other metabolisms in control were not enriched due to the low abundance of its metabolites.

II. High glucose treatment

Cells were treated with 80 mM glucose media for 24 hours.

➢ GC-MS graph

GC chromatogram of glucose treatment (given in Figure 22.1) depicts retention time (min) on X-axis and relative abundance (intensity) on Y-axis. A total of 137 metabolites (components) were identified in glucose-treated cells (given in Table 14.1). The most abundant metabolites are – 2-Ethylhexan-1-ol (28.794%), Acetamide (13.958%), 2-Ethylhexanoic acid (11.815%), Cholesterol (8.277%), and Phosphoric acid (6.841). The abundance is measured based on the % area of the peak of a specific component.

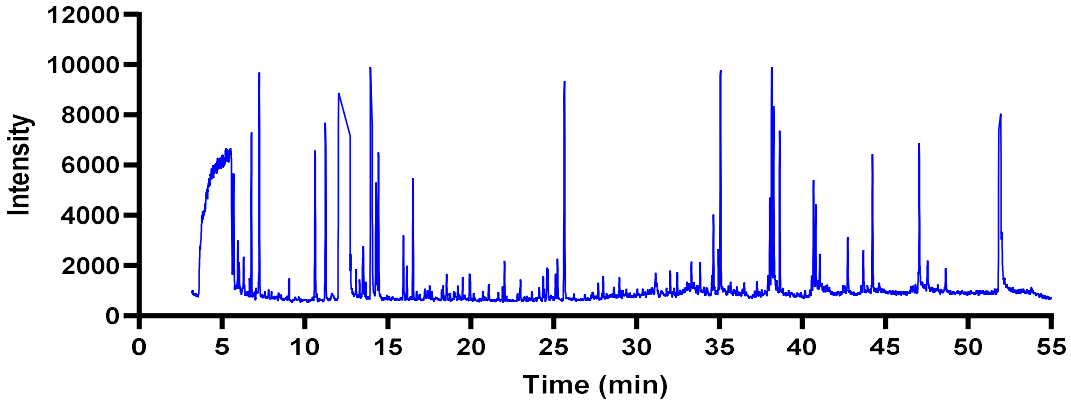

Figure 22.1: GC-MS graph obtained for glucose treatment

Table 14.1: Metabolites identified in glucose-treated cells

S.No.	Metabolites	Mol. Formula	MW (g/mol)	% Probability	RT (min)	Area	% Area
1	5,11-Dihydropyrido[2,3-b][1,4]benzodiazepin-6-one	$C_{12}H_9N_3O$	211.22	57.3	3.6485	219277	0.017
2	Propionic acid	$C_3H_6O_2$	74.08	16.8	3.69	101338	0.008
3	Isoquinoline-7-one	C_9H_7NO	145.16	43.6	3.741	622560	0.048
4	1,3-Benzodioxole	$C_7H_6O_2$	122.12	47.1	3.8125	11671	0.001
5	5H-Dibenzo[a,d]cycloheptene	$C_{15}H_{12}$	192.25	11.3	3.882	623317	0.048
6	Leucine	$C_6H_{13}NO_2$	131.17	3.82	3.9625	3826521	0.295
7	2,4(1H,3H)-Pyrimidinedione-14C	$C_4H_4N_2O_2$	114.08	5.84	4.0425	437102	0.034

8	5-Amino-3-methyl-1,2,4-thiadiazole	$C_3H_5N_3S$	115.16	18.3	4.077	110017	0.008
9	1-Benzoylpiperidine	$C_{12}H_{15}NO$	189.25	4.61	4.137	1308172	0.101
10	2-Aminothiazole	$C_3H_4N_2S$	100.14	11	4.1475	362340	0.028
11	Benzenesulfonamide	$C_6H_7NO_2S$	157.19	56.7	4.1925	38803	0.003
12	1,2,3,4-Tetrahydroisoquinoline	$C_9H_{11}N$	133.19	28.6	4.2625	324011	0.025
13	1,4,7-Trioxa-10-azacyclododecane	$C_8H_{17}NO_3$	175.23	10.2	4.2795	1850403	0.143
14	Dehydroemetine	$C_{29}H_{38}N_2O_4$	478.6	10.5	4.3325	501373	0.039
15	Pravadoline	$C_{23}H_{26}N_2O_3$	378.5	11.8	4.6425	1195380	0.092
16	Propyne, 1,3-diphenyl-	$C_{15}H_{12}$	192.25	11.9	4.657	303622	0.023
17	9-Phenanthrenecarboxylic acid	$C_{15}H_{10}O_2$	222.24	54.7	4.6825	145092	0.011
18	2-Phenyl-1H-indene	$C_{15}H_{12}$	192.25	12.5	4.7825	1048558	0.081
19	3-Methylphenanthrene	$C_{15}H_{12}$	192.25	17.3	4.8295	11412	0.001
20	Thiazole, 2-(phenylthio)-	$C_9H_7NS_2$	193.3	10.2	4.845	342056	0.026
21	8-Methylbenz[a]anthracene	$C_{19}H_{14}$	242.3	16.9	4.856	239767	0.019
22	Acetophenone	C_8H_8O	120.15	22.1	4.9015	205594	0.016
23	Valine	$C_5H_{11}NO_2$	117.15	14.7	4.9725	419614	0.032
24	Purine	$C_5H_4N_4$	120.11	34.5	5.006	458425	0.035
25	Indole	C_8H_7N	117.15	22.4	5.057	23405	0.002
26	Benz[c]acridine	$C_{17}H_{11}N$	229.27	32.7	5.072	75927	0.006
27	2-phenyl-2H-1,2,3-triazole	$C_8H_7N_3$	145.16	15	5.0895	17697	0.001
28	3-Nitro-9-vinylcarbazole	$C_{14}H_{10}N_2O_2$	238.24	11.9	5.1125	865771	0.067
29	Hydroquinone	$C_6H_6O_2$	110.11	16.8	5.127	164821	0.013
30	9-Phenanthrenemethyl cinnamate	$C_{24}H_{18}O_2$	338.4	17.2	5.1375	148643	0.011
31	2-Methylanthracene	$C_{15}H_{12}$	192.25	19.2	5.172	900985	0.070
32	7,8-Dimethylbenz(c)acridine	$C_{19}H_{15}N$	257.3	42.6	5.1925	83112	0.006
33	2-Amino-4-phenylthiazole	$C_9H_8N_2S$	176.24	8.12	5.217	392594	0.030
34	1-Methylanthracene	$C_{15}H_{12}$	192.25	11.4	5.229	32401	0.003
35	Benz[a]anthracene	$C_{18}H_{12}$	228.3	14.3	5.267	60504	0.005
36	1,4-Naphthoquinone	$C_{10}H_6O_2$	158.15	5.84	5.279	2706136	0.209
37	Morpholine-4-carboxylic acid	$C_5H_9NO_3$	131.13	38	5.302	25912	0.002
38	Phthalimide	$C_8H_5NO_2$	147.13	31.6	5.347	135882	0.010
39	Pyrrolidine-2-thione	C_4H_7NS	101.17	7.69	5.3765	2072944	0.160
40	8,9-Dihydrocyclopenta[def]phenanthrene	$C_{15}H_{12}$	192.25	35.3	5.3975	847285	0.065
41	4-Methylbenzoic acid	$C_8H_8O_2$	136.15	5.88	5.4145	53552	0.004
42	2-Aminopyrimidine	$C_4H_5N_3$	95.10	9.89	5.427	171442	0.013
43	l-Isoleucine	$C_6H_{13}NO_2$	131.17	5.57	5.4375	674564	0.052
44	2-Cyclohexen-1-one	C_6H_8O	96.13	11.1	5.4725	1669603	0.129
45	Benzofuran, 2-isopropenyl-3-methyl-	$C_{12}H_{12}O$	172.22	40.3	5.5045	1702843	0.131
46	Acetamide	C_2H_5NO	59.07	61.9	5.5465	180874660	13.958

47	3-Heptanone	$C_7H_{14}O$	114.19	70.5	5.698	14015797	1.082
48	Aniline	C_6H_7N	93.13	7.37	5.9075	736943	0.057
49	2,4-Dihydroxy-1,6-naphthyridine	$C_8H_6N_2O_2$	162.15	38.3	6.0345	337967	0.026
50	3-Methyl-3-pentanol	$C_6H_{14}O$	102.17	36.9	6.045	902500	0.070
51	1,1-Dicyclopropylethylene	C_8H_{12}	108.18	46.2	6.0875	174114	0.013
52	Ethylene Glycol	$C_2H_6O_2$	62.07	45.5	6.289	651804	0.050
53	Oxostephamiersine	$C_{21}H_{25}NO_7$	403.4	74.2	6.771	7297121	0.563
54	Acetamidine	$C_2H_6N_2$	58.08	75.4	6.773	45818684	3.536
55	Azetidine, 1-acetyl-2-methyl-	$C_6H_{11}NO$	113.16	71.3	7.13	962891	0.074
56	2-Ethylhexanal	$C_8H_{16}O$	128.21	86.9	7.2545	6345410	0.490
57	N,N,3,3-Tetramethylbutanamide	$C_8H_{17}NO$	143.23	15.3	7.7215	564087	0.044
58	Succinimide	$C_4H_5NO_2$	99.09	30.1	7.9415	269379	0.021
59	2,4,6-Trimethylpyridine	$C_8H_{11}N$	121.18	34.8	8.4045	1565350	0.121
60	2,4-Dimethyl-3-pentanol	$C_7H_{16}O$	116.20	47.6	8.7445	580242	0.045
61	Diethyl carbamate	$C_5H_{10}NO_2$	116.139	78.5	10.4405	1700788	0.131
62	2-Ethylhexyl formate	$C_9H_{18}O_2$	158.24	43.3	11.2515	21753363	1.679
63	Heptane	C_7H_{16}	100.20	19.8	11.6145	120741	0.009
64	6-Aza-2-thiothymine	$C_4H_5N_3OS$	143.17	61.1	12.0395	34277	0.003
65	[1,2,3]Triazolo[1,5-a]pyridine	$C_6H_5N_3$	119.12	12	12.0905	174462	0.013
66	Methylguanidine	$C_2H_7N_3$	73.10	14.4	12.153	241850	0.019
67	DL-Norleucine	$C_6H_{13}NO_2$	131.17	20.7	12.2125	44711	0.003
68	2,2'-Dithiodipyridine	$C_{10}H_8N_2S_2$	220.3	14.8	12.233	359058	0.028
69	Asparagine	$C_4H_8N_2O_3$	132.12	1	12.265	14987	0.001
70	Acetic acid	$C_2H_4O_2$	60.05	58.3	12.312	4091215	0.316
71	3,5-Dibutyl-2,3-dihydro-1H-inden-1-one	$C_{17}H_{24}O$	244.37	60.9	12.338	200930	0.016
72	Hexylcyclohexane	$C_{12}H_{24}$	168.32	43.1	12.38	787945	0.061
73	Tetrakis(4-cyanophenyl)ethylene	$C_{30}H_{16}N_4$	432.5	46	12.3955	2389761	0.184
74	Tert-butyl formate	$C_5H_{10}O_2$	102.13	22.2	12.4455	503852	0.039
75	1-Octanol	$C_8H_{18}O$	130.23	23.4	12.4575	3843038	0.297
76	Ethanol	C_2H_6O	46.07	63.8	12.672	54971	0.004
77	2-Ethylhexan-1-ol	$C_8H_{18}O$	130.23	78.3	12.7095	373114493	28.794
78	2(3H)-Furanone	$C_4H_4O_2$	84.07	16.1	12.7255	13110	0.001
79	3-Aminopiperidin-2-one	$C_5H_{10}N_2O$	114.15	24.4	13.539	238283	0.018
80	2-Buten-1-ol	C_4H_8O	72.11	11.9	14.0135	506426	0.039
81	Xanthotoxol	$C_{11}H_6O_4$	202.16	17.1	14.0275	14469376	1.117
82	2-Ethylhexanoic acid	$C_8H_{16}O_2$	144.21	97.6	14.0325	153106229	11.815
83	1H-pyrimidine-2,4-dione	$C_4H_4N_2O_2$	113.08	52.9	14.3645	6670836	0.515
84	Glutaric acid	$C_5H_8O_4$	132.11	5.08	15.912	652924	0.050
85	Glycidol	$C_3H_6O_2$	74.08	21.4	15.928	6780050	0.523
86	Benzoic acid	$C_7H_6O_2$	122.12	84.5	16.3575	1897575	0.146
87	Phosphoric acid	H_3PO_4	97.995	91.2	17.219	88648496	6.841
88	2-Propyl-1-pentanol	$C_8H_{18}O$	130.23	54.7	17.6475	2160275	0.167

89	4-Methyl-3-heptanol	$C_8H_{18}O$	130.23	15.8	18.423	739495	0.057
90	2-Ethylhexyl butyrate	$C_{12}H_{24}O_2$	200.32	86.3	18.5395	1981337	0.153
91	2-Methylacridine	$C_{14}H_{11}N$	193.24	16.4	18.953	67802	0.005
92	Isopentane	C_5H_{12}	72.15	48.3	18.9685	1267468	0.098
93	Methyl acetate	$C_3H_6O_2$	74.08	11.4	19.509	3697497	0.285
94	Pregnane-3,20-dione	$C_{21}H_{32}O_2$	316.5	12.6	19.931	2723221	0.210
95	n-hexane	C_6H_{14}	86.18	23	19.959	2789852	0.215
96	2-Ethyl-4-methylpentanoic acid	$C_8H_{16}O_2$	144.21	87.8	20.1715	1699579	0.131
97	Ethyl butyrate	$C_6H_{12}O_2$	116.16	27.9	20.5455	407172	0.031
98	Octanoic acid	$C_8H_{16}O_2$	144.21	31	20.729	1957770	0.151
99	Adamantane	$C_{10}H_{16}$	136.23	24.3	21.047	89108	0.007
100	2-Ethylhexyl valerate	$C_{13}H_{26}O_2$	214.34	64.5	21.084	1684184	0.130
101	1,2,4,5-Tetrazine	$C_2H_2N_4$	82.06	15.8	21.66	532615	0.041
102	Tetradecane	$C_{14}H_{30}$	198.39	38.5	22.03	648055	0.050
103	Methionine	$C_5H_{11}NO_2S$	149.21	90.5	23.645	49454	0.004
104	Proline	$C_5H_9NO_2$	115.13	76.6	23.6695	873384	0.067
105	Methyl diethylcarbamate	$C_6H_{13}NO_2$	131.17	42.9	24.2815	10474	0.001
106	Octanoic anhydride	$C_{16}H_{30}O_3$	270.41	9.44	24.595	621288	0.048
107	2-Methylundecane	$C_{12}H_{26}$	170.33	7.19	24.601	323250	0.025
108	4,6-Dimethyldodecane	$C_{14}H_{30}$	198.39	4.33	24.6055	716204	0.055
109	Octyl octanoate	$C_{16}H_{32}O_2$	256.42	10.4	25.2345	2036376	0.157
110	Hexanoic acid	$C_6H_{12}O_2$	116.16	94.4	25.6485	42998672	3.318
111	3-Methyloctane	C_9H_{20}	128.25	17.8	27.2625	740214	0.057
112	3-Heptyne	C_7H_{12}	96.17	10.2	27.266	192945	0.015
113	Heptacosane	$C_{27}H_{56}$	380.7	6.16	27.9945	2106381	0.163
114	Cyperaquinone	$C_{14}H_{10}O_4$	242.23	22.2	28.2135	37749	0.003
115	2,6-Diisopropylnaphthalene	$C_{16}H_{20}$	212.33	71.9	28.4355	365406	0.028
116	2,6,11,15-Tetramethylhexadecane	$C_{20}H_{42}$	282.5	7.62	28.9615	2145293	0.166
117	Terephthalic acid	$C_8H_6O_4$	166.13	93.2	29.8565	1036899	0.080
118	D-allofuranose	$C_6H_{12}O_6$	180.16	25.2	31.0645	2060918	0.159
119	2-Decanol	$C_{10}H_{22}O$	158.28	8.81	31.1155	2574331	0.199
120	D-Galactose	$C_6H_{12}O_6$	180.16	9.1	32.0315	21322151	1.645
121	Heneicosane	$C_{21}H_{44}$	296.6	6.91	32.453	2761732	0.213
122	Hentriacontane	$C_{31}H_{64}$	436.8	5.79	33.305	3506896	0.271
123	trans-2-Octenoic acid	$C_8H_{14}O_2$	142.20	42.3	33.329	381726	0.029
124	D-Talose	$C_6H_{12}O_6$	180.16	8.38	33.8355	39740872	3.067
125	Octane	C_8H_{18}	114.23	12.9	34.937	6131554	0.473
126	Palmitic acid	$C_{16}H_{32}O_2$	256.42	97.4	35.0545	17472461	1.348
127	2-Methyloctadecane	$C_{19}H_{40}$	268.5	5.36	36.485	2279073	0.176
128	Pentacosane	$C_{25}H_{52}$	352.7	8.61	37.253	2116825	0.163
129	D-Glucose	$C_6H_{12}O_6$	180.16	10.1	38.0535	2937500	0.227
130	Bisphenol A	$C_{15}H_{16}O_2$	228.29	72.3	38.139	11561436	0.892

131	Elaidic acid	$C_{18}H_{34}O_2$	282.5	23.2	38.1465	6210055	0.479
132	trans-Vaccenic acid	$C_{18}H_{34}O_2$	282.5	22.1	38.2695	2464624	0.190
133	Arachidonic acid	$C_{20}H_{32}O_2$	304.5	52	40.6735	1042278	0.080
134	Oleonitrile	$C_{18}H_{33}N$	263.5	68.4	42.7295	692471	0.053
135	Stearic acid	$C_{18}H_{36}O_2$	284.5	92.3	47.049	9582727	0.740
136	Cholesterol	$C_{27}H_{46}O$	386.7	79.7	51.92	107249824	8.277
137	Methyl alpha-D-galactopyranoside	$C_7H_{14}O_6$	194.18	23.8	52.0145	5981297	0.462

- **Enrichment analysis**

Disease signatures (Figure 22.2 and Table 14.2), metabolites enrichment from the KEGG database (Figure 22.3 and Table 14.3) and the SMPDB database (Figure 22.4 and Table 14.4), and different classes of metabolites (Figure 22.5 and Table 14.5) are given below. The enrichment ratio is no. of hits observed divided by no. of hits expected.

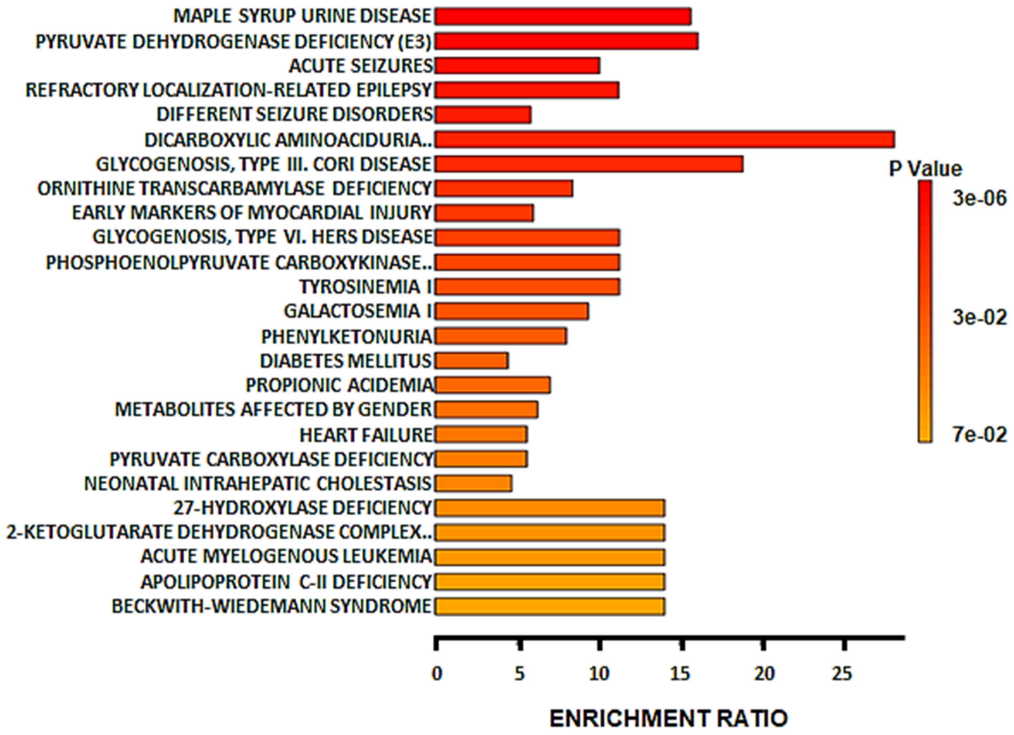

Figure 22.2: Disease signatures in glucose-treated cells

The top 25 disease signatures were identified. Significantly enriched signatures (↓) include maple syrup urine disease, pyruvate dehydrogenase deficiency (E3), acute seizures, refractory

localization-related epilepsy, and different seizure disorders. Highly enriched signatures (←) include dicarboxylic aminoaciduria, type III cori disease, pyruvate dehydrogenase deficiency (E3), maple syrup urine disease, 27-hydroxylase deficiency, 2-ketoglutarate dehydrogenase complex deficiency, acute myelogenous leukemia, apolipoprotein C-II deficiency, and beckwith-wiedemann syndrome.

Table 14.2: Disease signatures in glucose-treated cells

	Metabolite Set	Total	Hits	Expect	P Value	Holm P	FDR
	MAPLE SYRUP URINE DISEASE	9	5	0.319	3.48E-6	9.5E-4	9.5E-4
	PYRUVATE DEHYDROGENASE DEFICIENCY (E3)	7	4	0.248	3.6E-5	0.00979	0.00452
	ACUTE SEIZURES	14	5	0.497	4.96E-5	0.0135	0.00452
	REFRACTORY LOCALIZATION-RELATED EPILEPSY	10	4	0.355	2.02E-4	0.0545	0.0138
	DIFFERENT SEIZURE DISORDERS	24	5	0.852	8.49E-4	0.228	0.0463
	DICARBOXYLIC AMINOACIDURIA. GLUTAMATE-ASPARTATE TRANSPORT DEFECT	2	2	0.071	0.00119	0.318	0.0541
	GLYCOGENOSIS, TYPE III. CORI DISEASE, DEBRANCHER GLYCOGENOSIS	3	2	0.106	0.00349	0.932	0.131
	ORNITHINE TRANSCARBAMYLASE DEFICIENCY (OTC)	10	3	0.355	0.00383	1.0	0.131
	EARLY MARKERS OF MYOCARDIAL INJURY	14	3	0.497	0.0106	1.0	0.254
	GLYCOGENOSIS (TYPE IA, IB, IC) | GLYCOGENOSIS, TYPE VI. HERS DISEASE	5	2	0.177	0.0111	1.0	0.254
	PHOSPHOENOLPYRUVATE CARBOXYKINASE DEFICIENCY 2 (PEPCK2)	5	2	0.177	0.0111	1.0	0.254
	TYROSINEMIA I	5	2	0.177	0.0111	1.0	0.254
	GALACTOSEMIA I	6	2	0.213	0.0164	1.0	0.344
	85PHENYLKETONURIA	7	2	0.248	0.0224	1.0	0.438
	DIABETES MELLITUS (MODY), NON-INSULIN-DEPENDENT	19	3	0.674	0.0253	1.0	0.454
	PROPIONIC ACIDEMIA	8	2	0.284	0.0293	1.0	0.454
	METABOLITES AFFECTED BY GENDER	9	2	0.319	0.0369	1.0	0.454
	HEART FAILURE	10	2	0.355	0.0452	1.0	0.454

	PYRUVATE CARBOXYLASE DEFICIENCY	10	2	0.355	0.0452	1.0	0.454
	NEONATAL INTRAHEPATIC CHOLESTASIS	12	2	0.426	0.0635	1.0	0.454
	27-HYDROXYLASE DEFICIENCY	2	1	0.071	0.0698	1.0	0.454
	2-KETOGLUTARATE DEHYDROGENASE COMPLEX DEFICIENCY	2	1	0.071	0.0698	1.0	0.454
	ACUTE MYELOGENOUS LEUKEMIA	2	1	0.071	0.0698	1.0	0.454
	APOLIPOPROTEIN C-II DEFICIENCY | CHOLESTERYL ESTER STORAGE DISEASE | GLYCOGENOSIS, TYPE IXB	2	1	0.071	0.0698	1.0	0.454
	BECKWITH-WIEDEMANN SYNDROME. EXOMPHALOS-MAKROGLOSSIA-GIGANTISM SYNDROME | EXERCISE-INDUCED-HYPERINSULINSM [EIHI] | HYPOGLYCEMIA, FAMILIAL NEONATAL	2	1	0.071	0.0698	1.0	0.454

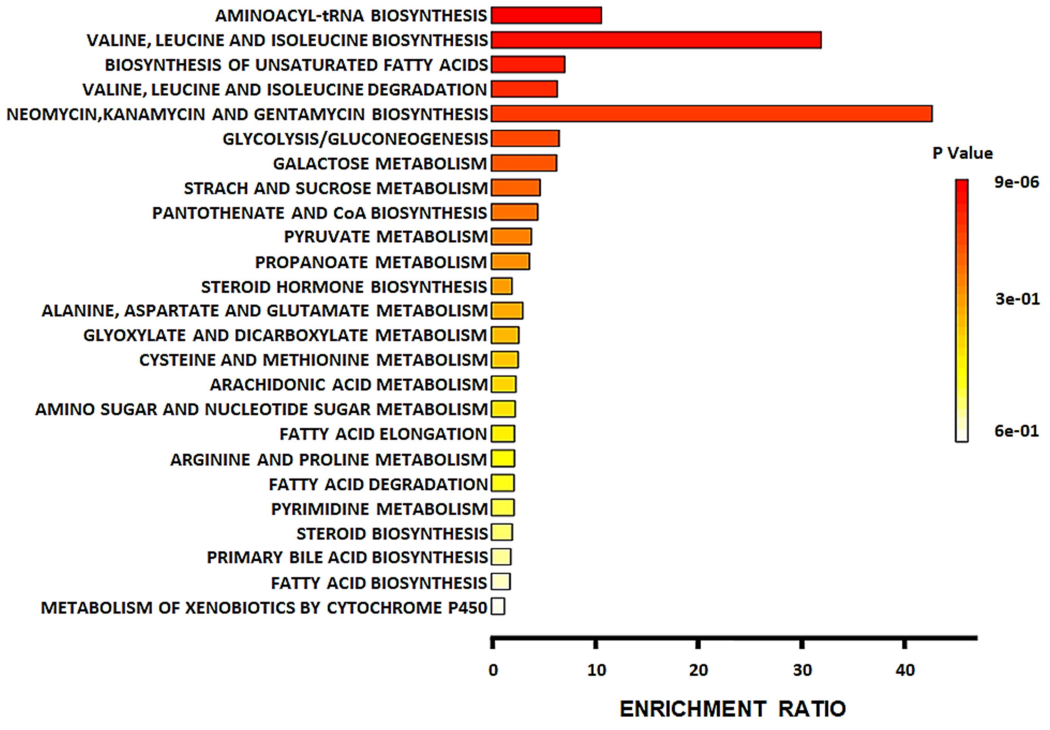

Figure 22.3: Glucose-specific metabolites enrichment from the KEGG database

The top 25 metabolic pathways were identified. Significantly enriched pathways (↓) include aminoacyl t-RNA biosynthesis, valine, leucine, and isoleucine biosynthesis, biosynthesis of

unsaturated fatty acids, valine, leucine, and isoleucine degradation, and neomycin, kanamycin, and gentamycin biosynthesis. Highly enriched pathways (←) include neomycin, kanamycin, and gentamycin biosynthesis, valine, leucine, and isoleucine biosynthesis, aminoacyl t-RNA biosynthesis, biosynthesis of unsaturated fatty acids, and glycolysis/gluconeogenesis.

Table 14.3: Glucose-specific metabolites enrichment from the KEGG database

	Metabolite Set	Total	Hits	Expect	P value	Holm P	FDR
	Aminoacyl-tRNA biosynthesis	48	6	0.562	9.48E-6	7.96E-4	7.96E-4
	Valine, leucine, and isoleucine biosynthesis	8	3	0.0938	7.31E-5	0.00606	0.00307
	Biosynthesis of unsaturated fatty acids	36	3	0.422	0.00758	0.622	0.212
	Valine, leucine and isoleucine degradation	40	3	0.469	0.0102	0.825	0.214
	Neomycin, kanamycin, and gentamicin biosynthesis	2	1	0.0234	0.0233	1.0	0.392
	Glycolysis / Gluconeogenesis	26	2	0.305	0.0357	1.0	0.46
	Galactose metabolism	27	2	0.316	0.0383	1.0	0.46
	Starch and sucrose metabolism	18	1	0.211	0.192	1.0	1.0
	Pantothenate and CoA biosynthesis	19	1	0.223	0.202	1.0	1.0
	Pyruvate metabolism	22	1	0.258	0.23	1.0	1.0
	Propanoate metabolism	23	1	0.27	0.239	1.0	1.0
	Steroid hormone biosynthesis	85	2	0.996	0.263	1.0	1.0
	Alanine, aspartate and glutamate metabolism	28	1	0.328	0.283	1.0	1.0
	Glyoxylate and dicarboxylate metabolism	32	1	0.375	0.317	1.0	1.0
	Cysteine and methionine metabolism	33	1	0.387	0.325	1.0	1.0
	Arachidonic acid metabolism	36	1	0.422	0.349	1.0	1.0
	Amino sugar and nucleotide sugar metabolism	37	1	0.434	0.357	1.0	1.0
	Fatty acid elongation	38	1	0.445	0.365	1.0	1.0
	Arginine and proline metabolism	38	1	0.445	0.365	1.0	1.0
	Fatty acid degradation	39	1	0.457	0.372	1.0	1.0
	Pyrimidine metabolism	39	1	0.457	0.372	1.0	1.0
	Steroid biosynthesis	42	1	0.492	0.395	1.0	1.0
	Primary bile acid biosynthesis	46	1	0.539	0.423	1.0	1.0
	Fatty acid biosynthesis	47	1	0.551	0.43	1.0	1.0
	Metabolism of xenobiotics by cytochrome P450	68	1	0.797	0.559	1.0	1.0

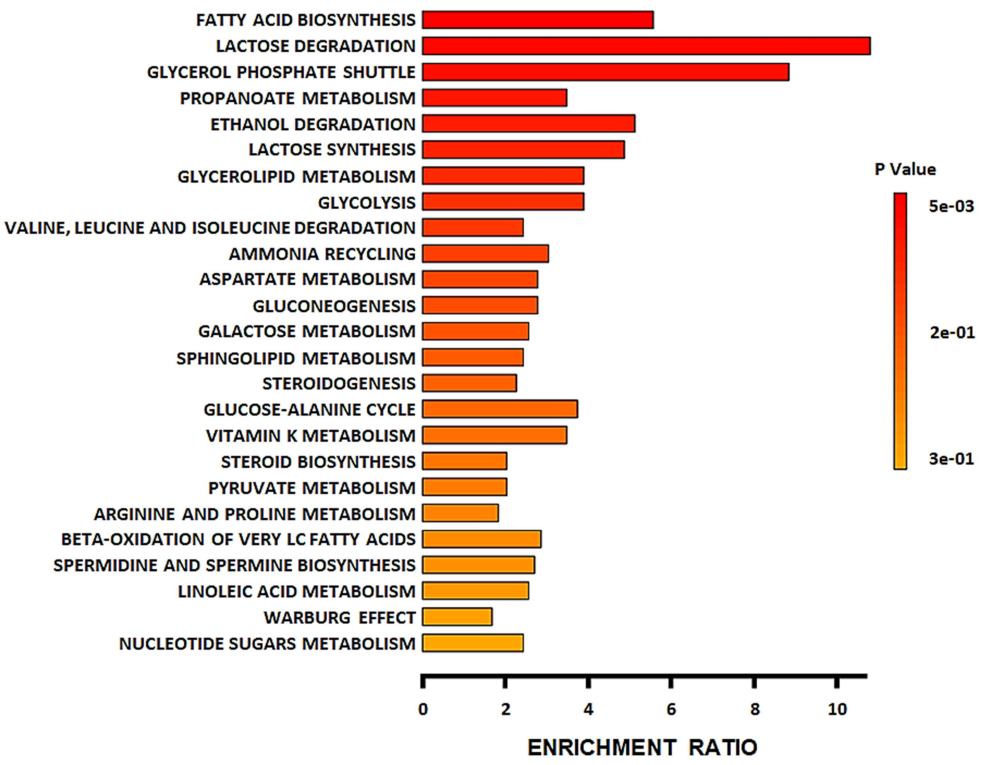

Figure 22.4: Glucose-specific metabolites enrichment from the SMPDB database

The top 25 metabolic pathways were identified. Significantly enriched pathways (↓) include fatty acid biosynthesis, lactose degradation, glycerol phosphate shuttle, propanoate metabolism, and ethanol degradation. Highly enriched pathways (←) include lactose degradation, glycerol phosphate shuttle, fatty acid biosynthesis, ethanol degradation, and lactose synthesis.

Table 14.4: Glucose-specific metabolites enrichment from the SMPDB database

	Metabolite Set	Total	Hits	Expect	P Value	Holm P	FDR
	Fatty acid biosynthesis	35	4	0.718	0.00453	0.444	0.444
	Lactose degradation	9	2	0.185	0.0132	1.0	0.644
	Glycerol phosphate shuttle	11	2	0.226	0.0197	1.0	0.644
	Propanoate metabolism	42	3	0.861	0.051	1.0	0.996
	Ethanol degradation	19	2	0.39	0.0555	1.0	0.996
	Lactose synthesis	20	2	0.41	0.061	1.0	0.996
	Glycerolipid metabolism	25	2	0.513	0.0905	1.0	1.0
	Glycolysis	25	2	0.513	0.0905	1.0	1.0
	Valine, leucine and isoleucine degradation	60	3	1.23	0.12	1.0	1.0

	Ammonia recycling	32	2	0.656	0.137	1.0	1.0
	Aspartate metabolism	35	2	0.718	0.159	1.0	1.0
	Gluconeogenesis	35	2	0.718	0.159	1.0	1.0
	Galactose metabolism	38	2	0.779	0.181	1.0	1.0
	Sphingolipid metabolism	40	2	0.82	0.196	1.0	1.0
	Steroidogenesis	43	2	0.882	0.219	1.0	1.0
	Glucose-alanine cycle	13	1	0.267	0.237	1.0	1.0
	Vitamin K metabolism	14	1	0.287	0.253	1.0	1.0
	Steroid biosynthesis	48	2	0.984	0.258	1.0	1.0
	Pyruvate metabolism	48	2	0.984	0.258	1.0	1.0
	Arginine and proline metabolism	53	2	1.09	0.297	1.0	1.0
	Beta oxidation of very long chain fatty acids	17	1	0.349	0.299	1.0	1.0
	Spermidine and spermine biosynthesis	18	1	0.369	0.313	1.0	1.0
	Alpha linolenic acid and linoleic acid metabolism	19	1	0.39	0.328	1.0	1.0
	Warburg effect	58	2	1.19	0.336	1.0	1.0
	Nucleotide sugars metabolism	20	1	0.41	0.342	1.0	1.0

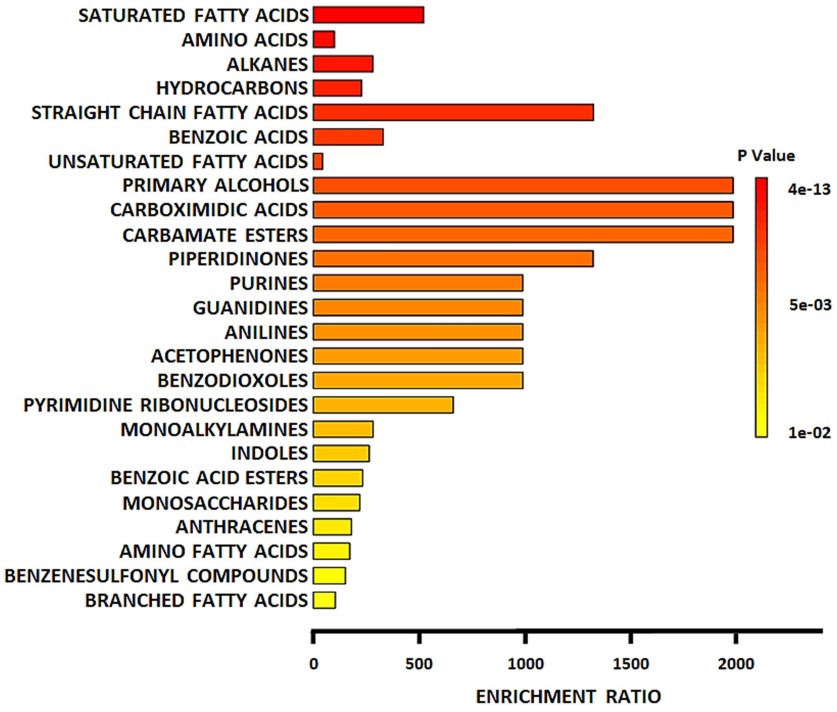

Figure 22.5: Different classes of identified metabolites in glucose-treated cells

The top 25 different classes of metabolites were identified. Significantly enriched classes (↓) include saturated fatty acids, amino acids, alkanes, hydrocarbons, and straight-chain fatty acids.

Highly enriched classes (←) include primary alcohols, carboximidic acids, carbamate esters, straight-chain fatty acids, and piperidinones.

Table 14.5: Different classes of identified metabolites in glucose-treated cells

	Metabolite Set	Total	Hits	Expect	P Value	Holm P	FDR
	Saturated fatty acids	38	5	0.00958	4.14E-13	3.02E-10	3.02E-10
	Amino acids	277	7	0.0698	9.13E-13	6.66E-10	3.34E-10
	Alkanes	42	3	0.0106	1.72E-7	1.25E-4	4.19E-5
	Hydrocarbons	52	3	0.0131	3.3E-7	2.41E-4	6.04E-5
	Straight-chain fatty acids	6	2	0.00151	9.34E-7	6.79E-4	1.37E-4
	Benzoic acids	24	2	0.00605	1.71E-5	0.0124	0.00209
	Unsaturated fatty acids	267	3	0.0673	4.51E-5	0.0327	0.00471
	Primary alcohols	2	1	5.04E-4	5.04E-4	0.365	0.0369
	Carboximidic acids	2	1	5.04E-4	5.04E-4	0.365	0.0369
	Carbamate esters	2	1	5.04E-4	5.04E-4	0.365	0.0369
	Piperidinones	3	1	7.56E-4	7.56E-4	0.545	0.0461
	Purines	4	1	0.00101	0.00101	0.726	0.0461
	Guanidines	4	1	0.00101	0.00101	0.726	0.0461
	Anilines	4	1	0.00101	0.00101	0.726	0.0461
	Acetophenones	4	1	0.00101	0.00101	0.726	0.0461
	Benzodioxoles	4	1	0.00101	0.00101	0.726	0.0461
	Pyrimidine ribonucleosides	6	1	0.00151	0.00151	1.0	0.065
	Monoalkylamines	14	1	0.00353	0.00352	1.0	0.143
	Indoles	15	1	0.00378	0.00378	1.0	0.145
	Benzoic acid esters	17	1	0.00429	0.00428	1.0	0.156
	Monosaccharides	18	1	0.00454	0.00453	1.0	0.158
	Anthracenes	22	1	0.00555	0.00553	1.0	0.184
	Amino fatty acids	23	1	0.0058	0.00578	1.0	0.184
	Benzenesulfonyl compounds	26	1	0.00656	0.00654	1.0	0.199
	Branched fatty acids	38	1	0.00958	0.00954	1.0	0.279

- **Pathway analysis**

Impacted pathways from the KEGG database (Figure 22.6 and Table 14.6), and the SMPDB database (Figure 22.7 and Table 14.7) are given below. Pathway impact is calculated by using centrality and pathway enrichment results.

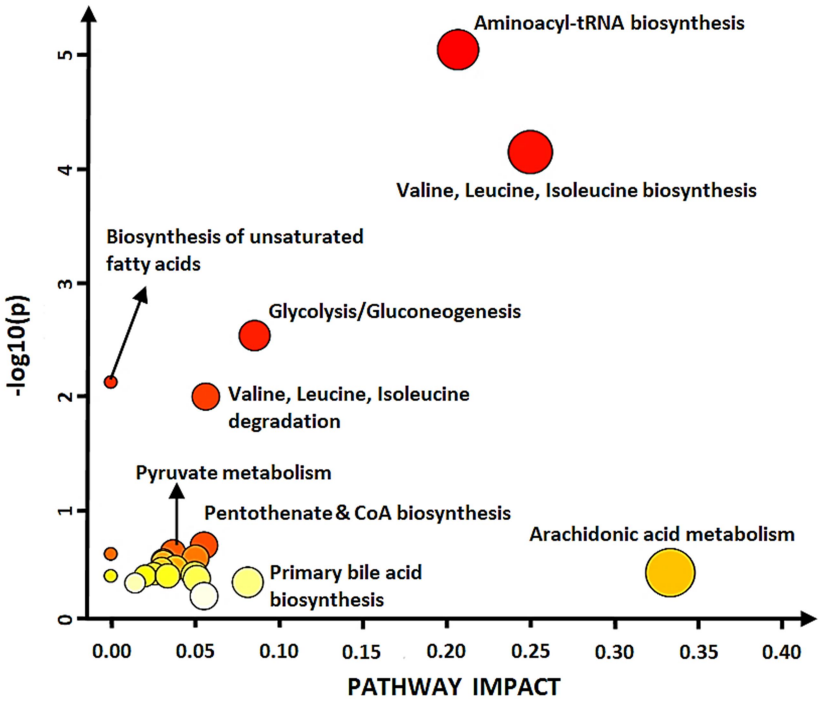

Figure 22.6: Glucose-specific pathway analysis from the KEGG database

The top 23 impacted pathways were identified. Highly impacted pathways (←) include arachidonic acid metabolism, valine, leucine, and isoleucine biosynthesis, aminoacyl t-RNA biosynthesis, glycolysis/gluconeogenesis, and primary bile acid biosynthesis. Significantly impacted pathways (↓) include aminoacyl t-RNA biosynthesis, valine, leucine, and isoleucine biosynthesis, glycolysis/gluconeogenesis, biosynthesis of unsaturated fatty acids, and valine, leucine, and isoleucine degradation.

Table 14.6: Glucose-specific pathway analysis from the KEGG database

Pathway Name	Match Status	p	-log(p)	Holm p	FDR	Impact
Aminoacyl-tRNA biosynthesis	6/48	8.9977E-6	5.0459	7.558E-4	7.558E-4	0.20688
Valine, leucine, and isoleucine biosynthesis	3/8	7.1126E-5	4.148	0.0059034	0.0029873	0.25
Glycolysis / Gluconeogenesis	3/26	0.0028956	2.5383	0.23744	0.081077	0.08571
Biosynthesis of unsaturated fatty acids	3/36	0.007392	2.1312	0.59875	0.15523	0.0
Valine, leucine, and isoleucine degradation	3/40	0.0099344	2.0029	0.79475	0.1669	0.05661

Pantothenate and CoA biosynthesis	1/19	0.20008	0.6988	1.0	1.0	0.05556
Pyruvate metabolism	1/22	0.22798	0.6421	1.0	1.0	0.03704
Propanoate metabolism	1/23	0.23708	0.62511	1.0	1.0	0.0
Steroid hormone biosynthesis	2/85	0.25911	0.58652	1.0	1.0	0.0505
Galactose metabolism	1/27	0.27245	0.56471	1.0	1.0	0.03125
Alanine, aspartate and glutamate metabolism	1/28	0.28105	0.55122	1.0	1.0	0.03125
Glyoxylate and dicarboxylate metabolism	1/32	0.31449	0.50239	1.0	1.0	0.03846
Cysteine and methionine metabolism	1/33	0.32262	0.4913	1.0	1.0	0.0303
Arachidonic acid metabolism	1/36	0.34647	0.46034	1.0	1.0	0.33333
Amino sugar and nucleotide sugar metabolism	1/37	0.35424	0.45071	1.0	1.0	0.02564
Arginine and proline metabolism	1/38	0.36192	0.44139	1.0	1.0	0.05
Fatty acid elongation	1/39	0.36951	0.43237	1.0	1.0	0.0
Fatty acid degradation	1/39	0.36951	0.43237	1.0	1.0	0.02041
Pyrimidine metabolism	1/39	0.36951	0.43237	1.0	1.0	0.0339
Steroid biosynthesis	1/42	0.39179	0.40694	1.0	1.0	0.05128
Primary bile acid biosynthesis	1/46	0.42035	0.37639	1.0	1.0	0.08163
Fatty acid biosynthesis	1/47	0.42728	0.36928	1.0	1.0	0.01449
Metabolism of xenobiotics by cytochrome P450	1/68	0.55607	0.25487	1.0	1.0	0.05556

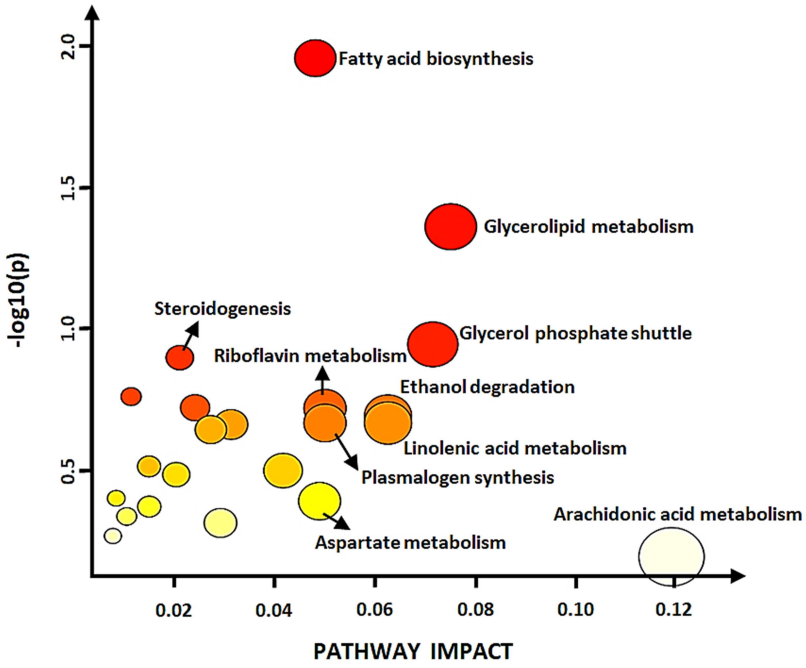

Figure 22.7: Glucose-specific pathway analysis from the SMPDB database

The top 22 impacted pathways were identified. Highly impacted pathways (←) include arachidonic acid metabolism, glycerolipid metabolism, glycerol phosphate shuttle, linolenic acid metabolism, and ethanol degradation. Significantly impacted pathways (↓) include fatty acid biosynthesis, glycerolipid metabolism, glycerol phosphate shuttle, steroidogenesis, and valine, leucine, and isoleucine degradation.

Table 14.7: Glucose-specific pathway analysis from the SMPDB database

Pathway Name	Match Status	p	-log(p)	Holm p	FDR	Impact
Fatty acid biosynthesis	3/33	0.011099	1.9547	1.0	1.0	0.048077
Glycerolipid metabolism	2/23	0.043596	1.3605	1.0	1.0	0.075
Glycerol phosphate shuttle	1/8	0.1133	0.94579	1.0	1.0	0.071429
Steroidogenesis	2/42	0.12615	0.8991	1.0	1.0	0.021116
Valine, leucine, and isoleucine degradation	2/51	0.1731	0.76171	1.0	1.0	0.011429
Pyrimidine metabolism	2/54	0.18941	0.72259	1.0	1.0	0.024155
Riboflavin metabolism	1/14	0.19028	0.72061	1.0	1.0	0.05
Ethanol degradation	1/15	0.20248	0.69361	1.0	1.0	0.0625
Plasmalogen synthesis	1/16	0.21452	0.66854	1.0	1.0	0.05
Alpha linolenic acid and linoleic acid metabolism	1/16	0.21452	0.66854	1.0	1.0	0.0625
Bile acid biosynthesis	2/59	0.21714	0.66327	1.0	1.0	0.031311
Mitochondrial beta-oxidation of short chain saturated fatty acids	1/17	0.22638	0.64515	1.0	1.0	0.027273
Mitochondrial beta-oxidation of long chain saturated fatty acids	1/24	0.30487	0.51588	1.0	1.0	0.015
Ammonia recycling	1/25	0.31546	0.50106	1.0	1.0	0.041667
Starch and sucrose metabolism	1/26	0.32589	0.48692	1.0	1.0	0.020408
Fatty acid elongation in mitochondria	1/33	0.39489	0.40353	1.0	1.0	0.0084746
Aspartate metabolism	1/34	0.40419	0.39342	1.0	1.0	0.048913
Porphyrin metabolism	1/36	0.42239	0.37429	1.0	1.0	0.015038
Fatty Acid metabolism	1/40	0.45724	0.33985	1.0	1.0	0.010563
Steroid biosynthesis	1/43	0.48209	0.31688	1.0	1.0	0.029197
Glycine and serine metabolism	1/50	0.53599	0.27085	1.0	1.0	0.0078125
Arachidonic acid metabolism	1/65	0.63435	0.19767	1.0	1.0	0.11888

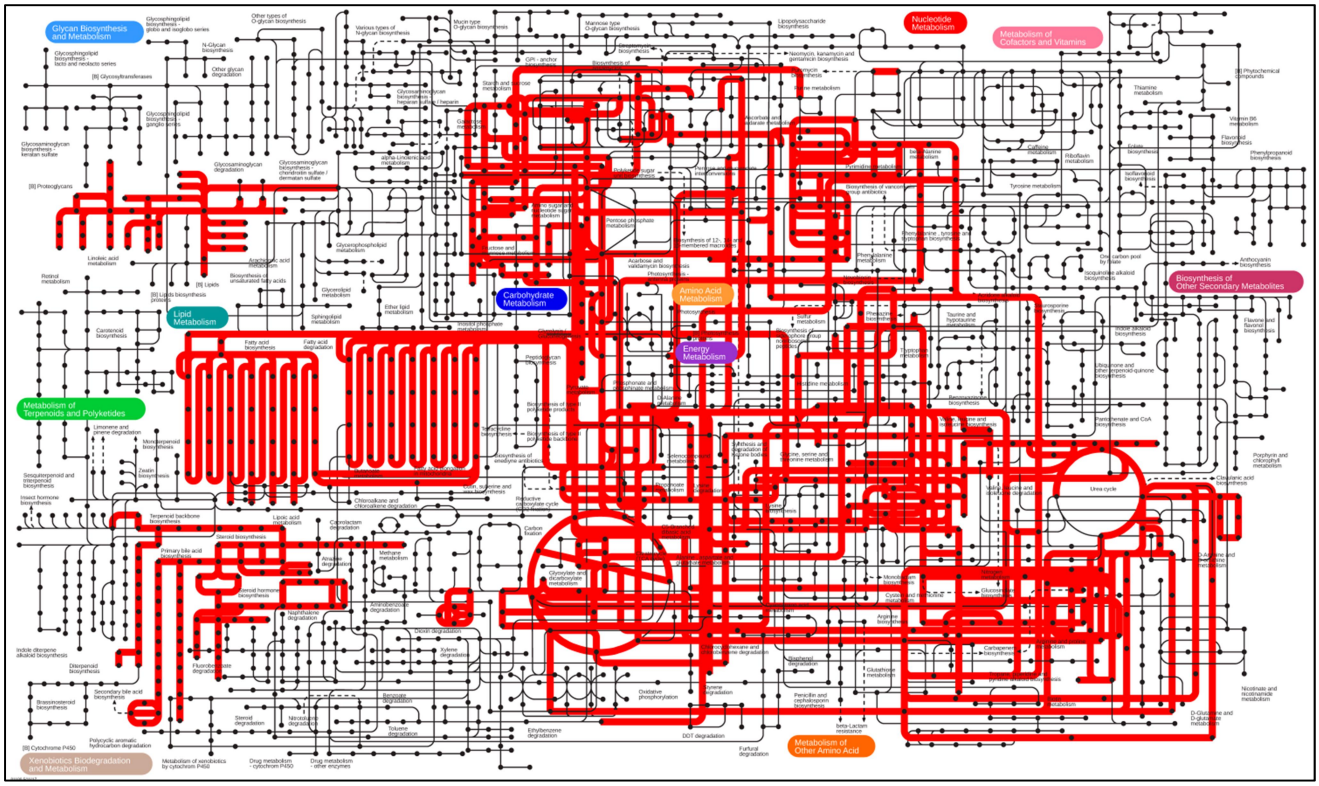

Figure 22.8: Metabolic pathways enriched in glucose treatment after mapping with the KEGG database. The highlighted metabolisms show enrichment specific to glucose treatment. This shows enrichment of energy metabolism, amino acid metabolism, carbohydrate metabolism, and other metabolic pathways.

III. High palmitic acid treatment

Cells were treated with 800 µM palmitic acid media for 24 hours.

➢ GC-MS graph

GC chromatogram of palmitic acid treatment (given in Figure 23.1) depicts retention time (min) on X-axis and relative abundance (intensity) on Y-axis. A total of 211 metabolites (components) were identified in palmitic acid-treated cells (given in Table 15.1). The most abundant metabolites are – 2-Ethylhexan-1-ol (33.58%), 2-Ethylhexanoic acid (15.707%), Phosphoric acid (14.908%), Acetamide (7.948%), and 2-Ethylhexyl 2-ethylhexanoate (4.397%). The abundance is measured based on the % area of the peak of specific components.

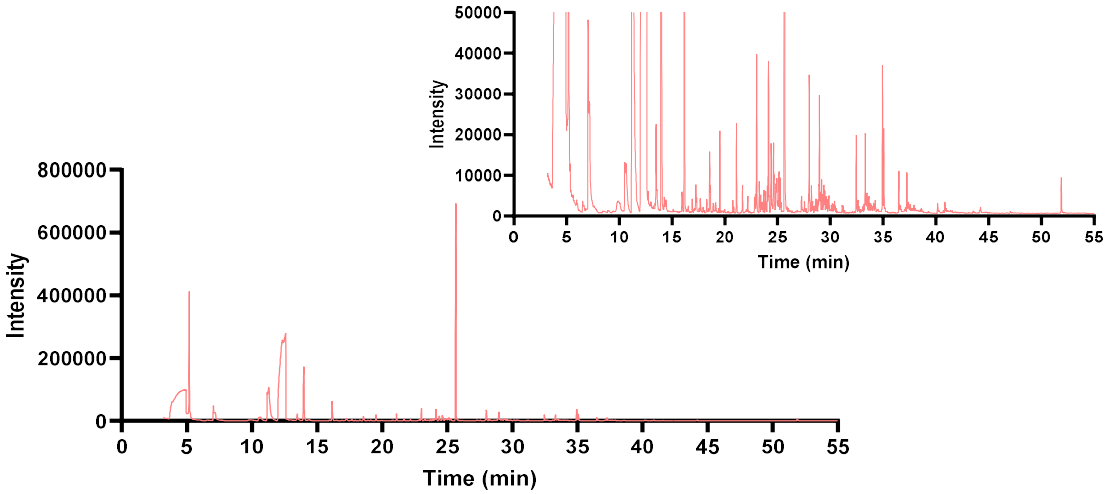

Figure 23.1: GC-MS graph obtained for palmitic acid treatment

Table 15.1: Metabolites identified in palmitic acid-treated cells

S.No.	Metabolites	Mol. Formula	MW (g/mol)	% Probability	RT (min)	Area	% Area
1	3-Cyclopentylpropionic acid	$C_8H_{14}O_2$	142.20	21	3.303	12006	0.002
2	D-proline	$C_5H_9NO_2$	115.13	5.52	3.3975	46159	0.007
3	D-Norleucine	$C_6H_{13}NO_2$	131.17	4.91	3.44	118165	0.017
4	1,3,6,9b-Tetraazaphenalene	$C_9H_6N_4$	170.17	34.5	3.494	108459	0.016
5	Parabanic acid	$C_3H_2N_2O_3$	114.06	5.3	3.683	27854	0.004
6	Morpholine	C_4H_9NO	87.12	33.2	3.7695	8103	0.001
7	Butyric Acid	$C_4H_8O_2$	88.11	73.4	3.8805	160842	0.023

8	N-Methyl-4-nitrobenzamide	$C_8H_8N_2O_3$	180.16	23.3	3.94	4777	0.001
9	Oxostephamiersine	$C_{21}H_{25}NO_7$	403.4	86.4	4.0945	4317415	0.631
10	5,5-Dimethylcyclohex-2-enone	$C_8H_{12}O$	124.18	29	4.113	1730421	0.253
11	2,6-Piperidinedione, 3-ethyl-3-phenyl-, (3R)-	$C_{13}H_{15}NO_2$	217.26	33.4	4.171	1194874	0.175
12	1,4,7-Trioxa-10-azacyclododecane	$C_8H_{17}NO_3$	175.23	7.31	4.2515	1716786	0.251
13	Leucine	$C_6H_{13}NO_2$	131.17	6.84	4.3295	2881913	0.421
14	6-Methoxy-2-methyl-1,2,3,4-tetrahydroisoquinoline	$C_{11}H_{15}NO$	177.24	64.9	4.386	508226	0.074
15	Phenanthridine	$C_{13}H_9N$	179.22	25.5	4.409	1956707	0.286
16	Thiazole, 2-(phenylthio)-	$C_9H_7NS_2$	193.3	13.7	4.486	745594	0.109
17	Di-tert-butyl disulfide	$C_8H_{18}S_2$	178.4	23	4.4915	1312	0.000
18	Dehydroemetine	$C_{29}H_{38}N_2O_4$	478.6	23.9	4.5295	1445104	0.211
19	1,2,3,4-Tetrahydroisoquinoline	$C_9H_{11}N$	133.19	14.2	4.533	39667	0.006
20	5,11-Dihydropyrido[2,3-b][1,4]benzodiazepin-6-one	$C_{12}H_9N_3O$	211.22	19.6	4.5405	948502	0.139
21	2-Methylanthracene	$C_{15}H_{12}$	192.25	21.4	4.5515	3874	0.001
22	3,5-Diacetyl-1,4-dihydrolutidine	$C_{11}H_{15}NO_2$	193.24	47.1	4.624	790953	0.116
23	2,5-Dimethyl-1,3,4-thiadiazole	$C_4H_6N_2S$	114.17	64.9	4.662	65182	0.010
24	Quinoline-4-carbothioamide	$C_{10}H_8N_2S$	188.25	24.8	4.7225	668241	0.098
25	Tridecane	$C_{13}H_{28}$	184.36	49.2	4.742	539916	0.079
26	1H-pyrazolo[3,4-b]quinolin-3-amine	$C_{10}H_8N_4$	184.20	7.44	4.754	1202438	0.176
27	Isoquinoline	C_9H_7N	129.16	16.6	4.765	980122	0.143
28	3-Phenylindole	$C_{14}H_{11}N$	193.24	25.1	4.778	594399	0.087
29	Thiophene-2-thiol	$C_4H_4S_2$	116.2	18.4	4.796	774536	0.113
30	Acetamide	C_2H_5NO	59.07	66	4.9225	54404648	7.948
31	1,3-Dioxolane	$C_3H_6O_2$	74.08	53	4.939	8184896	1.196
32	2H-Benzimidazole-2-thione	$C_7H_4N_2S$	148.19	33.2	4.9525	58958	0.009
33	2-Hydroxy-1,4-naphthoquinone	$C_{10}H_6O_3$	174.15	35.8	5.068	322080	0.047
34	Alanine	$C_3H_7NO_2$	89.09	4.35	5.095	7625	0.001
35	Isobutyric acid	$C_4H_8O_2$	88.11	44.6	5.142	486087	0.071
36	3-Heptanone	$C_7H_{14}O$	114.19	68.3	5.1815	4512118	0.659
37	1,4-Dimethyl-3-n-octadecylcyclohexane	$C_{26}H_{52}$	364.7	53.3	5.2715	125850	0.018
38	2(1H)-Quinazolinone	$C_8H_6N_2O$	146.15	15	5.4005	12961	0.002
39	4-Nitrophenyl benzoate	$C_{13}H_9NO_4$	243.21	11.8	5.5035	212725	0.031
40	n-Hexane	C_6H_{14}	86.18	38.3	5.581	80249	0.012
41	Fumaric Acid	$C_4H_4O_4$	116.07	6.82	5.612	92024	0.013
42	2-Butene	C_4H_8	56.11	12.1	5.691	89623	0.013
43	Thiourea	CH_4N_2S	76.12	19.9	5.7215	43176	0.006
44	(S)-3-Ethyl-4-methylpentanol	$C_8H_{18}O$	130.23	15.8	5.952	95853	0.014
45	N,N'-Diacetylethylenediamine	$C_6H_{12}N_2O_2$	144.17	32.8	6.4	63235	0.009
46	2-Ethyl-1-butanol	$C_6H_{14}O$	102.17	16.3	6.495	18546	0.003

47	Acetamidine	$C_2H_6N_2$	58.08	69.5	6.52	12090354	1.766
48	2,4-Dimethylpyridine	C_7H_9N	107.15	11.4	6.5495	149846	0.022
49	Acetone	C_3H_6O	58.08	52.7	6.6455	2371707	0.346
50	N-(2-Methoxy-phenyl)-formamide	$C_8H_9NO_2$	151.16	45.5	6.7875	6051	0.001
51	Methylenediformamide	$C_3H_6N_2O_2$	102.09	46.7	6.972	9199	0.001
52	2-Ethylhexanal	$C_8H_{16}O$	128.21	80.8	7.033	1021833	0.149
53	Benzoic anhydride	$C_{14}H_{10}O_3$	226.23	16.2	7.78	35211	0.005
54	2,4,6-Trimethylpyridine	$C_8H_{11}N$	121.18	21.2	8.3735	156768	0.023
55	2,3,6-Trimethylpyridine	$C_8H_{11}N$	121.18	30.6	8.381	4814	0.001
56	4-Methyl-3-heptanol	$C_8H_{18}O$	130.23	25.1	9.02	703557	0.103
57	Butane	C_4H_{10}	58.12	5.61	9.0505	245665	0.036
58	Ethyl diethylcarbamate	$C_7H_{15}NO_2$	145.20	56.4	10.405	231950	0.034
59	Lactic acid	$C_3H_6O_3$	90.08	19.2	10.546	224690	0.033
60	2,4,4-Trimethylpentan-1-ol	$C_8H_{18}O$	130.23	33.6	10.645	838379	0.122
61	2-Ethylhexyl formate	$C_9H_{18}O_2$	158.24	41	11.176	2889672	0.422
62	m-Cresol	C_7H_8O	108.14	42.7	12.1425	505235	0.074
63	1-Octanol	$C_8H_{18}O$	130.23	32.5	12.2635	670308	0.098
64	1,1-Dimethoxypropane	$C_5H_{12}O_2$	104.15	20.4	12.329	4617629	0.675
65	Acetic acid	$C_2H_4O_2$	60.05	20.2	12.3555	285780	0.042
66	Hexylcyclohexane	$C_{12}H_{24}$	168.32	41.4	12.378	826547	0.121
67	Trimethoxymethane	$C_4H_{10}O_3$	106.12	32.7	12.4225	757342	0.111
68	Valeric acid	$C_5H_{10}O_2$	102.13	44.2	12.4365	1133055	0.166
69	6-Phenyluracil	$C_{10}H_8N_2O_2$	188.18	10.3	12.4535	324870	0.047
70	2-Ethylhexan-1-ol	$C_8H_{18}O$	130.23	77.6	12.569	229869012	33.580
71	N-Methylsuccinimide	$C_5H_7NO_2$	113.11	25.9	12.7325	32616	0.005
72	Ethylphosphonic acid	$C_2H_7O_3P$	110.05	35	12.8695	44343	0.006
73	Methylmalonic acid	$C_4H_6O_4$	118.09	43.5	12.911	46298	0.007
74	1,2,4-Triazole	$C_2H_3N_3$	69.07	24.4	12.9545	10249	0.001
75	1,1-Dimethylcyclohexane	C_8H_{16}	112.21	6.35	13.0355	138026	0.020
76	Hex-4-enamide, N,N-dimethyl	$C_8H_{15}NO$	141.21	9.48	13.1355	3583	0.001
77	Desmetryn	$C_8H_{15}N_5S$	213.31	11.2	13.1395	23910	0.003
78	D-Lactic acid	$C_3H_6O_3$	90.08	7.52	13.389	77006	0.011
79	10,12-Docosadiynedioic acid	$C_{22}H_{34}O_4$	362.5	7.43	13.3935	10954	0.002
80	3-Heptene	C_7H_{14}	98.19	15.1	13.4445	332796	0.049
81	2-Ethylhexyl acetate	$C_{10}H_{20}O_2$	172.26	72.5	13.4795	1519160	0.222
82	Heptanoic anhydride	$C_{14}H_{26}O_3$	242.35	16.8	13.562	51726	0.008
83	5,8-Dimethoxy-2,4-dimethylquinoline	$C_{13}H_{15}NO_2$	217.26	13.5	13.9835	19502788	2.849
84	2-Ethylhexanoic acid	$C_8H_{16}O_2$	144.21	91.6	13.9865	107523021	15.707
85	gamma-Butyrolactone	$C_4H_6O_2$	86.09	33.4	14.2555	338050	0.049
86	(613C)1H-pyrimidine-2,4-dione	$C_4H_4N_2O_2$	113.08	51.5	14.3525	5140248	0.751
87	Dithioerythritol	$C_4H_{10}O_2S_2$	154.3	32.4	14.611	238839	0.035
88	Valine	$C_5H_{11}NO_2$	117.15	82.1	15.508	242128	0.035

89	Anthranilic acid	$C_7H_7NO_2$	137.14	24.8	15.66	199764	0.029
90	DL-Allylglycine	$C_5H_9NO_2$	115.13	62.1	15.8215	52478	0.008
91	Isopropyl alcohol	C_3H_8O	60.10	28.2	15.948	4732788	0.691
92	Benzoic acid	$C_7H_6O_2$	122.12	82.8	16.37	1837892	0.268
93	Benzyl alcohol	C_7H_8O	108.14	37.1	16.4625	30504	0.004
94	1,4-Butanediol	$C_4H_{10}O_2$	90.12	42.4	16.8435	60223	0.009
95	2,2,4,4,5,5,7,7-Octamethyloctane	$C_{16}H_{34}$	226.44	26.6	16.902	37629	0.005
96	Oxalic acid	$C_2H_2O_4$	90.03	42.9	17.0645	6811	0.001
97	L-Norleucine	$C_6H_{13}NO_2$	131.17	46.2	17.164	213322	0.031
98	Phosphoric acid	H_3PO_4	97.995	91.4	17.2525	102053916	14.908
99	Biphenyl	$C_{12}H_{10}$	154.21	38.8	17.279	98178	0.014
100	Glycerin	$C_3H_8O_3$	92.09	74	17.294	1117174	0.163
101	2,3,6-Trimethyldecane	$C_{13}H_{28}$	184.36	8.42	17.318	273168	0.040
102	alpha-D-galactose	$C_6H_{12}O_6$	180.16	4.47	17.415	60220	0.009
103	(214C)pyridine-3-carboxylic acid	$C_6H_5NO_2$	127.09	25.1	17.5005	7969	0.001
104	4-Hydroxypentanoic acid	$C_5H_{10}O_3$	118.13	26.9	17.5595	821723	0.120
105	2-Propyl-1-pentanol	$C_8H_{18}O$	130.23	41.3	17.6685	1491341	0.218
106	l-Isoleucine	$C_6H_{13}NO_2$	131.17	33.6	17.767	149357	0.022
107	4-Methylbenzamide	C_8H_9NO	135.16	22.4	18.2325	23394	0.003
108	4-Methylpentanoic acid	$C_6H_{12}O_2$	116.16	37.8	18.357	1368030	0.200
109	Harmaline	$C_{13}H_{14}N_2O$	214.26	13.2	18.522	334668	0.049
110	2-Ethylhexyl butyrate	$C_{12}H_{24}O_2$	200.32	86.9	18.5635	2084172	0.304
111	2-Hydroxy-3-methylbutyric acid	$C_5H_{10}O_3$	118.13	6.79	18.6115	807747	0.118
112	2-Hydroxypentanoic acid	$C_5H_{10}O_3$	118.13	42.1	18.6275	653202	0.095
113	4,7-Dimethylundecane	$C_{13}H_{28}$	184.36	9.61	18.8975	119657	0.017
114	Isopentane	C_5H_{12}	72.15	50.3	18.995	900691	0.132
115	Ethyl valerate	$C_7H_{14}O_2$	130.18	14.3	19.06	431806	0.063
116	2,4-Dimethyldecane	$C_{12}H_{26}$	170.33	9.04	19.1325	182928	0.027
117	Methyl vinyl ketone	C_4H_6O	70.09	55.1	19.1595	27063	0.004
118	Nonanoic acid	$C_9H_{18}O_2$	158.24	78.3	19.6555	41585	0.006
119	Nonan-1-ol	$C_9H_{20}O$	144.25	62	19.842	65077	0.010
120	Pregn-4-ene-3,20-dione-4-14C	$C_{21}H_{30}O_2$	316.5	4.99	19.9595	1819124	0.266
121	17alpha-Pregn-4-ene-3,11,20-trione	$C_{21}H_{28}O_3$	328.4	17.5	19.9735	2993069	0.437
122	Ethyl 4-methylpentanoate	$C_8H_{16}O_2$	144.21	85.4	20.193	1409889	0.206
123	1,3-Dihydro-2H-1,5-benzodiazepin-2-one	$C_9H_8N_2O$	160.17	11.3	20.2345	94128	0.014
124	Threonine	$C_4H_9NO_3$	119.12	96.3	20.3325	32235	0.005
125	Ethyl butyrate	$C_6H_{12}O_2$	116.16	26.2	20.567	293389	0.043
126	1-(4-Methoxyphenyl)-2,5-dimethylpyrrole	$C_{13}H_{15}NO$	201.26	9.16	20.7135	67120	0.010
127	Octanoic acid	$C_8H_{16}O_2$	144.21	40.6	20.748	1724901	0.252
128	2-Ethylhexyl valerate	$C_{13}H_{26}O_2$	214.34	70	21.1045	1117575	0.163
129	4-Hydroxy-3,4,6-trimethylhept-5-enoic acid lactone	$C_{10}H_{16}O_2$	168.23	25.4	21.6085	70910	0.010

130	1,2,4,5-Tetrazine, 1,4-dibutylhexahydro-	$C_{10}H_{24}N_4$	200.32	35	21.679	284140	0.042
131	2,5-Dimethylthiazole	C_5H_7NS	113.18	11.9	21.953	47635	0.007
132	Tetradecane	$C_{14}H_{30}$	198.39	33.8	22.044	310031	0.045
133	6-Methoxy-2-methylquinolin-4-ol	$C_{11}H_{11}NO_2$	189.21	33.6	22.1005	16305	0.002
134	2-Methylheptadecane	$C_{18}H_{38}$	254.5	8.7	22.893	111541	0.016
135	Plectaniaxanthin	$C_{40}H_{56}O_2$	568.9	7.16	22.969	380599	0.056
136	Heptadecane, 9-hexyl-	$C_{23}H_{48}$	324.6	34.4	23.3155	69865	0.010
137	Octadecane	$C_{18}H_{38}$	254.5	9.25	23.4005	182847	0.027
138	Hexanoic acid	$C_6H_{12}O_2$	116.16	22.6	23.532	277412	0.041
139	Proline	$C_5H_9NO_2$	115.13	75.3	23.682	407106	0.059
140	L-Pyroglutamic acid	$C_5H_7NO_3$	129.11	75.1	23.695	75387	0.011
141	2-Hexyl-1-decanol	$C_{16}H_{34}O$	242.44	8.51	23.7055	234875	0.034
142	Ethyl 4-ethoxybenzoate	$C_{11}H_{14}O_3$	194.23	80.4	23.8395	57059	0.008
143	Hexadecane	$C_{16}H_{34}$	226.44	9.1	23.8685	190911	0.028
144	Tetracosane	$C_{24}H_{50}$	338.7	6.29	23.9365	6037	0.001
145	Tridecanol, 2-ethyl-2-methyl-	$C_{16}H_{34}O$	242.44	6.47	24.0265	337952	0.049
146	Heneicosane	$C_{21}H_{44}$	296.6	6.77	24.138	1471353	0.215
147	2,2,4-Trimethylpentane	C_8H_{18}	114.23	16.1	24.29	8076	0.001
148	2,6,11-Trimethyldodecane	$C_{15}H_{32}$	212.41	6.8	24.3845	874421	0.128
149	Decane	$C_{10}H_{22}$	142.28	23.8	24.491	28161	0.004
150	2,5-Dimethyldodecane	$C_{14}H_{30}$	198.39	5.78	24.613	221031	0.032
151	Octanoic anhydride	$C_{16}H_{30}O_3$	270.41	22.2	24.6645	501966	0.073
152	3-Methyl-3-ethyldecane	$C_{13}H_{28}$	184.36	5.54	24.9225	319308	0.047
153	Nonane	C_9H_{20}	128.25	35.1	24.9275	38639	0.006
154	1-Methyl-4-nitro-1H-pyrazole	$C_4H_5N_3O_2$	127.10	21.4	24.9405	121461	0.018
155	2-Methyldecane	$C_{11}H_{24}$	156.31	6.77	25.005	25013	0.004
156	2-Methyldodecane	$C_{13}H_{28}$	184.36	10.2	25.145	317491	0.046
157	2,3,5-Trimethyldecane	$C_{13}H_{28}$	184.36	6.67	25.3195	65861	0.010
158	Isobutyric anhydride	$C_8H_{14}O_3$	158.19	24.6	25.41	14412	0.002
159	2-Ethylhexyl 2-ethylhexanoate	$C_{16}H_{32}O_2$	256.42	94.5	25.6575	30098807	4.397
160	2-Methyltetrahydrofuran	$C_5H_{10}O$	86.13	5.55	25.722	14016	0.002
161	Heptane	C_7H_{16}	100.20	20	25.8825	31722	0.005
162	Phenylalanine	$C_9H_{11}NO_2$	165.19	76.5	26.1905	36611	0.005
163	1,3,5-Trimethyl-2-octadecylcyclohexane	$C_{27}H_{54}$	378.7	29.6	26.2405	68281	0.010
164	Butyl succinate	$C_8H_{14}O_4$	174.194	28.2	26.6935	56548	0.008
165	Acethydrazide	$C_2H_6N_2O$	74.08	33.2	26.8555	34596	0.005
166	Lauric acid	$C_{12}H_{24}O_2$	200.32	89.3	26.8955	138464	0.020
167	Fucoxanthin	$C_{42}H_{58}O_6$	658.9	23.3	27.257	194090	0.028
168	7-Ethylisoxazolo(3,4-d)pyrimidine-4,6(5H,7H)-dione	$C_7H_7N_3O_3$	181.15	23.7	27.274	341656	0.050
169	5-methyl-4H-1,2,4-triazole-3-thiol	$C_3H_5N_3S$	115.16	40.4	27.4505	39149	0.006

170	5,11-Diethyl-8-methyl-7,9-dioxapentadecane	$C_{18}H_{38}O_2$	286.5	40.5	27.5465	146184	0.021
171	Triethylene glycol monomethyl ether	$C_7H_{16}O_4$	164.20	15.1	27.5955	95229	0.014
172	2-Cyclohexyl-3-isopropyl-4-penten-2-ol	$C_{14}H_{26}O$	210.356	23.8	27.693	70003	0.010
173	2-Methylhexadecane	$C_{17}H_{36}$	240.5	8.34	27.934	17350	0.003
174	Cyperaquinone	$C_{14}H_{10}O_4$	242.23	19.1	28.225	16157	0.002
175	2-Methylundecane	$C_{12}H_{26}$	170.33	5.75	28.852	113425	0.017
176	Tetratetracontane	$C_{44}H_{90}$	619.2	16.1	28.9155	192469	0.028
177	2-Methyltetradecane	$C_{15}H_{32}$	212.41	5.05	29.04	112782	0.016
178	S-(tert-Butyl) 4-allyl-2-tert-butyl-1,3-dioxolane-4-carbothioate	$C_{15}H_{26}O_3S$	286.16	32.6	29.05	23756	0.003
179	Glutaric acid	$C_5H_8O_4$	132.11	26.5	29.058	164139	0.024
180	2-Methyltricosane	$C_{24}H_{50}$	338.7	8.42	29.233	134083	0.020
181	2-Methyleicosane	$C_{21}H_{44}$	296.6	5.83	29.382	220936	0.032
182	Epinephrine	$C_9H_{13}NO_3$	183.20	23.6	29.5895	90914	0.013
183	L-Alanyl-L-alanine	$C_6H_{12}N_2O_3$	160.17	14.5	29.65	50514	0.007
184	Terephthalic acid	$C_8H_6O_4$	166.13	95.2	29.8635	578848	0.085
185	5-Phenylisoxazole-3-carboxylic acid	$C_{10}H_7NO_3$	189.17	36.5	29.916	31162	0.005
186	Azelaic acid	$C_9H_{16}O_4$	188.22	94.6	30.051	30817	0.005
187	3-Ethyl-3-methylheptane	$C_{10}H_{22}$	142.28	7.58	30.0995	31606	0.005
188	Pentadecane	$C_{15}H_{32}$	212.41	6.5	30.172	93164	0.014
189	Diethyl ethylmalonate	$C_9H_{16}O_4$	188.22	57.8	30.208	77532	0.011
190	1,2-Diisopropylhydrazine	$C_6H_{16}N_2$	116.20	10.6	30.375	103654	0.015
191	Heptadecane	$C_{17}H_{36}$	240.5	5.17	30.3945	149315	0.022
192	3,8-Dimethylundecane	$C_{13}H_{28}$	184.36	10.3	30.5315	36144	0.005
193	2-Decanol	$C_{10}H_{22}O$	158.28	31.1	31.1215	732400	0.107
194	Myristic acid	$C_{14}H_{28}O_2$	228.37	70.4	31.1575	143899	0.021
195	Hentriacontane	$C_{31}H_{64}$	436.8	7.17	32.4565	955497	0.140
196	2-Methyltridecane	$C_{14}H_{30}$	198.39	7.84	32.7005	37843	0.006
197	Undecane	$C_{11}H_{24}$	156.31	13.1	33.0895	48982	0.007
198	2,6,10,15-Tetramethylheptadecane	$C_{21}H_{44}$	296.6	7.28	33.1955	6264	0.001
199	Phthalic acid	$C_8H_6O_4$	166.13	8.86	33.2665	113039	0.017
200	Heptacosane	$C_{27}H_{56}$	380.7	6.79	33.312	1201257	0.175
201	trans-2-Octenoic acid	$C_8H_{14}O_2$	142.20	42.6	33.3315	92343	0.013
202	1-Hexadecanol	$C_{16}H_{34}O$	242.44	47	33.4215	41173	0.006
203	D-Galactose	$C_6H_{12}O_6$	180.16	8.85	33.836	793136	0.116
204	1-Pentene	C_5H_{10}	70.13	14.6	34.2225	53053	0.008
205	Octane	C_8H_{18}	114.23	10.1	34.9465	1552923	0.227
206	Palmitic acid	$C_{16}H_{32}O_2$	256.42	98	35.061	13755035	2.009
207	2-Methyloctadecane	$C_{19}H_{40}$	268.5	7.87	36.4905	526433	0.077
208	Oleic acid	$C_{18}H_{34}O_2$	282.5	30.3	38.1505	223581	0.033

209	Androst-2-en-17-amine	$C_{19}H_{31}N$	273.5	81.6	38.178	26765	0.004
210	Stearic acid	$C_{18}H_{36}O_2$	284.5	97.8	38.6365	308409	0.045
211	Cholesterol	$C_{27}H_{46}O$	386.7	79.7	51.8855	5737349	0.838

- **Enrichment analysis**

Disease signatures (Figure 23.2 and Table 15.2), metabolites enrichment from the KEGG database (Figure 23.3 and Table 15.3) and the SMPDB database (Figure 23.4 and Table 15.4), and different classes of metabolites (Figure 23.5 and Table 15.5) are given below. The enrichment ratio is no. of hits observed divided by no. of hits expected.

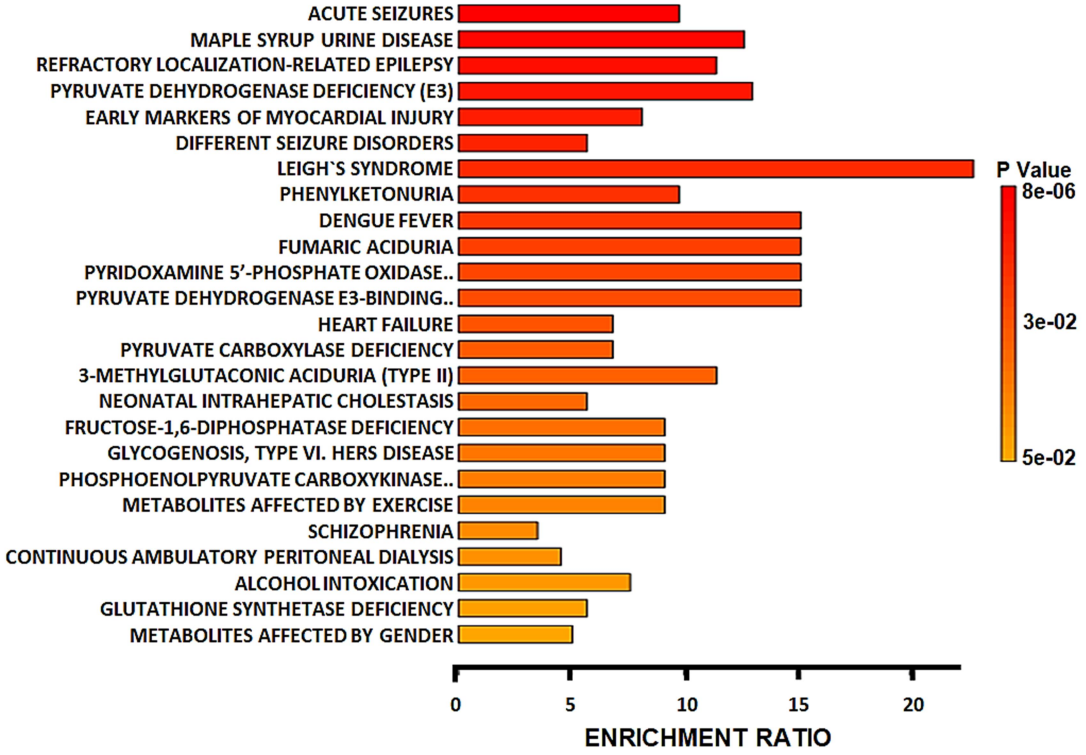

Figure 23.2: Disease signatures in palmitic acid-treated cells

The top 25 disease signatures were identified. Significantly enriched signatures (↓) include acute seizures, maple syrup urine disease, refractory localization-related epilepsy, pyruvate dehydrogenase deficiency (E3), and early markers of myocardial injury. Highly enriched

signatures (←) include leigh's syndrome, dengue fever, fumaric aciduria, pyridoxamine 5-prime phosphate oxidase deficiency, and pyruvate dehydrogenase E3 binding protein deficiency.

Table 15.2: Disease signatures in palmitic acid-treated cells

	Metabolite Set	Total	Hits	Expect	P Value	Holm P	FDR
	ACUTE SEIZURES	14	6	0.614	8.03E-6	0.00219	0.00152
	MAPLE SYRUP URINE DISEASE	9	5	0.395	1.11E-5	0.00302	0.00152
	REFRACTORY LOCALIZATION-RELATED EPILEPSY	10	5	0.438	2.16E-5	0.00585	0.00197
	PYRUVATE DEHYDROGENASE DEFICIENCY (E3)	7	4	0.307	8.86E-5	0.0239	0.00605
	EARLY MARKERS OF MYOCARDIAL INJURY	14	5	0.614	1.53E-4	0.0412	0.00835
	DIFFERENT SEIZURE DISORDERS	24	6	1.05	2.72E-4	0.0729	0.0124
	LEIGH`S SYNDROME, SUBACUTE NECROTIZING ENCEPHALOPATHY	2	2	0.0877	0.00183	0.49	0.0715
	PHENYLKETONURIA	7	3	0.307	0.00228	0.606	0.0778
	DENGUE FEVER	3	2	0.132	0.00536	1.0	0.122
	FUMARIC ACIDURIA	3	2	0.132	0.00536	1.0	0.122
	PYRIDOXAMINE 5-PRIME-PHOSPHATE OXIDASE DEFICIENCY	3	2	0.132	0.00536	1.0	0.122
	PYRUVATE DEHYDROGENASE E3-BINDING PROTEIN DEFICIENCY	3	2	0.132	0.00536	1.0	0.122
	HEART FAILURE	10	3	0.438	0.00717	1.0	0.14
	PYRUVATE CARBOXYLASE DEFICIENCY	10	3	0.438	0.00717	1.0	0.14
	3-METHYLGLUTACONIC ACIDURIA (TYPE II), X-LINKED	4	2	0.175	0.0104	1.0	0.19
	NEONATAL INTRAHEPATIC CHOLESTASIS	12	3	0.526	0.0124	1.0	0.212
	FRUCTOSE-1,6-DIPHOSPHATASE DEFICIENCY	5	2	0.219	0.0169	1.0	0.231
	GLYCOGENOSIS (TYPE IA, IB, IC) | GLYCOGENOSIS, TYPE VI. HERS DISEASE	5	2	0.219	0.0169	1.0	0.231
	PHOSPHOENOLPYRUVATE CARBOXYKINASE DEFICIENCY 2 (PEPCK2)	5	2	0.219	0.0169	1.0	0.231
	METABOLITES AFFECTED BY EXERCISE	5	2	0.219	0.0169	1.0	0.231
	SCHIZOPHRENIA	26	4	1.14	0.0217	1.0	0.283

	CONTINUOUS AMBULATORY PERITONEAL DIALYSIS (CAPD)	15	3	0.658	0.0236	1.0	0.292
	ALCOHOL INTOXICATION	6	2	0.263	0.0247	1.0	0.293
	GLUTATHIONE SYNTHETASE DEFICIENCY	8	2	0.351	0.0437	1.0	0.46
	METABOLITES AFFECTED BY GENDER	9	2	0.395	0.0548	1.0	0.46

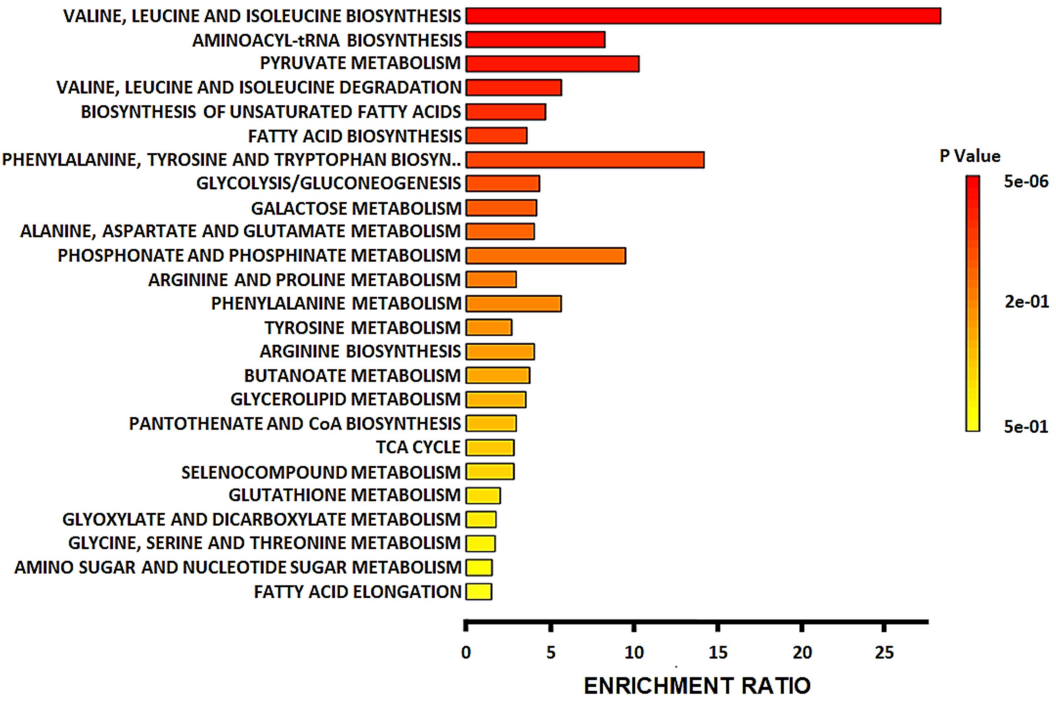

Figure 23.3: Palmitic acid-specific metabolites enrichment from the KEGG database

The top 25 metabolic pathways were identified. Significantly enriched pathways (↓) include valine, leucine, and isoleucine biosynthesis, aminoacyl t-RNA biosynthesis, pyruvate metabolism, valine, leucine, and isoleucine degradation, and biosynthesis of unsaturated fatty acids. Highly enriched pathways (←) include valine, leucine, and isoleucine biosynthesis, phenylalanine, tyrosine, and tryptophan biosynthesis, pyruvate metabolism, phosphonate, and phosphinate metabolism, and aminoacyl t-RNA biosynthesis.

Table 15.3: Palmitic acid-specific metabolites enrichment from the KEGG database

	Metabolite Set	Total	Hits	Expect	P Value	Holm P	FDR
	Valine, leucine, and isoleucine biosynthesis	8	4	0.141	5.07E-6	4.26E-4	4.26E-4
	Aminoacyl-tRNA biosynthesis	48	7	0.844	1.03E-5	8.54E-4	4.32E-4
	Pyruvate metabolism	22	4	0.387	4.47E-4	0.0367	0.0125
	Valine, leucine and isoleucine degradation	40	4	0.703	0.00449	0.364	0.0944
	Biosynthesis of unsaturated fatty acids	36	3	0.633	0.0235	1.0	0.395
	Fatty acid biosynthesis	47	3	0.826	0.047	1.0	0.657
	Phenylalanine, tyrosine, and tryptophan biosynthesis	4	1	0.0703	0.0685	1.0	0.714
	Glycolysis / Gluconeogenesis	26	2	0.457	0.0747	1.0	0.714
	Galactose metabolism	27	2	0.475	0.0798	1.0	0.714
	Alanine, aspartate and glutamate metabolism	28	2	0.492	0.085	1.0	0.714
	Phosphonate and phosphinate metabolism	6	1	0.105	0.101	1.0	0.772
	Arginine and proline metabolism	38	2	0.668	0.142	1.0	0.995
	Phenylalanine metabolism	10	1	0.176	0.163	1.0	1.0
	Tyrosine metabolism	42	2	0.738	0.167	1.0	1.0
	Arginine biosynthesis	14	1	0.246	0.221	1.0	1.0
	Butanoate metabolism	15	1	0.264	0.235	1.0	1.0
	Glycerolipid metabolism	16	1	0.281	0.248	1.0	1.0
	Pantothenate and CoA biosynthesis	19	1	0.334	0.287	1.0	1.0
	Citrate cycle (TCA cycle)	20	1	0.352	0.3	1.0	1.0
	Selenocompound metabolism	20	1	0.352	0.3	1.0	1.0
	Glutathione metabolism	28	1	0.492	0.394	1.0	1.0
	Glyoxylate and dicarboxylate metabolism	32	1	0.562	0.436	1.0	1.0
	Glycine, serine, and threonine metabolism	33	1	0.58	0.446	1.0	1.0
	Amino sugar and nucleotide sugar metabolism	37	1	0.65	0.485	1.0	1.0
	Fatty acid elongation	38	1	0.668	0.495	1.0	1.0

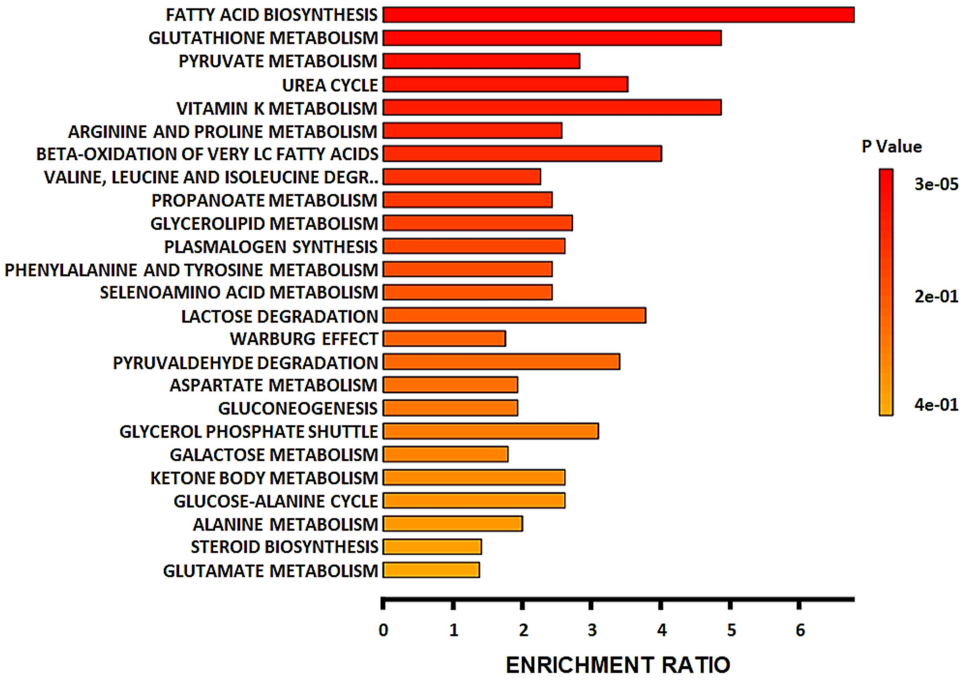

Figure 23.4: Palmitic acid-specific metabolites enrichment from the SMPDB database

The top 25 metabolic pathways were identified. Significantly enriched pathways (↓) include fatty acid biosynthesis, glutathione metabolism, pyruvate metabolism, urea cycle, and vitamin K metabolism. Highly enriched pathways (←) include fatty acid biosynthesis, glutathione metabolism, vitamin K metabolism, β-oxidation of very long chain fatty acids, and lactose degradation.

Table 15.4: Palmitic acid-specific metabolites enrichment from the SMPDB database

	Metabolite set	Total	Hits	Expect	P Value	Holm P	FDR
	Fatty acid biosynthesis	35	7	1.03	3.39E-5	0.00333	0.00333
	Glutathione metabolism	21	3	0.615	0.0211	1.0	1.0
	Pyruvate metabolism	48	4	1.41	0.0474	1.0	1.0
	Urea Cycle	29	3	0.85	0.0496	1.0	1.0
	Vitamin K metabolism	14	2	0.41	0.0607	1.0	1.0
	Arginine and proline metabolism	53	4	1.55	0.0645	1.0	1.0
	Beta oxidation of very long chain fatty acids	17	2	0.498	0.0859	1.0	1.0
	Valine, leucine and isoleucine degradation	60	4	1.76	0.0931	1.0	1.0
	Propanoate metabolism	42	3	1.23	0.121	1.0	1.0

	Glycerolipid metabolism	25	2	0.732	0.164	1.0	1.0
	Plasmalogen synthesis	26	2	0.762	0.175	1.0	1.0
	Phenylalanine and tyrosine metabolism	28	2	0.82	0.196	1.0	1.0
	Selenoamino acid metabolism	28	2	0.82	0.196	1.0	1.0
	Lactose degradation	9	1	0.264	0.236	1.0	1.0
	Warburg effect	58	3	1.7	0.239	1.0	1.0
	Pyruvaldehyde degradation	10	1	0.293	0.258	1.0	1.0
	Aspartate metabolism	35	2	1.03	0.274	1.0	1.0
	Gluconeogenesis	35	2	1.03	0.274	1.0	1.0
	Glycerol phosphate shuttle	11	1	0.322	0.28	1.0	1.0
	Galactose metabolism	38	2	1.11	0.307	1.0	1.0
	Ketone body metabolism	13	1	0.381	0.322	1.0	1.0
	Glucose-alanine cycle	13	1	0.381	0.322	1.0	1.0
	Alanine metabolism	17	1	0.498	0.399	1.0	1.0
	Steroid biosynthesis	48	2	1.41	0.416	1.0	1.0
	Glutamate metabolism	49	2	1.44	0.426	1.0	1.0

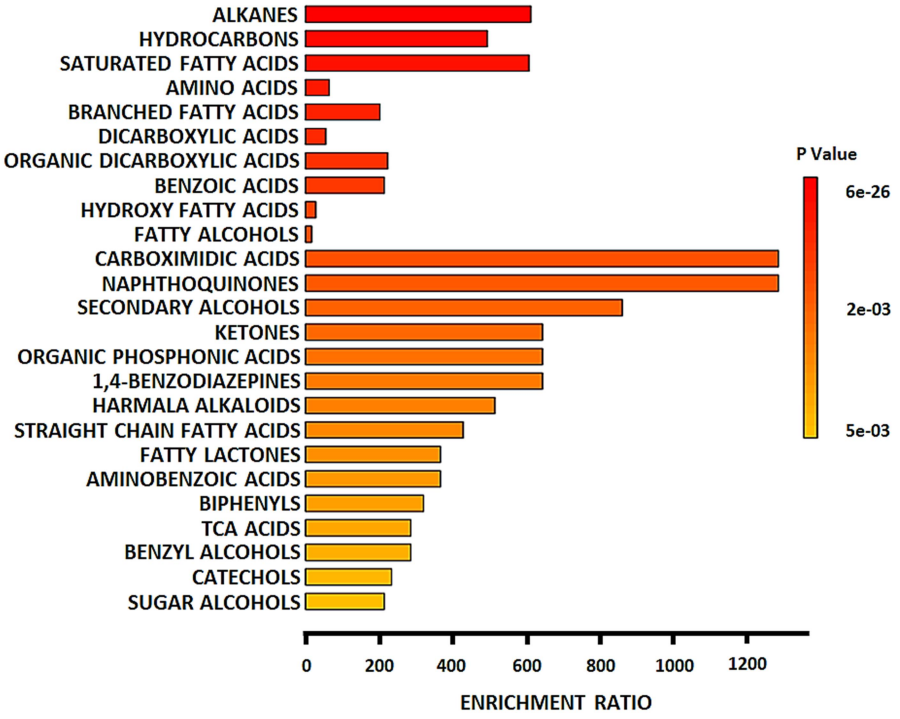

Figure 23.5: Different classes of identified metabolites in palmitic acid-treated cells

The top 25 different classes of metabolites were identified. Significantly enriched classes (↓) include alkanes, hydrocarbons, saturated fatty acids, amino acids, and branched fatty acids. Highly

enriched classes (←) include carboximidic acids, naphthoquinones, secondary alcohols, ketones, organic phosphonic acids, and 1,4- benzodiazepines.

Table 15.5: Different classes of identified metabolites in palmitic acid-treated cells

	Metabolite Set	Total	Hits	Expect	P Value	Holm P	FDR
	Alkanes	42	10	0.0163	6.17E-26	4.51E-23	4.51E-23
	Hydrocarbons	52	10	0.0202	6.62E-25	4.83E-22	2.42E-22
	Saturated fatty acids	38	9	0.0148	2.0E-23	1.46E-20	4.86E-21
	Amino acids	277	7	0.108	2.13E-11	1.55E-8	3.89E-9
	Branched fatty acids	38	3	0.0148	4.7E-7	3.42E-4	6.88E-5
	Dicarboxylic acids	140	3	0.0544	2.43E-5	0.0176	0.00295
	Organic dicarboxylic acids	23	2	0.00893	3.75E-5	0.0272	0.00373
	Benzoic acids	24	2	0.00932	4.09E-5	0.0296	0.00373
	Hydroxy fatty acids	274	3	0.106	1.77E-4	0.128	0.0144
	Fatty alcohols	452	3	0.176	7.59E-4	0.548	0.0473
	Carboximidic acids	2	1	7.77E-4	7.76E-4	0.56	0.0473
	Naphthoquinones	2	1	7.77E-4	7.76E-4	0.56	0.0473
	Secondary alcohols	3	1	0.00116	0.00116	0.837	0.0655
	Ketones	4	1	0.00155	0.00155	1.0	0.0709
	Organic phosphonic acids	4	1	0.00155	0.00155	1.0	0.0709
	1,4-benzodiazepines	4	1	0.00155	0.00155	1.0	0.0709
	Harmala alkaloids	5	1	0.00194	0.00194	1.0	0.0834
	Straight-chain fatty acids	6	1	0.00233	0.00233	1.0	0.0945
	Fatty lactones	7	1	0.00272	0.00272	1.0	0.0992
	Aminobenzoic acids	7	1	0.00272	0.00272	1.0	0.0992
	Biphenyls	8	1	0.00311	0.0031	1.0	0.108
	TCA acids	9	1	0.00349	0.00349	1.0	0.111
	Benzyl alcohols	9	1	0.00349	0.00349	1.0	0.111
	Catechols	11	1	0.00427	0.00426	1.0	0.13
	Sugar alcohols	12	1	0.00466	0.00465	1.0	0.136

- **Pathway analysis**

Impacted pathways from the KEGG database (Figure 23.6 and Table 15.6), and the SMPDB database (Figure 23.7 and Table 15.7) are given below. Pathway impact is calculated by using centrality and pathway enrichment results.

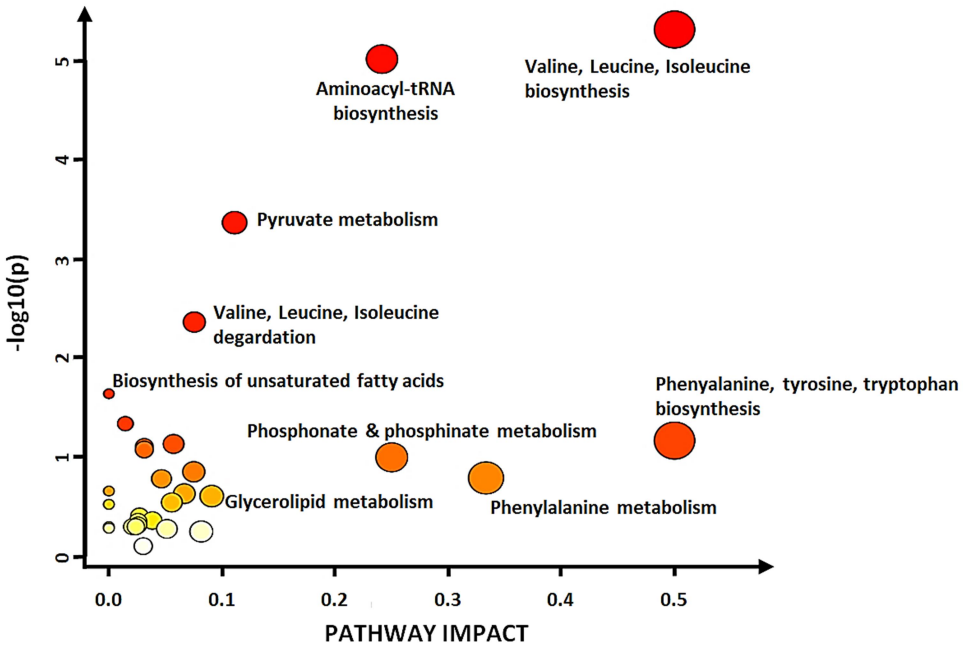

Figure 23.6: Palmitic acid-specific pathway analysis from the KEGG database

The top 31 impacted pathways were identified. Highly impacted pathways (←) include valine, leucine, and isoleucine biosynthesis, phenylalanine, tyrosine, and tryptophan biosynthesis, phenylalanine metabolism, phosphonate, and phosphinate metabolism, and aminoacyl t-RNA biosynthesis. Significantly impacted pathways (↓) include valine, leucine, and isoleucine biosynthesis, aminoacyl t-RNA biosynthesis, pyruvate metabolism, valine, leucine, and isoleucine degradation, and biosynthesis of unsaturated fatty acids.

Table 15.6: Palmitic acid-specific pathway analysis from the KEGG database

Pathway Name	Match Status	p	-log(p)	Holm p	FDR	Impact
Valine, leucine, and isoleucine biosynthesis	4/8	4.8881E-6	5.3109	4.106E-4	4.0741E-4	0.5
Aminoacyl-tRNA biosynthesis	7/48	9.7003E-6	5.0132	8.0512E-4	4.0741E-4	0.24136
Pyruvate metabolism	4/22	4.3196E-4	3.3646	0.035421	0.012095	0.11112
Valine, leucine, and isoleucine degradation	4/40	0.0043502	2.3615	0.35237	0.091355	0.07548
Biosynthesis of unsaturated fatty acids	3/36	0.022957	1.6391	1.0	0.38568	0.0
Fatty acid biosynthesis	3/47	0.045914	1.3381	1.0	0.6428	0.01449

Phenylalanine, tyrosine, and tryptophan biosynthesis	1/4	0.067942	1.1679	1.0	0.70293	0.5
Glycolysis / Gluconeogenesis	2/26	0.073486	1.1338	1.0	0.70293	0.05714
Galactose metabolism	2/27	0.07853	1.105	1.0	0.70293	0.03125
Alanine, aspartate and glutamate metabolism	2/28	0.083682	1.0774	1.0	0.70293	0.03125
Phosphonate and phosphinate metabolism	1/6	0.10022	0.99903	1.0	0.76534	0.25
Arginine and proline metabolism	2/38	0.14011	0.85353	1.0	0.98077	0.075
Phenylalanine metabolism	1/10	0.16159	0.79159	1.0	0.98755	0.33333
Tyrosine metabolism	2/42	0.16459	0.78359	1.0	0.98755	0.04651
Arginine biosynthesis	1/14	0.21891	0.65973	1.0	1.0	0.0
Butanoate metabolism	1/15	0.23264	0.63331	1.0	1.0	0.06667
Glycerolipid metabolism	1/16	0.24614	0.60882	1.0	1.0	0.09091
Pantothenate and CoA biosynthesis	1/19	0.28527	0.54474	1.0	1.0	0.05556
Citrate cycle (TCA cycle)	1/20	0.29788	0.52596	1.0	1.0	0.0
Selenocompound metabolism	1/20	0.29788	0.52596	1.0	1.0	0.0
Glutathione metabolism	1/28	0.39129	0.4075	1.0	1.0	0.02703
Glyoxylate and dicarboxylate metabolism	1/32	0.43339	0.36312	1.0	1.0	0.03846
Glycine, serine, and threonine metabolism	1/33	0.44347	0.35314	1.0	1.0	0.02564
Amino sugar and nucleotide sugar metabolism	1/37	0.48208	0.31688	1.0	1.0	0.02564
Fatty acid elongation	1/39	0.50041	0.30068	1.0	1.0	0.0
Fatty acid degradation	1/39	0.50041	0.30068	1.0	1.0	0.02041
Drug metabolism - other enzymes	1/39	0.50041	0.30068	1.0	1.0	0.02381
Tryptophan metabolism	1/41	0.51811	0.28558	1.0	1.0	0.0
Steroid biosynthesis	1/42	0.52673	0.27841	1.0	1.0	0.05128
Primary bile acid biosynthesis	1/46	0.55976	0.252	1.0	1.0	0.08163
Steroid hormone biosynthesis	1/85	0.78478	0.10525	1.0	1.0	0.0303

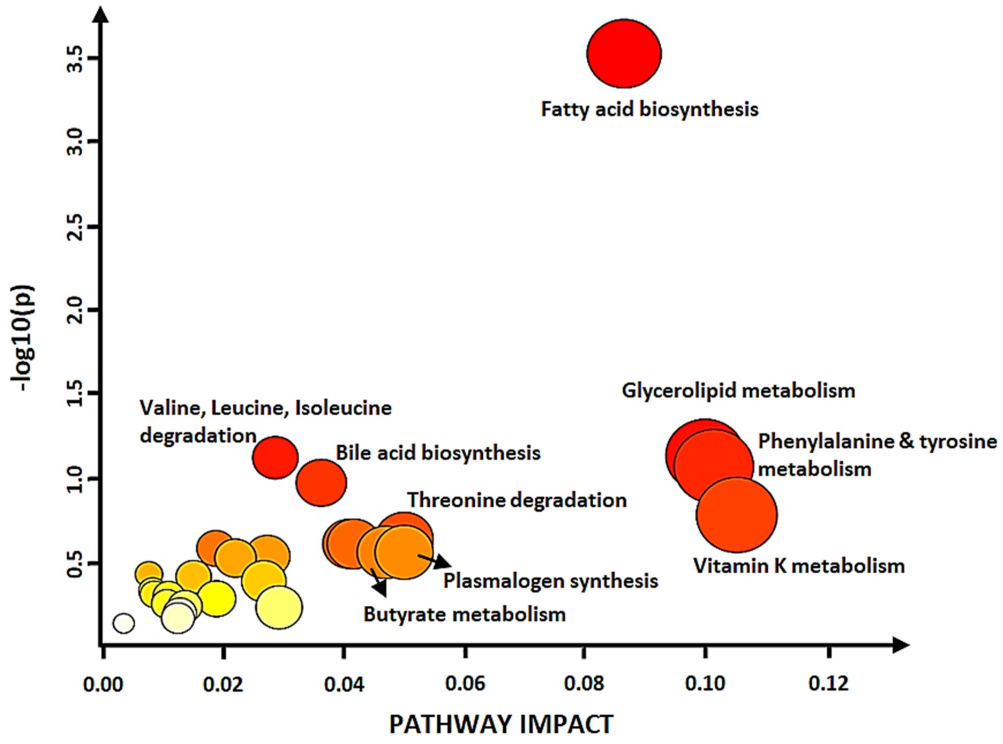

Figure 23.7: Palmitic acid-specific pathway analysis from the SMPDB database

The top 27 impacted pathways were identified. Highly impacted pathways (←) include vitamin K metabolism, phenylalanine and tyrosine metabolism, glycerolipid metabolism, fatty acid biosynthesis, threonine degradation, and plasmalogen synthesis. Significantly impacted pathways (↓) include fatty acid biosynthesis, glycerolipid metabolism, phenylalanine and tyrosine metabolism, valine, leucine, and isoleucine degradation, and bile acid biosynthesis.

Table 15.7: Palmitic acid-specific pathway analysis from the SMPDB database

Pathway Name	Match Status	p	-log(p)	Holm p	FDR	Impact
Fatty acid biosynthesis	5/33	2.9957E-4	3.5235	0.029657	0.029657	0.086538
Glycerolipid metabolism	2/23	0.07364	1.1329	1.0	1.0	0.1
Valine, leucine, and isoleucine degradation	3/51	0.07555	1.1218	1.0	1.0	0.028571
Phenylalanine and tyrosine metabolism	2/25	0.085289	1.0691	1.0	1.0	0.10145
Bile acid biosynthesis	3/59	0.1066	0.97223	1.0	1.0	0.036204
Vitamin K metabolism	1/9	0.16549	0.78123	1.0	1.0	0.10526

Threonine and 2-oxobutanoate degradation	1/13	0.23037	0.63757	1.0	1.0	0.05
Arginine and proline metabolism	2/48	0.24549	0.60996	1.0	1.0	0.040881
Catecholamine biosynthesis	1/14	0.24582	0.60937	1.0	1.0	0.041667
Mitochondrial electron transport chain	1/15	0.26098	0.58339	1.0	1.0	0.018692
Butyrate metabolism	1/16	0.27585	0.55932	1.0	1.0	0.046875
Plasmalogen synthesis	1/16	0.27585	0.55932	1.0	1.0	0.05
Mitochondrial beta-oxidation of short chain saturated fatty acids	1/17	0.29044	0.53695	1.0	1.0	0.027273
Tyrosine metabolism	2/55	0.29835	0.52527	1.0	1.0	0.021951
Urea cycle	1/23	0.37226	0.42916	1.0	1.0	0.0075758
Mitochondrial beta-oxidation of long chain saturated fatty acids	1/24	0.38499	0.41455	1.0	1.0	0.015
Citric acid cycle	1/26	0.40972	0.38751	1.0	1.0	0.026667
Galactose metabolism	1/31	0.46749	0.33023	1.0	1.0	0.0081967
Fatty acid elongation In mitochondria	1/33	0.48906	0.31064	1.0	1.0	0.0084746
Aspartate metabolism	1/34	0.49953	0.30144	1.0	1.0	0.01087
Porphyrin metabolism	1/36	0.51986	0.28411	1.0	1.0	0.018797
Fatty acid metabolism	1/40	0.55819	0.25321	1.0	1.0	0.010563
Steroidogenesis	1/42	0.57625	0.23939	1.0	1.0	0.013575
Steroid biosynthesis	1/43	0.58502	0.23283	1.0	1.0	0.029197
Warburg effect	1/49	0.63409	0.19785	1.0	1.0	0.012698
Tryptophan metabolism	1/55	0.67762	0.16901	1.0	1.0	0.012384
Purine metabolism	1/63	0.72806	0.13784	1.0	1.0	0.0033898

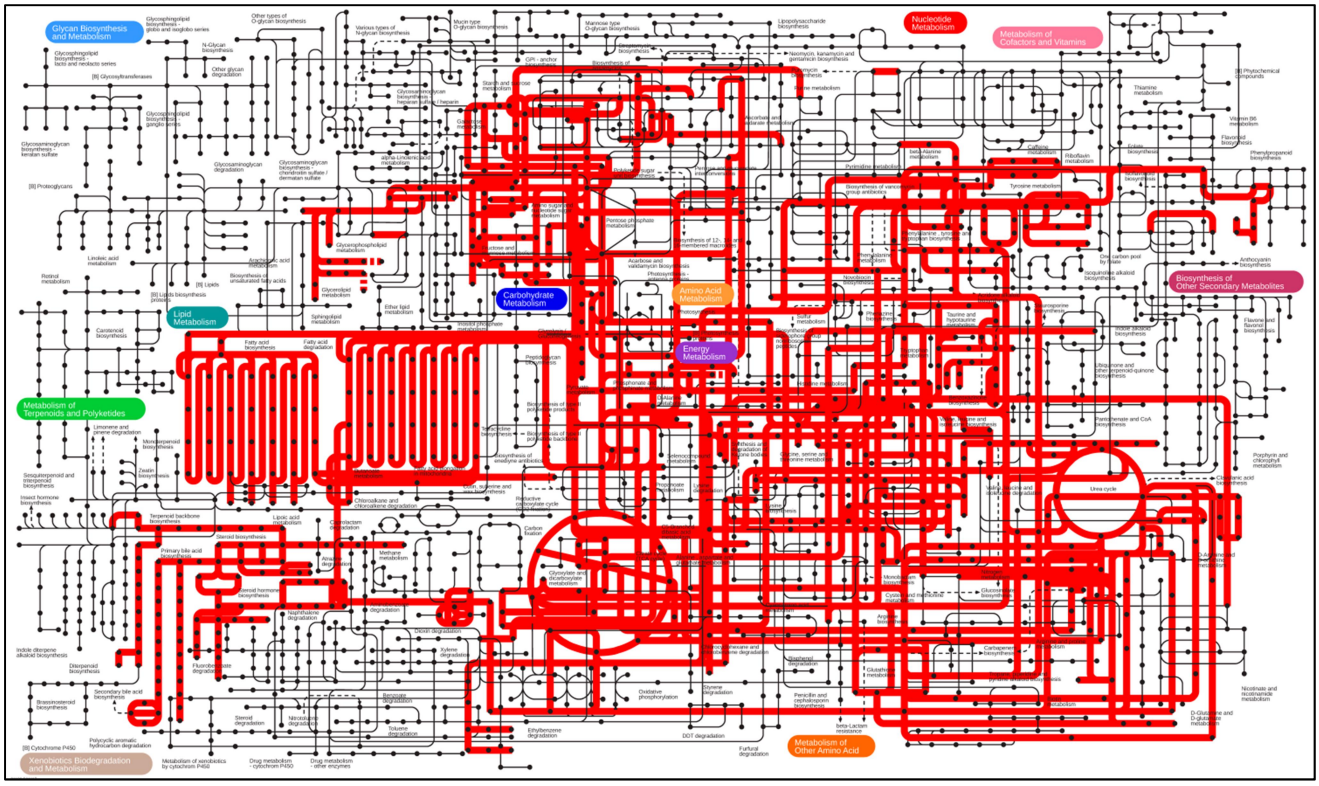

Figure 23.8: Metabolic pathways enriched in palmitic acid treatment after mapping with the KEGG database. The highlighted metabolisms show enrichment specific to palmitic acid treatment. This shows enrichment of energy metabolism, amino acid metabolism, glycerophospholipid metabolism, and other metabolic pathways.

IV. High sodium chloride treatment

Cells were treated with 200 mM NaCl media for 24 hours.

➢ GC-MS graph

GC chromatogram of NaCl treatment (given in Figure 24.1) depicts retention time (min) on X-axis and relative abundance (intensity) on Y-axis. A total of 92 metabolites (components) were identified in NaCl-treated cells (given in Table 16.1). The most abundant metabolites are – 2-Ethylhexan-1-ol (54.336%), Acetamide (24.888%), Phosphoric Acid (5.032%), Cholest-5-en-3-ol (3.710%), and 2-Ethylhexanoic acid (3.7%). The abundance is measured based on the % area of the peak of a specific component.

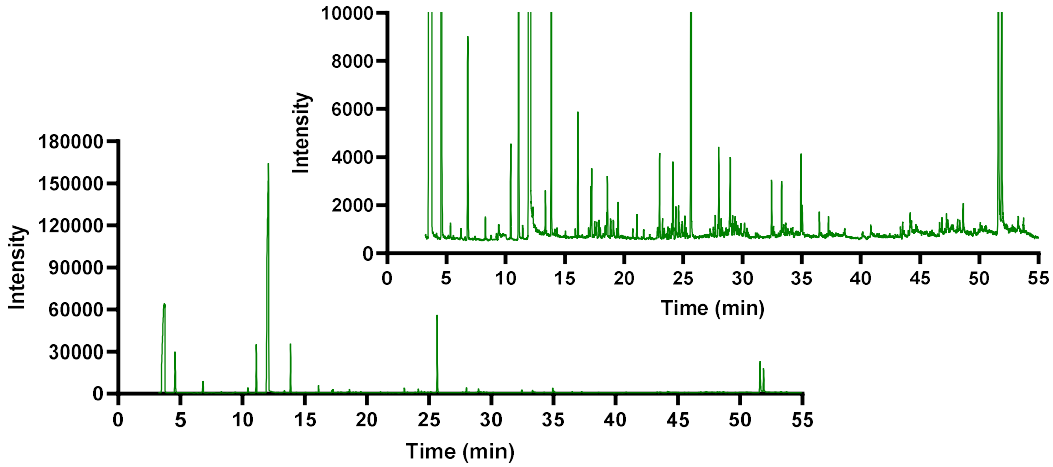

Figure 24.1: GC-MS graph obtained for NaCl treatment

Table 16.1: Metabolites identified in NaCl-treated cells

S.No.	Metabolites	Mol. Formula	MW (g/mol)	% Probability	RT (min)	Area	% Area
1	3-Nitro-1H-pyrazole	$C_3H_3N_3O_2$	113.08	1	3.4635	5681	0.001
2	3,5-Dimethyl-1H-pyrazol-4-amine	$C_5H_9N_3$	111.15	83.4	3.5095	3964	0.001
3	1,4,7-Trioxa-10-azacyclododecane	$C_8H_{17}NO_3$	175.23	48.4	3.578	176289	0.041
4	3-Hydroxy-3-phenylbutan-2-one	$C_{10}H_{12}O_2$	164.20	25.4	3.612	2256160	0.529
5	DL-Norleucine	$C_6H_{13}NO_2$	131.17	9.04	3.6355	868783	0.204
6	Leucine	$C_6H_{13}NO_2$	131.17	4.62	3.662	39213	0.009

7	2alpha-Isopropenyl-2,3-dihydrobenzofuran-4-ol	$C_{11}H_{12}O_2$	176.21	15.8	3.678	778901	0.183
8	6,7-Dimethoxy-1-(4-methoxybenzyl)-1,2,3,4-tetrahydroisoquinoline	$C_{19}H_{23}NO_3$	313.4	14.8	3.706	3924	0.001
9	Isoquinoline	C_9H_7N	129.16	11.6	3.715	1040471	0.244
10	5,6,6a,7,8,12b-Hexahydro-benzo[a]phenanthridine-10,11-diol	$C_{17}H_{17}NO_2$	267.32	30.4	3.725	311072	0.073
11	Glycinamide	$C_2H_6N_2O$	74.08	73.3	3.7425	8029564	1.881
12	Acetamide	C_2H_5NO	59.07	53.2	3.749	106214924	24.888
13	3-Heptanone	$C_7H_{14}O$	114.19	40.5	4.563	647300	0.152
14	N,N-Dimethylacetamide	C_4H_9NO	87.12	75.8	4.7805	25314	0.006
15	1-Acetylisatin	$C_{10}H_7NO_3$	189.17	7.72	5.06	19511	0.005
16	Acetamidine	$C_2H_6N_2$	58.08	62	6.223	1907167	0.447
17	N,N-Diethylformamide	$C_5H_{11}NO$	101.15	50.1	6.317	25911	0.006
18	1,2,4-Triazolo[4,3-b][1,2,4,5]tetrazine	$C_3H_2N_6$	122.09	25.3	6.7265	43816	0.010
19	2-Ethylhexanal	$C_8H_{16}O$	128.21	73.1	6.803	184293	0.043
20	2,4,6-Trimethylpyridine	$C_8H_{11}N$	121.18	43.2	8.29	57322	0.013
21	Ethyl diethylcarbamate	$C_7H_{15}NO_2$	145.20	87.5	10.2745	59611	0.014
22	2,4,4-Trimethylpentan-1-ol	$C_8H_{18}O$	130.23	33.6	10.4275	1109875	0.260
23	Propionic acid	$C_3H_6O_2$	74.08	31.4	10.4425	88719	0.021
24	2-Ethylhexyl formate	$C_9H_{18}O_2$	158.24	41.7	11.0915	1002891	0.235
25	2-Ethylhexan-1-ol	$C_8H_{18}O$	130.23	79.8	12.0755	231890732	54.336
26	2-Ethylhexyl acetate	$C_{10}H_{20}O_2$	172.26	43.7	13.357	68499	0.016
27	2-Ethylhexanoic acid	$C_8H_{16}O_2$	144.21	97.3	13.851	15790889	3.700
28	(613C)1H-pyrimidine-2,4-dione	$C_4H_4N_2O_2$	113.08	60.7	14.279	143014	0.034
29	Mevalonolactone	$C_6H_{10}O_3$	130.14	14.8	15.8795	133196	0.031
30	Valproic Acid	$C_8H_{16}O_2$	144.21	35.3	15.884	24230	0.006
31	Benzoic Acid	$C_7H_6O_2$	122.12	75.9	16.3105	69551	0.016
32	1-Ethyl-1,2,4-triazole	$C_4H_7N_3$	97.12	15.7	17.01	31630	0.007
33	Phosphoric acid	H_3PO_4	97.995	91.8	17.1865	21476490	5.032
34	Glycerin	$C_3H_8O_3$	92.09	51.1	17.252	92435	0.022
35	Hexadecane	$C_{16}H_{34}$	226.44	9.55	17.2665	108454	0.025
36	2-Ethoxy-2,3-dihydro-6-methoxy-1,4-benzoxathiin	$C_{11}H_{14}O_3S$	226.29	9.1	17.382	21388	0.005
37	Thiazolo[4,5-f]quinoline, 2,7-dimethyl-	$C_{12}H_{10}N_2S$	214.29	19.3	17.4475	16850	0.004
38	Ethyl heptanoate	$C_9H_{18}O_2$	158.24	4.29	17.513	21469	0.005
39	Succinic acid	$C_4H_6O_4$	118.09	12.5	17.5215	2322	0.001
40	2-Propyl-1-pentanol	$C_8H_{18}O$	130.23	31.3	17.623	107498	0.025
41	4,6-Dimethyldodecane	$C_{14}H_{30}$	198.39	7.4	17.8925	11027	0.003
42	Octanoic acid	$C_8H_{16}O_2$	144.21	59.7	18.3235	95799	0.022
43	2-Ethylhexyl butyrate	$C_{12}H_{24}O_2$	200.32	84.6	18.529	66323	0.016
44	Pregna-3,5-dien-9-ol-20-one	$C_{21}H_{30}O_2$	314.5	25.7	18.747	23187	0.005

45	Pentitol	$C_5H_{12}O_5$	152.15	51.7	18.966	31916	0.007
46	Acetic acid	$C_2H_4O_2$	60.05	69.3	19.2245	7339	0.002
47	Methyl 1-Methylcyclopropane-1-carboxylate	$C_6H_{10}O_2$	114.14	15.2	19.505	90871	0.021
48	Acetaldehyde	C_2H_4O	44.05	5.72	19.9655	8166	0.002
49	Ethyl 4-methylpentanoate	$C_8H_{16}O_2$	144.21	79.3	20.171	36460	0.009
50	6-Hydroxyheptanoic acid	$C_7H_{14}O_3$	146.18	70.8	20.549	3937	0.001
51	Ethyl 2-ethylbutanoate	$C_8H_{16}O_2$	144.21	17.5	20.729	42020	0.010
52	Butyric acid	$C_4H_8O_2$	88.11	16.5	20.735	3433	0.001
53	2-Ethylhexyl valerate	$C_{13}H_{26}O_2$	214.34	62.6	21.0835	35050	0.008
54	Cyclohexene	C_6H_{10}	82.14	47.7	22.8165	42118	0.010
55	2-Methyltridecane	$C_{14}H_{30}$	198.39	6.18	23.0015	108152	0.025
56	3,3-Dimethylhexane	C_8H_{18}	114.23	14.5	23.856	5492	0.001
57	Heptadecane	$C_{17}H_{36}$	240.5	7.52	24.128	132230	0.031
58	2,6,11-Trimethyldodecane	$C_{15}H_{32}$	212.41	19.5	24.372	43556	0.010
59	2-Benzylidenecyclohexanone	$C_{13}H_{14}O$	186.25	13.1	24.4335	6478	0.002
60	2,3,5,8-Tetramethyldecane	$C_{14}H_{30}$	198.39	6.4	24.613	51371	0.012
61	5,8-Diethyldodecane	$C_{16}H_{34}$	226.44	20.8	24.657	76301	0.018
62	2-Hydroxypyrimidine	$C_4H_4N_2O$	96.087	11.4	25.226	46585	0.011
63	Heneicosane	$C_{21}H_{44}$	296.6	9.25	27.996	107207	0.025
64	Sulfurous acid	H_2SO_3	82.08	5.87	28.199	16523	0.004
65	Octadecane	$C_{18}H_{38}$	254.5	7.68	28.965	107106	0.025
66	2-Methyldodecane	$C_{13}H_{28}$	184.36	8.71	29.169	20551	0.005
67	2-Methylanthraquinone	$C_{15}H_{10}O_2$	222.24	88.7	29.861	11961	0.003
68	Octacosane	$C_{28}H_{58}$	394.8	16.9	31.112	48745	0.011
69	6,10,14-Trimethylpentadecan-2-ol	$C_{18}H_{38}O$	270.5	19.5	31.1175	3576	0.001
70	2-Decanol	$C_{10}H_{22}O$	158.28	20.3	31.22	34129	0.008
71	Heptacosane	$C_{27}H_{56}$	380.7	5.25	32.4565	93453	0.022
72	1,2-O-Isopropylidene-D-glucofuranose	$C_9H_{16}O_6$	220.22	16.4	32.7985	24308	0.006
73	Octadecane, 3-ethyl-5-(2-ethylbutyl)-	$C_{26}H_{54}$	366.7	17.9	33.3025	220893	0.052
74	D-Mannose	$C_6H_{12}O_6$	180.16	12.7	33.833	51586	0.012
75	Octane	C_8H_{18}	114.23	15.8	34.9405	110991	0.026
76	Palmitic acid	$C_{16}H_{32}O_2$	256.42	98.3	35.0525	608620	0.143
77	Stearic acid	$C_{18}H_{36}O_2$	284.5	96.7	38.6325	79933	0.019
78	1,2,3-Benzotriazin-4-amine	$C_7H_6N_4$	146.15	12.6	41.8715	118118	0.028
79	Phenanthridinic acid	$C_{14}H_9NO_2$	223.23	6.78	42.5865	64901	0.015
80	Triphenylphosphine oxide	$C_{18}H_{15}OP$	278.3	74.3	43.121	109480	0.026
81	Phthalic acid	$C_8H_6O_4$	166.13	22.6	43.341	24992	0.006
82	Cholesta-3,5-diene	$C_{27}H_{44}$	368.6	24	46.849	184013	0.043
83	Cholestane-3,5-diol, diacetate (3beta, 5alpha)	$C_{31}H_{52}O_4$	488.7	11	48.162	122418	0.029
84	Cholesta-4,6-dien-3-ol, (3beta)-	$C_{27}H_{44}O$	384.6	93.6	48.339	120719	0.028

85	Cholesteryl propionate	$C_{30}H_{50}O_2$	442.7	13.7	48.64	528892	0.124
86	1,3,5-Triphenylbenzene	$C_{24}H_{18}$	306.4	25.7	49.265	17647	0.004
87	Cholest-5-en-3-ol	$C_{27}H_{46}O$	386.7	44.2	51.603	15831939	3.710
88	Quinoline-5-carboxylic acid	$C_{10}H_7NO_2$	173.17	9.92	51.625	41623	0.010
89	Picolinohydrazide	$C_6H_7N_3O$	137.14	11.5	51.8595	3515	0.001
90	Cholesterol	$C_{27}H_{46}O$	386.7	77.5	51.8845	11950886	2.800
91	Cholest-4-en-3-one	$C_{27}H_{44}O$	384.6	88.9	53.28	224358	0.053
92	Cholesta-4,6-dien-3-one	$C_{27}H_{42}O$	382.6	38.9	53.7265	19947	0.005

- **Enrichment analysis**

Disease signatures (Figure 24.2 and Table 16.2), metabolites enrichment from the KEGG database (Figure 24.3 and Table 16.3) and from the SMPDB database (Figure 24.4 and Table 16.4), and different classes of metabolites (Figure 24.5 and Table 16.5) are given below. The enrichment ratio is no. of hits observed divided by no. of hits expected.

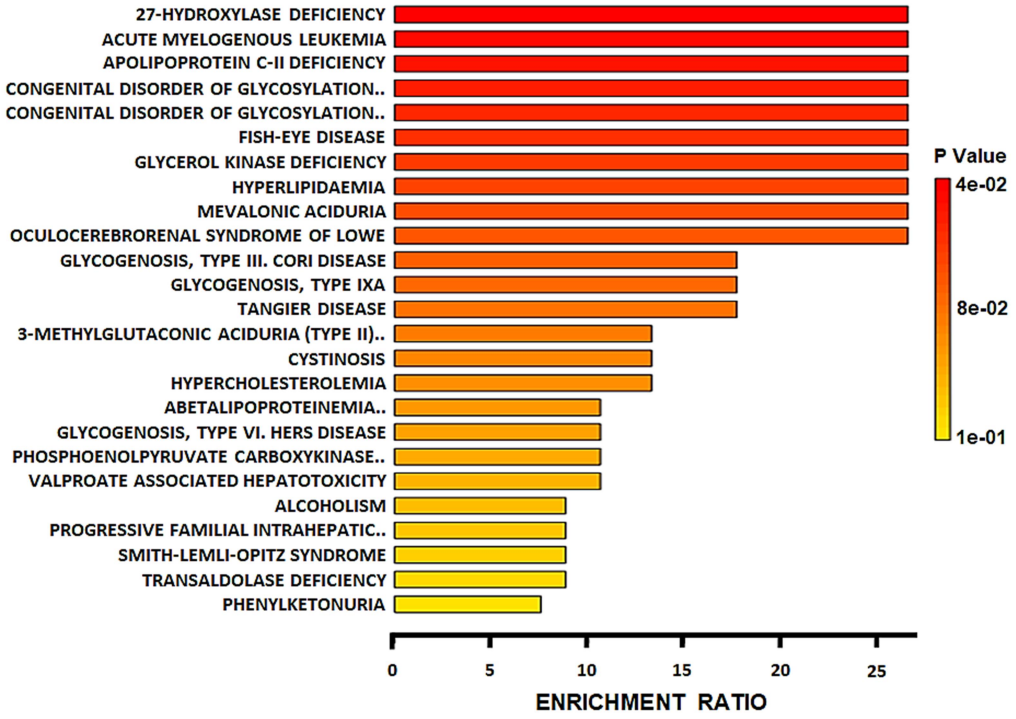

Figure 24.2: Disease signatures in NaCl-treated cells

The top 25 disease signatures were identified. Significantly enriched signatures (↓) include 27-hydroxylase deficiency, acute myelogenous leukemia, apolipoprotein C-II deficiency, a congenital

disorder of glycosylation CDG-IA and CDG-IB, and fish-eye disease. Highly enriched signatures (←) include 27-hydroxylase deficiency, acute myelogenous leukemia, apolipoprotein C-II deficiency, a congenital disorder of glycosylation CDG-IA and CDG-IB, fish-eye disease, glycerol kinase deficiency, hyperlipidaemia, mevalonic aciduria, and oculocerebrorenal syndrome of lowe.

Table 16.2: Disease signatures in NaCl-treated cells

	Metabolite Set	Total	Hits	Expect	P Value	Holm P	FDR
	27-HYDROXYLASE DEFICIENCY	2	1	0.0376	0.0373	1.0	1.0
	ACUTE MYELOGENOUS LEUKEMIA	2	1	0.0376	0.0373	1.0	1.0
	APOLIPOPROTEIN C-II DEFICIENCY | CHOLESTERYL ESTER STORAGE DISEASE | GLYCOGENOSIS, TYPE IXB	2	1	0.0376	0.0373	1.0	1.0
	CONGENITAL DISORDER OF GLYCOSYLATION CDG-IA	2	1	0.0376	0.0373	1.0	1.0
	CONGENITAL DISORDER OF GLYCOSYLATION CDG-IB	2	1	0.0376	0.0373	1.0	1.0
	FISH-EYE DISEASE	2	1	0.0376	0.0373	1.0	1.0
	GLYCEROL KINASE DEFICIENCY	2	1	0.0376	0.0373	1.0	1.0
	HYPERLIPIDAEMIA	2	1	0.0376	0.0373	1.0	1.0
	MEVALONIC ACIDURIA	2	1	0.0376	0.0373	1.0	1.0
	OCULOCEREBRORENAL SYNDROME OF LOWE	2	1	0.0376	0.0373	1.0	1.0
	GLYCOGENOSIS, TYPE III. CORI DISEASE, DEBRANCHER GLYCOGENOSIS	3	1	0.0564	0.0554	1.0	1.0
	GLYCOGENOSIS, TYPE IXA	3	1	0.0564	0.0554	1.0	1.0
	TANGIER DISEASE	3	1	0.0564	0.0554	1.0	1.0
	3-METHYLGLUTACONIC ACIDURIA (TYPE II), X-LINKED	4	1	0.0752	0.0733	1.0	1.0
	CYSTINOSIS	4	1	0.0752	0.0733	1.0	1.0
	HYPERCHOLESTEROLEMIA	4	1	0.0752	0.0733	1.0	1.0
	ABETALIPOPROTEINEMIA, BASSEN-KORNZWEIG-SYNDROME, ACANTHOCYTOSIS (ABL)	5	1	0.0939	0.0908	1.0	1.0
	GLYCOGENOSIS (TYPE IA, IB, IC) | GLYCOGENOSIS, TYPE VI. HERS DISEASE	5	1	0.0939	0.0908	1.0	1.0
	PHOSPHOENOLPYRUVATE CARBOXYKINASE DEFICIENCY 2 (PEPCK2)	5	1	0.0939	0.0908	1.0	1.0

	VALPROATE THERAPY: ANTICONVULASANT HYPERSENSITIVITY SYNDROME VALPROATE-ASSOCIATED HEPATOTOXICITY	5	1	0.0939	0.0908	1.0	1.0
	ALCOHOLISM	6	1	0.113	0.108	1.0	1.0
	PROGRESSIVE FAMILIAL INTRAHEPATIC CHOLESTASIS	6	1	0.113	0.108	1.0	1.0
	SMITH-LEMLI-OPITZ SYNDROME	6	1	0.113	0.108	1.0	1.0
	TRANSALDOLASE DEFICIENCY	6	1	0.113	0.108	1.0	1.0
	PHENYLKETONURIA	7	1	0.132	0.125	1.0	1.0

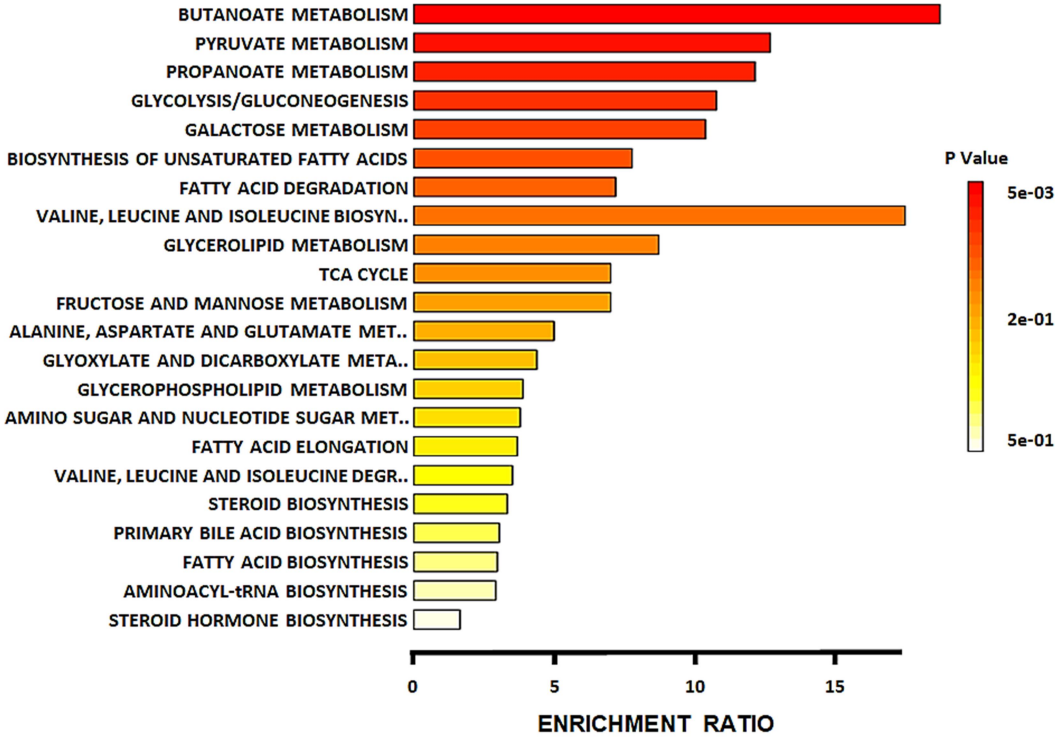

Figure 24.3: NaCl-specific metabolites enrichment from the KEGG database

The top 22 metabolic pathways were identified. Significantly enriched pathways (↓) include butanoate metabolism, pyruvate metabolism, propanoate metabolism, glycolysis/gluconeogenesis, and galactose metabolism. Highly enriched pathways (←) include butanoate metabolism, valine, leucine, and isoleucine biosynthesis, pyruvate metabolism, propanoate metabolism, and glycolysis/gluconeogenesis.

Table 16.3: NaCl-specific metabolites enrichment from the KEGG database

	Metabolite Set	Total	Hits	Expect	P Value	Holm P	FDR
	Butanoate metabolism	15	2	0.107	0.00466	0.391	0.249
	Pyruvate metabolism	22	2	0.158	0.00996	0.827	0.249
	Propanoate metabolism	23	2	0.165	0.0109	0.891	0.249
	Glycolysis / Gluconeogenesis	26	2	0.186	0.0138	1.0	0.249
	Galactose metabolism	27	2	0.193	0.0148	1.0	0.249
	Biosynthesis of unsaturated fatty acids	36	2	0.258	0.0257	1.0	0.359
	Fatty acid degradation	39	2	0.279	0.0299	1.0	0.359
	Valine, leucine, and isoleucine biosynthesis	8	1	0.0573	0.056	1.0	0.588
	Glycerolipid metabolism	16	1	0.115	0.109	1.0	1.0
	Citrate cycle (TCA cycle)	20	1	0.143	0.135	1.0	1.0
	Fructose and mannose metabolism	20	1	0.143	0.135	1.0	1.0
	Alanine, aspartate and glutamate metabolism	28	1	0.201	0.184	1.0	1.0
	Glyoxylate and dicarboxylate metabolism	32	1	0.229	0.207	1.0	1.0
	Glycerophospholipid metabolism	36	1	0.258	0.23	1.0	1.0
	Amino sugar and nucleotide sugar metabolism	37	1	0.265	0.236	1.0	1.0
	Fatty acid elongation	38	1	0.272	0.242	1.0	1.0
	Valine, leucine and isoleucine degradation	40	1	0.286	0.253	1.0	1.0
	Steroid biosynthesis	42	1	0.301	0.264	1.0	1.0
	Primary bile acid biosynthesis	46	1	0.329	0.285	1.0	1.0
	Fatty acid biosynthesis	47	1	0.337	0.29	1.0	1.0
	Aminoacyl-tRNA biosynthesis	48	1	0.344	0.296	1.0	1.0
	Steroid hormone biosynthesis	85	1	0.609	0.467	1.0	1.0

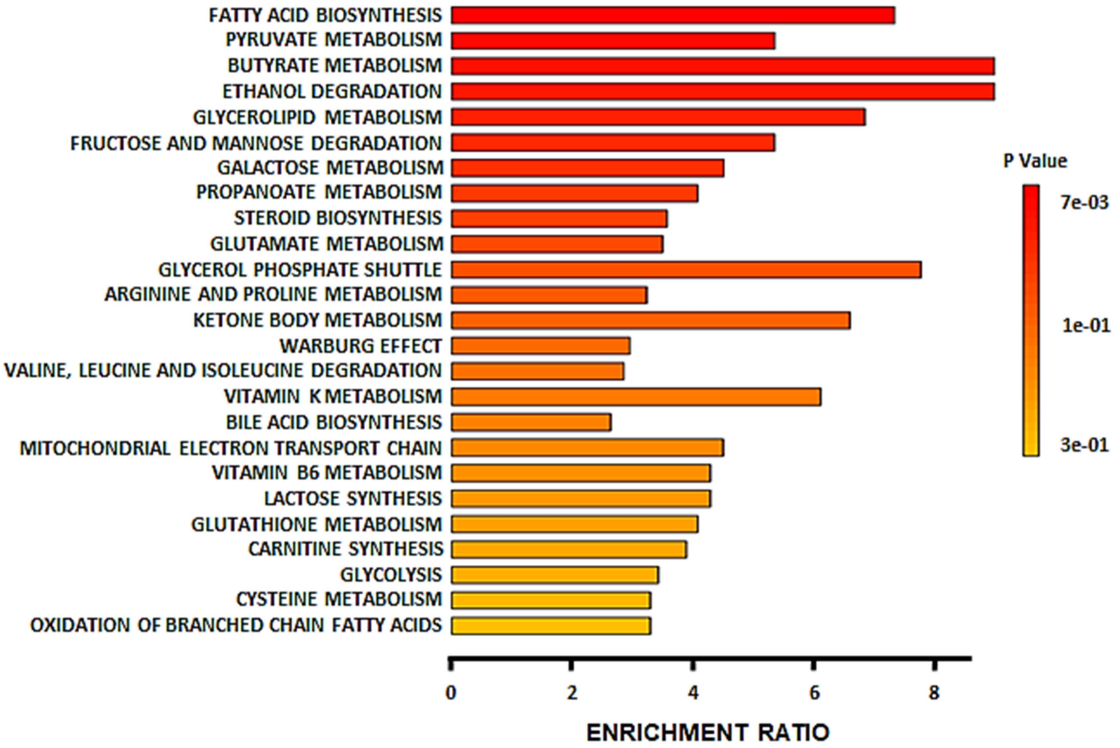

Figure 24.4: NaCl-specific metabolites enrichment from the SMPDB database

The top 25 metabolic pathways were identified. Significantly enriched pathways (↓) include fatty acid biosynthesis, pyruvate metabolism, butyrate metabolism, ethanol degradation, and glycerolipid metabolism. Highly enriched pathways (←) include butyrate metabolism, ethanol degradation, glycerol phosphate shuttle, fatty acid biosynthesis, and glycerolipid metabolism.

Table 16.4: NaCl-specific metabolites enrichment from SMPDB database

	Metabolite Set	Total	Hits	Expect	P Value	Holm P	FDR
	Fatty acid biosynthesis	35	3	0.41	0.00652	0.639	0.472
	Pyruvate metabolism	48	3	0.562	0.0158	1.0	0.472
	Butyrate metabolism	19	2	0.223	0.0193	1.0	0.472
	Ethanol degradation	19	2	0.223	0.0193	1.0	0.472
	Glycerolipid metabolism	25	2	0.293	0.0325	1.0	0.638
	Fructose and mannose degradation	32	2	0.375	0.0514	1.0	0.839
	Galactose metabolism	38	2	0.445	0.07	1.0	0.861
	Propanoate metabolism	42	2	0.492	0.0836	1.0	0.861
	Steroid biosynthesis	48	2	0.562	0.105	1.0	0.861

	Glutamate metabolism	49	2	0.574	0.109	1.0	0.861
	Glycerol phosphate shuttle	11	1	0.129	0.122	1.0	0.861
	Arginine and proline metabolism	53	2	0.621	0.125	1.0	0.861
	Ketone body metabolism	13	1	0.152	0.143	1.0	0.861
	Warburg effect	58	2	0.68	0.145	1.0	0.861
	Valine, leucine and isoleucine degradation	60	2	0.703	0.153	1.0	0.861
	Vitamin K metabolism	14	1	0.164	0.153	1.0	0.861
	Bile acid biosynthesis	65	2	0.762	0.174	1.0	0.861
	Mitochondrial electron transport chain	19	1	0.223	0.202	1.0	0.861
	Vitamin B6 metabolism	20	1	0.234	0.212	1.0	0.861
	Lactose synthesis	20	1	0.234	0.212	1.0	0.861
	Glutathione metabolism	21	1	0.246	0.221	1.0	0.861
	Carnitine synthesis	22	1	0.258	0.231	1.0	0.861
	Glycolysis	25	1	0.293	0.258	1.0	0.861
	Cysteine metabolism	26	1	0.305	0.267	1.0	0.861
	Oxidation of branched chain fatty acids	26	1	0.305	0.267	1.0	0.861

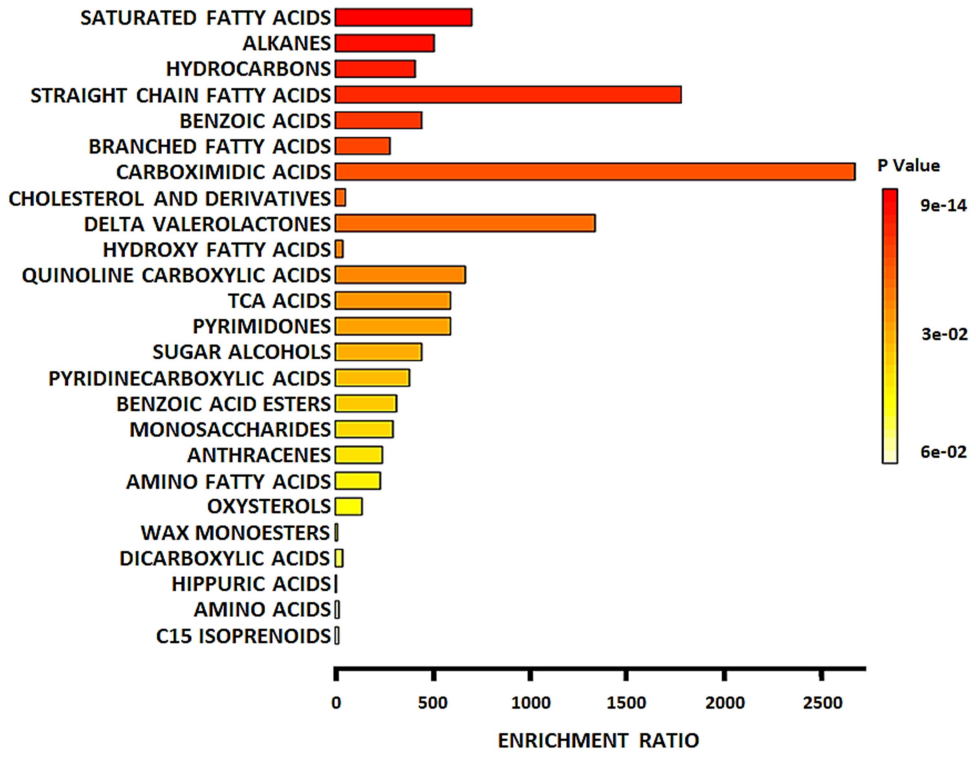

Figure 24.5: Different classes of identified metabolites in NaCl-treated cells

The top 25 different classes of metabolites were identified. Significantly enriched classes (↓) include saturated fatty acids, alkanes, hydrocarbons, straight-chain fatty acids, and benzoic acids.

Highly enriched classes (←) include carboximidic acids, straight-chain fatty acids, δ-valerolactones, saturated fatty acids, and quinoline carboxylic acids.

Table 16.5: Different classes of identified metabolites in NaCl-treated cells

	Metabolite Set	Total	Hits	Expect	P value	Holm P	FDR
	Saturated fatty acids	38	5	0.00709	8.53E-14	6.23E-11	6.23E-11
	Alkanes	42	4	0.00784	1.14E-10	8.34E-8	4.17E-8
	Hydrocarbons	52	4	0.0097	2.76E-10	2.01E-7	6.72E-8
	Straight-chain fatty acids	6	2	0.00112	5.08E-7	3.7E-4	9.28E-5
	Benzoic acids	24	2	0.00448	9.33E-6	0.00678	0.00136
	Branched fatty acids	38	2	0.00709	2.37E-5	0.0172	0.00289
	Carboximidic acids	2	1	3.73E-4	3.73E-4	0.271	0.039
	Cholesterol and derivatives	203	2	0.0379	6.78E-4	0.491	0.0606
	Delta valerolactones	4	1	7.46E-4	7.46E-4	0.539	0.0606
	Hydroxy fatty acids	274	2	0.0511	0.00123	0.886	0.0897
	Quinoline carboxylic acids	8	1	0.00149	0.00149	1.0	0.0944
	TCA acids	9	1	0.00168	0.00168	1.0	0.0944
	Pyrimidones	9	1	0.00168	0.00168	1.0	0.0944
	Sugar alcohols	12	1	0.00224	0.00224	1.0	0.117
	Pyridinecarboxylic acids	14	1	0.00261	0.00261	1.0	0.127
	Benzoic acid esters	17	1	0.00317	0.00317	1.0	0.144
	Monosaccharides	18	1	0.00336	0.00335	1.0	0.144
	Anthracenes	22	1	0.00411	0.0041	1.0	0.165
	Amino fatty acids	23	1	0.00429	0.00428	1.0	0.165
	Oxysterols	39	1	0.00728	0.00725	1.0	0.265
	Wax monoesters	949	2	0.177	0.0136	1.0	0.475
	Dicarboxylic acids	140	1	0.0261	0.0258	1.0	0.857
	Hippuric acids	1470	2	0.274	0.0307	1.0	0.977
	Amino acids	277	1	0.0517	0.0504	1.0	1.0
	C15 isoprenoids	333	1	0.0621	0.0603	1.0	1.0

➢ **Pathway analysis**

Impacted pathways from the KEGG database (Figure 24.6 and Table 16.6), and the SMPDB database (Figure 24.7 and Table 16.7) are given below. Pathway impact is calculated by using centrality and pathway enrichment results.

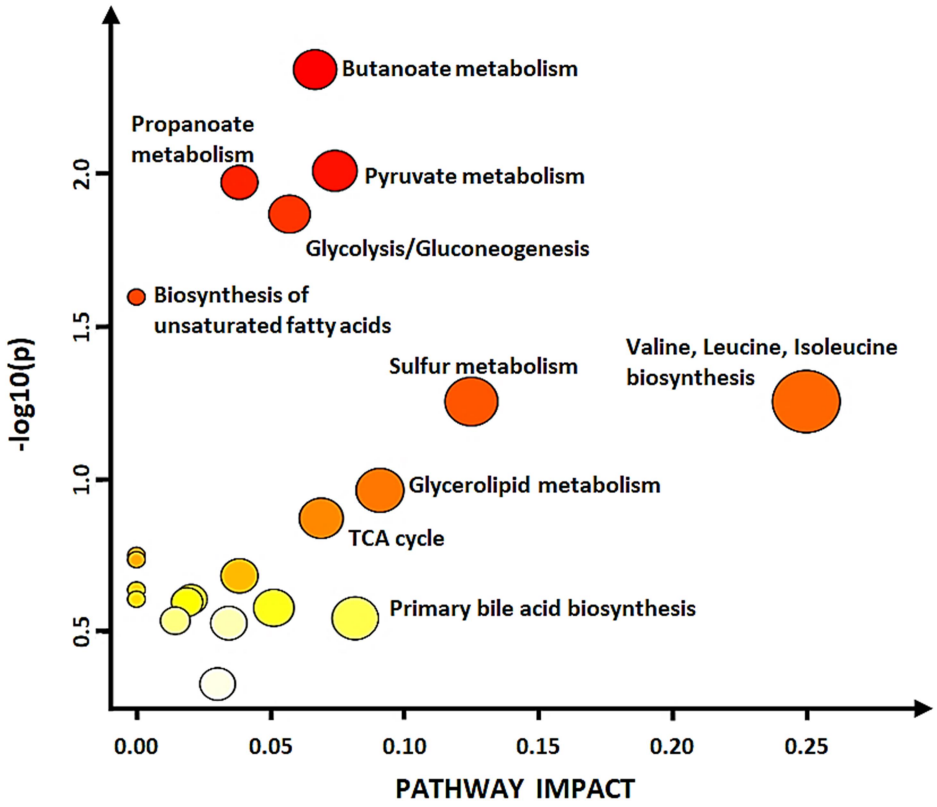

Figure 24.6: NaCl-specific pathway analysis from the KEGG database

The top 21 impacted pathways were identified. Highly impacted pathways (←) include valine, leucine, and isoleucine biosynthesis, sulfur metabolism, glycerolipid metabolism, primary bile acid biosynthesis, and pyruvate metabolism. Significantly impacted pathways (↓) include butanoate metabolism, pyruvate metabolism, propanoate metabolism, glycolysis/gluconeogenesis, and biosynthesis of unsaturated fatty acids.

Table 16.6: NaCl-specific pathway analysis from the KEGG database

Pathway Name	Match Status	p	-log(p)	Holm p	FDR	Impact
Butanoate metabolism	2/15	0.0045738	2.3397	0.3842	0.28486	0.06667
Pyruvate metabolism	2/22	0.0097925	2.0091	0.81278	0.28486	0.07408
Propanoate metabolism	2/23	0.010684	1.9713	0.87605	0.28486	0.03846
Glycolysis / Gluconeogenesis	2/26	0.013565	1.8676	1.0	0.28486	0.05714
Biosynthesis of unsaturated fatty acids	2/36	0.025294	1.597	1.0	0.42494	0.0
Sulfur metabolism	1/8	0.055506	1.2557	1.0	0.66607	0.125
Valine, leucine, and isoleucine biosynthesis	1/8	0.055506	1.2557	1.0	0.66607	0.25
Glycerolipid metabolism	1/16	0.1082	0.96578	1.0	1.0	0.09091
Citrate cycle (TCA cycle)	1/20	0.13353	0.87443	1.0	1.0	0.06897
Galactose metabolism	1/27	0.17629	0.75378	1.0	1.0	0.0
Alanine, aspartate and glutamate metabolism	1/28	0.18224	0.73936	1.0	1.0	0.0
Glyoxylate and dicarboxylate metabolism	1/32	0.20565	0.68688	1.0	1.0	0.03846
Glycerophospholipid metabolism	1/36	0.22844	0.64122	1.0	1.0	0.0
Fatty acid elongation	1/39	0.24515	0.61057	1.0	1.0	0.0
Fatty acid degradation	1/39	0.24515	0.61057	1.0	1.0	0.02041
Valine, leucine and isoleucine degradation	1/40	0.25064	0.60094	1.0	1.0	0.01887
Steroid biosynthesis	1/42	0.26153	0.58248	1.0	1.0	0.05128
Primary bile acid biosynthesis	1/46	0.28286	0.54843	1.0	1.0	0.08163
Fatty acid biosynthesis	1/47	0.2881	0.54045	1.0	1.0	0.01449
Aminoacyl-tRNA biosynthesis	1/48	0.29332	0.53267	1.0	1.0	0.03448
Steroid hormone biosynthesis	1/85	0.46338	0.33406	1.0	1.0	0.0303

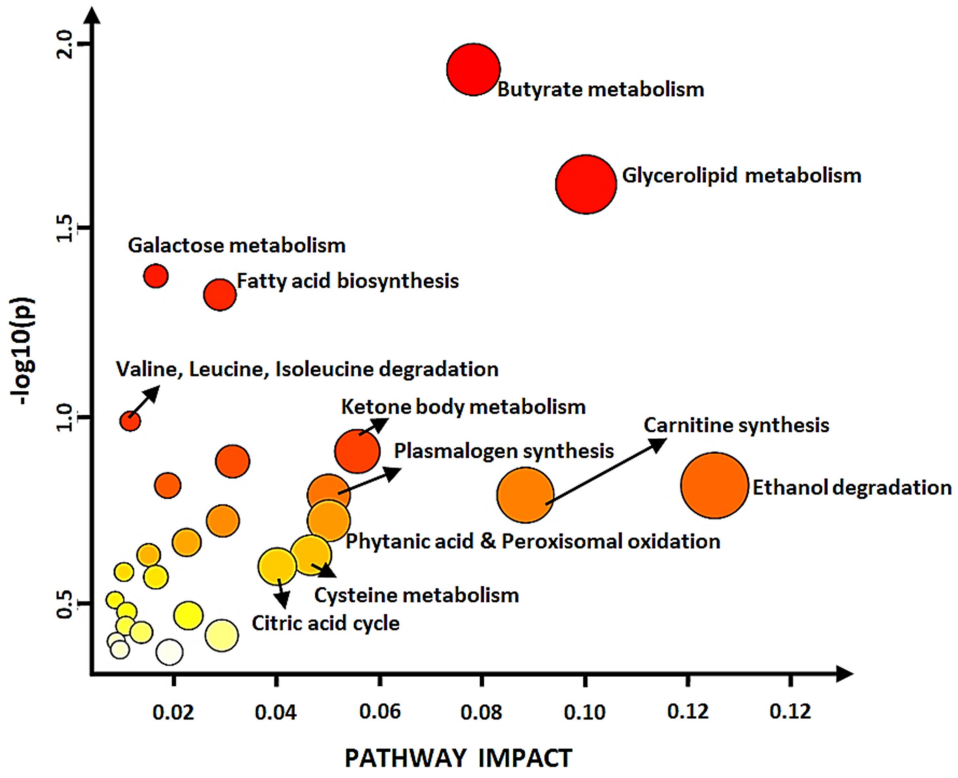

Figure 24.7: NaCl -specific pathway analysis from the SMPDB database

The top 28 impacted pathways were identified. Highly impacted pathways (←) include ethanol degradation, glycerolipid metabolism, carnitine synthesis, butyrate metabolism, and ketone body metabolism. Significantly impacted pathways (↓) include butyrate metabolism, glycerolipid metabolism, galactose metabolism, fatty acid biosynthesis, valine, leucine, and isoleucine degradation.

Table 16.7: NaCl -specific pathway analysis from the SMPDB database

Pathway Name	Match Status	p	-log(p)	Holm p	FDR	Impact
Butyrate metabolism	2/16	0.011937	1.9231	1.0	1.0	0.078125
Glycerolipid metabolism	2/23	0.024136	1.6173	1.0	1.0	0.1
Galactose metabolism	2/31	0.042292	1.3737	1.0	1.0	0.016393
Fatty acid biosynthesis	2/33	0.047452	1.3237	1.0	1.0	0.028846
Valine, leucine, and isoleucine degradation	2/51	0.10292	0.98748	1.0	1.0	0.011429
Ketone body metabolism	1/12	0.12389	0.90695	1.0	1.0	0.055556
Bile acid biosynthesis	2/59	0.1317	0.88043	1.0	1.0	0.031311

Mitochondrial electron transport chain	1/15	0.1526	0.81644	1.0	1.0	0.018692
Ethanol degradation	1/15	0.1526	0.81644	1.0	1.0	0.125
Plasmalogen synthesis	1/16	0.16198	0.79054	1.0	1.0	0.05
Carnitine synthesis	1/16	0.16198	0.79054	1.0	1.0	0.088235
Sulfate/Sulfite metabolism	1/19	0.18955	0.72228	1.0	1.0	0.029412
Phytanic acid peroxisomal oxidation	1/19	0.18955	0.72228	1.0	1.0	0.05
Oxidation of branched chain fatty acids	1/22	0.21629	0.66496	1.0	1.0	0.022388
Mitochondrial beta-oxidation of long chain saturated fatty acids	1/24	0.23367	0.63139	1.0	1.0	0.015
Cysteine metabolism	1/24	0.23367	0.63139	1.0	1.0	0.046512
Citric acid cycle	1/26	0.2507	0.60084	1.0	1.0	0.04
Pentose phosphate pathway	1/27	0.25909	0.58656	1.0	1.0	0.010204
Fructose and mannose degradation	1/28	0.26739	0.57286	1.0	1.0	0.016393
Fatty acid elongation in mitochondria	1/33	0.30763	0.51197	1.0	1.0	0.0084746
Propanoate metabolism	1/36	0.3308	0.48044	1.0	1.0	0.010753
Pyruvate metabolism	1/37	0.33836	0.47061	1.0	1.0	0.022727
Fatty acid metabolism	1/40	0.3606	0.44298	1.0	1.0	0.010563
Steroidogenesis	1/42	0.37504	0.42592	1.0	1.0	0.013575
Steroid biosynthesis	1/43	0.38215	0.41777	1.0	1.0	0.029197
Glutamate metabolism	1/45	0.39615	0.40214	1.0	1.0	0.0087209
Arginine and proline metabolism	1/48	0.4166	0.38028	1.0	1.0	0.009434
Warburg effect	1/49	0.42328	0.37337	1.0	1.0	0.019048

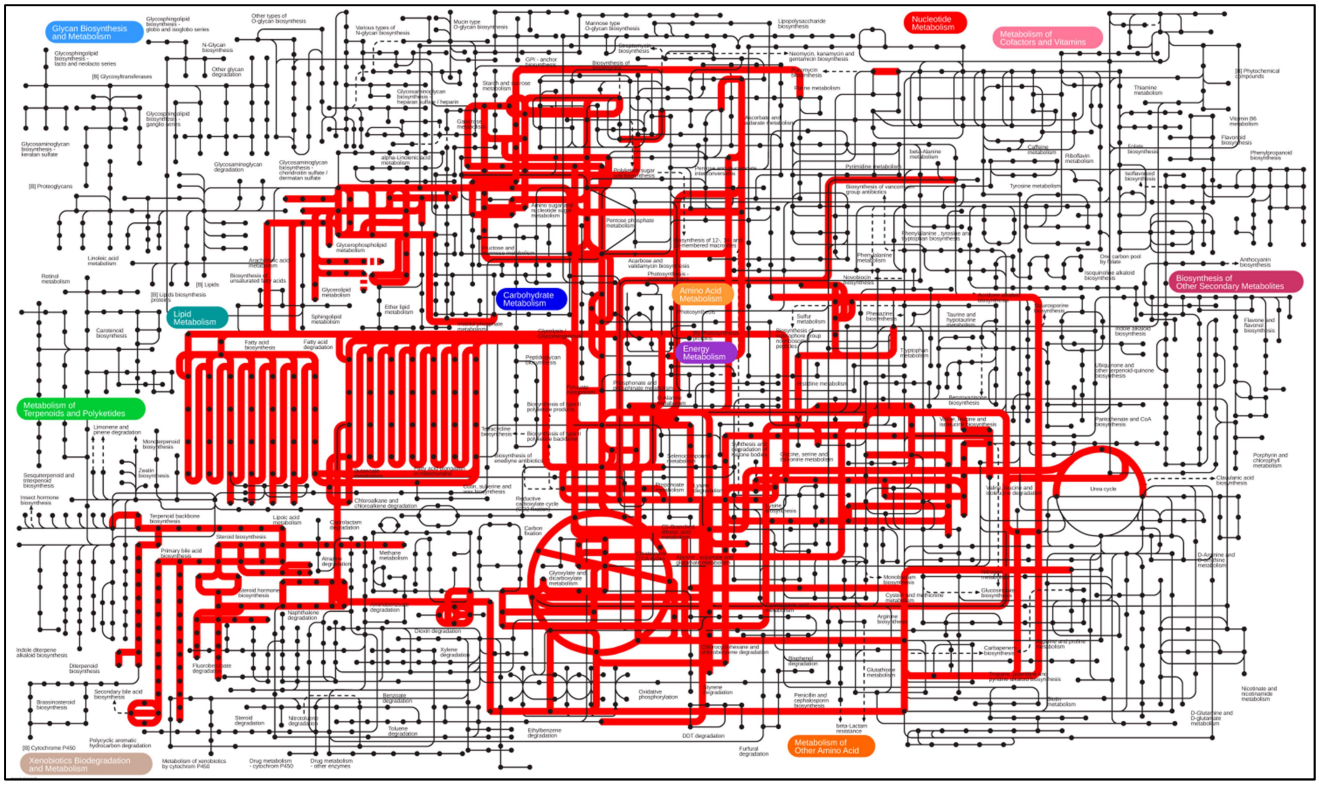

Figure 24.8: Metabolic pathways enriched in NaCl treatment after mapping with the KEGG database. The highlighted metabolisms show enrichment specific to NaCl treatment. This shows the enrichment of propanoate metabolism, TCA cycle, energy metabolism, glycerophospholipid metabolism, and other metabolic pathways.

V. High bovine serum albumin treatment

Cells were treated with 5 mM BSA media for 24 hours.

➢ GC-MS graph

GC chromatogram of BSA treatment (given in Figure 25.1) depicts retention time (min) on X-axis and relative abundance (intensity) on Y-axis. A total of 231 metabolites (components) were identified in BSA-treated cells (given in Table 17.1). The most abundant metabolites are – Acetamide (68.881%), Cholesterol (17.046%), Palmitic Acid (4.492%), 2-Propyl-1-pentanol (3.66%), and Guaiacol (1.186%). The abundance is measured based on the % area of the peak of specific components.

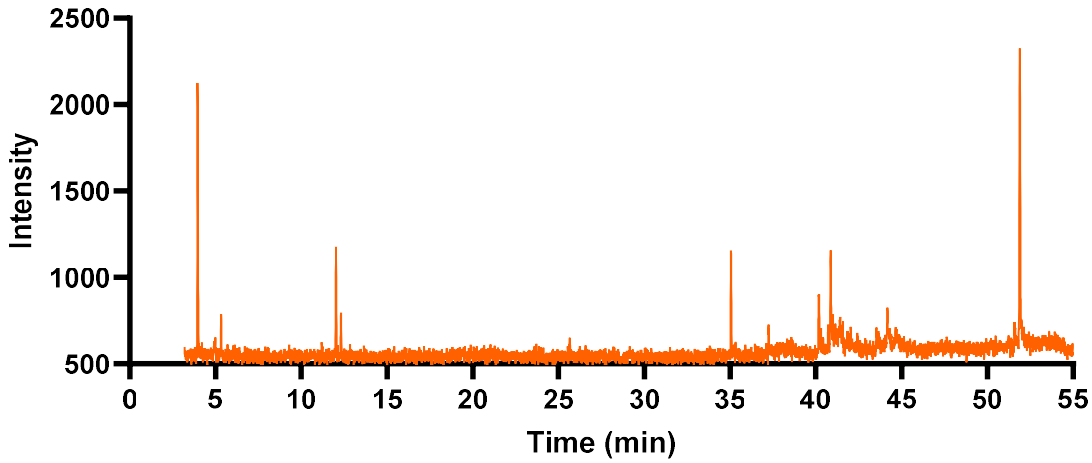

Figure 25.1: GC-MS graph obtained for BSA treatment

Table 17.1: Metabolites identified in BSA-treated cells

S.No.	Metabolites	Mol. Formula	MW (g/mol)	% Probability	RT (min)	Area	% Area
1	Azadirachtin	$C_{35}H_{44}O_{16}$	720.7	24.1	3.246	98	0.001
2	Oleanane	$C_{30}H_{52}$	412.7	39.6	3.374	343	0.005
3	Benzene, [3-(2-cyclohexylethyl)-6-cyclopentylhexyl]-	$C_{25}H_{40}$	340.6	34.9	3.831	546	0.008
4	Alanine	$C_3H_7NO_2$	89.09	38.2	3.9355	19477	0.276
5	Acetamide	C_2H_5NO	59.07	54.2	3.9575	4863660	68.881
6	Butylphosphonic acid	$C_4H_{11}O_3P$	138.10	51.4	4.1645	148	0.002

7	Carbamazepine	$C_{15}H_{12}N_2O$	236.27	22.6	4.203	188	0.003
8	Triazatriphosphorine	N_3P_3	134.942	88.8	4.5245	99	0.001
9	D-Glucose	$C_6H_{12}O_6$	180.16	77.5	5.763	189	0.003
10	Protoporphyrin IX	$C_{34}H_{34}N_4O_4$	562.7	49.8	5.8345	445	0.006
11	D-Glycero-L-manno-heptono-gamma-lactone	$C_7H_{12}O_7$	208.17	26.6	5.8765	170	0.002
12	Quinazoline-4-acetic Acid	$C_{10}H_8N_2O_2$	188.18	32.5	6.138	399	0.006
13	Daphnetoxin	$C_{27}H_{30}O_8$	482.5	36.6	6.5945	212	0.003
14	Tetraphosphorus	P_4	123.89	73	6.7345	46	0.001
15	D-alanine	$C_3H_7NO_2$	89.09	50.9	6.898	244	0.003
16	1,4-Dioxa-8-azaspiro[4.5]decane	$C_7H_{13}NO_2$	143.18	40.1	7.115	150	0.002
17	Propanenitrile-25	C_3H_5N	55.08	64.7	7.237	131	0.002
18	9-Thiabicyclo[3.3.1]nonan-3-one 9,9-dioxide	$C_8H_{12}O_3S$	188.25	3.16	7.3345	139	0.002
19	2-Methylbenzyl p-toluate	$C_{16}H_{16}O_2$	240.30	33.9	7.4195	59	0.001
20	Lycopene	$C_{40}H_{56}$	536.9	6.9	7.68	856	0.012
21	2,2-Dimethoxypropane	$C_5H_{12}O_2$	104.15	46.6	7.7655	108	0.002
22	1-Phenyl-2-propanone	$C_9H_{10}O$	135.17	49.8	7.898	337	0.005
23	Carpesterol benzoate	$C_{44}H_{58}O_5$	666.9	60.8	8.1135	149	0.002
24	Norgestrel	$C_{21}H_{28}O_2$	312.4	70.9	8.495	107	0.002
25	Phenol, 2-(4,6-diamino-1,3,5-triazin-2-yl)-	$C_9H_9N_5O$	203.20	62.9	8.9595	561	0.008
26	Chroman-2-ol	$C_9H_{10}O_2$	150.17	25.5	8.996	612	0.009
27	Cycloartane	$C_{30}H_{52}$	412.7	58.4	9.027	126	0.002
28	2,5-Diaminobenzophenone	$C_{13}H_{12}N_2O$	212.25	7.76	9.7245	47	0.001
29	2-Methylthiazolidine	C_4H_9NS	103.19	13.2	9.9405	293	0.004
30	Acridine	$C_{13}H_9N$	179.22	72.7	10.0445	127	0.002
31	2H-1-Benzopyran-6-carbaldehyde	$C_{10}H_8O_2$	160.17	14.5	10.8215	504	0.007
32	Ethylcyclobutane	C_6H_{12}	84.16	39.6	10.9095	49	0.001
33	Diethyl malonate	$C_7H_{12}O_4$	160.17	28.1	11.166	51	0.001
34	3-Hexene	C_6H_{12}	84.16	13.3	11.2045	428	0.006
35	1h-Pyrido[3,4-b]indol-1-one	$C_{11}H_6N_2O$	182.18	61.3	11.544	180	0.003
36	Torosanin	$C_{32}H_{28}O_9$	556.6	90.6	12.1715	280	0.004
37	Phenyl 3-methylbenzoate	$C_{14}H_{12}O_2$	212.24	6.1	12.2365	816	0.012
38	3-Thiophenecarboxaldehyde	C_5H_4OS	112.15	34.3	12.2995	83472	1.182
39	2-Propyl-1-pentanol	$C_8H_{18}O$	130.23	32.4	12.3105	258408	3.660
40	Isoquinoline-1-carboxylic acid	$C_{10}H_7NO_2$	173.17	58.2	12.489	686	0.010
41	Phosphinic amide, N-hexyl-P,P-diphenyl-	$C_{18}H_{24}NOP$	301.4	58.9	12.6485	254	0.004
42	2,5-Cyclohexadienone	C_6H_6O	94.11	14.5	12.875	110	0.002
43	alpha-Carotene	$C_{40}H_{56}$	536.9	26.1	12.91	329	0.005
44	Methyl 3-oxo-2-phenylpropanoate	$C_{10}H_{10}O_3$	178.18	22.6	13.2095	155	0.002

45	N,N'-Bis-(4-methyl-benzylidene)-hydrazine	$C_{16}H_{16}N_2$	236.31	75.7	13.3595	143	0.002
46	Leucine	$C_6H_{13}NO_2$	131.17	13.8	13.649	140	0.002
47	5alpha-Cholestane-3,11-dione	$C_{27}H_{44}O_2$	400.6	58.5	14.033	63	0.001
48	cis-1-Nitro-1-propene	$C_3H_5NO_2$	87.08	8.57	14.7545	389	0.006
49	Cyclohexane	C_6H_{12}	84.16	5.38	14.796	343	0.005
50	2H,8H-Benzo[1,2-b:5,4-b']dipyran-10-propanol, 5-methoxy-2,2,8,8-tetramethyl-	$C_{20}H_{26}O_4$	330.4	11.8	14.9235	302	0.004
51	7,3',4'-Trimethoxyflavone	$C_{18}H_{16}O_5$	312.3	73.7	15.0775	499	0.007
52	Methyl 2,3,4,6-tetra-O-methyl-alpha-D-glucopyranoside	$C_{11}H_{22}O_6$	250.29	29.5	15.5725	137	0.002
53	2,3-Dibenzyl-1,3-butadiene	$C_{18}H_{18}$	234.3	55.1	15.8975	191	0.003
54	7-Hydroxy-2,2-dimethylchromene	$C_{11}H_{12}O_2$	176.21	63.5	16.05	242	0.003
55	Isopropyl decanoate	$C_{13}H_{26}O_2$	214.34	70.3	16.1005	81	0.001
56	Isoxazole	C_3H_3NO	69.06	15.2	16.5045	394	0.006
57	Pyridine-3,5-dicarboxylic acid	$C_7H_5NO_4$	167.12	55	16.916	73	0.001
58	1,3,5-Triazin-2-amine	$C_3H_4N_4$	96.09	42.8	17.0495	130	0.002
59	Phenol	C_6H_6O	94.11	77.3	17.4985	36	0.001
60	Malonic acid	$C_3H_4O_4$	104.06	67.5	18.087	203	0.003
61	2-Methylbenzylamine	$C_8H_{11}N$	121.18	25.7	18.4695	123	0.002
62	Octa-3,5-diene-2,7-dione	$C_8H_{10}O_2$	138.16	25.6	18.6855	227	0.003
63	trans-Stilbene-alpha,alpha'-D2	$C_{14}H_{12}$	182.26	52.7	18.931	230	0.003
64	1,3-Dinitrobenzene	$C_6H_4N_2O_4$	168.11	32	18.9655	53	0.001
65	Retigeradiol	$C_{30}H_{52}O_2$	444.7	62.2	19.4675	406	0.006
66	1H-1,2,4-Triazole-3-carboxamide	$C_3H_4N_4O$	112.09	62.8	19.749	435	0.006
67	Benzaldehyde	C_7H_6O	106.12	24.7	20.0895	149	0.002
68	Ethyl p-toluenesulfonate	$C_9H_{12}O_3S$	200.26	29.1	20.2295	112	0.002
69	Urs-20-en-16-yl acetate	$C_{32}H_{52}O_2$	468.8	28.2	20.606	376	0.005
70	Methanesulfonamide	CH_5NO_2S	95.12	17.7	20.6625	348	0.005
71	Chamaecydin	$C_{30}H_{40}O_3$	448.6	68.5	20.7405	412	0.006
72	Xanthodactynaphin-jc-1	$C_{30}H_{28}O_{12}$	580.5	65.9	20.917	284	0.004
73	Retigeric acid B	$C_{30}H_{46}O_6$	502.7	12.3	21.2815	268	0.004
74	2-Methyl-1,3-oxazolidin-2-ol	$C_4H_9NO_2$	103.12	64.4	21.311	132	0.002
75	Galactitol	$C_6H_{14}O_6$	182.17	63.9	21.7105	161	0.002
76	1H-pyrazole-5-carbohydrazide	$C_4H_6N_4O$	126.12	11.3	21.85	82	0.001
77	Glycylglycine	$C_4H_8N_2O_3$	132.12	51.1	21.927	64	0.001
78	Methanone, bis(3-methoxyphenyl)-, hydrazone	$C_{15}H_{16}N_2O_2$	256.30	14.4	22.1555	336	0.005
79	Pyridine	C_5H_5N	79.10	7.8	22.551	322	0.005
80	Fumaric acid	$C_4H_4O_4$	116.07	33	22.83	449	0.006
81	3-Butenamide	C_4H_7NO	85.10	70.6	23.026	182	0.003
82	Proline	$C_5H_9NO_2$	115.13	35	23.261	121	0.002
83	Octadecadienoic acid	$C_{18}H_{32}O_2$	280.4	13.6	23.3725	343	0.005

84	Methoxamine acetate	$C_{13}H_{19}NO_4$	253.29	45.4	23.476	320	0.005
85	3H-[1,2,4]triazolo[4,3-b][1,2,4]triazole-3,6-diamine	$C_3H_5N_7$	139.12	11.1	23.5215	317	0.004
86	5h-Cyclopenta[d]pyrimidine	$C_7H_6N_2$	118.14	23.2	23.8755	948	0.013
87	2-Methylquinoxaline	$C_9H_8N_2$	144.17	17.8	24.737	279	0.004
88	Propionamide	C_3H_7NO	73.09	36.6	25.3735	378	0.005
89	4-Nitro-1H-pyrazole-3-carboxamide	$C_4H_4N_4O_3$	156.10	7.51	25.5445	179	0.003
90	Naphthalene	$C_{10}H_8$	128.17	84.9	25.6075	133	0.002
91	Cinchophen	$C_{16}H_{11}NO_2$	249.26	15.9	25.719	299	0.004
92	Grayanotoxin II 3,6-diacetate	$C_{24}H_{36}O_7$	436.5	47.9	25.786	117	0.002
93	Racemosol	$C_{21}H_{24}O_4$	340.4	23.3	25.9	129	0.002
94	Butane	C_4H_{10}	58.12	39.6	25.9555	82	0.001
95	1,3,5-Triazine	$C_3H_3N_3$	81.08	36.2	26.1905	206	0.003
96	1,2-Diphenylhydrazine	$C_{12}H_{12}N_2$	184.24	7.21	26.3995	302	0.004
97	Thiazine	C_4H_5NS	99.16	29.9	26.619	58	0.001
98	Terephthalic acid	$C_8H_6O_4$	166.13	19.5	26.689	85	0.001
99	D:A-Friedooleanan-1-one, 25,26-epoxy-	$C_{30}H_{48}O_2$	440.7	51.2	27.191	46	0.001
100	Cholest-5-en-3-yl acetate	$C_{29}H_{48}O_2$	428.7	20.9	27.2705	118	0.002
101	Phthalic acid	$C_8H_6O_4$	166.13	18.8	27.484	129	0.002
102	6H-Dibenzo[b,d]pyran-6-one	$C_{13}H_8O_2$	196.20	39.7	27.5705	141	0.002
103	(S)-Pyrrolidine-3-carboxylic acid	$C_5H_9NO_2$	115.13	4.46	27.6295	130	0.002
104	Thalidomide	$C_{13}H_{10}N_2O_4$	258.23	5.82	27.935	515	0.007
105	Phenylacetic acid	$C_8H_8O_2$	136.15	7.89	28.298	339	0.005
106	Pregnane-3,20-diamine	$C_{21}H_{38}N_2$	318.54	61.5	28.774	254	0.004
107	Benzoic acid	$C_7H_6O_2$	122.12	23.8	28.838	259	0.004
108	Monensin	$C_{36}H_{62}O_{11}$	670.9	52.5	28.897	185	0.003
109	Cylindrocarine	$C_{21}H_{28}N_2O_3$	356.5	54.3	29.0995	154	0.002
110	4H-1,3-Benzothiazine-4-one	C_8H_5NOS	163.20	30.4	29.1525	221	0.003
111	Pregnane	$C_{21}H_{36}$	288.5	39.4	29.315	169	0.002
112	Diphenyl sulfone	$C_{12}H_{10}O_2S$	218.27	49.9	29.544	533	0.008
113	Benzamide	C_7H_7NO	121.14	18.4	29.7935	91	0.001
114	d:c-Friedo-b':a'-neogammacer-9(11)-ene-2,3-diol, diacetate, (2alpha,3beta)-	$C_{34}H_{54}O_4$	526.8	70.5	30.125	163	0.002
115	1-Aminoisoquinoline	$C_9H_8N_2$	144.17	11.3	30.2195	112	0.002
116	Ethane-1,1-diamine	$C_2H_8N_2$	60.10	7.11	30.588	520	0.007
117	Glutaric acid	$C_5H_8O_4$	132.11	26.5	31.043	90	0.001
118	Propionic acid	$C_3H_6O_2$	74.08	15.5	31.1625	209	0.003
119	2,3-Dimethyltetradecane	$C_{16}H_{34}$	226.44	17.8	31.2865	309	0.004
120	Vinylporphyrin	$C_{22}H_{16}N_4$	336.4	18.5	31.5185	186	0.003
121	2-Dibenzofurancarboxylic acid	$C_{13}H_8O_3$	212.20	78.3	32.185	130	0.002
122	Terephthalamide	$C_8H_8N_2O_2$	164.16	28.7	32.2475	464	0.007

123	5-(4-Carboxyphenyl)-10,15,20-triphenylporphyrin	$C_{45}H_{30}N_4O_2$	658.7	49.2	32.4125	301	0.004
124	9,10-Dihydrophenanthrene	$C_{14}H_{12}$	180.24	12	32.5605	177	0.003
125	2,4,6,8-Tetrahydroxypyrimido[5,4-d]pyrimidine	$C_6H_4N_4O_4$	196.12	45.6	32.604	152	0.002
126	3',4',5,7-Tetramethoxyflavone	$C_{19}H_{18}O_6$	342.3	6.59	32.729	784	0.011
127	Benzodiazepinone	$C_9H_6N_2O$	158.16	59.3	32.945	284	0.004
128	Rhodopinal	$C_{40}H_{56}O_2$	568.9	12	33.047	1108	0.016
129	Benzanilide	$C_{13}H_{11}NO$	197.23	66.1	33.2085	205	0.003
130	Dibenzo-18-crown-6	$C_{20}H_{24}O_6$	360.4	11.9	33.6555	348	0.005
131	Aniline	C_6H_7N	93.13	10.3	33.7	408	0.006
132	2-Deoxy-alpha-ecdysone, 3-O-acetate 22-O-benzoate	$C_{36}H_{50}O_7$	594.8	13.3	34.4345	673	0.010
133	Indene	C_9H_8	116.16	59.2	34.4965	136	0.002
134	Valine	$C_5H_{11}NO_2$	117.15	40.3	34.6735	76	0.001
135	Quaterrylene	$C_{40}H_{20}$	500.6	20.3	34.7495	149	0.002
136	Butyric acid	$C_4H_8O_2$	88.11	12.3	35.01	869	0.012
137	Palmitic acid	$C_{16}H_{32}O_2$	256.42	97.7	35.0595	317159	4.492
138	3-(Pyrrolidin-1-yl)propanoic acid	$C_7H_{13}NO_2$	143.18	27	35.4935	85	0.001
139	3beta-Acetoxyolean-18-en-28-oic acid	$C_{32}H_{50}O_4$	498.7	64.2	36.444	96	0.001
140	6,7-Dihydro-5H-dibenzo[c,e]azepine-5-one	$C_{14}H_{11}NO$	209.24	12.5	37.1115	158	0.002
141	Glycine	$C_2H_5NO_2$	75.07	6.77	37.507	494	0.007
142	Prosta 5,13-dien-1-oic acid	$C_{20}H_{34}O_2$	306.5	22.8	37.5585	71	0.001
143	1,14-Tetradecanediamine	$C_{14}H_{32}N_2$	228.42	38.7	37.6505	186	0.003
144	p-Phenylenediamine	$C_6H_8N_2$	108.14	22.2	37.6875	59	0.001
145	Bis[4-[4-hydroxy]piperidino-3-aminophenyl]sulfone	$C_{22}H_{30}N_4O_4S$	446.6	35.9	37.8755	118	0.002
146	2-Oxa-5alpha-androstane-3,17-dione	$C_{18}H_{26}O_3$	290.4	43.8	38.471	197	0.003
147	Acridinone	$C_{13}H_9NO$	195.22	72.3	38.852	169	0.002
148	2',3',4',5,7-Pentamethoxyflavone	$C_{20}H_{20}O_7$	372.4	14.3	39.084	150	0.002
149	Allobetulane	$C_{30}H_{50}O$	426.7	53.3	39.1505	108	0.002
150	Tetracyclo[5.5.0.02,5.08,11]dodecane	$C_{12}H_{18}$	162.27	43.9	39.277	192	0.003
151	18-Methyleicosanoic acid	$C_{21}H_{42}O_2$	326.6	62.8	39.493	98	0.001
152	Anthraquinone	$C_{14}H_8O_2$	208.21	9.49	39.9835	246	0.003
153	Hexadecane	$C_{16}H_{34}$	226.44	11.6	40.17	10970	0.155
154	Hexacosanoic acid, pyrrolidide	$C_{30}H_{59}NO$	449.8	44.3	40.528	120	0.002
155	Dodecane	$C_{12}H_{26}$	170.33	14	40.8505	13073	0.185
156	Guaiacol	$C_7H_8O_2$	124.14	13.5	40.874	83740	1.186
157	Quinazoline	$C_8H_6N_2$	130.15	51.6	41.3555	53	0.001
158	5-Acetoxymethyl-2,6,10-trimethyl-2,9-undecadien-6-ol	$C_{17}H_{30}O_3$	282.4	16.6	41.3895	149	0.002

159	Spiro[bicyclo[3.1.0]hexane-6,3'(2'H)-as-indacen]-2-one, decahydro-6'-hydroxy-1,4,5'a-trimethyl-, acetate	$C_{22}H_{32}O_3$	344.5	23.9	42.121	224	0.003
160	1-Amino-1,2,4-triazole	$C_2H_4N_4$	84.08	47.8	42.212	147	0.002
161	7-O-methylisoorientin	$C_{22}H_{24}O_{11}$	464.4	49	42.8045	184	0.003
162	3,4-Dihydrocoumarin	$C_9H_8O_2$	148.16	13.7	42.9145	288	0.004
163	Succinamide	$C_4H_8N_2O_2$	116.12	44.9	43.2525	133	0.002
164	Fluorene	$C_{13}H_{10}$	166.22	26.9	43.335	299	0.004
165	Rodiasine	$C_{38}H_{42}N_2O_6$	622.7	19	43.587	818	0.012
166	2-Methylbenzyl benzoate	$C_{15}H_{14}O_2$	226.27	20.5	43.7255	66	0.001
167	1,2,3,5-Tetramethylbenzene	$C_{10}H_{14}$	134.22	38.2	43.8015	193	0.003
168	1,3-Dithiolium-4-olate	$C_3H_2OS_2$	118.18	20.8	43.8625	73	0.001
169	But-2-enoic acid	$C_4H_6O_2$	86.09	71.1	44.536	42	0.001
170	S-(4-(Acetylamino)phenyl) 4-(acetylamino)benzenesulfonothioate	$C_{16}H_{16}N_2O_4S_2$	364.4	65.4	44.772	93	0.001
171	Pyrrolo[1,2-a]pyrimidine	$C_7H_6N_2$	118.14	21.7	45.5115	833	0.012
172	Xanthopterin	$C_6H_5N_5O_2$	179.14	44.7	45.657	118	0.002
173	Peracetic acid	$C_2H_4O_3$	76.05	33.1	47.0875	65	0.001
174	Cyclohexane-1,2,4-trione	$C_6H_6O_3$	126.11	38.3	47.7295	96	0.001
175	Prost-13-en-1-oic acid, 9,11,15-tris(acetyloxy)-, methyl ester, (9alpha,11alpha,13E,15S)-	$C_{27}H_{44}O_8$	496.6	6.23	47.7645	1724	0.024
176	Diisopropyl methylphosphonate	$C_7H_{17}O_3P$	180.18	9.27	47.771	703	0.010
177	Trimetozine	$C_{14}H_{19}NO_5$	281.30	33.5	47.9925	46	0.001
178	Phenothiazine	$C_{12}H_9NS$	199.27	13.1	48.317	1082	0.015
179	(R)-5-Phenyl-2-cyclohexene-1-one	$C_{12}H_{12}O$	172.22	26.1	48.365	307	0.004
180	4-oxo-4H-Pyran-3-carboxylic acid	$C_6H_4O_4$	140.09	46.7	48.556	108	0.002
181	Succinamic acid	$C_4H_7NO_3$	117.10	56.8	48.62	254	0.004
182	Dienestrol	$C_{18}H_{18}O_2$	266.3	40.6	48.629	223	0.003
183	Dimethylphosphine	C_2H_7P	62.05	11.8	48.646	306	0.004
184	2,2-Diphenyl-2H-1-benzopyran-6-ol	$C_{21}H_{16}O_2$	300.3	33.9	48.68	1227	0.017
185	D-Arabinitol	$C_5H_{12}O_5$	152.15	89.7	48.849	73	0.001
186	5,6-Diphenylpyrazin-2-ol	$C_{16}H_{12}N_2O$	248.28	72.2	48.921	106	0.002
187	Pregnan-20-one	$C_{21}H_{34}O$	302.5	4.74	49.015	1615	0.023
188	Pyrrole-trione	C_4HNO_3	111.06	45.2	49.214	407	0.006
189	Azepinone	C_6H_5NO	107.11	71.2	49.3895	222	0.003
190	7H-Benzo[c]phenothiazine	$C_{16}H_{11}NS$	249.3	12.9	49.4615	809	0.011
191	Imidazolidin-4-one	$C_3H_6N_2O$	86.09	43.9	49.497	256	0.004
192	Biphenyl	$C_{12}H_{10}$	154.21	4.02	49.521	634	0.009
193	Anthracene	$C_{14}H_{10}$	178.23	14.9	49.9955	1085	0.015
194	3,5-Dimethylaniline	$C_8H_{11}N$	121.18	48.9	50.05	154	0.002

195	2-Penten-1-ol	$C_5H_{10}O$	86.13	10.4	50.1615	53	0.001
196	4-Quinolinamine	$C_9H_8N_2$	144.173	51.3	50.43	741	0.010
197	2,4-Cyclohexadienone	C_6H_6O	94.11	20.9	50.469	28804	0.408
198	Simplexin	$C_{30}H_{44}O_8$	532.7	49.9	50.7165	107	0.002
199	Benzene, 1-acetyl-3-ethyl-2-(2-ethenyl-6-ethylphenylazo)-	$C_{20}H_{22}N_2O$	306.4	8.54	50.775	261	0.004
200	Pyrazolo[1,4]diazepine	$C_6H_4N_4$	132.12	34.6	50.928	914	0.013
201	4-Phenylphenol	$C_{12}H_{10}O$	170.21	41.2	51.281	769	0.011
202	Undecane	$C_{11}H_{24}$	156.31	95.1	51.3625	731	0.010
203	1H-Pyrazole-3-carboxylic acid	$C_4H_4N_2O_2$	112.09	47.9	51.4555	1225	0.017
204	Benzilic acid	$C_{14}H_{12}O_3$	228.24	59.7	51.4585	919	0.013
205	Paracyclophane	$C_{16}H_{16}$	208.30	84.2	51.629	1052	0.015
206	N-Hydroxyacetamidine	$C_2H_6N_2O$	74.08	20.7	51.757	452	0.006
207	Cholesterol	$C_{27}H_{46}O$	386.7	78.6	51.8795	1203592	17.046
208	6-Methyl-2H-1,4-benzoxazin-3(4H)-one	$C_9H_9NO_2$	163.17	36.9	51.9225	909	0.013
209	Anthracen-9-one, 10-heptyl-10-hydroxy-	$C_{21}H_{24}O_2$	308.4	9.84	52.0145	637	0.009
210	Gniditrin	$C_{37}H_{42}O_{10}$	646.7	22.2	52.09	438	0.006
211	Benzene	C_6H_6	78.11	18.9	52.35	23774	0.337
212	Benzimidazole	$C_7H_6N_2$	118.14	21.3	52.4585	250	0.004
213	1-Hepten-3-ol	$C_7H_{14}O$	114.19	1.99	52.4845	426	0.006
214	1H-1,5-Benzodiazepine	$C_9H_8N_2$	144.17	13.6	52.7495	110	0.002
215	Carbohydrazide	CH_6N_4O	90.09	28.3	52.844	615	0.009
216	[2.2](2,5)Pyridinophane	$C_{14}H_{14}N_2$	210.27	13.2	52.9355	713	0.010
217	8-Isopropyl-5-methyl-5,6,7,8-tetrahydro-2,4-quinazolinedione	$C_{12}H_{18}N_2O_2$	222.28	49.4	52.9605	1573	0.022
218	Conessine	$C_{24}H_{40}N_2$	356.6	31.1	52.9845	18895	0.268
219	3-Phenyl-1H-1,2,4-triazole	$C_8H_7N_3$	145.16	30.9	53.092	288	0.004
220	4-Ethyl-4-methylcyclohexanone	$C_9H_{16}O$	140.22	48.1	53.1495	1748	0.025
221	Pyrimidine	$C_4H_4N_2$	80.09	10.8	53.4945	395	0.006
222	8-Methoxy-6-nitro-2H-chromene	$C_{10}H_9NO_4$	207.18	7.1	53.626	349	0.005
223	1,2,4-Benzenetricarboxylic acid	$C_9H_6O_6$	210.14	26.2	53.7035	25458	0.361
224	Ethylamine, N-methyl-N-hexadecyl-	$C_{19}H_{41}N$	283.5	28.2	53.7215	8180	0.116
225	Sarcosine	$C_3H_7NO_2$	89.09	16.6	53.821	259	0.004
226	2-(Methylthio)pyrimidin-4-ol	$C_5H_6N_2OS$	142.18	37.3	53.991	1329	0.019
227	4-Chromanone	$C_9H_8O_2$	148.16	34.5	54.0665	23948	0.339
228	5,6-Quinolinedione	$C_9H_5NO_2$	159.14	8.6	54.28	1077	0.015
229	2,6,10-Dodecatrien-1-ol	$C_{12}H_{20}O$	180.29	22.2	54.3245	2003	0.028
230	4-Methyl-1-pentene	C_6H_{12}	84.16	47.1	54.7255	2770	0.039
231	1,2,4-Triazole	$C_2H_3N_3$	69.07	19.8	54.899	2771	0.039

➢ **Enrichment analysis**

Disease signatures (Figure 25.2 and Table 17.2), metabolites enrichment from the KEGG database (Figure 25.3 and Table 17.3) and the SMPDB database (Figure 25.4 and Table 17.4), and different classes of metabolites (Figure 25.5 and Table 17.5) are given below. The enrichment ratio is no. of hits observed divided by no. of hits expected.

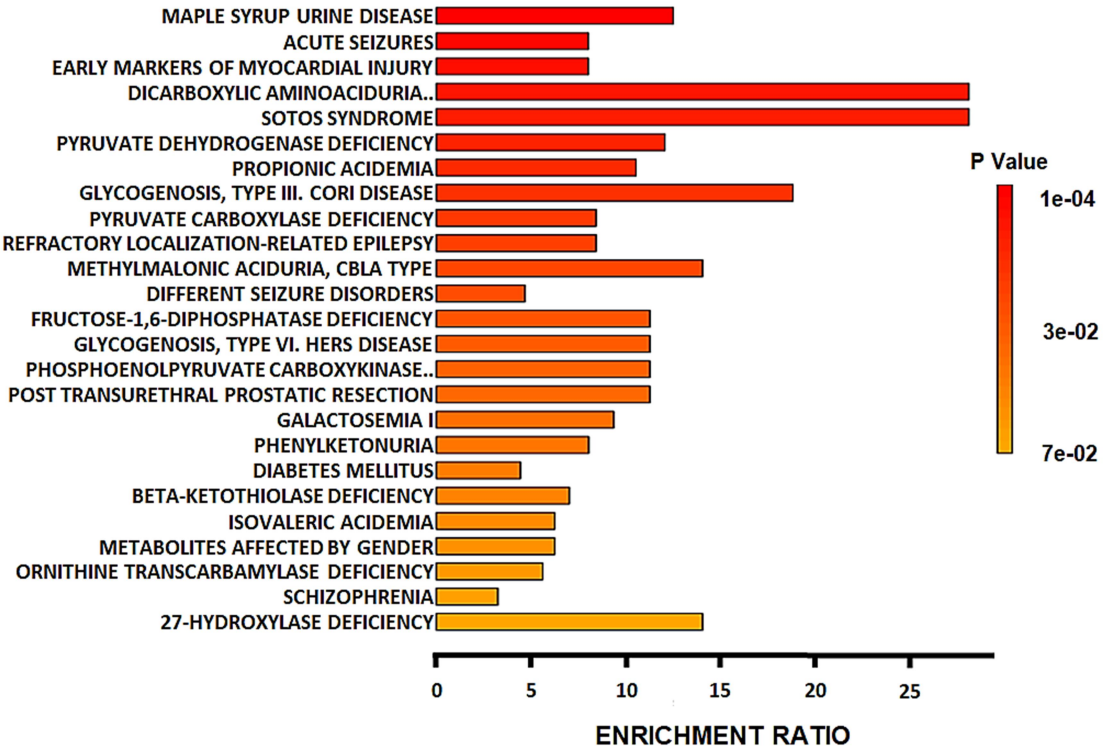

Figure 25.2: Disease signatures in BSA treated cells

The top 25 disease signatures were identified. Significantly enriched signatures (↓) maple syrup urine disease, acute seizures, early markers of myocardial injury, dicarboxylic aminoaciduria, and sotos syndrome. Highly enriched signatures (←) include dicarboxylic aminoaciduria, sotos syndrome, type III cori disease, methylmalonic aciduria, and maple syrup urine disease.

Table 17.2: Disease signatures in BSA-treated cells

	Metabolite Set	Total	Hits	Expect	P Value	Holm P	FDR
	MAPLE SYRUP URINE DISEASE	9	4	0.319	1.24E-4	0.0338	0.0338
	ACUTE SEIZURES	14	4	0.497	8.81E-4	0.24	0.0544
	EARLY MARKERS OF MYOCARDIAL INJURY	14	4	0.497	8.81E-4	0.24	0.0544
	DICARBOXYLIC AMINOACIDURIA. GLUTAMATE-ASPARTATE TRANSPORT DEFECT	2	2	0.071	0.00119	0.321	0.0544
	SOTOS SYNDROME	2	2	0.071	0.00119	0.321	0.0544
	PYRUVATE DEHYDROGENASE DEFICIENCY (E3)	7	3	0.248	0.0012	0.321	0.0544
	PROPIONIC ACIDEMIA	8	3	0.284	0.00187	0.5	0.073
	GLYCOGENOSIS, TYPE III. CORI DISEASE, DEBRANCHER GLYCOGENOSIS	3	2	0.106	0.00349	0.928	0.105
	PYRUVATE CARBOXYLASE DEFICIENCY	10	3	0.355	0.00383	1.0	0.105
	REFRACTORY LOCALIZATION-RELATED EPILEPSY	10	3	0.355	0.00383	1.0	0.105
	METHYLMALONIC ACIDURIA, CBLA TYPE	4	2	0.142	0.00683	1.0	0.17
	DIFFERENT SEIZURE DISORDERS	24	4	0.852	0.00747	1.0	0.17
	FRUCTOSE-1,6-DIPHOSPHATASE DEFICIENCY	5	2	0.177	0.0111	1.0	0.19
	GLYCOGENOSIS (TYPE IA, IB, IC) | GLYCOGENOSIS, TYPE VI. HERS DISEASE	5	2	0.177	0.0111	1.0	0.19
	PHOSPHOENOLPYRUVATE CARBOXYKINASE DEFICIENCY 2 (PEPCK2)	5	2	0.177	0.0111	1.0	0.19
	POST TRANSURETHRAL PROSTATIC RESECTION	5	2	0.177	0.0111	1.0	0.19
	GALACTOSEMIA I	6	2	0.213	0.0164	1.0	0.263
	PHENYLKETONURIA	7	2	0.248	0.0224	1.0	0.34
	DIABETES MELLITUS (MODY), NON-INSULIN-DEPENDENT	19	3	0.674	0.0253	1.0	0.364
	BETA-KETOTHIOLASE DEFICIENCY	8	2	0.284	0.0293	1.0	0.4
	ISOVALERIC ACIDEMIA	9	2	0.319	0.0369	1.0	0.423
	METABOLITES AFFECTED BY GENDER	9	2	0.319	0.0369	1.0	0.423
	ORNITHINE TRANSCARBAMYLASE DEFICIENCY (OTC)	10	2	0.355	0.0452	1.0	0.423
	SCHIZOPHRENIA	26	3	0.923	0.0581	1.0	0.423
	27-HYDROXYLASE DEFICIENCY	2	1	0.071	0.0698	1.0	0.423

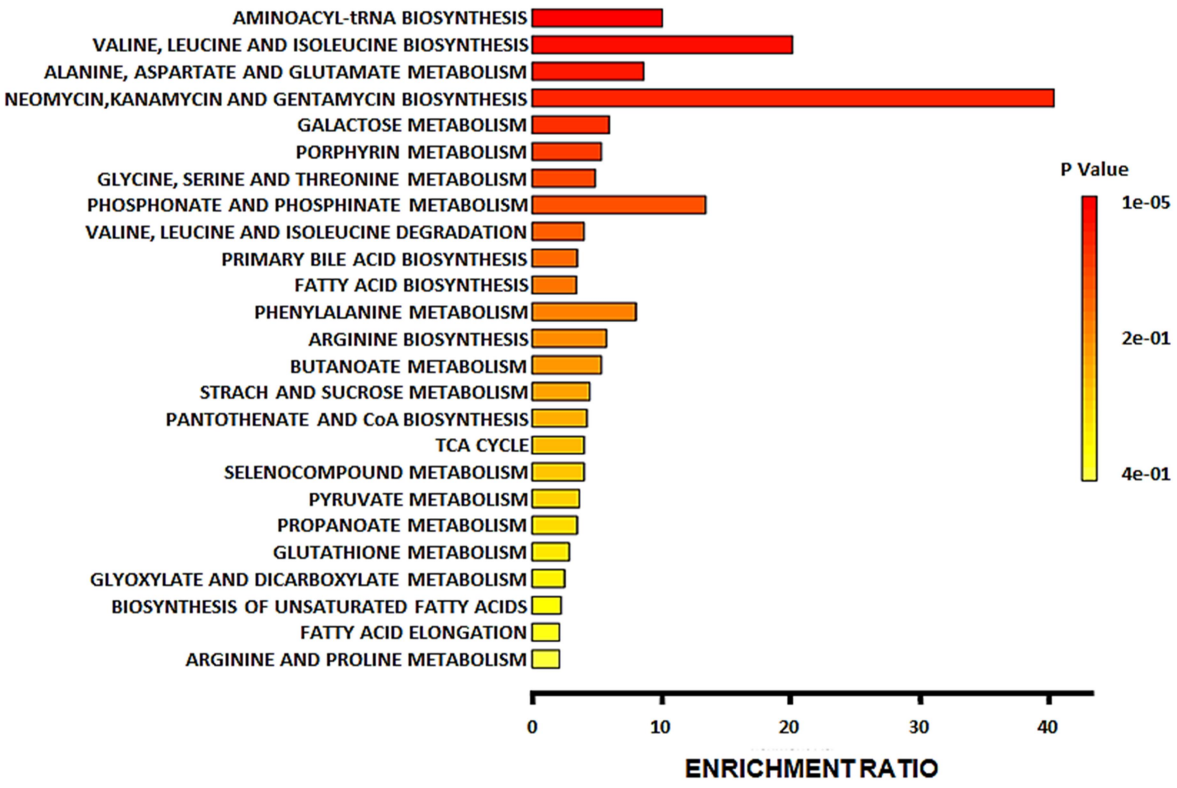

Figure 25.3: BSA-specific metabolites enrichment from the KEGG database

The top 25 metabolic pathways were identified. Significantly enriched pathways (↓) include aminoacyl t-RNA biosynthesis, valine, leucine, and isoleucine biosynthesis, alanine, aspartate, and glutamate metabolism, neomycin, kanamycin, and gentamycin biosynthesis, and galactose metabolism. Highly enriched pathways (←) include neomycin, kanamycin, and gentamycin biosynthesis, valine, leucine, and isoleucine biosynthesis, phosphonate and phosphinate metabolism, aminoacyl t-RNA biosynthesis, and alanine, aspartate, and glutamate metabolism.

Table 17.3: BSA-specific metabolites enrichment from the KEGG database

	Metabolite Set	Total	Hits	Expect	P Value	Holm P	FDR
	Aminoacyl-tRNA biosynthesis	48	6	0.594	1.35E-5	0.00114	0.00114
	Valine, leucine, and isoleucine biosynthesis	8	2	0.099	0.00388	0.322	0.121
	Alanine, aspartate and glutamate metabolism	28	3	0.346	0.00433	0.355	0.121
	Neomycin, kanamycin, and gentamicin biosynthesis	2	1	0.0247	0.0246	1.0	0.516
	Galactose metabolism	27	2	0.334	0.0423	1.0	0.711
	Porphyrin metabolism	30	2	0.371	0.0513	1.0	0.719
	Glycine, serine, and threonine metabolism	33	2	0.408	0.061	1.0	0.732
	Phosphonate and phosphinate metabolism	6	1	0.0742	0.0721	1.0	0.757
	Valine, leucine and isoleucine degradation	40	2	0.495	0.0856	1.0	0.799
	Primary bile acid biosynthesis	46	2	0.569	0.109	1.0	0.822
	Fatty acid biosynthesis	47	2	0.581	0.113	1.0	0.822
	Phenylalanine metabolism	10	1	0.124	0.117	1.0	0.822
	Arginine biosynthesis	14	1	0.173	0.161	1.0	1.0
	Butanoate metabolism	15	1	0.186	0.171	1.0	1.0
	Starch and sucrose metabolism	18	1	0.223	0.202	1.0	1.0
	Pantothenate and CoA biosynthesis	19	1	0.235	0.212	1.0	1.0
	Citrate cycle (TCA cycle)	20	1	0.247	0.222	1.0	1.0
	Selenocompound metabolism	20	1	0.247	0.222	1.0	1.0
	Pyruvate metabolism	22	1	0.272	0.241	1.0	1.0
	Propanoate metabolism	23	1	0.285	0.251	1.0	1.0
	Glutathione metabolism	28	1	0.346	0.296	1.0	1.0
	Glyoxylate and dicarboxylate metabolism	32	1	0.396	0.331	1.0	1.0
	Biosynthesis of unsaturated fatty acids	36	1	0.445	0.364	1.0	1.0
	Fatty acid elongation	38	1	0.47	0.38	1.0	1.0
	Arginine and proline metabolism	38	1	0.47	0.38	1.0	1.0

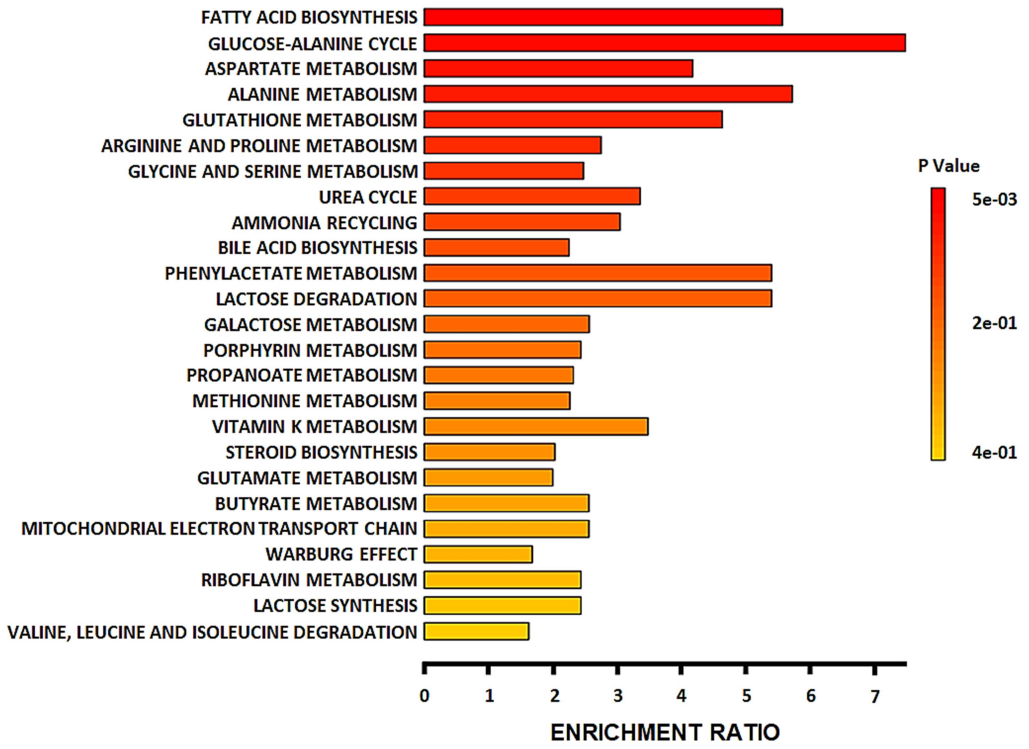

Figure 25.4: BSA-specific metabolites enrichment from the SMPDB database

The top 25 metabolic pathways were identified. Significantly enriched pathways (↓) include fatty acid biosynthesis, glucose-alanine cycle, aspartate metabolism, alanine metabolism, and glutathione metabolism. Highly enriched pathways (←) include glucose-alanine cycle, alanine metabolism, fatty acid biosynthesis, lactose degradation, and phenylacetate metabolism.

Table 17.4: BSA-specific metabolites enrichment from SMPDB database

	Metabolite Set	Total	Hits	Expect	P Value	Holm P	FDR
	Fatty acid biosynthesis	35	4	0.718	0.00453	0.444	0.444
	Glucose-alanine cycle	13	2	0.267	0.0273	1.0	1.0
	Aspartate metabolism	35	3	0.718	0.0319	1.0	1.0
	Alanine metabolism	17	2	0.349	0.0453	1.0	1.0
	Glutathione metabolism	21	2	0.431	0.0666	1.0	1.0
	Arginine and proline metabolism	53	3	1.09	0.09	1.0	1.0
	Glycine and serine metabolism	59	3	1.21	0.115	1.0	1.0
	Urea cycle	29	2	0.595	0.117	1.0	1.0
	Ammonia recycling	32	2	0.656	0.137	1.0	1.0
	Bile acid biosynthesis	65	3	1.33	0.143	1.0	1.0

	Phenylacetate metabolism	9	1	0.185	0.171	1.0	1.0
	Lactose degradation	9	1	0.185	0.171	1.0	1.0
	Galactose metabolism	38	2	0.779	0.181	1.0	1.0
	Porphyrin metabolism	40	2	0.82	0.196	1.0	1.0
	Propanoate metabolism	42	2	0.861	0.212	1.0	1.0
	Methionine metabolism	43	2	0.882	0.219	1.0	1.0
	Vitamin K metabolism	14	1	0.287	0.253	1.0	1.0
	Steroid biosynthesis	48	2	0.984	0.258	1.0	1.0
	Glutamate metabolism	49	2	1.0	0.266	1.0	1.0
	Butyrate metabolism	19	1	0.39	0.328	1.0	1.0
	Mitochondrial electron transport chain	19	1	0.39	0.328	1.0	1.0
	Warburg effect	58	2	1.19	0.336	1.0	1.0
	Riboflavin metabolism	20	1	0.41	0.342	1.0	1.0
	Lactose synthesis	20	1	0.41	0.342	1.0	1.0
	Valine, leucine, and isoleucine degradation	60	2	1.23	0.351	1.0	1.0

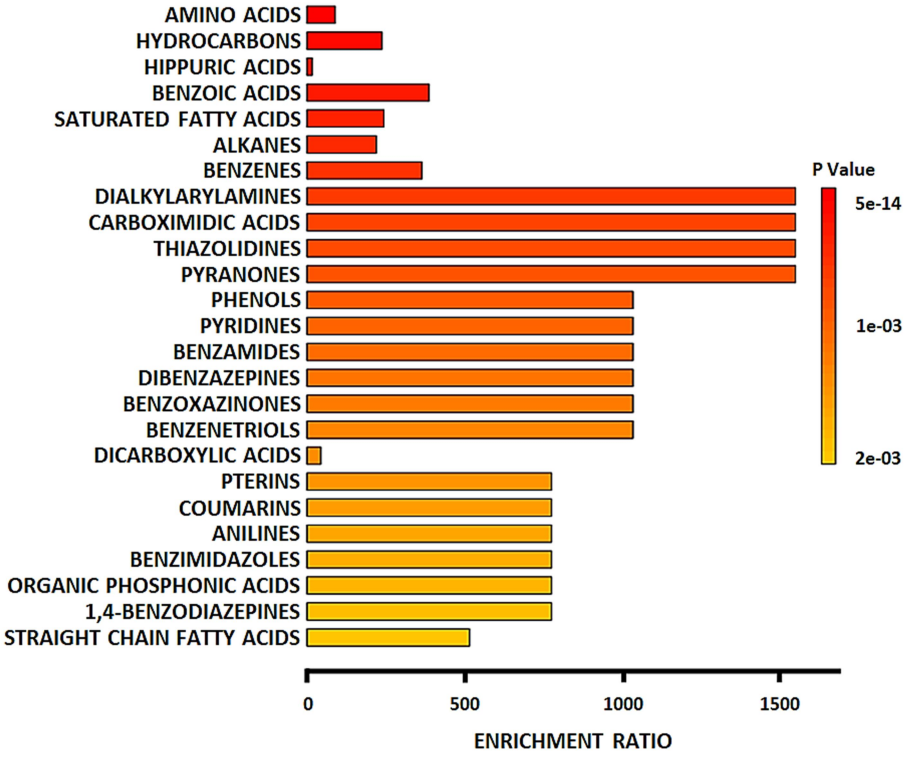

Figure 25.5: Different classes of identified metabolites in BSA-treated cells

The top 25 different classes of metabolites were identified. Significantly enriched classes (↓) include amino acids, hydrocarbons, hirrupic acids, benzoic acids, and saturated fatty acids. Highly

enriched classes (←) include dialkylarylamines, carboximidic acids, thiazolidines, pyranones, phenols, pyridines, benzamides, dibenzazepines, benzoxazinones, and benzenetriols

Table 17.5: Different classes of identified metabolites in BSA-treated cells

	Metabolite Set	Total	Hits	Expect	P Value	Holm P	FDR
	Amino acids	277	8	0.0894	5.42E-14	3.96E-11	3.96E-11
	Hydrocarbons	52	4	0.0168	2.64E-9	1.93E-6	9.65E-7
	Hippuric acids	1470	8	0.474	2.72E-8	1.98E-5	6.62E-6
	Benzoic acids	24	3	0.00775	6.46E-8	4.7E-5	1.18E-5
	Saturated fatty acids	38	3	0.0123	2.68E-7	1.95E-4	3.92E-5
	Alkanes	42	3	0.0136	3.65E-7	2.65E-4	4.44E-5
	Benzenes	17	2	0.00549	1.39E-5	0.0101	0.00145
	Dialkylarylamines	2	1	6.46E-4	6.45E-4	0.467	0.0393
	Carboximidic acids	2	1	6.46E-4	6.45E-4	0.467	0.0393
	Thiazolidines	2	1	6.46E-4	6.45E-4	0.467	0.0393
	Pyranones	2	1	6.46E-4	6.45E-4	0.467	0.0393
	Phenols	3	1	9.68E-4	9.68E-4	0.697	0.0393
	Pyridines	3	1	9.68E-4	9.68E-4	0.697	0.0393
	Benzamides	3	1	9.68E-4	9.68E-4	0.697	0.0393
	Dibenzazepines	3	1	9.68E-4	9.68E-4	0.697	0.0393
	Benzoxazinones	3	1	9.68E-4	9.68E-4	0.697	0.0393
	Benzenetriols	3	1	9.68E-4	9.68E-4	0.697	0.0393
	Dicarboxylic acids	140	2	0.0452	9.7E-4	0.697	0.0393
	Pterins	4	1	0.00129	0.00129	0.92	0.0393
	Coumarins	4	1	0.00129	0.00129	0.92	0.0393
	Anilines	4	1	0.00129	0.00129	0.92	0.0393
	Benzimidazoles	4	1	0.00129	0.00129	0.92	0.0393
	Organic phosphonic acids	4	1	0.00129	0.00129	0.92	0.0393
	1,4-benzodiazepines	4	1	0.00129	0.00129	0.92	0.0393
	Straight-chain fatty acids	6	1	0.00194	0.00194	1.0	0.0566

- **Pathway analysis**

Impacted pathways from the KEGG database (Figure 25.6 and Table 17.6), and the SMPDB database (Figure 25.7 and Table 17.7) are given below. Pathway impact is calculated by using centrality and pathway enrichment results.

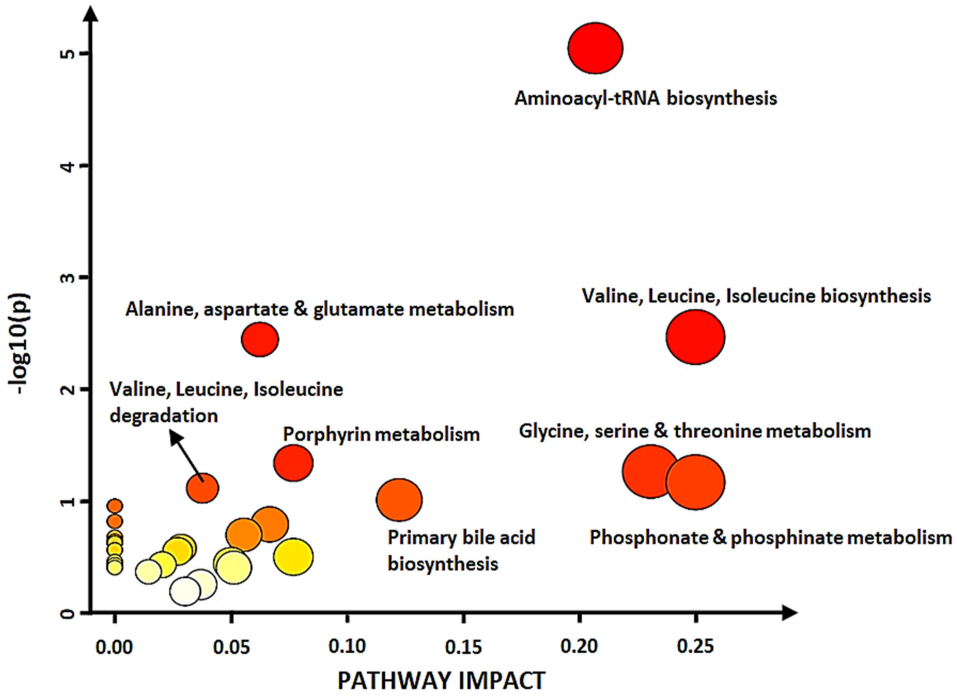

Figure 25.6: BSA-specific pathway analysis from the KEGG database

The top 29 impacted pathways were identified. Highly impacted pathways (←) include valine, leucine, and isoleucine biosynthesis, phosphonate and phosphinate metabolism, glycine, serine, and threonine metabolism, aminoacyl t-RNA biosynthesis, and primary bile acid biosynthesis. Significantly impacted pathways (↓) include aminoacyl t-RNA biosynthesis, valine, leucine, and isoleucine biosynthesis, alanine, aspartate and glutamate biosynthesis, porphyrin metabolism, and glycine, serine, and threonine metabolism.

Table 17.6: BSA-specific pathway analysis from the KEGG database

Pathway Name	Match Status	p	-log(p)	Holm p	FDR	Impact
Aminoacyl-tRNA biosynthesis	6/48	8.9977E-6	5.0459	7.558E-4	7.558E-4	0.20688
Valine, leucine, and isoleucine biosynthesis	2/8	0.0034237	2.4655	0.28417	0.10068	0.25
Alanine, aspartate and glutamate metabolism	3/28	0.0035956	2.4442	0.29484	0.10068	0.0625
Porphyrin metabolism	2/30	0.045731	1.3398	1.0	0.91362	0.07692
Glycine, serine, and threonine metabolism	2/33	0.054382	1.2645	1.0	0.91362	0.23077

Phosphonate and phosphinate metabolism	1/6	0.067792	1.1688	1.0	0.91915	0.25
Valine, leucine, and isoleucine degradation	2/40	0.076596	1.1158	1.0	0.91915	0.03774
Primary bile acid biosynthesis	2/46	0.097579	1.0106	1.0	1.0	0.12245
Phenylalanine metabolism	1/10	0.11055	0.95644	1.0	1.0	0.0
Arginine biosynthesis	1/14	0.15145	0.81973	1.0	1.0	0.0
Butanoate metabolism	1/15	0.16139	0.79211	1.0	1.0	0.06667
Pantothenate and CoA biosynthesis	1/19	0.20008	0.6988	1.0	1.0	0.05556
Citrate cycle (TCA cycle)	1/20	0.20948	0.67885	1.0	1.0	0.0
Selenocompound metabolism	1/20	0.20948	0.67885	1.0	1.0	0.0
Pyruvate metabolism	1/22	0.22798	0.6421	1.0	1.0	0.0
Propanoate metabolism	1/23	0.23708	0.62511	1.0	1.0	0.0
Glycolysis / Gluconeogenesis	1/26	0.26376	0.5788	1.0	1.0	0.02857
Galactose metabolism	1/27	0.27245	0.56471	1.0	1.0	0.0
Glutathione metabolism	1/28	0.28105	0.55122	1.0	1.0	0.02703
Glyoxylate and dicarboxylate metabolism	1/32	0.31449	0.50239	1.0	1.0	0.07692
Biosynthesis of unsaturated fatty acids	1/36	0.34647	0.46034	1.0	1.0	0.0
Arginine and proline metabolism	1/38	0.36192	0.44139	1.0	1.0	0.05
Fatty acid elongation	1/39	0.36951	0.43237	1.0	1.0	0.0
Fatty acid degradation	1/39	0.36951	0.43237	1.0	1.0	0.02041
Tyrosine metabolism	1/42	0.39179	0.40694	1.0	1.0	0.0
Steroid biosynthesis	1/42	0.39179	0.40694	1.0	1.0	0.05128
Fatty acid biosynthesis	1/47	0.42728	0.36928	1.0	1.0	0.01449
Metabolism of xenobiotics by cytochrome P450	1/68	0.55607	0.25487	1.0	1.0	0.03704
Steroid hormone biosynthesis	1/85	0.63975	0.19399	1.0	1.0	0.0303

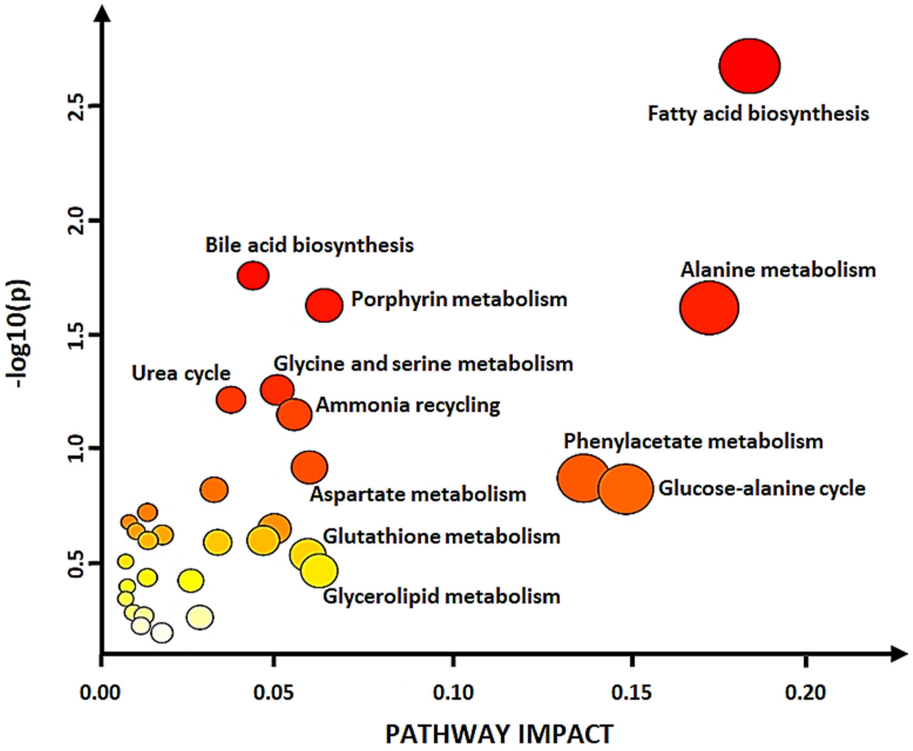

Figure 25.7: BSA-specific pathway analysis from the SMPDB database

The top 31 impacted pathways were identified. Highly impacted pathways (←) include fatty acid biosynthesis, alanine metabolism, glucose-alanine cycle, phenylacetate metabolism, and porphyrin metabolism. Significantly impacted pathways (↓) include fatty acid biosynthesis, bile acid biosynthesis, alanine metabolism, porphyrin metabolism, and glycine and serine metabolism.

Table 17.7: BSA-specific pathway analysis from the SMPDB database

Pathway Name	Match Status	p	-log(p)	Holm p	FDR	Impact
Fatty acid biosynthesis	4/33	0.0021041	2.6769	0.20831	0.20831	0.18269
Bile acid biosynthesis	4/59	0.01742	1.759	1.0	0.59659	0.044031
Porphyrin metabolism	3/36	0.02355	1.628	1.0	0.59659	0.06391
Alanine metabolism	2/14	0.024105	1.6179	1.0	0.59659	0.17143
Glycine and serine metabolism	3/50	0.055241	1.2577	1.0	1.0	0.050781
Urea cycle	2/23	0.060953	1.215	1.0	1.0	0.037879
Ammonia recycling	2/25	0.070774	1.1501	1.0	1.0	0.055556
Aspartate metabolism	2/34	0.12047	0.91913	1.0	1.0	0.059783
Phenylacetate metabolism	1/8	0.13455	0.8711	1.0	1.0	0.13636
Glucose-alanine cycle	1/9	0.15012	0.82357	1.0	1.0	0.14815

Methionine metabolism	2/39	0.15106	0.82084	1.0	1.0	0.033149
Glutamate metabolism	2/45	0.18968	0.72198	1.0	1.0	0.014535
Arginine and proline metabolism	2/48	0.20954	0.67872	1.0	1.0	0.009434
Riboflavin metabolism	1/14	0.22404	0.64967	1.0	1.0	0.05
Valine, leucine, and isoleucine degradation	2/51	0.22966	0.63891	1.0	1.0	0.011429
Mitochondrial electron transport chain	1/15	0.23808	0.62327	1.0	1.0	0.018692
Carnitine synthesis	1/16	0.25188	0.59881	1.0	1.0	0.014706
Butyrate metabolism	1/16	0.25188	0.59881	1.0	1.0	0.046875
Tyrosine metabolism	2/55	0.25676	0.59047	1.0	1.0	0.034146
Glutathione metabolism	1/19	0.29187	0.53481	1.0	1.0	0.059322
Purine metabolism	2/63	0.31128	0.50685	1.0	1.0	0.0084746
Glycerolipid metabolism	1/23	0.34206	0.4659	1.0	1.0	0.0625
Phenylalanine and tyrosine metabolism	1/25	0.36587	0.43667	1.0	1.0	0.014493
Citric acid cycle	1/26	0.37747	0.42312	1.0	1.0	0.026667
Selenoamino acid metabolism	1/28	0.40007	0.39786	1.0	1.0	0.0089286
Fatty acid elongation in mitochondria	1/33	0.45323	0.34368	1.0	1.0	0.0084746
Fatty acid metabolism	1/40	0.52023	0.28381	1.0	1.0	0.010563
Steroidogenesis	1/42	0.53789	0.2693	1.0	1.0	0.013575
Steroid biosynthesis	1/43	0.5465	0.26241	1.0	1.0	0.029197
Warburg effect	1/49	0.59501	0.22547	1.0	1.0	0.012698
Tryptophan metabolism	1/55	0.6386	0.19477	1.0	1.0	0.018576

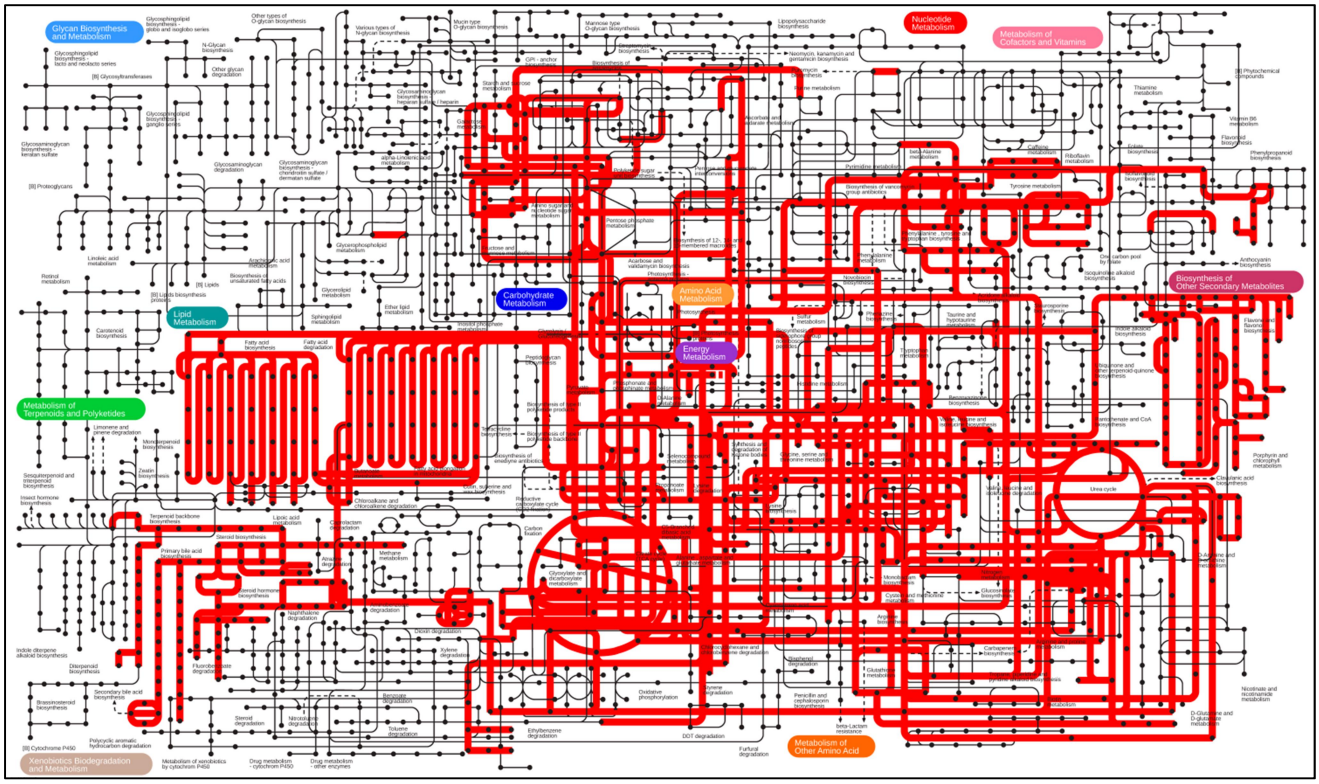

Figure 25.8: Metabolic pathways enriched in BSA treatment after mapping with the KEGG database. The highlighted metabolisms show enrichment specific to BSA treatment. This shows the enrichment of amino acid metabolism, energy metabolism, porphyrin metabolism, amino sugar and nucleotide sugar metabolism, and other metabolic pathways.

VI. High sodium butyrate treatment

Cells were treated with 20 mM sodium butyrate media for 24 hours.

➢ GC-MS graph

GC chromatogram of butyrate treatment (given in Figure 26.1) depicts retention time (min) on X-axis and relative abundance (intensity) on Y-axis. A total of 122 metabolites (components) were identified in sodium butyrate-treated cells (given in Table 18.1). The most abundant metabolites are – Acetamide (42.812%), 2-Ethylhexan-1-ol (39.873%), Phosphoric Acid (4.813%), 2-Ethylhexanoic acid (3.187%), and Cholesterol (3.050%). The abundance is measured based on the % area of the peak of a specific component.

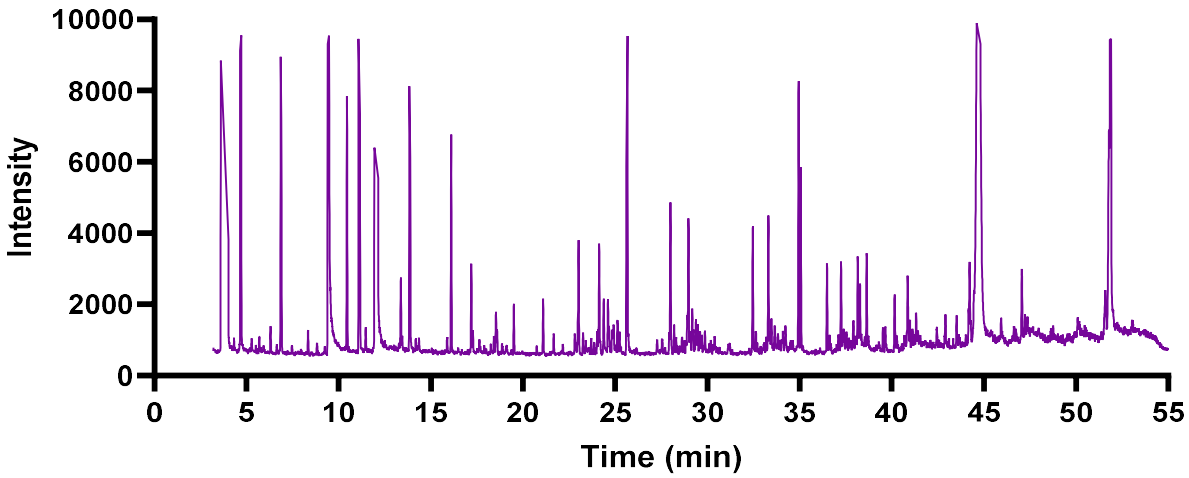

Figure 26.1: GC-MS graph obtained for butyrate treatment

Table 18.1: Metabolites identified in sodium butyratetreated cells

S.No.	Metabolites	Mol. Formula	MW (g/mol)	% Probability	RT (min)	Area	% Area
1	Phosphonothioic acid, ethyl-	$C_2H_7O_2PS$	126.12	23.8	3.583	4853	0.001
2	Semicarbazide	CH_5N_3O	75.07	21.7	3.65	22945	0.004
3	1,3-Dioxolane	$C_3H_6O_2$	74.08	27.4	3.802	5705305	0.934
4	1,4,7-Trioxa-10-azacyclododecane	$C_8H_{17}NO_3$	175.23	8.59	3.817	1575203	0.258
5	Piperidin-4-ol	$C_5H_{11}NO$	101.15	9.64	3.84	15516	0.003
6	6,7-Dimethoxy-1,2,3,4-tetrahydroisoquinoline	$C_{11}H_{15}NO_2$	193.24	8.56	3.8635	341922	0.056

7	Benzenesulfonamide	$C_6H_7NO_2S$	157.19	20.3	3.923	64863	0.011
8	Valine	$C_5H_{11}NO_2$	117.15	23	3.987	1859398	0.304
9	Acetamide	C_2H_5NO	59.07	51.7	3.9995	261487138	42.812
10	1,1-Dimethoxyethane	$C_4H_{10}O_2$	90.12	23.1	4.016	60219	0.010
11	Butyric acid	$C_4H_8O_2$	88.11	63.3	4.6225	271137	0.044
12	5-Methylhexan-3-one	$C_7H_{14}O$	114.19	43.2	4.686	1034795	0.169
13	2,2-Dimethyl-3-pentanol	$C_7H_{16}O$	116.20	17.4	4.697	239397	0.039
14	D-Lactic acid	$C_3H_6O_3$	90.08	51.9	4.9865	18036	0.003
15	4-Nitrophenyl benzoate	$C_{13}H_9NO_4$	243.21	11.6	5.134	18321	0.003
16	S,S'-Dimethyl dithiocarbonate	$C_3H_6OS_2$	122.21	8.38	5.195	24487	0.004
17	2-Hydroxypentanoic acid	$C_5H_{10}O_3$	118.13	10.1	5.338	88732	0.015
18	Pentane	C_5H_{12}	72.15	18.1	5.35	3137	0.001
19	Styrylacetic acid	$C_{10}H_{10}O_2$	162.18	18	5.3575	58217	0.010
20	2-Methylpropanal phenyl hydrazone	$C_{10}H_{14}N_2$	162.23	5.56	5.3745	101399	0.017
21	Ether, 3-butenyl propyl	$C_7H_{14}O$	114.19	78.1	6.161	16715	0.003
22	Acetamidine	$C_2H_6N_2$	58.08	70	6.301	2405603	0.394
23	6-Amino-6-methylfulvene	C_7H_9N	107.15	5.12	6.3275	108737	0.018
24	Anodendroside E 2	$C_{30}H_{38}O_{11}$	574.6	8.98	6.351	331561	0.054
25	1,1-Dimethyl-2-pentylhydrazine	$C_7H_{18}N_2$	130.23	47.7	6.436	7549	0.001
26	3-Hexen-1-yne	C_6H_8	80.13	11	6.647	3321	0.001
27	5-Ethyl-5-methylhydantoin	$C_6H_{10}N_2O_2$	142.16	24.4	6.779	61993	0.010
28	Chimonanthine	$C_{22}H_{26}N_4$	346.5	12.8	6.8015	68310	0.011
29	Glycolic acid	$C_2H_4O_3$	76.05	22.8	6.853	144741	0.024
30	2-Ethylhexanal	$C_8H_{16}O$	128.21	71	6.87	395533	0.065
31	2-Propanone, o-methyloxime	C_4H_9NO	87.12	37.4	7.443	14861	0.002
32	Ethylene Glycol	$C_2H_6O_2$	62.07	78.1	7.903	10655	0.002
33	2,4,6-Trimethylpyridine	$C_8H_{11}N$	121.18	65.8	8.276	54015	0.009
34	2,4-Dimethyl-3-pentanol	$C_7H_{16}O$	116.20	55.9	8.5125	26795	0.004
35	Ethyl diethylcarbamate	$C_7H_{15}NO_2$	145.20	85.1	10.2975	109831	0.018
36	2-Propyl-1-pentanol	$C_8H_{18}O$	130.23	35.8	10.4535	1682948	0.276
37	Lactic acid	$C_3H_6O_3$	90.08	42.4	10.468	246392	0.040
38	2-Ethylhexyl formate	$C_9H_{18}O_2$	158.24	42.5	11.114	1370544	0.224
39	Heptyl 2-methylpropanoate	$C_{11}H_{22}O_2$	186.29	80.7	11.457	20194	0.003
40	N-Methoxy-N-methylacetamide	$C_4H_9NO_2$	103.12	54.5	11.5285	8792	0.001
41	Leucine	$C_6H_{13}NO_2$	131.17	12.3	12.0515	2327794	0.381
42	2-Ethylhexan-1-ol	$C_8H_{18}O$	130.23	79	12.113	243534467	39.873
43	Acrylic acid	$C_3H_4O_2$	72.06	36.8	12.8505	9313	0.002
44	2-Ethylhexyl acetate	$C_{10}H_{20}O_2$	172.26	42.5	13.375	86793	0.014
45	2-Ethylhexanoic acid	$C_8H_{16}O_2$	144.21	97.3	13.8645	19467245	3.187
46	gamma-Butyrolactone	$C_4H_6O_2$	86.09	30.9	14.169	24126	0.004
47	Methyl propionate	$C_4H_8O_2$	88.11	66.1	14.2865	350606	0.057
48	Dithioerythritol	$C_4H_{10}O_2S_2$	154.3	17.6	14.5475	10671	0.002

49	Isopropyl alcohol	C_3H_8O	60.10	26.3	15.89	55747	0.009
50	Benzoic acid	$C_7H_6O_2$	122.12	80.7	16.319	118654	0.019
51	Mesitylene, 2-propadienyl-	$C_{12}H_{14}$	158.24	6.15	17.1215	5436	0.001
52	Nicotyrine	$C_{10}H_{10}N_2$	158.20	6.15	17.1215	5436	0.001
53	Phosphoric acid	H_3PO_4	97.995	90.8	17.1845	29398584	4.813
54	Glycerin	$C_3H_8O_3$	92.09	63.1	17.253	73945	0.012
55	2,4,4-Trimethylpentan-1-ol	$C_8H_{18}O$	130.23	25	17.6285	123227	0.020
56	L-Norleucine	$C_6H_{13}NO_2$	131.17	30.2	17.7275	6371	0.001
57	Octanoic acid	$C_8H_{16}O_2$	144.21	67.9	18.3255	148783	0.024
58	2-Ethylhexyl butyrate	$C_{12}H_{24}O_2$	200.32	87.2	18.531	93875	0.015
59	Pentitol	$C_5H_{12}O_5$	152.15	32.5	18.9675	50576	0.008
60	9Z-octadecenoic acid (d5)	$C_{18}H_{34}O_2$	287.5	17.2	19.0365	17160	0.003
61	17alpha-Pregn-4-ene-3,11,20-trione	$C_{21}H_{28}O_3$	328.4	24.8	19.932	454736	0.074
62	Pregnanediol	$C_{21}H_{36}O_2$	320.5	7.55	19.935	13433	0.002
63	Pregna-3,5-dien-20-one	$C_{21}H_{30}O$	298.5	19.1	19.9595	163515	0.027
64	Ethyl 4-methylpentanoate	$C_8H_{16}O_2$	144.21	85.9	20.172	70101	0.011
65	Ethyl 2-ethylbutanoate	$C_8H_{16}O_2$	144.21	29.2	20.731	76565	0.013
66	2-Ethylhexyl valerate	$C_{13}H_{26}O_2$	214.34	59	21.086	55136	0.009
67	1,2,4,5-Tetrazine, 1,4-dibutylhexahydro-	$C_{10}H_{24}N_4$	200.32	54.7	21.66	14167	0.002
68	2,7-Dimethyloctane	$C_{10}H_{22}$	142.28	7.89	22.8805	8791	0.001
69	4,6-Dimethyldodecane	$C_{14}H_{30}$	198.39	7.88	23.003	95272	0.016
70	Proline	$C_5H_9NO_2$	115.13	49.3	23.67	24211	0.004
71	2,7,10-Trimethyldodecane	$C_{15}H_{32}$	212.41	7.8	24.376	50804	0.008
72	Nonadecane	$C_{19}H_{40}$	268.5	6.54	24.6105	50008	0.008
73	1-(4-tert-Butoxy-3-thienyl)ethanone	$C_{10}H_{14}O_2S$	198.28	8.62	24.6565	62380	0.010
74	Octanoic anhydride	$C_{16}H_{30}O_3$	270.41	16	24.668	23104	0.004
75	Propylphosphonic acid	$C_3H_9O_3P$	124.08	32.5	25.1135	27965	0.005
76	3-Ethyl-3-methylheptane	$C_{10}H_{22}$	142.28	9.06	25.1425	15030	0.002
77	Zearalenone	$C_{18}H_{22}O_5$	318.4	19.8	25.2285	174516	0.029
78	Lauric acid	$C_{12}H_{24}O_2$	200.32	60.3	26.8895	11084	0.002
79	Hexadecane	$C_{16}H_{34}$	226.44	9.15	28.198	17471	0.003
80	5,8-Diethyldodecane	$C_{16}H_{34}$	226.44	11.8	28.3135	10218	0.002
81	Heptadecane	$C_{17}H_{36}$	240.5	7.04	28.968	138335	0.023
82	Octadecane	$C_{18}H_{38}$	254.5	6.61	29.1705	32449	0.005
83	3-Methyl-3-ethyldecane	$C_{13}H_{28}$	184.36	7.11	29.373	22110	0.004
84	Terephthalic acid	$C_8H_6O_4$	166.13	90.2	29.86	71729	0.012
85	Cinnamic acid	$C_9H_8O_2$	148.16	9.06	31.116	18673	0.003
86	Myristic acid	$C_{14}H_{28}O_2$	228.37	86.9	31.1555	219073	0.036
87	6,10,14-Trimethylpentadecan-2-ol	$C_{18}H_{38}O$	270.5	36.3	31.223	69802	0.011
88	D-Galactose	$C_6H_{12}O_6$	180.16	11.9	32.032	369957	0.061
89	Heneicosane	$C_{21}H_{44}$	296.6	7.39	32.454	159013	0.026
90	Dodecane	$C_{12}H_{26}$	170.33	30.5	32.629	15021	0.002

91	Phthalic acid	$C_8H_6O_4$	166.13	5.19	33.2635	72429	0.012
92	Heptacosane	$C_{27}H_{56}$	380.7	3.84	33.3045	238795	0.039
93	Benzamide	C_7H_7NO	121.14	15.6	33.418	3149	0.001
94	3-Methyldodecane	$C_{13}H_{28}$	184.36	4.55	33.467	49556	0.008
95	D-Glucose	$C_6H_{12}O_6$	180.16	10.5	33.8335	881504	0.144
96	4-Azaphenanthrene, 1-methyl-3-phenylethynyl-	$C_{22}H_{15}N$	293.4	39.4	34.215	8435	0.001
97	9-Hexadecenoic acid	$C_{16}H_{30}O_2$	254.41	52.3	34.636	367939	0.060
98	2-Methylheptane	C_8H_{18}	114.23	14.9	34.939	282113	0.046
99	Palmitic acid	$C_{16}H_{32}O_2$	256.42	97.1	35.055	3368495	0.552
100	2-Methylhexadecane	$C_{17}H_{36}$	240.5	5.06	37.252	13141	0.002
101	2,2-Bis(2-hydroxyphenyl)propane	$C_{15}H_{16}O_2$	228.29	91.2	37.832	49302	0.008
102	Linoleic acid	$C_{18}H_{32}O_2$	280.4	86	38.025	35031	0.006
103	9,12-Octadecadienoic acid	$C_{18}H_{32}O_2$	280.4	66.2	38.03	4565	0.001
104	Oleic acid	$C_{18}H_{34}O_2$	282.5	19.5	38.1485	3093945	0.507
105	Androst-2-en-17-amine	$C_{19}H_{31}N$	273.5	59.6	38.17	33275	0.005
106	trans-Vaccenic acid	$C_{18}H_{34}O_2$	282.5	18.6	38.27	1804407	0.295
107	Stearic acid	$C_{18}H_{36}O_2$	284.5	98	38.6325	1285661	0.210
108	3-Cyclopentylpropionic acid	$C_8H_{14}O_2$	142.20	30.1	39.3165	30982	0.005
109	cis-11-Eicosenoic acid	$C_{20}H_{38}O_2$	310.5	35.5	41.505	23723	0.004
110	13-Eicosenoic acid	$C_{20}H_{38}O_2$	310.5	53.7	41.6165	8296	0.001
111	Ethanamine, 2,2'-oxybis-	$C_4H_{12}N_2O$	104.15	42.3	42.2015	17527	0.003
112	Carbonic acid	CH_2O_3	62.025	19	42.636	10321	0.002
113	Hexacosane	$C_{26}H_{54}$	366.7	9.38	44.1595	56519	0.009
114	Orotic acid	$C_5H_4N_2O_4$	156.10	24.3	44.733	206788	0.034
115	4-Pyrimidinecarboxylic acid	$C_5H_4N_2O_2$	124.10	44.3	44.7355	40668	0.007
116	Cholesta-3,5-diene	$C_{27}H_{44}$	368.6	8.93	48.6205	49050	0.008
117	Cholest-5-en-3-ol	$C_{27}H_{46}O$	386.7	24.3	51.584	11308	0.002
118	4-tert-Butylcalix[4]arene	$C_{44}H_{56}O_4$	648.9	41.5	51.7805	654177	0.107
119	Lycoxanthin	$C_{40}H_{56}O$	552.9	6.84	51.7915	666212	0.109
120	Estra-1,3,5(10)-triene-3,17-diol	$C_{18}H_{24}O_2$	272.4	78.8	51.842	90421	0.015
121	Cholesterol	$C_{27}H_{46}O$	386.7	77.1	51.873	18629465	3.050
122	Acetic acid	$C_2H_4O_2$	60.05	6.64	52.0105	161225	0.026

- **Enrichment analysis**

Disease signatures (Figure 26.2 and Table 18.2), metabolites enrichment from the KEGG database (Figure 26.3 and Table 18.3) and from the SMPDB database (Figure 26.4 and Table 18.4), and different classes of metabolites (Figure 26.5 and Table 18.5) are given below. The enrichment ratio is no. of hits observed divided by no. of hits expected.

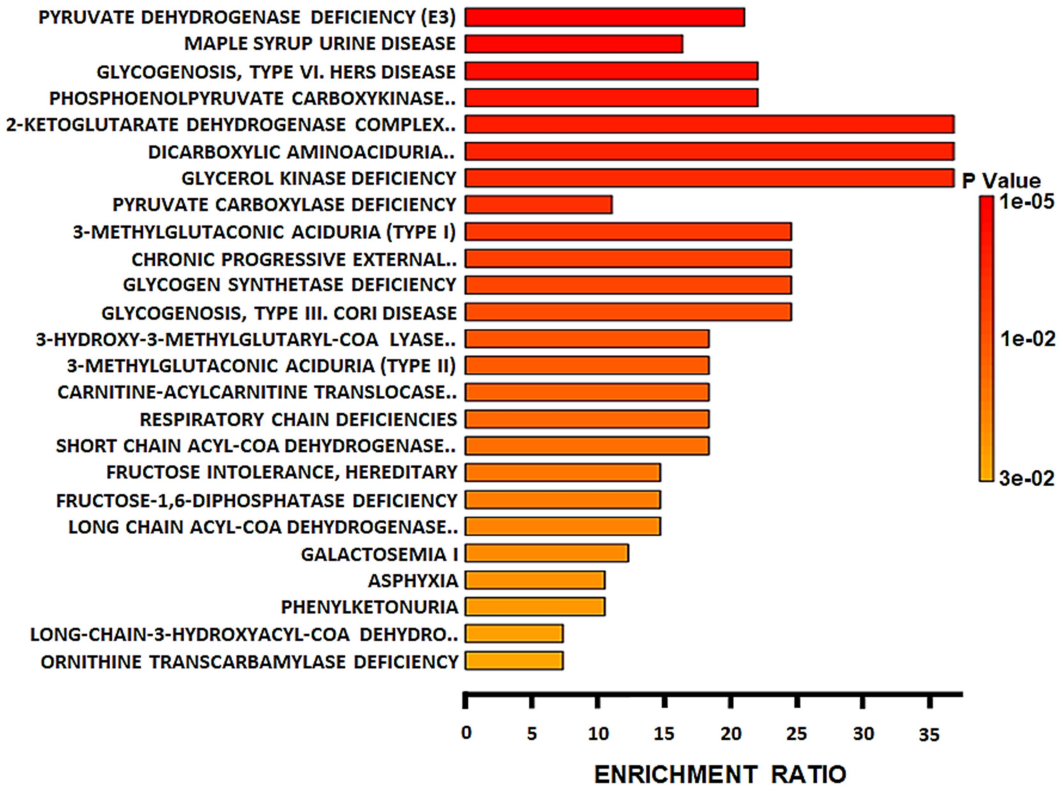

Figure 26.2: Disease signatures in butyrate-treated cells

The top 25 disease signatures were identified. Significantly enriched signatures (↓) pyruvate dehydrogenase deficiency (E3), maple syrup urine disease, type VI. hers disease, phosphoenolpyruvate carboxykinase deficiency 2, and 2-ketoglutarate dehydrogenase complex deficiency. Highly enriched signatures (←) include 2-ketoglutarate dehydrogenase complex deficiency, dicarboxylic aminoaciduria, glycerol kinase deficiency, 3- methylglutaconic aciduria, chronic progressive external ophthalmoplegia, glycogen synthetase deficiency, and type III cori disease.

Table 18.2: Disease signatures in butyrate-treated cells

	Metabolite Set	Total	Hits	Expect	P Value	Holm P	FDR
	PYRUVATE DEHYDROGENASE DEFICIENCY (E3)	7	4	0.19	1.1E-5	0.00301	0.00301
	MAPLE SYRUP URINE DISEASE	9	4	0.244	3.85E-5	0.0105	0.00526
	GLYCOGENOSIS (TYPE IA, IB, IC) | GLYCOGENOSIS, TYPE VI. HERS DISEASE	5	3	0.136	1.52E-4	0.0412	0.0104
	PHOSPHOENOLPYRUVATE CARBOXYKINASE DEFICIENCY 2 (PEPCK2)	5	3	0.136	1.52E-4	0.0412	0.0104
	2-KETOGLUTARATE DEHYDROGENASE COMPLEX DEFICIENCY	2	2	0.0543	6.81E-4	0.183	0.0266
	DICARBOXYLIC AMINOACIDURIA. GLUTAMATE-ASPARTATE TRANSPORT DEFECT	2	2	0.0543	6.81E-4	0.183	0.0266
	GLYCEROL KINASE DEFICIENCY	2	2	0.0543	6.81E-4	0.183	0.0266
	PYRUVATE CARBOXYLASE DEFICIENCY	10	3	0.271	0.00169	0.449	0.0458
	3-METHYLGLUTACONIC ACIDURIA (TYPE I)	3	2	0.0814	0.00201	0.533	0.0458
	CHRONIC PROGRESSIVE EXTERNAL OPHTHALMOPLEGIA AND KEARNS-SAYRE SYNDROM	3	2	0.0814	0.00201	0.533	0.0458
	GLYCOGEN SYNTHETASE DEFICIENCY	3	2	0.0814	0.00201	0.533	0.0458
	GLYCOGENOSIS, TYPE III. CORI DISEASE, DEBRANCHER GLYCOGENOSIS	3	2	0.0814	0.00201	0.533	0.0458
	3-HYDROXY-3-METHYLGLUTARYL-COA LYASE DEFICIENCY	4	2	0.109	0.00396	1.0	0.0636
	3-METHYLGLUTACONIC ACIDURIA (TYPE II), X-LINKED	4	2	0.109	0.00396	1.0	0.0636
	CARNITINE-ACYLCARNITINE TRANSLOCASE DEFICIENCY	4	2	0.109	0.00396	1.0	0.0636
	RESPIRATORY CHAIN DEFICIENCIES	4	2	0.109	0.00396	1.0	0.0636
	SHORT CHAIN ACYL-COA DEHYDROGENASE DEFICIENCY (SCAD)	4	2	0.109	0.00396	1.0	0.0636
	FRUCTOSE INTOLERANCE, HEREDITARY	5	2	0.136	0.0065	1.0	0.0888
	FRUCTOSE-1,6-DIPHOSPHATASE DEFICIENCY	5	2	0.136	0.0065	1.0	0.0888

	LONG CHAIN ACYL-COA DEHYDROGENASE DEFICIENCY (LCAD)	5	2	0.136	0.0065	1.0	0.0888
	GALACTOSEMIA I	6	2	0.163	0.00961	1.0	0.125
	ASPHYXIA [DD]	7	2	0.19	0.0132	1.0	0.157
	PHENYLKETONURIA	7	2	0.19	0.0132	1.0	0.157
	LONG-CHAIN-3-HYDROXYACYL-COA DEHYDROGENASE DEFICIENCY (LCHAD)	10	2	0.271	0.0271	1.0	0.266
	ORNITHINE TRANSCARBAMYLASE DEFICIENCY (OTC)	10	2	0.271	0.0271	1.0	0.266

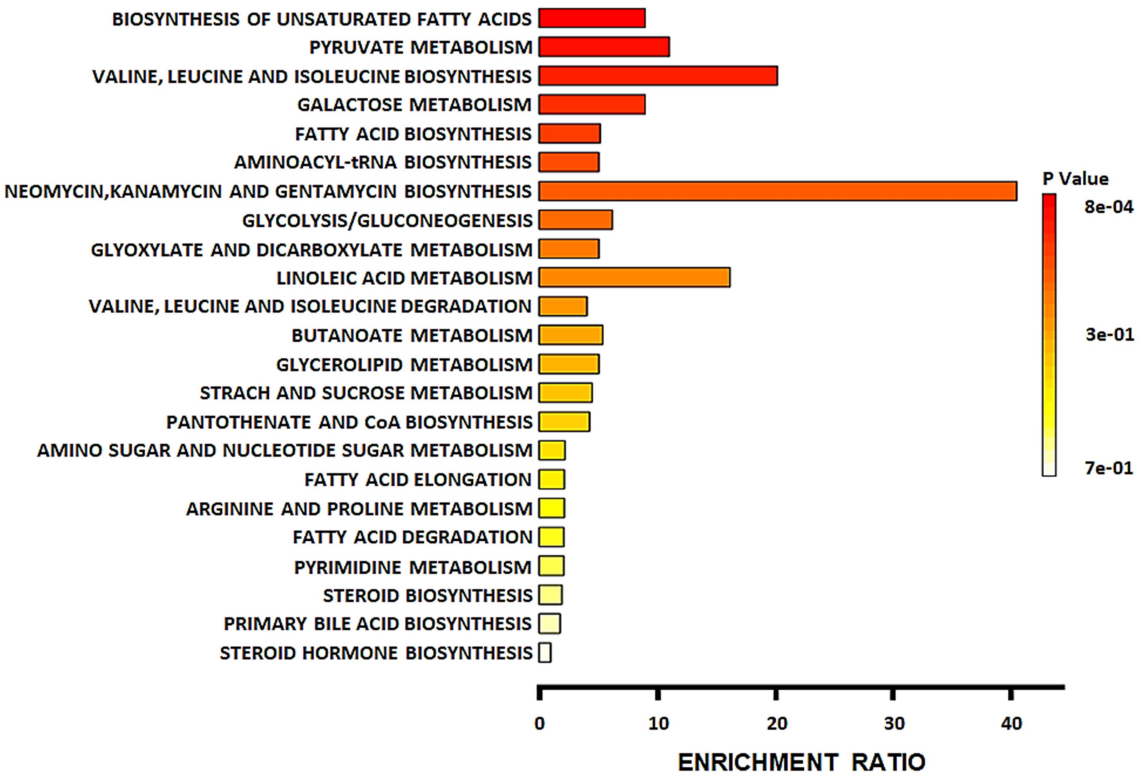

Figure 26.3: Butyrate-specific metabolites enrichment from the KEGG database

The top 23 metabolic pathways were identified. Significantly enriched pathways (↓) include biosynthesis of unsaturated fatty acids, pyruvate metabolism, valine, leucine, and isoleucine biosynthesis, galactose metabolism, and fatty acid biosynthesis. Highly enriched pathways (←) include neomycin, kanamycin, and gentamycin biosynthesis, valine, leucine, and isoleucine

biosynthesis, linoleic acid metabolism, pyruvate metabolism, biosynthesis of unsaturated fatty acids, and galactose metabolism.

Table 18.3: Butyrate-specific metabolites enrichment from the KEGG database

	Metabolite Set	Total	Hits	Expect	P Value	Holm P	FDR
	Biosynthesis of unsaturated fatty acids	36	4	0.445	7.68E-4	0.0645	0.0645
	Pyruvate metabolism	22	3	0.272	0.00213	0.177	0.0818
	Valine, leucine, and isoleucine biosynthesis	8	2	0.099	0.00388	0.319	0.0818
	Galactose metabolism	27	3	0.334	0.00389	0.319	0.0818
	Fatty acid biosynthesis	47	3	0.581	0.0184	1.0	0.273
	Aminoacyl-tRNA biosynthesis	48	3	0.594	0.0195	1.0	0.273
	Neomycin, kanamycin, and gentamicin biosynthesis	2	1	0.0247	0.0246	1.0	0.295
	Glycolysis / Gluconeogenesis	26	2	0.322	0.0395	1.0	0.415
	Glyoxylate and dicarboxylate metabolism	32	2	0.396	0.0577	1.0	0.507
	Linoleic acid metabolism	5	1	0.0618	0.0604	1.0	0.507
	Valine, leucine and isoleucine degradation	40	2	0.495	0.0856	1.0	0.653
	Butanoate metabolism	15	1	0.186	0.171	1.0	1.0
	Glycerolipid metabolism	16	1	0.198	0.181	1.0	1.0
	Starch and sucrose metabolism	18	1	0.223	0.202	1.0	1.0
	Pantothenate and CoA biosynthesis	19	1	0.235	0.212	1.0	1.0
	Amino sugar and nucleotide sugar metabolism	37	1	0.458	0.373	1.0	1.0
	Fatty acid elongation	38	1	0.47	0.38	1.0	1.0
	Arginine and proline metabolism	38	1	0.47	0.38	1.0	1.0
	Fatty acid degradation	39	1	0.482	0.388	1.0	1.0
	Pyrimidine metabolism	39	1	0.482	0.388	1.0	1.0
	Steroid biosynthesis	42	1	0.52	0.411	1.0	1.0
	Primary bile acid biosynthesis	46	1	0.569	0.441	1.0	1.0
	Steroid hormone biosynthesis	85	1	1.05	0.663	1.0	1.0

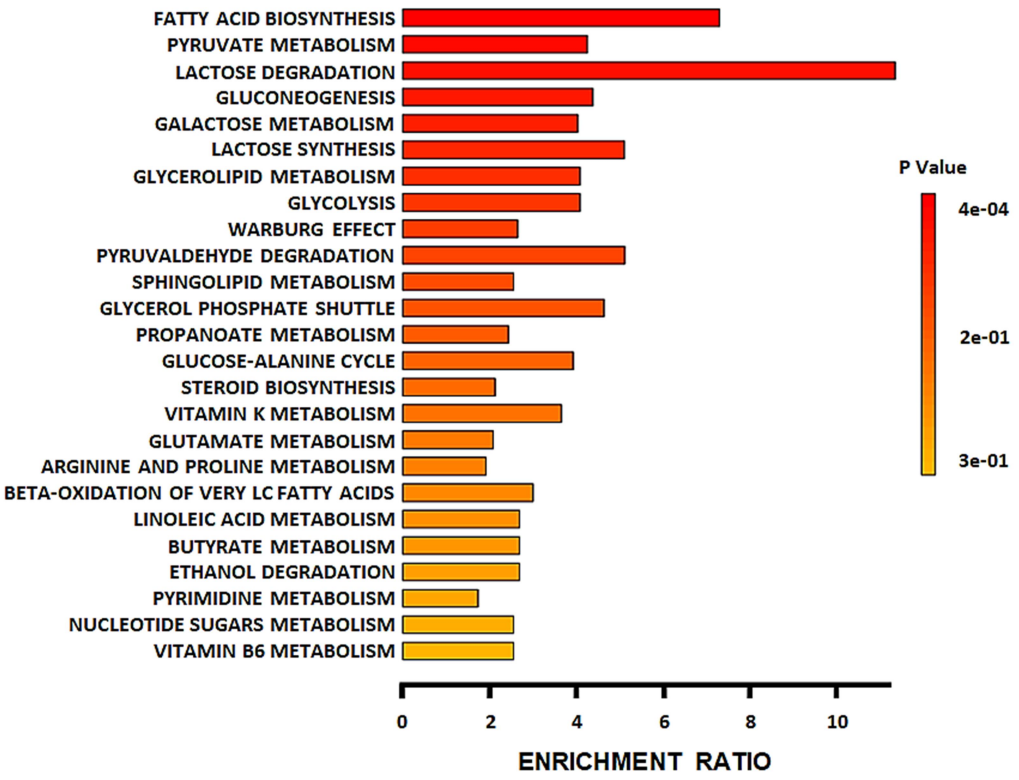

Figure 26.4: Butyrate-specific metabolites enrichment from the SMPDB database

The top 25 metabolic pathways were identified. Significantly enriched pathways (↓) include fatty acid biosynthesis, pyruvate metabolism, lactose degradation, gluconeogenesis, and galactose metabolism. Highly enriched pathways (←) include lactose degradation, fatty acid biosynthesis, lactose synthesis, pyruvaldehyde degradation, and glycerol phosphate shuttle.

Table 18.4: Butyrate-specific metabolites enrichment from the SMPDB database

	Metabolite Set	Total	Hits	Expect	P Value	Holm P	FDR
	Fatty acid biosynthesis	35	5	0.684	3.73E-4	0.0366	0.0366
	Pyruvate metabolism	48	4	0.938	0.0118	1.0	0.393
	Lactose degradation	9	2	0.176	0.012	1.0	0.393
	Gluconeogenesis	35	3	0.684	0.028	1.0	0.681
	Galactose metabolism	38	3	0.742	0.0347	1.0	0.681
	Lactose synthesis	20	2	0.391	0.0558	1.0	0.911
	Glycerolipid metabolism	25	2	0.488	0.0831	1.0	1.0
	Glycolysis	25	2	0.488	0.0831	1.0	1.0
	Warburg effect	58	3	1.13	0.099	1.0	1.0

	Pyruvaldehyde degradation	10	1	0.195	0.18	1.0	1.0
	Sphingolipid metabolism	40	2	0.781	0.182	1.0	1.0
	Glycerol phosphate shuttle	11	1	0.215	0.196	1.0	1.0
	Propanoate metabolism	42	2	0.82	0.196	1.0	1.0
	Glucose-alanine cycle	13	1	0.254	0.227	1.0	1.0
	Steroid biosynthesis	48	2	0.938	0.24	1.0	1.0
	Vitamin K metabolism	14	1	0.273	0.243	1.0	1.0
	Glutamate metabolism	49	2	0.957	0.248	1.0	1.0
	Arginine and proline metabolism	53	2	1.04	0.277	1.0	1.0
	Beta oxidation of very long chain fatty acids	17	1	0.332	0.287	1.0	1.0
	Alpha linolenic acid and linoleic Acid metabolism	19	1	0.371	0.315	1.0	1.0
	Butyrate metabolism	19	1	0.371	0.315	1.0	1.0
	Ethanol degradation	19	1	0.371	0.315	1.0	1.0
	Pyrimidine metabolism	59	2	1.15	0.322	1.0	1.0
	Nucleotide sugars metabolism	20	1	0.391	0.328	1.0	1.0
	Vitamin B6 metabolism	20	1	0.391	0.328	1.0	1.0

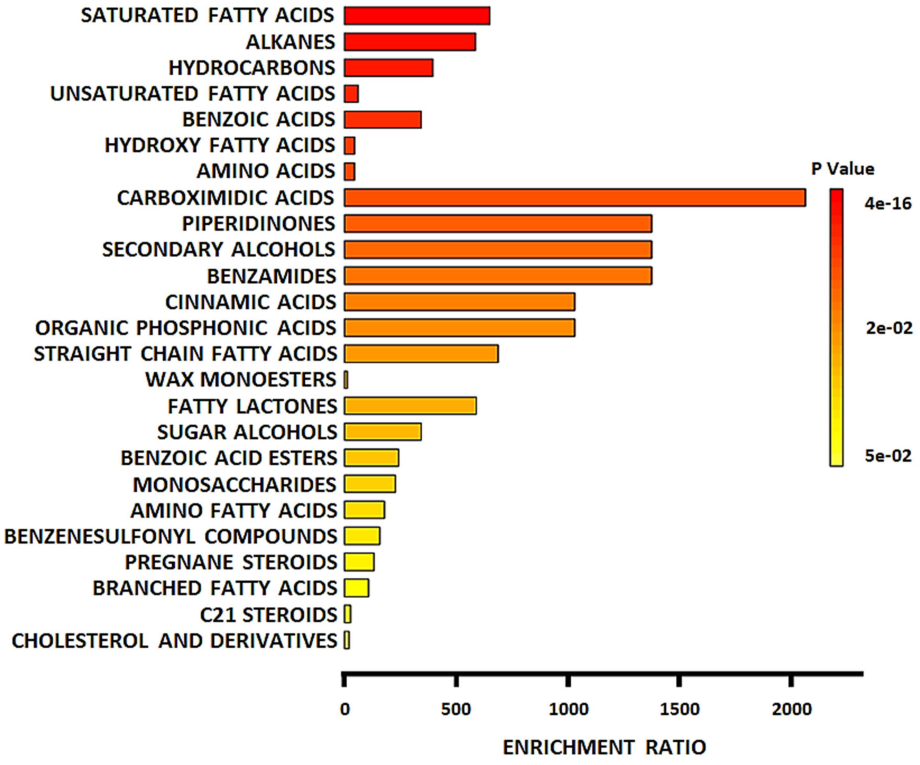

Figure 26.5: Different classes of identified metabolites in butyrate-treated cells

The top 25 different classes of metabolites were identified. Significantly enriched classes (↓) include saturated fatty acids, alkanes, hydrocarbons, unsaturated fatty acids, and benzoic acids. Highly enriched classes (←) include carboximidic acids, piperidinones, secondary alcohols, benzamides, cinnamic acids, and organic phosphonic acids.

Table 18.5: Different classes of identified metabolites in butyrate-treated cells

	Metabolite Set	Total	Hits	Expect	P Value	Holm P	FDR
	Saturated fatty acids	38	6	0.0092	3.99E-16	2.92E-13	2.77E-13
	Alkanes	42	6	0.0102	7.58E-16	5.53E-13	2.77E-13
	Hydrocarbons	52	5	0.0126	1.73E-12	1.26E-9	4.21E-10
	Unsaturated fatty acids	267	4	0.0646	5.97E-7	4.35E-4	1.09E-4
	Benzoic acids	24	2	0.00581	1.58E-5	0.0115	0.00231
	Hydroxy fatty acids	274	3	0.0663	4.31E-5	0.0313	0.00465
	Amino acids	277	3	0.0671	4.45E-5	0.0323	0.00465
	Carboximidic acids	2	1	4.84E-4	4.84E-4	0.35	0.0442
	Piperidinones	3	1	7.26E-4	7.26E-4	0.525	0.0482
	Secondary alcohols	3	1	7.26E-4	7.26E-4	0.525	0.0482
	Benzamides	3	1	7.26E-4	7.26E-4	0.525	0.0482
	Cinnamic acids	4	1	9.68E-4	9.68E-4	0.697	0.0544
	Organic phosphonic acids	4	1	9.68E-4	9.68E-4	0.697	0.0544
	Straight-chain fatty acids	6	1	0.00145	0.00145	1.0	0.0758
	Wax monoesters	949	3	0.23	0.00161	1.0	0.0774
	Fatty lactones	7	1	0.00169	0.00169	1.0	0.0774
	Sugar alcohols	12	1	0.0029	0.0029	1.0	0.125
	Benzoic acid esters	17	1	0.00412	0.00411	1.0	0.167
	Monosaccharides	18	1	0.00436	0.00435	1.0	0.167
	Amino fatty acids	23	1	0.00557	0.00555	1.0	0.203
	Benzenesulfonyl compounds	26	1	0.00629	0.00628	1.0	0.218
	Pregnane steroids	31	1	0.0075	0.00748	1.0	0.248
	Branched fatty acids	38	1	0.0092	0.00916	1.0	0.291
	C21 steroids	148	1	0.0358	0.0352	1.0	1.0
	Cholesterol and derivatives	203	1	0.0491	0.048	1.0	1.0

➢ **Pathway analysis**

Impacted pathways from the KEGG database (Figure 26.6 and Table 18.6), and the SMPDB database (Figure 26.7 and Table 18.7) are given below. Pathway impact is calculated by using centrality and pathway enrichment results.

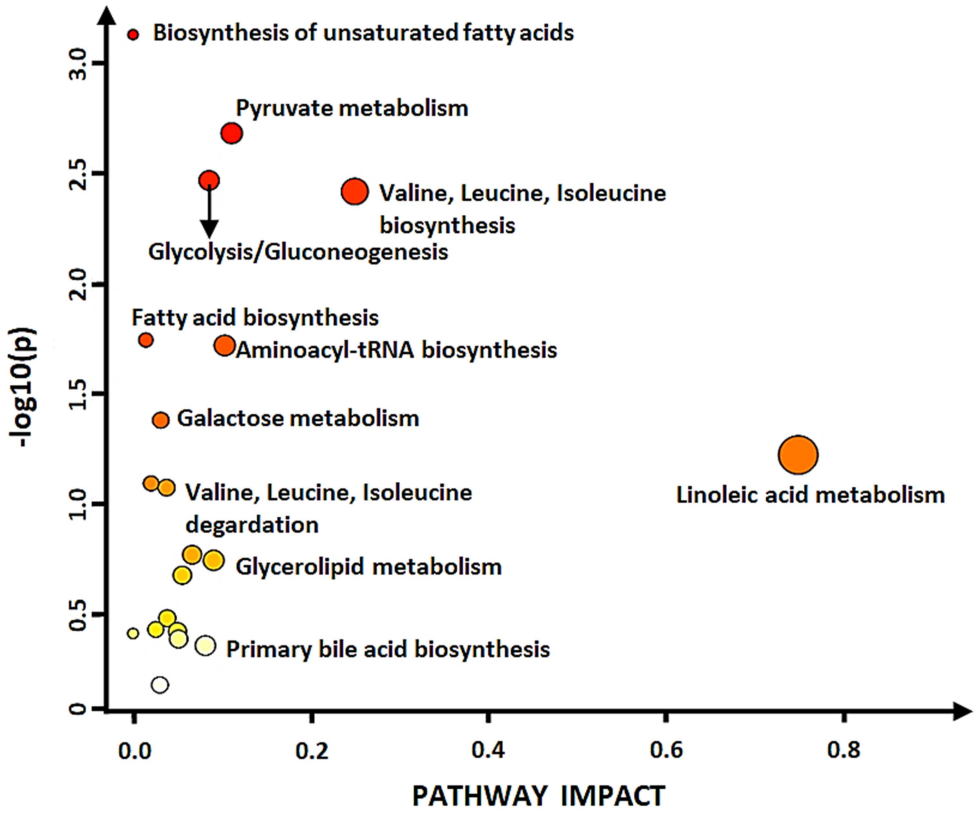

Figure 26.6: Butyrate-specific pathway analysis from the KEGG database

The top 21 impacted pathways were identified. Highly impacted pathways (←) include linoleic acid metabolism, valine, leucine, and isoleucine biosynthesis, pyruvate metabolism, aminoacyl t-RNA biosynthesis, and glycerolipid metabolism. Significantly impacted pathways (↓) include biosynthesis of unsaturated fatty acids, pyruvate metabolism, glycolysis/gluconeogenesis, valine, leucine, and isoleucine biosynthesis, and fatty acid biosynthesis.

Table 18.6: Butyrate-specific pathway analysis from the KEGG database

Pathway Name	Match Status	p	-log(p)	Holm p	FDR	Impact
Biosynthesis of unsaturated fatty acids	4/36	7.4211E-4	3.1295	0.062337	0.062337	0.0
Pyruvate metabolism	3/22	0.0020778	2.6824	0.17245	0.080148	0.11112
Glycolysis / Gluconeogenesis	3/26	0.0034004	2.4685	0.27883	0.080148	0.08571
Valine, leucine, and isoleucine biosynthesis	2/8	0.0038166	2.4183	0.30914	0.080148	0.25
Fatty acid biosynthesis	3/47	0.018011	1.7445	1.0	0.26688	0.01449
Aminoacyl-tRNA biosynthesis	3/48	0.019063	1.7198	1.0	0.26688	0.10344
Galactose metabolism	2/27	0.04165	1.3804	1.0	0.4998	0.03125
Linoleic acid metabolism	1/5	0.059881	1.2227	1.0	0.62876	0.75
Fatty acid degradation	2/39	0.080611	1.0936	1.0	0.70765	0.02041
Valine, leucine, and isoleucine degradation	2/40	0.084244	1.0745	1.0	0.70765	0.03774
Butanoate metabolism	1/15	0.1696	0.77056	1.0	1.0	0.06667
Glycerolipid metabolism	1/16	0.17988	0.74501	1.0	1.0	0.09091
Pantothenate and CoA biosynthesis	1/19	0.21	0.67778	1.0	1.0	0.05556
Glyoxylate and dicarboxylate metabolism	1/32	0.32881	0.48305	1.0	1.0	0.03846
Amino sugar and nucleotide sugar metabolism	1/37	0.36983	0.432	1.0	1.0	0.02564
Arginine and proline metabolism	1/38	0.37775	0.4228	1.0	1.0	0.05
Fatty acid elongation	1/39	0.38557	0.4139	1.0	1.0	0.0
Pyrimidine metabolism	1/39	0.38557	0.4139	1.0	1.0	0.0
Steroid biosynthesis	1/42	0.40847	0.38884	1.0	1.0	0.05128
Primary bile acid biosynthesis	1/46	0.43775	0.35877	1.0	1.0	0.08163
Steroid hormone biosynthesis	1/85	0.65974	0.18063	1.0	1.0	0.0303

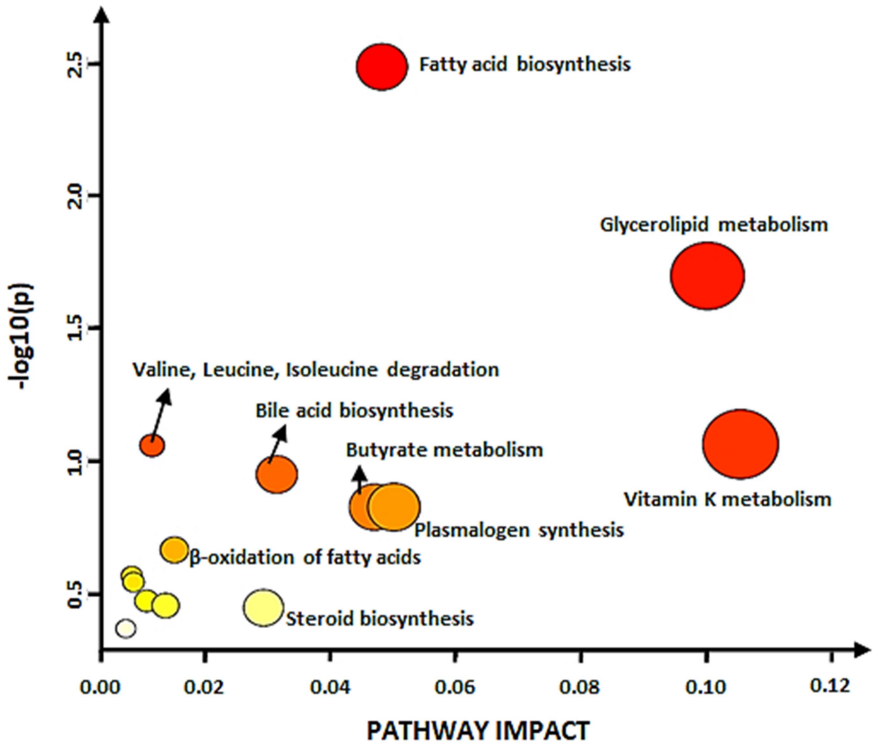

Figure 26.7: Butyrate-specific pathway analysis from the SMPDB database

The top 14 impacted pathways were identified. Highly impacted pathways (←) include vitamin K metabolism, glycerolipid metabolism, plasmalogen synthesis, fatty acid biosynthesis, and butyrate metabolism. Significantly impacted pathways (↓) include fatty acid biosynthesis, glycerolipid metabolism, vitamin K metabolism, valine, leucine, and isoleucine degradation, and bile acid biosynthesis.

Table 18.7: Butyrate-specific pathway analysis from the SMPDB database

Pathway Name	Match Status	p	-log(p)	Holm p	FDR	Impact
Fatty acid biosynthesis	3/33	0.0032751	2.4848	0.32423	0.32423	0.048077
Glycerolipid metabolism	2/23	0.020024	1.6985	1.0	0.99118	0.1
Vitamin K metabolism	1/9	0.08607	1.0651	1.0	1.0	0.10526
Valine, leucine and isoleucine degradation	2/51	0.08695	1.0607	1.0	1.0	0.011429
Bile acid biosynthesis	2/59	0.11182	0.95147	1.0	1.0	0.031311
Butyrate metabolism	1/16	0.14834	0.82874	1.0	1.0	0.046875
Plasmalogen synthesis	1/16	0.14834	0.82874	1.0	1.0	0.05

Mitochondrial beta-oxidation of long chain saturated fatty acids	1/24	0.21481	0.66795	1.0	1.0	0.015
Galactose metabolism	1/31	0.2691	0.57009	1.0	1.0	0.0081967
Fatty acid elongation in mitochondria	1/33	0.28398	0.54672	1.0	1.0	0.0084746
Fatty acid metabolism	1/40	0.33393	0.47635	1.0	1.0	0.010563
Steroidogenesis	1/42	0.34761	0.45891	1.0	1.0	0.013575
Steroid biosynthesis	1/43	0.35436	0.45056	1.0	1.0	0.029197
Pyrimidine metabolism	1/54	0.42453	0.37209	1.0	1.0	0.0072464

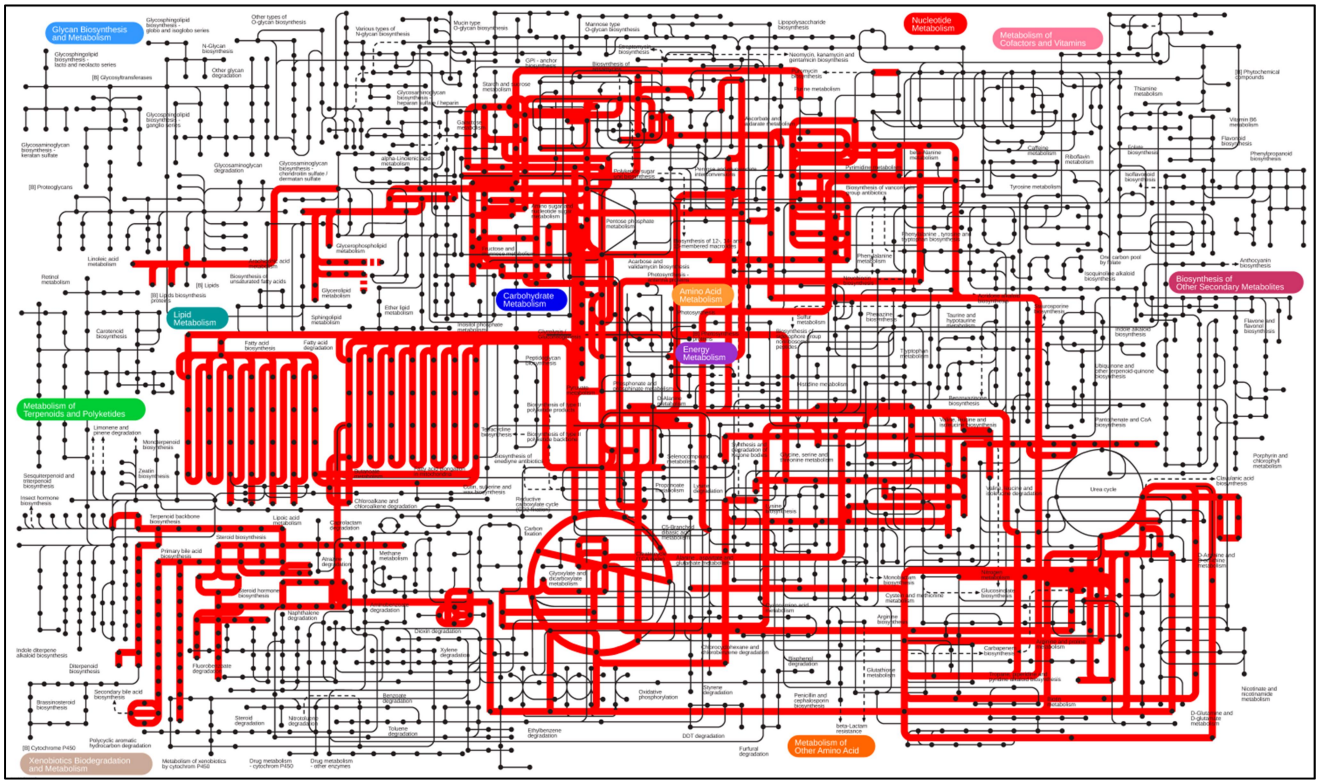

Figure 26.8: Metabolic pathways enriched in butyrate treatment after mapping with the KEGG database. The highlighted metabolisms show enrichment specific to butyrate treatment. This shows the enrichment of amino sugar and nucleotide sugar metabolism, fructose and mannose metabolism, primary bile acid biosynthesis, and other metabolic pathways.

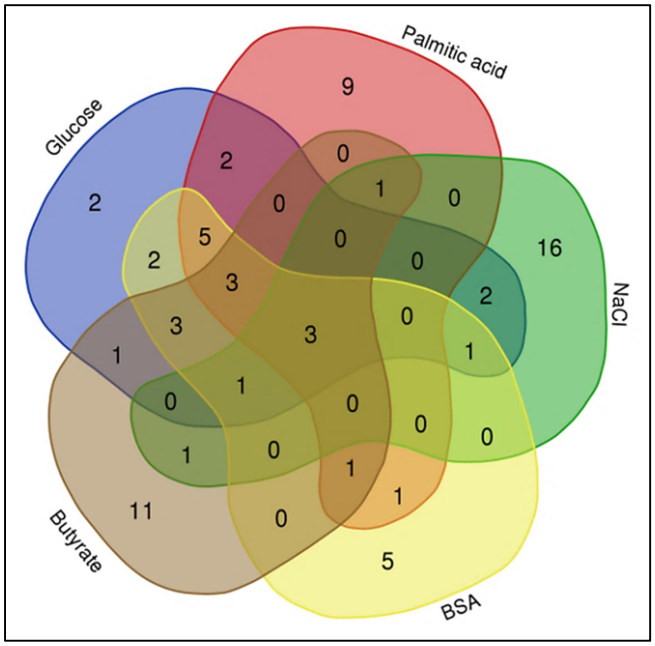

Figure 27.1: Venn diagram representing common disease signatures among all treatments

Three disease signatures were found to be common in all treatments (as in Figure 27.1) –

1. Phenylketonuria
2. PEPCK deficiency
3. Type VI hers disease

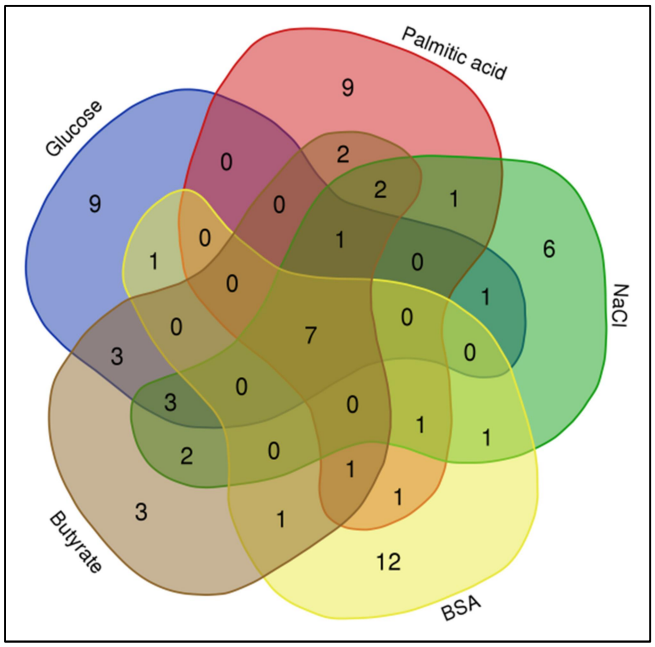

Figure 27.2: Venn diagram representing common classes of metabolites in all treatments

Seven classes of metabolites were found to be common in all treatments (as in Figure 27.2) –

1. Straight chain fatty acids
2. Benzoic acids
3. Carboximidic acids
4. Amino acids
5. Hydrocarbons
6. Saturated fatty acids
7. Alkanes

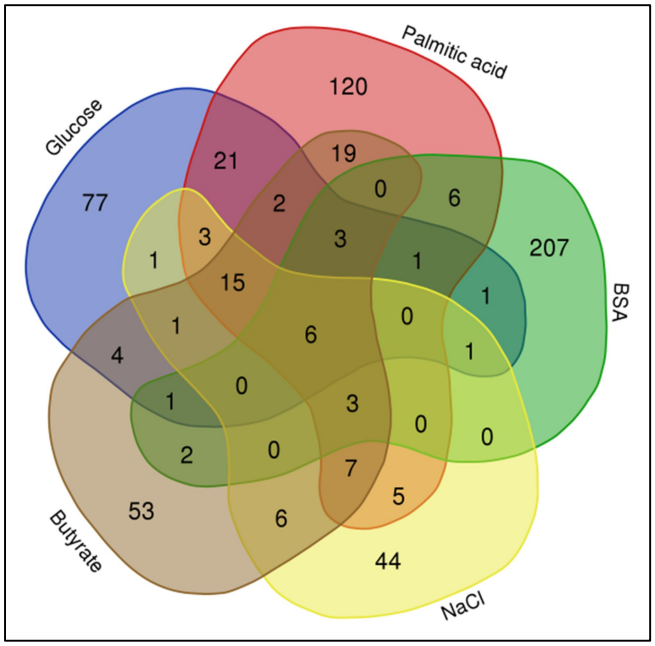

Figure 27.3: Venn diagram representing common metabolites in all treatments

Six metabolites were found to be common in all treatments (as in Figure 27.3) –

1. Cholesterol
2. 2-Propyl-1-pentanol
3. Palmitic acid
4. Benzoic acid
5. Acetamide
6. Leucine

By comparing the metabolites from each nutritional stress to control, some common metabolites were identified, given as follows –

18 common metabolites were identified	
2-Ethylhexan-1-ol	Octanoic acid
2-Ethylhexanal	Terephthalic acid
4-Methylbenzoic acid	Acetamide
2-Ethylhexyl formate	Stearic acid
Valine	2-Ethylhexanoic acid
Cholesterol	2-Propyl-1-pentanol
Palmitic acid	2-Ethylhexyl butyrate
1,2,3,4-Tetrahydroisoquinoline	2,4,6-Trimethylpyridine
Benzoic acid	2-Buten-1-ol

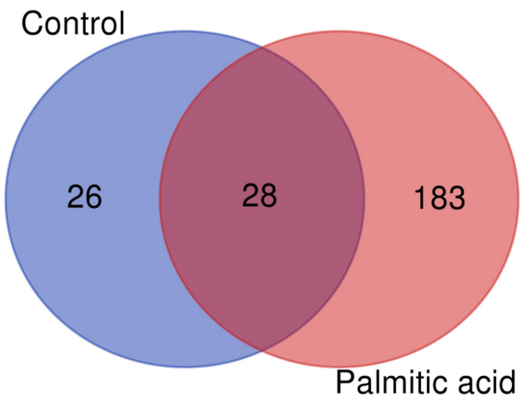

28 common metabolites were identified	
1,2,3,4-Tetrahydroisoquinoline	2-Methyltridecane
Benzoic acid	2-Ethylhexan-1-ol
Oleic acid	2-Ethylhexanal
2,4,4-Trimethylpentan-1-ol	2-Ethylhexyl formate
Lactic Acid	Valine
Valeric acid	Cholesterol
Stearic acid	2-Ethylhexyl 2-ethylhexanoate
2-Ethylhexanoic acid	Palmitic acid
2-Propyl-1-pentanol	Octanoic acid
Hexadecane	Terephthalic acid
2-Ethylhexyl acetate	Acetamide
3-Ethyl-3-methylheptane	Butyric acid
3,8-Dimethylundecane	2-Ethylhexyl butyrate
2,4,6-Trimethylpyridine	Ethyl diethylcarbamate

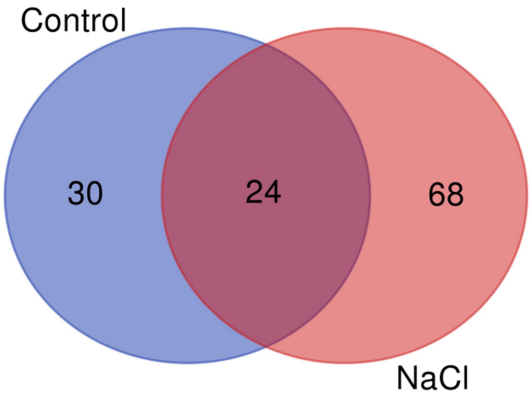

24 common metabolites were identified	
Benzoic acid	2-Methyltridecane
2-Propyl-1-pentanol	2-Ethylhexan-1-ol
2-Ethylhexanoic acid	2-Ethylhexanal
Hexadecane	Acetamide
2-Ethylhexyl acetate	2-Ethylhexyl formate
2,4,4-Trimethylpentan-1-ol	Butyric acid
D-Mannose	Cholesterol
2-Ethylhexyl butyrate	Stearic acid
Pentitol	Pregna-3,5-dien-9-ol-20-one
Octanoic acid	Sulfurous acid
Ethyl diethylcarbamate	Palmitic acid
2,4,6-Trimethylpyridine	6-Hydroxyheptanoic acid

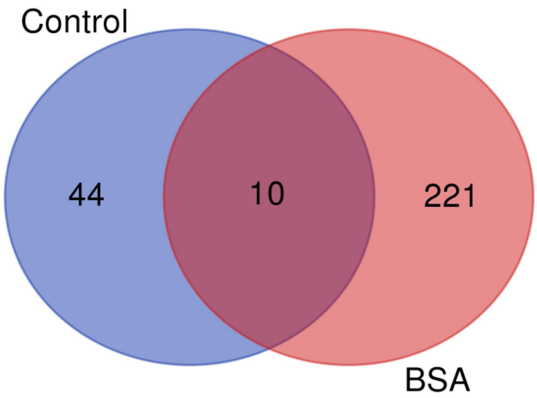

10 common metabolites were identified	
Palmitic acid	Valine
Propionamide	Cholesterol
Terephthalic acid	Benzoic acid
Butyric acid	Acetamide
Hexadecane	2-Propyl-1-pentanol

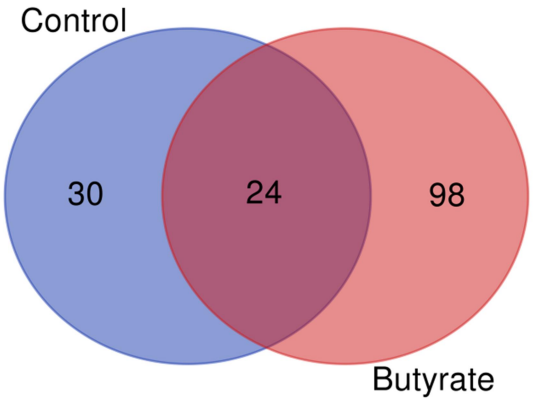

24 common metabolites were identified	
Acetamide	2-Ethylhexan-1-ol
Butyric acid	2-Ethylhexanal
Stearic acid	2-Ethylhexyl formate
2-Ethylhexanoic acid	Valine
2-Propyl-1-pentanol	Cholesterol
Hexadecane	Palmitic acid
2-Ethylhexyl acetate	Benzoic acid
3-Ethyl-3-methylheptane	Oleic acid
2-Ethylhexyl butyrate	2,4,4-Trimethylpentan-1-ol
Pentitol	Lactic acid
Ethyl diethylcarbamate	Octanoic acid
2,4,6-Trimethylpyridine	Terephthalic acid

DISCUSSION

Metabolism permeates every element of physiology. There are more metabolites formed in the body than genes itself as one gene can help in the production of multiple metabolites. A cell cannot change its morphology, physiology, functions, or behavior without altering its metabolism. Also, the biochemical pathways do not generate end products; rather every product of a specific pathway is an intermediate for another (Adrain, 2021). These metabolites have a significant impact on the normal functioning of the body as it affects chromatin state, gene expression, and protein folding at the molecular level and may cause diseases at physiological levels. The metabolites produced by cells can be induced by specific treatments given or in response to each dietary stress or simply indicate normal functioning of the cell. The metabolites identified enrich certain metabolisms or impact certain pathways which could justify the changes in the liver after specific dietary stress at physiological and genetic levels. Also, the pathways that are enriched or identified can represent the effect of treatments given or may indicate regular cellular processes and functions. Moreover, the observation and results are based on only metabolite studies.

Metabolic pathways impacted or enriched in control are general metabolism occurring inside normal cells including amino acid metabolism, fat metabolism, carbohydrate metabolism, CoA biosynthesis, butyrate metabolism, plasmalogen synthesis, glycerolipid metabolism, glycerol phosphate shuttle, sulfur metabolism, bile acid synthesis, and steroid metabolism. These are the metabolic pathways that help in maintaining normal cell functioning.

The top 25 disease signatures were identified in each treatment. Disease signatures identified in control could be due to false recognition (internal software algorithm) or lack of nutrients. Out of all disease signatures, three were common in all including phenylketonuria, PEPCK deficiency,

and type VI hers disease. These diseases may be common to all treatments but differ in enrichment ratios. Phenylketonuria is caused to due to accumulation of phenylalanine and phenylpyruvate. It is associated with protein feeding and glycolysis (Cox & Nelson, 2000). Type VI hers disease is liver phosphorylase dysfunction in which glycogen is not degraded. It is a kind of metabolic disorder that prevents the release of glucose (Aeppli *et al.*, 2020). PEPCK is an important enzyme for gluconeogenesis, glyceroneogenesis, serine biosynthesis, and amino acid metabolism. It helps in the regulation of lipogenesis and SREBP activation. HCC progression is promoted by the transcription of lipogenesis genes upon activation of SREBPs (Yu *et al.*, 2021).

Out of all metabolites classes, seven were found to be common among all treatments which include straight-chain fatty acids, benzoic acids, carboximidic acids, amino acids, hydrocarbons, saturated fatty acids, and alkanes. Carboximidic acids (CHEBI: 48378) are highly enriched in all treatments. It is a structural derivative of oxoacids and includes imidic acid and organonitrogen compounds. Amino acids in all treatments have a very less enrichment ratio. This could be due to the usage of non-polar columns or handling errors. Hydrocarbons and alkanes are involved in every pathway and have a sufficiently good enrichment ratio in each treatment. Elevated benzoic acid levels indicate glycine deficiency and liver dysfunction (Lee *et al.*, 2022). But the enrichment ratio of benzoic acid is less than 500 and surprisingly out of all treatments benzoic acid was the least in palmitic acid treatment. Benzoic acids can combine with glycine to form hippuric acid. Low hippuric acid levels indicate hypertension (Lee *et al.*, 2022) and this is following our result as after salt treatment, the hippuric acid enrichment ratio is close to zero and salt is known to cause hypertension (Li *et al.*, 2021). Identification of straight-chain fatty acids and saturated fatty acids is probably due to the usage of non-polar column. The saturated fatty acid is not healthy for the body and palmitic acid treatment has more saturated fatty acid metabolites according to enrichment

ratio. The discussion for individual treatment and corresponding enriched or impacted pathways is given as follows –

High glucose treatment

Enriched neomycin, kanamycin, and gentamycin biosynthesis were seen after high glucose treatment. Although this metabolism is not present in humans, the metabolites identified after the analysis can be the same or similar for this pathway. According to Kudo & Eguchi, 2009, neomycin, kanamycin, and gentamycin are 2-deoxystreptamine-containing aminoglycosides. D-glucose-6-phosphate (from glycolysis) forms 2-deoxystreptamine and 2-deoxy-scyllo-inosose. The latter is a cyclohexanone having a 4-hydroxy group. Similar identification in GC-MS analysis was also done for "2-cyclohexe-1-one" with an abundance of 0.129%. In the KEGG database (ID: map00524) D-glucose is the precursor for this pathway. Valine, leucine, and isoleucine biosynthesis was impacted and enriched after high glucose treatment. These are BCAAs and essential amino acids which are not produced in the human body but metabolites obtained could be the same or similar to this pathway. Pyruvate helps in the biosynthesis of BCAAs (Cox & Nelson, 2000). These are the indicators for obesity and associated disorders (Kim *et al.*, 2011) (Cai *et al.*, 2021) and cause metabolic diseases (Pesta & Samuel, 2014). They increase glucose mobility from the liver, induce insulin release (De Chiara *et al.,* 2019), cause mitochondrial dysfunction, and interept fat oxidation (Pesta & Samuel, 2014). BCAAs are biomarkers for insulin resistance (Würtz *et al.*, 2013) and their biosynthesis detection indicates deteriorating cell health. But interestingly, it was also seen that leucine may play a functional role by inducing muscle protein synthesis and regulating cellular signaling for protein production. Also, BCAAs feeding in rats elevated the protein production dealing with insulin to cause insulin sensitivity (Wolfe, 2017).

Another enriched and impacted pathway includes the biosynthesis of aminoacyl t-RNA. This is the charging of t-RNA with compatible amino acids for protein synthesis. This indicates the possible increase in protein expression as according to Chandrasekaran *et al.*, 2010, glucose in HepG2 cells tends to increase the expression and production of human apolipoprotein A-II that cause hyperglycemia. Also, enhanced protein production can cause the induction of MAPKs and NF-κB signaling (Panahi *et al.*, 2018). Glucose feeding may generate more ATP (Félix-Martínez *et al.*, 2013) which is a source of energy for t-RNA charging. Moreover, excess glucose can be converted into amino acids (Rui, 2014), and possibly more amino acids are available for t-RNA charging (Wolfe, 2017). Biosynthesis of unsaturated fatty acids was also enriched which could be due to fatty acid production liver using glucose or pyruvate as substrate (Rui, 2014). More glucose tends to degrade in the body and glycolysis was observed as an enriched and impacted pathway. Also, Chen *et al.*, 2013 observed that glucose feeding induces glycolysis in Chang liver cells. Glycerol phosphate shuttle enrichment was also seen which could be due to an increase in glycolysis as this shuttle helps in the regeneration of NAD^+ from NADH and NAD^+ helps in glycolysis and oxidative phosphorylation (Cox & Nelson, 2000). Lactose metabolism was also enriched as glucose can form lactose (Cox & Nelson, 2000).

Arachidonic acid metabolism was impacted after glucose treatment. Arachidonic acid generates pro-inflammatory and signaling molecules. Its metabolites enhance inflammatory responses (induced by high glucose) for accumulating immune cells, leukocytes, and cytokines at the site for clearance. Later it maintains the inflammatory signals by generating metabolites that protect the host (Hanna & Hafez, 2018). Primary bile acid biosynthesis and glycerolipid metabolism were also impacted pathway as acetyl CoA from glucose induces cholesterol uptake and biosynthesis and fatty acid formation (glycerolipid formation) (Cox & Nelson, 2000), and cholesterol induces the

formation of primary bile acid synthesis in the liver (Cai *et al.*, 2021). Enrichment of ethanol degradation indicated the possible production of acetyl CoA for ATP production and fatty acid biosynthesis (as given in Figure 28) (Wilson & Matschinsky, 2020).

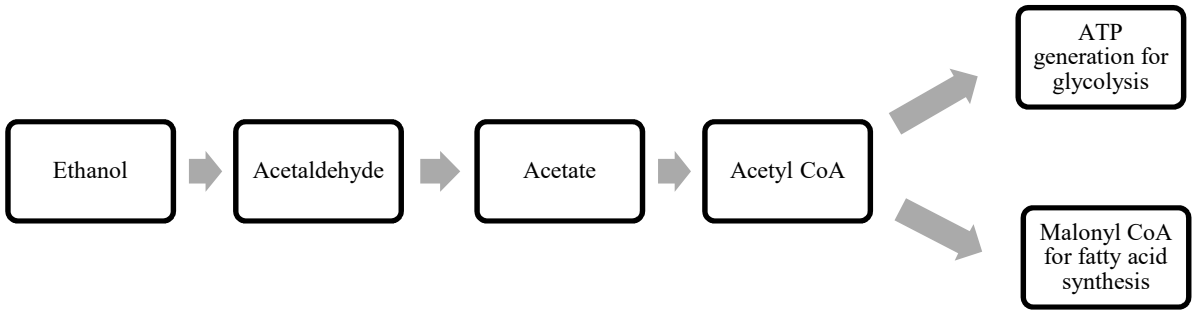

Figure 28: Flow chart representing ethanol degradation; Ethanol is degraded into acetyl CoA for ATP production and fat synthesis, (Wilson & Matschinsky, 2020).

Linolenic acid metabolism was also impacted. According to Cabout *et al.*, 2017, less linolenic acid in blood is linked to insulin resistance and diabetes and Cai *et al.*, 2021 explained that linolenic acid is associated with inflammation and insulin resistance reduction.

High palmitic acid treatment

Valine, leucine, isoleucine, phenylalanine, tyrosine, and tryptophan biosynthesis was enriched and impacted after palmitic acid treatment. As discussed earlier, valine, leucine, and isoleucine are BCAAs and according to Kim *et al.*, 2011, it acts as a marker for obesity. This can affect fat oxidation (Pesta & Samuel, 2014). Phenylalanine, tyrosine, and tryptophan are AAAs and only tyrosine is produced in humans. According to De Chiara *et al*., 2019, BCAA/AAA helps in the diagnosis of liver disease and accessing liver dysfunction. AAAs can cause metabolic disorders (Pesta & Samuel, 2014) and according to Würtz *et al.*, 2013 valine, isoleucine, leucine, tyrosine,

and phenylalanine can cause insulin resistance. Phenylalanine and tyrosine metabolism was also impacted after this treatment. Phenylalanine can be converted into tyrosine which is related to insulin resistance development (Würtz *et al.*, 2013) and insulin resistance can lead to steatosis (characteristic of NAFLD) (Chandrasekaran *et al.*, 2010). So, the detection of biosynthesis of these could indicate the harmful effects of palmitic acids on HepG2 cells.

Pyruvate metabolism was enriched as it generates ATP via the TCA cycle and oxidative phosphorylation, which could enhance fatty acid activation for oxidation. Acetyl CoA is a common end product for fatty acid degradation and pyruvate metabolism, so it can be inferred that pyruvate metabolism may get enriched due to acetyl CoA formation. This enrichment may also indicate the possible oxidation of fatty acids for eradication or ATP generation. Other enriched pathways include β-oxidation of very long-chain fatty acids, which is similar to the above inferred enrichment. The increased feeding of palmitic acid may lead to its oxidation for energy generation and ketone body formation (Rui, 2014). A similar observation was recorded by Mato *et al.*, 2019 in which elevated rates of β-oxidation of fat were present in the liver of NAFLD patients. But previous observations by Kim *et al*., 2011, were the opposite as the function of carnitine palmitoyltransferase 1 (involved in β-oxidation of fat) declined after a high-fat diet in mice.

Threonine degradation was also impacted after analysis. Threonine can be converted to pyruvate (Gray *et al.*, 2014). This could lead to enrichment in pyruvate metabolism. Also, threonine can be degraded to the ketone body and ketone bodies are also formed by β-oxidation of fatty acids (Rui, 2014), so the threonine degradation pathway may get enriched due to the formation of ketone bodies. Aminoacyl t-RNA biosynthesis was increased and impacted due to possible enhanced protein expression. High palmitic acid feeding may generate more ATP and this is required for aminoacyl t-RNA synthesis, as according to Rui, 2014, insulin resistance and hepatic steatosis can

be developed due to overexpression of LPL in the liver, and Boyce *et al.*, 2020 observed increase in 23 metabolites after high-fat diet which is mainly involved in carnitine and amino acid metabolism.

Surprisingly, fatty acid biosynthesis was also impacted and enriched after palmitic acid treatment. This may indicate a regular cellular process or a positive feedback loop. Previously also, it was seen that the biosynthesis of unsaturated fatty acids (specifically, oleic acid) was significantly enriched after high-fat treatment (Cai *et al.*, 2021). Palmitic acid can form long chain fatty acids (steric acid, oleic acid, and palmitoleic acid) and increase in palmitoleic acid is related to liver steatosis (Maciejewska-Markiewicz *et al.*, 2022). This could also explain the possible enrichment of glycerolipid metabolism as high palmitic acid treatment could provide high fatty acids to cells which could be converted to glycerolipid (Cox & Nelson, 2000). Plasmalogen synthesis was also impacted after fat treatment. Plasmalogen synthesis occurs in the peroxisome and β-oxidation of fatty acids occurs in mitochondria and peroxisome (Kim *et al.*, 2011). Plasmalogen is a sub-class of glycerophospholipids, which can be produced by fatty acids (Cox & Nelson, 2000). Similarly, it was observed that after a high-fat diet, glycerophospholipid metabolism was significantly enriched (Cai *et al.*, 2021).

Glutathione metabolism was enriched after fat treatment. Glutathione is an anti-oxidant in animals and prevents cellular damage. Metabolism involves both anabolism and catabolism. Palmitic acid breakdown to form ATP (β-oxidation) and glutathione synthase requires ATP for glutathione production (Pizzorno, 2014). Also, it is well known that high fat causes inflammation in mice liver (Rui, 2014) and (Kim *et al.*, 2011) and according to Pizzorno, 2014, glutathione gets reduced due to inflammation and oxidative stress. It was also observed that cysteine plays a vital role in glutathione production (Pizzorno, 2014), and high fat in mice decreases betaine titers in the liver

which depletes the methionine-homocysteine cycle (Kim *et al.*, 2011) which may negatively affect glutathione production and cells are prone to damage. The high enrichment of vitamin K metabolism could be due to the identification of napthoquinone (0.047%) after GC-MS analysis. Vitamin K is a fat-soluble vitamin. According to Wang *et al.*, 2023, vitamin K metabolism (deficiency) can lead to liver damage as vitamin K helps in protecting cells from lipid peroxidation, maintaining redox reactions and inflammation.

High sodium chloride treatment

Butanoate (butyrate) metabolism was highly impacted and enriched after high salt treatment. Butanoate can lead to the formation of cholesterol and fatty acids (Nathani *et al.*, 2016), and previously also, it was observed that a high salt diet leads to an increase in cholesterol formation (da Silva Ferreira *et al.*, 2023). Valine, leucine, and isoleucine biosynthesis was another highly enriched and impacted pathway which indicates the development of insulin resistance and metabolic syndrome (Pesta & Samuel, 2014), and pyruvate degradation (Cox & Nelson, 2000). Simultaneously, pyruvate metabolism was also impacted and enriched. Pyruvate can degrade into acetyl CoA for energy production and fat and cholesterol synthesis (Cox & Nelson, 2000) which could also be the possible reason for high enrichment in fatty acid biosynthesis and glycerolipid metabolism. This is similar to the observation by da Silva Ferreira *et al.*, 2023, which confirms the increase in cholesterol levels after a high-salt diet. According to da Silva Ferreira *et al.*, 2023, ALT and AST levels elevate after high sodium treatment. ALT forms pyruvate from alanine (Gray *et al.*, 2014) and later pyruvate can undergo various metabolic pathways. Propanoate metabolism was also enriched after a high salt diet. Propanoate can produce succinyl CoA, which enriches the TCA cycle, and malonyl CoA which helps in the production of fat and cholesterol, as given in Figure 29 (PubChem pathway ID: SMP0087480).

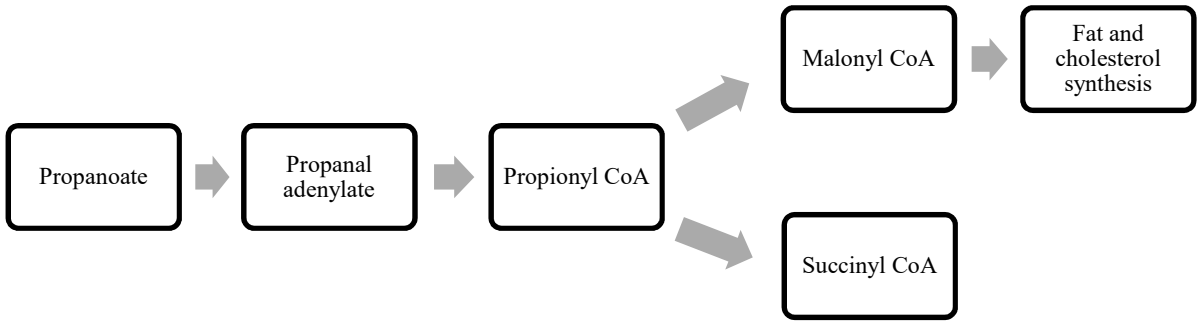

Figure 29: Flow chart representing propanoate metabolism; Propanaote helps in the production of propionyl CoA, malonyl CoA, and succinyl CoA.

Glycolysis/ gluconeogenesis pathways were also enriched. This could be explained by ALT and AST levels elevation after high sodium treatment (da Silva Ferreira *et al.*, 2023). AST actively participates in the malate-aspartate shuttle (involved in glycolysis) and gluconeogenesis in the liver (Otto-Ślusarczyk *et al.*, 2016). Thus increase in glycolysis could explain the enrichment in the glycerol phosphate shuttle. The ethanol degradation pathway was impacted and enriched after high salt treatment which indicated the possible production of acetyl CoA for ATP production and fatty acid biosynthesis (Wilson & Matschinsky, 2020). A high salt diet causes shifts in sulfur metabolism. It was earlier observed that saline injection could possibly deteriorate the levels of metabolites containing reduced sulfur (sulfane sulfur and H_2S). Cysteine metabolism was also affected by salt injections (Iciek *et al.*, 2017). According to Pizzorno, 2014 cysteine plays a vital role in gluthathione production and disturbances in cysteine metabolism can affect glutathione production which can lead to cellular damage.

Primary bile acids (cholic acid and chenodexycholic acid) are synthesized from cholesterol (Cai *et al.*, 2021). The above evidences and da Silva Ferreira *et al.*, 2023 observations confirm that a high salt diet induces cholesterol formation and hence primary bile acid biosynthesis pathway is highly

impacted. High salt treatment also impacted carnitine synthesis. This could be explained as ALT and AST levels elevate after high sodium treatment (da Silva Ferreira *et al.*, 2023), ALT promotes pyruvate formation (Gray *et al.*, 2014) and pyruvate breaks down into acetyl CoA and fatty acids are produced (Cox & Nelson, 2000). High fatty acids produced can further induce L-carnitine formation (Boyce *et al.*, 2020). This observation matches with the Shojaei-Zarghani *et al.*, 2022 observation that when a rat was given high salt water there was an increase in concentrations of trimethylamine N-oxide, a metabolite of choline, betaine, and carnitine, which is responsible for steatosis in the liver. As mentioned above, high salt treatment may promote pyruvate and fatty acid production. Both cause the formation of ketone bodies in the body (Cox & Nelson, 2000). So, due to this reason, ketone body metabolism was also impacted after high salt treatment.

High BSA treatment

Neomycin, kanamycin, and gentamycin biosynthesis were enriched after high protein feeding. According to Pesta & Samuel, 2014, high protein leads to the formation of glucose (gluconeogenesis) in the liver and glucose plays a vital role in the formation of these antibiotics through 2-deoxystreptamine and 2-deoxy-scyllo-inosose, as mentioned above. The evidence for the direct role of glutamate in biosynthesis is not present. But according to the KEGG database (ID: map00524), glutamate seems to be involved in it. 2-deoxy-scyllo-inosose is one of the metabolites involved in the biosynthesis of antibiotics ((Kudo & Eguchi, 2009)) and this metabolite is a cyclohexanone having a 4-hydroxy group. Similar compounds were identified after GC-MS analysis - (R)-5-Phenyl-2-cyclohexene-1-one (0.004%), 2,4-Cyclohexadienone (0.408%), 4-Ethyl-4-methylcyclohexanone (0.025%), and 2,5-Cyclohexadienone (0.002%). Valine, leucine, and isoleucine biosynthesis were enriched and impacted after a protein treatment. This may indicate a positive feedback loop. These are BCAAs which indicate fatty liver disease (Stachowska *et al.*,

2022) and obesity (Cai *et al.*, 2021). But consumption of vegetables rich in BCAAs tends to benefit cirrhotic patients' health and reduce HCC development (De Chiara *et al.*, 2019). High intake of BCAAs is linked to metabolic disorders, insulin resistance, and mitochondrial dysfunction (Pesta & Samuel, 2014). Leucine helps in regulating cellular signaling for protein synthesis in muscles. Also, BCAAs feeding in rats elevated the protein production dealing with insulin to cause insulin sensitivity (Wolfe, 2017).

High-protein diet enriches aminoacyl t-RNA biosynthesis. A high protein diet may provide more amino acids for t-RNA synthesis as previously it was seen that intake of BCAAs can increase the protein formation in rat muscle (Wolfe, 2017). It also promotes gluconeogenesis (Rui, 2014) and glucose may produce energy for the t-RNA charging process. Also, increased expression of glucose-6-phosphatase and PEPCK was observed (Pesta & Samuel, 2014). Enrichment in alanine, aspartate, and glutamate metabolism could be due to the breakdown of these amino acids or a positive feedback loop for production. Alanine is produced by proteins and later can form glucose (Gray *et al.*, 2014) and (Rui, 2014). Alanine biosynthesis can cause insulin resistance (Würtz *et al.*, 2013). Alanine can also be used to produce pyruvate (Gray *et al.*, 2014). Aspartate is a part of a shuttle for glycolysis, can also form oxaloacetate (causing TCA enrichment), and act as a nitrogen donor in the urea cycle (Cox & Nelson, 2000). The development of liver fibrosis is caused by alterations in glutamate titers (Stachowska *et al.*, 2022). Glutamate is involved in the production of glutathione (Cox & Nelson, 2000).

Glucose-alanine cycle enrichment indicates carbohydrate anabolism and amino acid metabolism (Cox & Nelson, 2000). Protein releases alanine to produce glucose (Rui, 2014). This cycle balances the glucose concentrations in blood between the meals (Cox & Nelson, 2000). This could also explain the enrichment of alanine metabolism. Alanine can be converted to glucose and glutamate,

and later glutamate can be useful for glutathione production (Cox & Nelson, 2000). Amino acids can form glucose (Cox & Nelson, 2000) and glucose can further form fatty acids (Rui, 2014). This could explain the enrichment of fatty acid biosynthesis. This hypothesis matches with (De Chiara *et al.*, 2019) observations that amino acids can form long-chain and short-chain fatty acids.

As amino acids tend to form fatty acids, then primary bile acid biosynthesis also gets impacted as high fat can induce the formation of primary bile acids (Cai *et al.*, 2021). Protein feeding also resulted in the enrichment of phenylacetate metabolism. Phenylacetate is formed due to the accumulation of phenylalanine. Phenylalanine forms phenylpyruvate which further produces phenylacetate. High protein intake can cause phenylalanine and phenylpyruvate accumulation in the body, causing phenylketonuria, and phenylacetate (produced from phenylpyruvate) helps in detecting it (Cox & Nelson, 2000). Glycine, serine, and threonine metabolism was impacted after high protein feeding. These 3 amino acids are involved in nucleotide synthesis (Mato *et al.*, 2019). Glycine conjugates with primary bile acids to form secondary bile acids (Cai *et al.*, 2021). It also helps in the production of glutathione (Pizzorno, 2014). Shifts in glycine titers can cause the development of liver fibrosis (Stachowska *et al.*, 2022). Serine and glycine are taken up by M1 macrophages and maintain lipid and nucleotide synthesis, redox reactions, and expression of pro-inflammatory factors (Adrain, 2021). Serine and threonine play a significant role in insulin signaling (Chandrasekaran *et al.*, 2010) and their catabolism can form pyruvate (Gray *et al.*, 2014).

Porphyrin metabolism was also impacted due to protein feeding. It can occur because glycine acts as a precursor for porphyrin production and the breakdown of porphyrin (heme) produces bilirubin which is essential for bile pigment production. Succinyl CoA can also form porphyrin. Porphyrin serves as an electron and oxygen carrier in the body (Cox & Nelson, 2000).

High sodium butyrate treatment

Fiber has the potential to produce glucose (gluconeogenesis) (Kieffer, Martin*, et al.*, 2016). Glucose is involved in the production of neomycin, kanamycin, and gentamycin, as discussed above. Hence, this could explain the enrichment of neomycin, kanamycin, and gentamycin biosynthesis after butyrate treatment. Similarly, glucose produced by fiber can later form pyruvate (glycolysis), and pyruvate act as a precursor for valine, leucine, and isoleucine production (Cox & Nelson, 2000). This could justify the enrichment of valine, leucine, and isoleucine production, lactose production, and pyruvate metabolism. Also, Kieffer, Piccolo*, et al.*, 2016, observed an increase in glycolysis after fiber feeding in mice, which could indicate more pyruvate generation and production of these three amino acids. As the glycerol phosphate shuttle is a part of glycolysis, it also gets enriched after high fiber treatment.

Aminoacyl t-RNA synthesis was also impacted. This indicates the possible increase in protein expression. As high fiber converts to glucose (Kieffer, Martin*, et al.*, 2016) and glucose produces energy in the form of ATP (Félix-Martínez *et al.*, 2013) which may be required for t-RNA charging. Linoleic acid metabolism was impacted and enriched after fiber treatment. Kieffer, Piccolo*, et al.*, 2016, also observed significant depletion in linoleic acid after HAMRS2 treatment in mice. Glucose produced from fiber (Kieffer, Martin*, et al.*, 2016) can increase the production of fat (Rui, 2014) and high fat produced can alter the amounts of linoleic acids in the body (Kim *et al.*, 2011). Also, linoleic acid can produce arachidonic acid, which is beneficial to the body as it produces signaling molecules and pro-inflammatory factors (Hanna & Hafez, 2018).

The formation of fat from glucose could explain the enrichment of biosynthesis of unsaturated fatty acids and fatty acid biosynthesis. High fat helps in the production of unsaturated fatty acids

(Cai *et al.*, 2021). This is similar to the observation by Maciejewska-Markiewicz *et al.*, 2022, that high fiber in the body can produce more monounsaturated fatty acids (oleic acid and palmitoleic acid) and it leads to the expression of SREBP-1 that helps in the fatty acid biosynthesis. Simultaneously, glycerolipid metabolism was also impacted as glycerolipid is produced from fat (Cox & Nelson, 2000). Butyrate metabolism was highly impacted after high fiber treatment as sodium butyrate treatment was given. Butanoate (butyrate) can lead to the formation of cholesterol and fatty acids (Nathani *et al.*, 2016) which could also enrich fatty acid synthesis and impact plasmalogen synthesis. Plasmalogen is a sub-class of glycerophospholipids, which can be produced by fatty acids (Cox & Nelson, 2000). The observation is following the above explanation as fat is produced by fiber.

High fiber leads to pyruvaldehyde degradation. Pyruvaldehyde is also called methylglyoxal which is a by-product of glycolysis. It is highly reactive and causes damage to DNA and proteins. It leads to the development of type 2 diabetes (Cox & Nelson, 2000). After a fiber diet, it gets degraded which is beneficial to the body. Another impacted pathway was vitamin K metabolism. As discussed earlier, it protects cells against inflammation and lipid peroxidation and regulates lipid and glucose metabolic disorders. This may indicate the normal functioning of cells.

RESEARCH LIMITATIONS

Although this research was carried out with proper experimental design and a good literature survey, still potential limitations stand by and some of them include –

1. The cancer cell line (HepG2 cells) was used to understand liver functions. Cancer cells are not normal cells and certainly have mutations that are not present in normal liver cells which means that the metabolites obtained may not solely represent normal cell functioning. Also, primary cells are not easily available.
2. Observations, results, and discussion are based on only metabolomics studies. No gene expression and morphological studies were conducted to confirm the results of metabolite-induced changes in metabolic pathways. As genes are involved in all metabolic functions and gene expression studies would have confirmed that the shifts in metabolome are solely due to diet and no other parameter was involved.
3. Nutritional stress dosage was identified using MTT assay and sub-lethal dosage was used to confer the effects of dietary stress on HepG2 cells. The sub-lethal dose that we have selected may not be the actual sub-lethal dose as the dose range between lethal and sub-lethal values is high.
4. Several metabolites were not identified in GC-MS analysis due to less abundance or low/high molecular weight of the metabolite as the mass range for the analysis was 50-650 amu. Less abundance of metabolites could be due to the usage of less cell volume for sample preparation.
5. Metabolanalyst (5.0) tool was used to identify the metabolites but it may reject certain metabolites (no hits obtained) due to an internal algorithm or a less updated version of the tool.
6. This study is solely based on *in vitro* cell culture. So, the endocrine system and hormonal aspects were not covered in this study.

7. HepG2 cells share certain characteristics with hepatocytes. But the liver consists of multiple cell types and the effects of each dietary stress on different cells of the liver could not be inferred.
8. 5Sil MS column was used for GC-MS analysis. This is a non-polar column. So, some of the metabolites could not have been identified due to their polar characteristics.
9. Treatment of cells with each dietary stress was given for only 24 hours. So, this study is only based on dose-dependent effects. Some of the changes due to dietary stress can be induced in different time intervals.
10. This study was conducted using different dietary stress with different dosage concentrations. But the aspect of using different dietary stress with the same concentration could have yielded different results.
11. The homeostatic regulation present inside the body (metabolic integration, nervous system, and endocrine system) is absent *in vitro* culture, this could indicate that the results are more precise to liver functionalities. Also, the results obtained for dietary stresses are devoid of other tissue responses.

CONCLUSION

This study helps in concluding the effects of dietary stresses (high glucose, high palmitic acid, high NaCl, high BSA, and high butyrate) on liver function and diseases. Out of all five treatments, glucose and palmitic acid treatment showed ill effects on the liver concerning the metabolic pathways identified after metabolite analysis. Palmitic acid showed more negative and disease-associated effects on cells which include biosynthesis of BCAAs and AAAs, glutathione degradation, and ketone body formation. Butyrate showed enrichment of beneficial factors like degradation of pyruvaldehyde in cell culture which is healthy for the body. BSA showed a mixture of effects which can include normal cellular metabolism, glutathione production, and insulin resistance. Proteins tend to show negative and positive effects on the body and this is dependent on the type of protein that is consumed. Since BSA is a standard protein for various experiments, it showed a variety of effects on cells. Salt also showed mild or no effect on cells. Major metabolic pathways identified were associated with normal cellular functions including carnitine synthesis, butyrate and propanoate metabolism, pyruvate metabolism, and glycolysis/gluconeogenesis.

Hence, it could be concluded that palmitic acid possesses more deteriorating effects on the liver than glucose or any other nutritional stress. High fiber intake is beneficial to the body specifically the liver. The effects of salt on the liver are mild in terms of metabolic disorders and protein may show different effects in the liver based on the protein source and type.

REFERENCES

Acierno, C., Caturano, A., Pafundi, P. C., Nevola, R., Adinolfi, L. E., & Sasso, F. C. (2020). Nonalcoholic fatty liver disease and type 2 diabetes: pathophysiological mechanisms shared between the two faces of the same coin. *Exploration of Medicine*, *1*(5), 287-306. https://doi.org/10.37349/emed.2020.00019

Adrain, C. (2021). Systemic and cellular metabolism: the cause of and remedy for disease? *Febs journal*, *288*(12), 3624-3627. https://doi.org/10.1111/febs.16033

Aeppli, T. R. J., Rymen, D., Allegri, G., Bode, P. K., & Häberle, J. (2020). Glycogen storage disease type VI: clinical course and molecular background. *European Journal of Pediatrics*, *179*(3), 405-413. https://doi.org/10.1007/s00431-019-03499-1

Arzumanian, V. A., Kiseleva, O. I., & Poverennaya, E. V. (2021). The Curious Case of the HepG2 Cell Line: 40 Years of Expertise. *International Journal of Molecular Sciences*, *22*(23). https://doi.org/10.3390/ijms222313135

Bi, X., & Henry, C. J. (2017). Plasma-free amino acid profiles are predictors of cancer and diabetes development. *Nutrition & Diabetes*, *7*(3), e249-e249. https://doi.org/10.1038/nutd.2016.55

Boyce, G., Shoeb, M., Kodali, V., Meighan, T., Roberts, J. R., Erdely, A., Kashon, M., & Antonini, J. M. (2020). Using liquid chromatography mass spectrometry (LC-MS) to assess the effect of age, high-fat diet, and rat strain on the liver metabolome. *PLoS One*, *15*(7), e0235338. https://doi.org/10.1371/journal.pone.0235338

Brookes, M. J., & Cooper, B. T. (2007). Hypertension and fatty liver: guilty by association? *Journal of Human Hypertension*, *21*(4), 264-270. https://doi.org/10.1038/sj.jhh.1002148

Cabout, M., Alssema, M., Nijpels, G., Stehouwer, C. D. A., Zock, P. L., Brouwer, I. A., Elshorbagy, A. K., Refsum, H., & Dekker, J. M. (2017). Circulating linoleic acid and alpha-linolenic acid and glucose metabolism: the Hoorn Study. *European Journal of Nutrition*, *56*(6), 2171-2180. https://doi.org/10.1007/s00394-016-1261-6

Cai, H., Wen, Z., Meng, K., & Yang, P. (2021). Metabolomic signatures for liver tissue and cecum contents in high-fat diet-induced obese mice based on UHPLC-Q-TOF/MS. *Nutrition & Metabolism*, *18*(1), 69. https://doi.org/10.1186/s12986-021-00595-8

Chandrasekaran, K., Swaminathan, K., Chatterjee, S., & Dey, A. (2010). Apoptosis in HepG2 cells exposed to high glucose. *Toxicology In Vitro*, *24*(2), 387-396. https://doi.org/10.1016/j.tiv.2009.10.020

Chen, J. Y., Chou, H. C., Chen, Y. H., & Chan, H. L. (2013). High glucose-induced proteome alterations in hepatocytes and its possible relevance to diabetic liver disease. *Journal of Nutritional Biochemistry*, *24*(11), 1889-1910. https://doi.org/10.1016/j.jnutbio.2013.05.006

Cox, M., & Nelson, D. (2000). *Lehninger Principles of Biochemistry* (Vol. 5). https://doi.org/10.1007/978-3-662-08289-8

da Silva Ferreira, G., Catanozi, S., & Passarelli, M. (2023). Dietary Sodium and Nonalcoholic Fatty Liver Disease: A Systematic Review. *Antioxidants*, *12*(3), 599. https://www.mdpi.com/2076-3921/12/3/599

De Chiara, F., Ureta Checcllo, C., & Ramón Azcón, J. (2019). High Protein Diet and Metabolic Plasticity in Non-Alcoholic Fatty Liver Disease: Myths and Truths. *Nutrients*, *11*(12), 2985. https://www.mdpi.com/2072-6643/11/12/2985

Delimaris, I. (2013). Adverse Effects Associated with Protein Intake above the Recommended Dietary Allowance for Adults. *International Scholarly Research Notices*, *2013*, 126929. https://doi.org/10.5402/2013/126929

Félix-Martínez, G., Azpiroz, J., Roberto, Á.-P., & Fernández, J. R. (2013). Effects of Impaired ATP Production and Glucose Sensitivity on Human β-Cell Function: A Simulation Study. *Revista mexicana de ingeniería biomédica*, *35*, 157-170.

Golabi, P., Paik, J., Hwang, J. P., Wang, S., Lee, H. M., & Younossi, Z. M. (2019). Prevalence and outcomes of non-alcoholic fatty liver disease (NAFLD) among Asian American adults in the United States. *Liver International*, *39*(4), 748-757. https://doi.org/10.1111/liv.14038

Gray, L. R., Tompkins, S. C., & Taylor, E. B. (2014). Regulation of pyruvate metabolism and human disease. *Cellular and Molecular Life Sciences*, *71*(14), 2577-2604. https://doi.org/10.1007/s00018-013-1539-2

Griffin, J. W. D., & Bradshaw, P. C. (2019). Effects of a high protein diet and liver disease in an in silico model of human ammonia metabolism. *Theoretical Biology and Medical Modelling*, *16*(1), 11. https://doi.org/10.1186/s12976-019-0109-1

Hajdarevic, B., Vehabovic, I., Catic, T., & Masic, I. (2020). The Role of Diet Therapy in the Treatment of Liver Disease. *Materia Socio Medica*, *32*(3), 200-206. https://doi.org/10.5455/msm.2020.32.196-199

Hamed, A. E., Elsahar, M., Elwan, N. M., El-Nakeep, S., Naguib, M., Soliman, H. H., Ahmed Aboubakr, A., AbdelMaqsod, A., Sedrak, H., Assaad, S. N., Elwakil, R., Esmat, G., Salh, S., Mostafa, T., Mogawer, S., Sadek, S. E., Saber, M. M., Ezelarab, H., Mahmoud, A. A., Moussa, S. (2018). Managing diabetes and liver disease association. *Arab Journal of Gastroenterology*, *19*(4), 166-179. https://doi.org/10.1016/j.ajg.2018.08.003

Hanna, V. S., & Hafez, E. A. A. (2018). Synopsis of arachidonic acid metabolism: A review. *Journal of Advanced Research*, *11*, 23-32. https://doi.org/10.1016/j.jare.2018.03.005

Iciek, M., Kotańska, M., Knutelska, J., Bednarski, M., Zygmunt, M., Kowalczyk-Pachel, D., Bilska-Wilkosz, A., Górny, M., & Sokołowska-Jeżewicz, M. (2017). The effect of NaCl on the level of reduced sulfur compounds in rat liver. Implications for blood pressure increase. *Postepy Higieny Medycyny Doswiadczalnej (Online)*, *71*(0), 564-576. https://doi.org/10.5604/01.3001.0010.3837

Johnson, R. J., Perez-Pozo, S. E., Sautin, Y. Y., Manitius, J., Sanchez-Lozada, L. G., Feig, D. I., Shafiu, M., Segal, M., Glassock, R. J., Shimada, M., Roncal, C., & Nakagawa, T. (2009). Hypothesis: could excessive fructose intake and uric acid cause type 2 diabetes? *Endocrine Reviews*, *30*(1), 96-116. https://doi.org/10.1210/er.2008-0033

Kieffer, D. A., Martin, R. J., & Adams, S. H. (2016). Impact of Dietary Fibers on Nutrient Management and Detoxification Organs: Gut, Liver, and Kidneys. *Advances in Nutrition*, *7*(6), 1111-1121. https://doi.org/10.3945/an.116.013219

Kieffer, D. A., Piccolo, B. D., Marco, M. L., Kim, E. B., Goodson, M. L., Keenan, M. J., Dunn, T. N., Knudsen, K. E., Martin, R. J., & Adams, S. H. (2016). Mice Fed a High-Fat Diet Supplemented with Resistant Starch Display Marked Shifts in the Liver Metabolome Concurrent with Altered Gut Bacteria. *Journal of Nutrition*, *146*(12), 2476-2490. https://doi.org/10.3945/jn.116.238931

Kim, H. J., Kim, J. H., Noh, S., Hur, H. J., Sung, M. J., Hwang, J. T., Park, J. H., Yang, H. J., Kim, M. S., Kwon, D. Y., & Yoon, S. H. (2011). Metabolomic analysis of livers and serum from high-fat diet induced obese mice. *Journal of Proteome Research*, *10*(2), 722-731. https://doi.org/10.1021/pr100892r

Kudo, F., & Eguchi, T. (2009). Biosynthetic genes for aminoglycoside antibiotics. *The Journal of Antibiotics*, *62*(9), 471-481. https://doi.org/10.1038/ja.2009.76

Lee, Y. T., Huang, S. Q., Lin, C. H., Pao, L. H., & Chiu, C. H. (2022). Quantification of Gut Microbiota Dysbiosis-Related Organic Acids in Human Urine Using LC-MS/MS. *Molecules*, *27*(17). https://doi.org/10.3390/molecules27175363

Li, Y., Lyu, Y., Huang, J., Huang, K., & Yu, J. (2021). Transcriptome sequencing reveals high-salt diet-induced abnormal liver metabolic pathways in mice. *BMC Gastroenterology*, *21*(1), 335. https://doi.org/10.1186/s12876-021-01912-4

Maciejewska-Markiewicz, D., Drozd, A., Palma, J., Ryterska, K., Hawryłkowicz, V., Załęska, P., Wunsh, E., Kozłowska-Petriczko, K., & Stachowska, E. (2022). Fatty Acids and Eicosanoids Change during High-Fiber Diet in NAFLD Patients-Randomized Control Trials (RCT). *Nutrients*, *14*(20). https://doi.org/10.3390/nu14204310

Mato, J. M., Alonso, C., Noureddin, M., & Lu, S. C. (2019). Biomarkers and subtypes of deranged lipid metabolism in non-alcoholic fatty liver disease. *World Journal of Gastroenterology*, *25*(24), 3009-3020. https://doi.org/10.3748/wjg.v25.i24.3009

Meissen, J. K., Hirahatake, K. M., Adams, S. H., & Fiehn, O. (2015). Temporal metabolomic responses of cultured HepG2 liver cells to high fructose and high glucose exposures. *Metabolomics*, *11*(3), 707-721. https://doi.org/10.1007/s11306-014-0729-8

Narayan, K. M. V., & Kanaya, A. M. (2020). Why are South Asians prone to type 2 diabetes? A hypothesis based on underexplored pathways. *Diabetologia*, *63*(6), 1103-1109. https://doi.org/10.1007/s00125-020-05132-5

Nathani, N. M., Duggirala, S. M., Bhatt, V. D., Patel, A. K., Kothari, R. K., & Joshi, C. G. (2016). Correlation between genomic analyses with metatranscriptomic study reveals various functional

pathways of Clostridium sartagoforme AAU1, a buffalo rumen isolate. *Journal of Applied Animal Research*, *44*(1), 498-507. https://doi.org/10.1080/09712119.2015.1091346

Otto-Ślusarczyk, D., Graboń, W., & Mielczarek-Puta, M. (2016). [Aspartate aminotransferase--key enzyme in the human systemic metabolism]. *Postepy Higieny Medycyny Doswiadczalnej (Online)*, *70*, 219-230. https://doi.org/10.5604/17322693.1197373 (Aminotransferaza asparaginianowa--kluczowy enzym w metabolizmie ogólnoustrojowym człowieka.)

Panahi, G., Pasalar, P., Zare, M., Rizzuto, R., & Meshkani, R. (2018). High glucose induces inflammatory responses in HepG2 cells via the oxidative stress-mediated activation of NF-κB, and MAPK pathways in HepG2 cells. *Archieves of Physiology and Biochemistry*, *124*(5), 468-474. https://doi.org/10.1080/13813455.2018.1427764

Perdomo, C. M., Frühbeck, G., & Escalada, J. (2019). Impact of Nutritional Changes on Nonalcoholic Fatty Liver Disease. *Nutrients*, *11*(3). https://doi.org/10.3390/nu11030677

Pesta, D. H., & Samuel, V. T. (2014). A high-protein diet for reducing body fat: mechanisms and possible caveats. *Nutrition and Metabolism (Lond)*, *11*(1), 53. https://doi.org/10.1186/1743-7075-11-53

Pitsavos, C., Panagiotakos, D., Weinem, M., & Stefanadis, C. (2006). Diet, exercise and the metabolic syndrome. *Review of Diabetic Studies*, *3*(3), 118-126. https://doi.org/10.1900/rds.2006.3.118

Pizzorno, J. (2014). Glutathione! *Integrative Medicine (Encinitas)*, *13*(1), 8-12.

Powles, J., Fahimi, S., Micha, R., Khatibzadeh, S., Shi, P., Ezzati, M., Engell, R. E., Lim, S. S., Danaei, G., Mozaffarian, D., Nutrition, o. b. o. t. G. B. o. D., & Group, C. D. E. (2013). Global, regional and national sodium intakes in 1990 and 2010: a systematic analysis of 24 h urinary

sodium excretion and dietary surveys worldwide. *BMJ Open*, *3*(12), e003733. https://doi.org/10.1136/bmjopen-2013-003733

Rojas, Á., García-Lozano, M. R., Gil-Gómez, A., Romero-Gómez, M., & Ampuero, J. (2022). Glutaminolysis-ammonia-urea Cycle Axis, Non-alcoholic Fatty Liver Disease Progression and Development of Novel Therapies. *Journal of clinical and translational hepatology*, *10*(2), 356-362. https://doi.org/10.14218/jcth.2021.00247

Rui, L. (2014). Energy metabolism in the liver. *Comprehensive Physiology*, *4*(1), 177-197. https://doi.org/10.1002/cphy.c130024

Sharma, M., Kishore, A., Roy, D., & Joshi, K. (2020). A comparison of the Indian diet with the EAT-Lancet reference diet. *BMC Public Health*, *20*(1), 812. https://doi.org/10.1186/s12889-020-08951-8

Shojaei-Zarghani, S., Safarpour, A. R., Fattahi, M. R., & Keshtkar, A. (2022). Sodium in relation with nonalcoholic fatty liver disease: A systematic review and meta-analysis of observational studies. *Food Science and Nutrition*, *10*(5), 1579-1591. https://doi.org/10.1002/fsn3.2781

Stachowska, E., Maciejewska-Markiewicz, D., Palma, J., Mielko, K. A., Qasem, B., Kozłowska-Petriczko, K., Ufnal, M., Sokolowska, K. E., Hawryłkowicz, V., Załęska, P., Jakubczyk, K., Wunsch, E., Ryterska, K., Skonieczna-Żydecka, K., & Młynarz, P. (2022). Precision Nutrition in NAFLD: Effects of a High-Fiber Intervention on the Serum Metabolome of NAFD Patients—A Pilot Study. *Nutrients*, *14*(24), 5355. https://www.mdpi.com/2072-6643/14/24/5355

Stanhope, K. L., Schwarz, J. M., Keim, N. L., Griffen, S. C., Bremer, A. A., Graham, J. L., Hatcher, B., Cox, C. L., Dyachenko, A., Zhang, W., McGahan, J. P., Seibert, A., Krauss, R. M., Chiu, S., Schaefer, E. J., Ai, M., Otokozawa, S., Nakajima, K., Nakano, T., Havel, P. J. (2009).

Consuming fructose-sweetened, not glucose-sweetened, beverages increases visceral adiposity and lipids and decreases insulin sensitivity in overweight/obese humans. *Journal of Clinical Investigation*, *119*(5), 1322-1334. https://doi.org/10.1172/jci37385

Wang, G., Yeung, C. K., Wong, W. Y., Zhang, N., Wei, Y. F., Zhang, J. L., Yan, Y., Wong, C. Y., Tang, J. J., Chuai, M., Lee, K. K., Wang, L. J., & Yang, X. (2016). Liver Fibrosis Can Be Induced by High Salt Intake through Excess Reactive Oxygen Species (ROS) Production. *Journal of Agricultural and Food Chemistry*, *64*(7), 1610-1617. https://doi.org/10.1021/acs.jafc.5b05897

Wang, X., Zhang, W., Huang, J., Li, H., & Gao, J. (2023). The relationship between vitamin K and metabolic dysfunction-associated fatty liver disease among the United States population: National Health and Nutrition Examination Survey 2017-2018. *Frontiers in Nutrition*, *10*, 1086477. https://doi.org/10.3389/fnut.2023.1086477

Wilson, D. F., & Matschinsky, F. M. (2020). Ethanol metabolism: The good, the bad, and the ugly. *Medical Hypotheses*, *140*, 109638. https://doi.org/https://doi.org/10.1016/j.mehy.2020.109638

Wolfe, R. R. (2017). Branched-chain amino acids and muscle protein synthesis in humans: myth or reality? *Journal of International Society of Sports Nutrition*, *14*, 30. https://doi.org/10.1186/s12970-017-0184-9

Würtz, P., Soininen, P., Kangas, A. J., Rönnemaa, T., Lehtimäki, T., Kähönen, M., Viikari, J. S., Raitakari, O. T., & Ala-Korpela, M. (2013). Branched-chain and aromatic amino acids are predictors of insulin resistance in young adults. *Diabetes Care*, *36*(3), 648-655. https://doi.org/10.2337/dc12-0895

Yu, S., Meng, S., Xiang, M., & Ma, H. (2021). Phosphoenolpyruvate carboxykinase in cell metabolism: Roles and mechanisms beyond gluconeogenesis. *Molecular Metabolism*, *53*, 101257. https://doi.org/10.1016/j.molmet.2021.101257

Plagiarism report

Document Information

Analyzed document	Nehal_302101015_thesis.doc (D172106116)
Submitted	2023-07-15 08:03:00
Submitted by	Dr. Priyankar Dey
Submitter email	priyankar.dey@thapar.edu
Similarity	0%
Analysis address	priyankar.dey.thapar@analysis.urkund.com

Sources included in the report

Nehal

17/07/23.

Entire Document

ABSTRACT

Normal body function is based on the metabolic processes going inside the body. The metabolic pathways require energy (ATP) as fuel for the formation of metabolic intermediates to enrich other metabolic pathways and perform cellular functions. This energy is provided by diet which includes carbohydrates, fats, proteins, fiber, and minerals. The diet consumed is digested in the small intestine and enters the liver via the portal vein. The liver plays a significant role in the metabolism of gut-derived dietary components. Metabolism of these components includes degradation or modification for the production of metabolites conferring physiological roles. Consumption of these dietary elements in adequate amounts maintains metabolic homeostasis. But excess intake for prolonged periods may cause toxicity and affect the metabolic processes and metabolites composition in the human body. This can lead to the development of metabolic syndrome (MetS) which may cause several metabolic diseases. These metabolomic shifts may negatively affect the liver and its function as the liver is the first line of detoxification for gut-derived metabolites. Non-alcoholic fatty liver disease (NAFLD) is a common liver disease that occurs due to metabolic disorders in the liver. NAFLD spectrum includes fat accumulation, inflammation, fibrosis, cirrhosis, and development of hepatocellular carcinoma (HCC). In this

THAPAR INSTITUTE
OF ENGINEERING & TECHNOLOGY
(Deemed to be University)

NEHAL . <nnehal_msc21@thapar.edu>

Fwd: [Ouriginal] 0% similarity - priyankar.dey@thapar.edu

2 messages

PRIYANKAR DEY <priyankar.dey@thapar.edu> Sat, Jul 15, 2023 at 11:31 AM
To: "NEHAL ." <nnehal_msc21@thapar.edu>

---------- Forwarded message ---------
From: <noreply@urkund.com>
Date: Sat, Jul 15, 2023 at 11:33 AM
Subject: [Ouriginal] 0% similarity - priyankar.dey@thapar.edu
To: <priyankar.dey@thapar.edu>

Document sent by: priyankar.dey@thapar.edu
Document received: 7/15/2023 8:03:00 AM
Report generated 7/15/2023 8:03:42 AM by Ouriginal's system for automatic control.

Student message: Nehal_Thesis

Document : Nehal_302101015_thesis.doc[D172106116]
IMPORTANT! The analysis contains 1 warning(s).
About 0% of this document consists of text similar to text found in 1 sources. The largest marking is 0 words long and is 0% similar to its primary source.

PLEASE NOTE that the above figures do not automatically mean that there is plagiarism in the document. There may be good reasons as to why parts of a text also appear in other sources. For a reasonable suspicion of academic dishonesty to present itself, the analysis, possibly found sources and the original document need to be examined closely.

Click here to open the analysis:
https://secure.urkund.com/view/164470447-466602-124943

Click here to download the document:
https://secure.ouriginal.com/archive/download/172106116-710013-587786

17/7/23

--

THAPAR INSTITUTE
OF ENGINEERING & TECHNOLOGY
(Deemed to be University)

Priyankar Dey, M.S., Ph.D.
Assistant Professor & Ph.D. Coordinator
Department of Biotechnology
Thapar Institute of Engineering & Technology
Bhadson Road, Patiala
Punjab, Pin -147004, India

Nehal

3M Lab Webpage
Email: priyankar.dey@thapar.edu; priyankardey28@gmail.com
Mob: +91-9064275660